HEMODYNAMICS, VENTILATION EFFECTS, ENERGETICS, AND TIME OFFSETS IN VARIOUS MODIFIED FONTAN CIRCULATIONS

Mark E. Ketner

A dissertation submitted to the faculty of the University of North Carolina at Chapel Hill in partial fulfillment of the requirements for the degree of Doctor of Philosophy in the Department of Biomedical Engineering.

Chapel Hill
2006

Approved by

Advisor: Carol Lucas, Ph.D.

Reader: Timothy Johnson, Ph.D.

Reader: Weili Lin, Ph.D.

Reader: Michael Mill, M.D.

Reader: Ajit Yoganathan, Ph.D.

ABSTRACT

MARK E. KETNER: Hemodynamics, Ventilation Effects, Energetics, and Time Offsets in Various Modified Fontan Circulations

(Under the direction of Carol Lucas)

Approximately two out of every one thousand live births have a complex congenital heart defect (CHD) that creates a univentricular physiology. As a result of the altered physiology, the overloaded single ventricle pumps both oxygenated and deoxygenated blood to parallel pulmonary and systemic circulations. Since 1971, when Fontan and Baudet were first successful in treating patients with tricuspid atresia with an atriopulmonary (AP) repair, operations that place the pulmonary and systemic circulations in series with the single pump have been termed “Fontan Repairs”. The current repair of choice bypasses the right side of the heart, connecting the superior and inferior cava directly to the pulmonary arteries. Such repairs are termed total cavopulmonary connections (TCP) and have various modifications: graft size, connection angles, materials used, etc. Though most Fontan patients lead relatively normal lives, most also suffer some complications, ranging from exercise intolerance to life threatening GI disorders, whose causes are yet to be determined. One prominent characteristic of the Fontan circulation is an increased influence of respiration, which also is not well understood, but may be related to other complications.

This research investigated various Fontan modifications not available via computer simulation by implementing surgical designs in-vivo in lambs and collecting pressure and

flow data in various vessels and chambers. Data were obtained in four models, the AP connection and three models of the TCP connection: total cavopulmonary connection without a synthetic graft (TCPC), extracardiac total cavopulmonary connection with graft (TCPX), and the total cavopulmonary connection using a Y-shaped graft (TCPY). The overall hypothesis is that a fundamental understanding of modified Fontan repairs will lead to improved surgical planning and designs and thus the potential for long term outcomes in patients. Specific Aims were to: 1) Investigate the effects of ventilation parameters on hemodynamics under normal and various Fontan modifications, 2) Determine power losses of various Fontan circulations under varying physiological parameters, 3) Determine time offsets regarding positive pressure ventilation (PPV) for implementation in an electrical computer simulation model and 4) Determine feasibility and establish protocol at UNC for geometry and velocity mapping via MRI.

To my wife and daughter, Kelli and Carson Adele Ketner.

Your love, prayers, and support were the motivation to reach this goal.

I love you.

ACKNOWLEDGEMENTS

I would like to thank my advisor, mentor, and friend, Dr. Carol Lucas, for having the utmost patience and faith in me. Her knowledge, guidance, and support were instrumental in helping achieve this goal. Her friendship and advice are cherished and will remain for years to come.

I would like to thank the surgeons, Dr. Michael Mill and Dr. Brett Sheridan, for providing the expertise in making this research possible. Their time, knowledge, and interest in this research project are invaluable. Thank you to the anesthesiologist, Dr. Luke Lucas, for his humor, "pharmaceutical magic", and knowledge. Too many to name, but thank you to the perfusionists, technicians, surgical assistants, and DLAM personnel that have helped the animal models become successful.

Thank you to all of my committee members, Dr. Timothy Johnson, Dr. Weili Lin, Dr. Michael Mill, and Dr. Ajit Yoganathan, for research direction, advice, dissertation reviews, and project insights throughout the years.

Thanks to Dr. Brian Hyslop and Maggie Morris for making Fontan MRI possible here at UNC.

Thanks for Dr. Brooke Steele for laboratory and technical support over the last two years.

I would like to thank my entire family for enduring the many trials and tribulations that were involved in achieving this goal. They never lost faith in me and for that I am most grateful.

Thank you to the University of North Carolina at Chapel Hill and the entire Department of Biomedical Engineering faculty and staff that have provided a great education and a degree for which I am very proud.

Thank you to Sharon Womble and Tiffany Harris, without your unselfish help on countless occasions, I would not have graduated, much less registered for class or paid tuition.

Thanks to Don Weyel and James Jordan for keeping the department technology current and always available.

Thanks to my lab partner, Dr. Jonathan Masters, whose intelligence and friendship helped me through many educational roadblocks in pursuit of this degree.

I am grateful for the many friendships that have been formed with students, faculty, and staff through the years. I hope they will remain strong in the future.

Thank you to the National Institutes of Health for funding this research.

I would like to thank God, for without Him, none of this is possible.

TABLE OF CONTENTS

Page

LIST OF TABLES

Appendix III:

Appendix IV:

LIST OF FIGURES

Appendix II:

Appendix III:

Appendix IV:

LIST OF ABBREVIATIONS AND SYMBOLS

φ_m	Phase shift of moving spins
Φ	Phase angle from MRI image
$\theta(f)$	Phase Angle from Transfer Function
$\Phi(T)$	Phase shift at time T
τ	Duration of the Magnetic Gradient
γ	Gyromagnetic Ratio
v	Velocity
t	Time
3D	Three Dimensional
AIRP	Airway Pressure
AIRQ	Airway Flow
AO	Aorta
AOP	Arterial Pressure or Aortic Pressure
AP	Atriopulmonary
ASD	Atrial Septal Defect
BDG	Bidirectional Glenn
cc	cubic centimeter
CFD	Computational Fluid Dynamics
CHD	Congenital Heart Defect
CI	Confidence Interval
CO	Cardiac Output

CO_2	Carbon Dioxide
DILV	Double Inlet Left Ventricle
$\dot{E}$	Power
$G(f)_{II}$	Auto-Spectra
$G(f)_{IO}$	Cross-Spectra
F	Female
FFT	Fast Fourier Transform
FISP	Fast Imaging with Steady Precession
G	Gradient Waveform and Strength
GI	Gastrointestinal
GUI	Graphical User Interface
$H_{imaginary}(f)$	Imaginary part of Transfer Function
$H_{real}(f)$	Real part of Transfer Function
$H(f)$	Transfer Function
HASTE	Half-Fourier single shot turbo spin-echo
HIPAA	Health Insurance Portability and Accountability Act
HLV	Hypoplastic Left Ventricle
HPLH	Hypoplastic Left Heart
HRH	Hypoplastic Right Heart
HRU	Hybrid Resistance Unit
HRV	Hypoplastic Right Ventricle
Hg	Mercury
Hz	Hertz

iNO	inhaled Nitric Oxide
IVC	Inferior Vena Cava
IVCP	Inferior Vena Cava Pressure
IVCQ	Inferior Vena Cava Flow
IRB	Institutional Review Board
LA	Left Atria
LAP	Left Atria Pressure
LPA	Left Pulmonary Artery
LPAQ	Left Pulmonary Artery Flow
LV	Left Ventricle
LVP	Left Ventricle Pressure
mL	Milliliter
min	Minute
M	Male
mm	millimeters
mW	milliwatt
MPA	Main Pulmonary Artery
MPAP	Main Pulmonary Artery Pressure
MPAQ	Main Pulmonary Artery Flow
MRI	Magnetic Resonance Imaging
P	Pressure
PA	Pulmonary Artery
PAP	Pulmonary Artery Pressure

PAQ	Pulmonary Artery Flow
PC	Phase Contrast Imaging
PLE	Protein-losing Enteropathy
PPV	Positive Pressure Ventilation
PTFE	Polytetrafluoroethylene
PVR	Pulmonary Vascular Resistance
Q	Flow
RA	Right Atria
RAP	Right Atria Pressure
RPA	Right Pulmonary Artery
RV	Right Ventricle
S_m	Moving spin contribution of the MRI image
SD	Standard Deviation
sec	Second
SVC	Superior Vena Cava
SVCP	Superior Vena Cava Pressure
SVCQ	Superior Vena Cava Flow
SVR	Systemic Vascular Resistance
TCP	Total Cavopulmonary
TCPC	Total Cavopulmonary Connection
TCPX	Total Cavopulmonary Connection with Synthetic Extracardiac Shunt
TCPY	Total Cavopulmonary Connection with Y-shaped anastomoses.
TGA	Transposition of the Great Arteries

UNC	University of North Carolina at Chapel Hill
VAD	Ventricular Assist Device
VSD	Ventricular Septal Defect

CHAPTER I

INTRODUCTION AND HYPOTHESIS

1.1 General Introduction

1.1.1 Physiology

Approximately two out of every one thousand live births have a complex congenital heart defect (CHD) that effectively creates a univentricular physiology. Examples of such defects include multiple ventricular septal defects, tricuspid atresia, hypoplastic left heart (HPLH) syndrome, and double outlet ventricle. As a result of this altered physiology, the overloaded single ventricle pumps both oxygenated and deoxygenated blood to parallel pulmonary and systemic circulations. This mixing of blood impairs the atriopulmonary (AP) pathway.

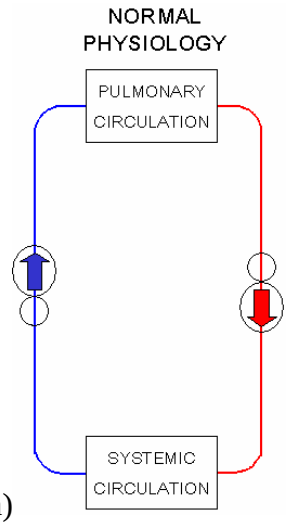

a)

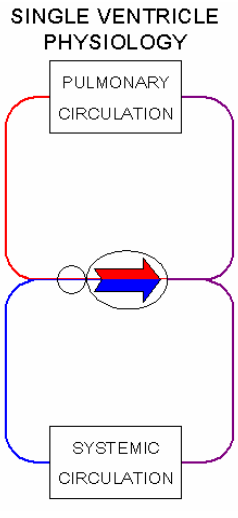

b)

Figure 1.1 Schematics showing a) normal two ventricle physiology with two distinct pumps separating oxygenated and deoxygenated blood and b) single ventricle physiology having a single pump that mixes oxygenated and deoxygenated blood.

Therefore researchers, clinicians, and surgeons' efforts have focused towards reducing the load required by the ventricle and eliminating the mixing of oxygenated and deoxygenated blood. This is achieved by separating the pulmonary and systemic circulations and placing them in series with each other where the hemodynamic energy is supplied by a single univentricular pump.

Early work, 1948, consisted of right ventricular bypass in dogs by Rodbard and Wagner. In 1958, Glenn was successful in clinically implementing a shunt between the superior vena cava (SVC) and the right pulmonary artery (RPA). The configuration was partially successful because it reduced the volume load on the ventricle. However, the shunt did not prevent the mixing of oxygenated and deoxygenated blood.

1.1.2 Palliative Fontan Procedure

The mixing of venous with oxygenated blood problem was solved using a palliative procedure developed by Fontan and Baudet in 1971 (Fontan and Baudet 1971). This procedure drains the entire caval blood return into the lungs. Therefore, only oxygenated blood is returned to the left side of the heart. The right atria (RA) takes the place of the functioning ventricle by directing the inferior vena cava (IVC) blood flow to the left lung. Fontan successfully performed this procedure in two patients having tricuspid atresia.

Normal pulmonary physiology and the absence of pulmonary hypertension and low pulmonary vascular resistance (PVR) were requirements needed for these patients.

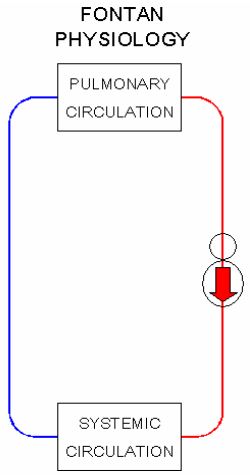

Figure 1.2 Fontan physiology separating the systemic and pulmonary circulations preventing the mixing of oxygenated and deoxygenated blood. This circuit utilizes the energy of one ventricle to pump blood throughout the low-pressure circulation.

The surgical technique was performed through a median sternotomy. The operation consisted of five steps. The first step was an end-to-side anastomosis using a Blalock continuous suture of the SVC to the distal end of the RPA. This was the same procedure used earlier by Glenn. Next, an aortic homograft was used to connect the RA appendage to the proximal end of the RPA by end-to-end anastomosis. The homograft was used to prevent blood reflux into the RA from the left pulmonary artery (LPA) during atrial diastole. The third step was placing the patient under cardiopulmonary bypass via cannulation of the SVC and the right external iliac vein. The RA is opened and the atrial septal defect (ASD) is closed. A pulmonary valve homograft was next inserted where the IVC enters the RA. This homograft prevented blood reflux into the IVC during atrial systole. Finally, the main pulmonary artery (MPA) was either ligated or transected and the patient taken off

cardiopulmonary bypass. The portion of the SVC used to cannulate was then transected. Postoperative measures after this first technique include mass infusions of blood and maintaining tachycardia.

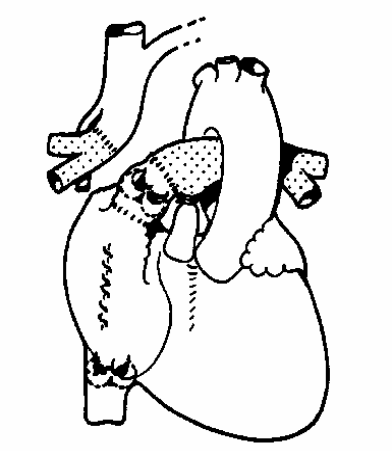

Figure 1.3 Illustration of first Fontan procedure for tricuspid atresia (Fontan and Baudet 1971).

The term "Fontan" has become the generic term applied to numerous surgical procedures that separate the systemic and pulmonary circuits in patients with only one functional ventricle.

1.1.3 Valves

Successive investigators and even Fontan questioned the use of valves. One of Fontan's first patients had the procedure successfully implemented without grafts due to small vascular geometry. Aortic valves formed secondary calcifications and valvular stenosis tended to be the major cause of conduit failure. Also, the pliability and plasticity of the valves was questioned (Fontan and Baudet 1971). Other work found that blood flow through the atriopulmonary conduits was primarily influenced by the RA pressure and was therefore not affected by the presence or absence of a valve (Shemin, Merrill et al. 1979).

1.1.4 Role of the Pulsatile Right Atria

Once valves were proven unnecessary, the next major contribution arose from debates about the role of a pulsatile RA in aiding pulmonary circulation. Also, the development of arrhythmias due to high pressures in the RA caused concern for including the RA in single ventricle circulations. Other complications of the traditional atriopulmonary connection include atrial arrhythmias, thromboembolism, and right pulmonary vein obstruction, which usually occur secondary to RA enlargement (McElhinney, Reddy et al. 1996). An element of the atriopulmonary (AP) procedure, described earlier by Fontan and Baudet and modified by the removal of vales, that remains unpredictable is the patient response to the changes in hemodynamics and the consequences of an eventual atrial disturbance such as atrial flutter or fibrillation (Fontan and Baudet 1971).

1.1.5 The Intra-atrial Total Cavopulmonary Connection

In 1988, de Leval performed experiments *in-vitro* on a pulsating valveless chamber in a continuous flow circuit (de Leval, Kilner et al. 1988). de Leval's experiments showed that the atrial chamber generates turbulence and therefore increases resistance to forward flow. Results also illustrated the importance in streamlining around corners and through cavities in order to minimize energy losses. From the *in-vitro* results, de Leval developed an alternative procedure to the classical AP connection that excluded either most or all of the RA called the intra-atrial total cavopulmonary connection (TCPC). The TCPC connection consisted of an end-to-side anastomosis of the SVC to the RPA, construction of an intra-atrial tunnel using composite material, part of the RA wall, and use of a synthetic graft to channel the IVC to the

inferior side of the RPA. This connection projected diminished energy losses, less turbulence, a decreased risk of atrial thrombosis, and a lower RA pressure thereby reducing the risk of arrhythmias. The intra-atrial TCPC connection is often called the lateral tunnel Fontan.

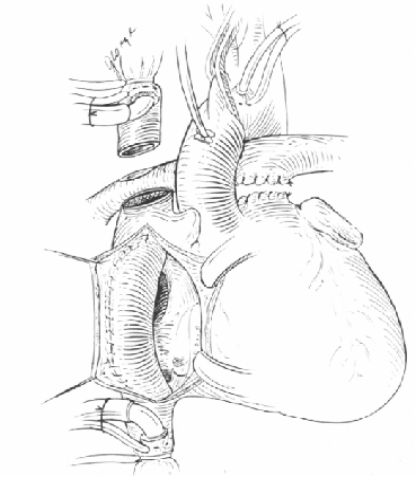

Figure 1.4 Illustration of lateral or intra-atrial tunnel Fontan procedure (de Leval, Kilner et al. 1988).

1.1.6 Research Modalities

Since de Leval's discovery of the necessity of streamlines, reduced turbulence, and absence of stagnant flow, many surgical techniques have been investigated to improve blood flow and diminish energy losses. Energy maintenance is of utmost importance due to the fact that only one functioning ventricle is responsible for providing the energy to move the blood throughout the entire circulation. Major areas under investigation are anastomoses types (end-to-end or end-to-side), connection parameters (straight, flared, curved, or cowled), planar and non-planar caval arrangements, the degree of offset between anastomoses,

bifurcation angles, as well as shunt types, materials, and size. In order to calculate energy dissipation and flow distribution to the lungs, numerous finite element and finite volume methods have been developed. These methods use computational software packages in order to solve the fluid mass and momentum equations (Navier-Stokes equations).

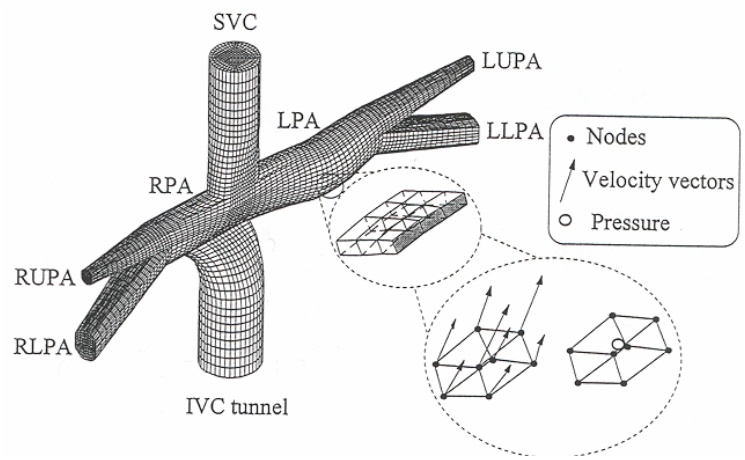

Figure 1.5 Schematic example of finite element mesh of the total cavopulmonary connection (de Leval, Dubini et al. 1996).

An example of a finite element mesh generation for a TCPC procedure is illustrated in Figure 1.5. Solutions to these computer simulations should help determine optimal surgical procedures and protocol based on individual anatomy and physiology. Along with computational fluid dynamics (CFD), in-vitro models have been studied in order to simulate Fontan modifications and minimize energy loss. Particles are introduced into the flow and photographed. This process is called particle velocimetry. Results (Figure 1.6) show recirculation regions, stagnation regions, high shear regions, and flow distribution between the lungs.

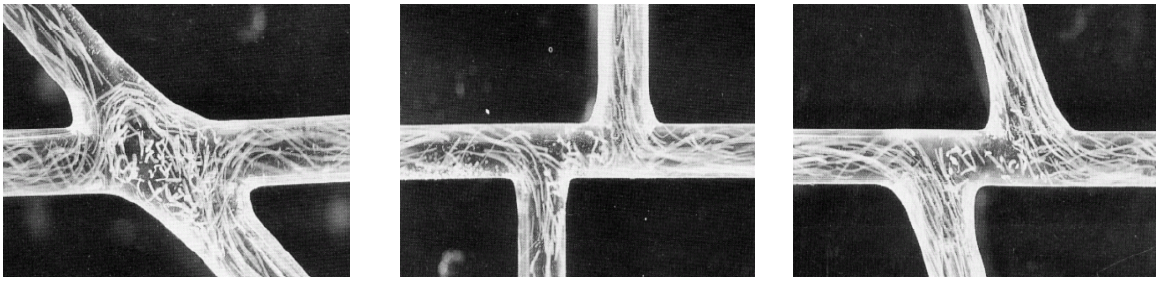

A) **B)** **C)**

Figure 1.6 In-vitro models of particle velocimetry showing different A) incidence angles B) offset and C) flaring options (Kim, Walker et al. 1995).

Advances in magnetic resonance imaging (MRI) techniques have enabled the measurement of three dimensional flow dynamics of Fontan circulations (Figure 1.7) through phase contrast imaging sequences. Comprehensive flow patterns can be determined in-vivo.

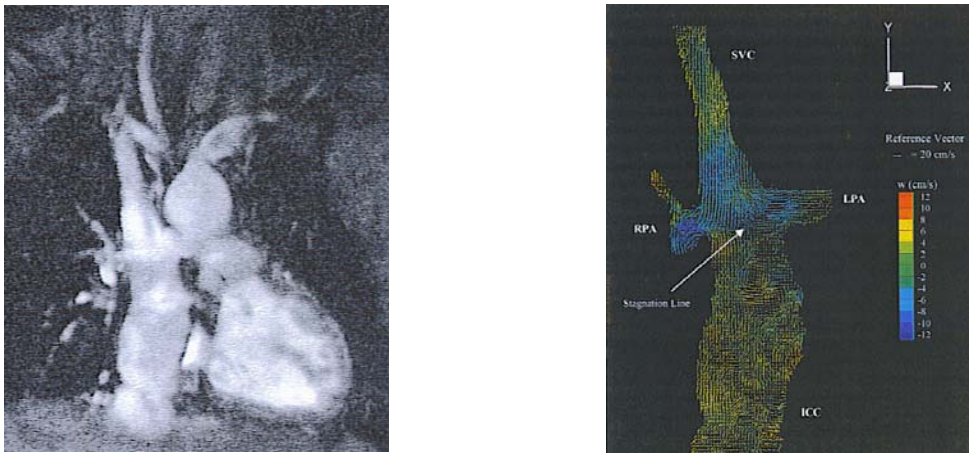

Figure 1.7 MRI phase contrast image and resulting velocity vector map of total cavopulmonary connection (Sharma, Ensley et al. 2001).

Many different modalities are being used in order to help minimize energy loss and provide the optimal surgical procedure. Correlation between modalities and patient databases will enable surgeons to optimize protocols based on individual patient geometry.

Both the AP and lateral tunnel TCPC connections have been used in clinical practice. Generally, the AP was used for cases of tricuspid atresia and the lateral tunnel TCPC for univentricular heart cases. One major advantage of the TCPC is that it can be applied to almost any complex cardiac anatomy. The intra-atrial or lateral tunnel concept is now widely accepted among surgeons and is usually constructed with the use of aortic crossclamping. Other advantages of the lateral tunnel TCPC include construction without cardiac ischemia, easy fenestration if necessary in the postoperative period, and the properties of the compressible, non- thrombogenic conduit, which is capable of some growth. Therefore, the procedure can be performed in early infancy. The use of synthetic grafts to partially form intra-atrial conduits can result in pulmonary and systemic emboli from clotting within or external to the conduit but within the atrium (Gundry, Razzouk et al. 1997).

1.1.7 The Extracardiac Total Cavopulmonary Connection

In 1990, Marcelleti and colleagues suggested the use of an extracardiac conduit from the IVC to the PA in replacement of the conventional lateral tunnel procedure (Marcelletti, Corno et al. 1990). This procedure suggested numerous advantages. As the name implies, the tunnel can be constructed outside the heart. This procedure has been performed with the patient on cardiopulmonary bypass without arresting the heart and without cardiopulmonary bypass (Tam, Miller et al. 1999). The extracardiac conduit also eliminates the need for extensive atrial suture lines, avoids aortic cross-clamping, avoids exposure of the RA to high venous pressures perhaps preventing arrhythmias, and provides a more realistic laminar flow profile, which has been shown to diminish energy losses. Left sided emboli should be eliminated due to no foreign material existing within the heart. With the exclusion of the

RA, the atria wall is no longer subject to high shear stresses that will in turn lower the incidence of atrial flutter (Gardiner, Dhillon et al. 1996). Further advantages include a decrease in hospital stay, improved postoperative hemodynamics due to lack of cardiopulmonary bypass, and a more rapid recovery time.

Disadvantages of the extracardiac shunt include the inability for growth and the complex determination of shunt material. In the past, studies have been performed using large enough grafts to theoretically allow for growth. However, the issue of thrombosis formation is still a major concern (Alexi-Meskishvili, Ovroutski et al. 2000). Homografts have been investigated as a solution. Extracardiac conduits with homografts are extremely expensive and require the use of a limited resource (Gundry, Razzouk et al. 1997). Further research into conduit materials needs to be performed and a database of graft properties, sizes, etc. needs to be collected. Optimal size of the conduit according to patient age or size as well as the IVC and pulmonary artery diameters has not yet been determined. Furthermore, the lack of growth potential limits the application of these conduits in very young children.

Either an intra-atrial or extracardiac conduit seems to be a viable option for patients with AP complications or atrial defects (McElhinney, Reddy et al. 1996). The extracardiac conduit is the procedure of choice when converting from a conventional AP connection to a tunnel connection because no additional suture lines are necessary that may exacerbate existing atrial conditions. A summary of surgical conditions during and postoperatively between procedures is illustrated in Figure 1.8.

Parameters	Intra-atrial Tunnel	Extracardiac Tunnel	Extracardiac Conduit
Aortic Crossclamping	Yes	Not routinely required	Not routinely required
Intra-atrial suture lines	Extensive	Superficial and epicardial	No
Atriotomy	Yes	No	No
Intracardiac prosthetic material	Intra-atrial baffle	No	No
Thrombogenicity	Intra-atrial baffle material	Epicardial surface and tunnel material	Conduit material
Growth potential	Moderate	Moderate	No
Late percutaneous fenestrations	Yes	Yes	No
Intimal peel concern	Moderate	Moderate	High

Table 1.1 Attributes of three different Fontan procedures and possible complications (Lardo, Webber et al. 1999).

Surgical procedures have been performed in which no prosthetic material was used. In 1995, van Son performed a procedure in which the right and left SVCs were anastomosed to their respective pulmonary arteries (end-to-side) and the IVC was anstomosed to the MPA in an end-to-end fashion (van Son, Reddy et al. 1995). This procedure is inevitably only feasible in patients with appropriate anatomy. Another viable option includes using the pericardium to construct part or the entire cavopulmonary conduit.

Figure 1.8 Illustration of complete extracardiac Fontan procedure (Tam, Miller et al. 1999).

1.1.8 Fenestration

In either the lateral tunnel or extracardiac conduit method, a hole or "fenestration" is often made between the Fontan circuit and the right atrium so that if pressures become very high in the Fontan circuit, there is a "pop-off" into the heart (Figure 1.9). Patients with fenestrations may have a more stable post-operative course with smaller and less prolonged pleural effusions. Many fenestrations close spontaneously many months after surgery, but can also be closed during a cardiac catheterization procedure if deemed necessary. Surgical methods include baffles or adjustable ASDs for the lateral tunnel and shunts and punctures in the atrial wall for extracardiac Fontan procedures. Fenestrations can be closed temporarily by pursestring sutures and transcatheters or permanently by umbrella devices. The belief is that fenestration diminishes the dramatic effects of the Fontan circulation after cardiopulmonary bypass. Altered hemodynamics include increased pulmonary vascular resistance and decreased ventricular function (Thompson, Petrossian et al. 1999). Fenestration also reduces the RA pressure and thereby reduces arrhythmias. Centers that have routinely performed fenestrations report a decrease in postoperative hospital stay as well as fewer days required for chest tube drainage (Cetta, Feldt et al. 1996). Disadvantages of fenestration include increased patient risk, possible need for multiple procedures, and cost. Theory suggests that this right-to-left shunting will allow cardiac output to be maintained after the procedure. The expense is the mixing of blood and the lack of oxygenation. Also, the risk for morbidity, including embolism and complications as a result of oxygen desaturation, is greater. Lung collapse may occur or severe congestion of the SVC or IVC. Also, venous collaterals may develop between the two vascular beds (Bridges, Lock et al.

1990). The importance of fenestrations is still undetermined and further research needs to be performed. Recently, studies have found that fenestration after an extracardiac TCPC procedure is not necessary in most patients. Evaluation and fenestration decisions should be made after cardiopulmonary bypass at which time hemodynamics can be monitored (Thompson, Petrossian et al. 1999). The addition of a fenestration can be placed and revised easily without the use of bypass and with minimal intervention and risk in patients with an extracardiac TCPC. In practice, this technique seems to rely on surgeon preference and the severity of risk of the patient.

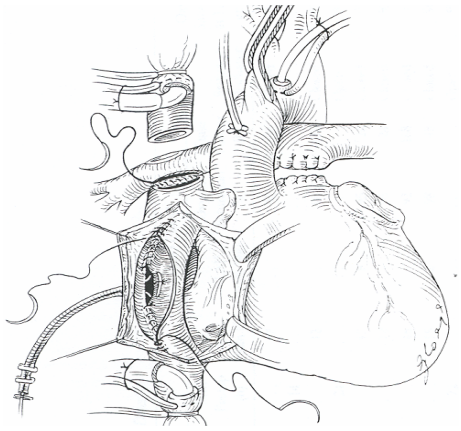

Fig. 1.9 Illustration of unidirectional TCPC tunnel with adjustable ASD. Fenestration provides communication between the tunnel and the left atrium (Laks, Pearl et al. 1991).

1.1.9 Patient Selection Criteria

Problems with patients not reaching an age sufficient to tolerate drastic surgical procedures and patients at high risk have led to further developments in the Fontan surgical pathway. Criteria for Fontan patients and classification of high-risk patients are continually debated. High-risk parameters that have been considered include: patient less than two years

of age, mean PA pressure greater than 20 mmHg, pulmonary vascular resistance greater than 3 Woods units, atrioventricular valve regurgitation, distortion and size (Nakata index) of the pulmonary artery, anomalous pulmonary venous return, and depressed ventricular function (Masuda, Kado et al. 1998), subaortic stenosis, a transpulmonary gradient greater than 15 mm Hg, and distortion of the pulmonary artery (Laks, Pearl et al. 1991). Only elevated pulmonary vascular resistance and depressed ventricular function seem to be agreed on by all. Most authors suggest that the mean PA pressure should be less than 18 mm Hg, ideally less than 15 mm Hg, and pulmonary vascular resistance less than 2 woods units. Studies have shown an association with early failure and high PA pressure, PA distortion, increased bypass time, ventricular hypertrophy, and significant pulmonary hypertension (Gentles, Mayer et al. 1997).

The debate about the ideal age to undergo a Fontan procedure is ongoing. The original selection criteria recommended that the child's age be greater than 4 years but less than 15 years. Most researchers now believe the ideal age is between 18 months and 6 years (Veldtman, Nishimoto et al. 2001). However, the extracardiac TCPC is thought to be low risk in adults because conduit growth is no longer a concern. If a patient is at high risk, an extracardiac TCPC with an adjustable ASD is usually performed (Gates, Laks et al. 1997).

1.1.10 Evolution of Staged Procedures

In order to increase survival rate, the Fontan procedure has evolved to take the form of staging the operations. Early results have proved beneficial for patient success rate as well as lower mortality and morbidity. In practice, two main staging procedures are most widely used: the Norwood procedure followed by Fontan completion and the bidirectional Glenn

shunt (BDG) followed by Fontan completion. Fontan completion means construction of either an intra-atrial (lateral) or an extracardiac conduit (by various methods) connecting the IVC to the PA.

A major factor in patient mortality is the dramatic decrease in cardiac output following a Fontan procedure. A complete Fontan procedure dramatically reduces the ventricular load resulting in changes in ventricular geometry and function. This decrease in cardiac output may be linked to the risk factors mentioned earlier. One of the most common congenital heart defects (CHD) is the hypoplastic left-heart syndrome, which occurs when the left ventricle and aorta are severely hypoplastic and unable to support systemic circulation. A procedure was investigated in which a shunt was placed between the proximal subclavian artery and the pulmonary arteries (Norwood and Jacobs 1993). The operation, termed “Norwood procedure”, also included an atrial sepectomy and reconstruction of the ascending aorta and aortic arch. Several experienced centers have reported survival rates for the Norwood procedure between 63% and 94%. An imbalance of pulmonary and systemic blood flow is the leading cause of morbidity and mortality following a Norwood procedure. Currently, a balance is achieved by manipulating the vascular resistance through medications. Decreasing the high mortality remains a challenging step following this procedure (Sano, Ishino et al. 2003). This stage would help reduce some of the ventricular volume load and minimize the effect of the complete Fontan procedure.

The second widely used staging procedure is the BDG. This connection consists of an end-to-side anastomosis of the SVC to the RPA and subsequent closure of the SVC to the RA. An important preoperative strategy is to perform an early BDG anastomosis to preserve ventricular function by relieving the volume load on the single ventricle physiology. Also,

the BDG provides a controlled source of low pressure pulmonary blood flow (McElhinney, Marianeschi et al. 1998; Petrossian, Reddy et al. 1999). Controversies exist concerning both the BDG and the Norwood procedures. Clinical data has proven that these procedures provide excellent early and midterm palliation. Furthermore, incidence of reoperation remains low. The use and role of additional accessory blood flow is being examined. The addition of a source of pulmonary blood flow either through a patent pulmonary valve or by means of a systemic to pulmonary artery (PA) shunt has been theorized as a means of preventing arteriovenous fistulas and stimulating overall PA growth. However, there is little published data to confirm this claim (McElhinney, Marianeschi et al. 1998). Researchers contend that accessory blood flow increases hospital stay and incidence of pleural effusions. The effect of the BDG on growth of the pulmonary arteries is also of concern. Reports show a decreased mean PA pressure and a significant decrease in PA diameter (Mendelsohn, Bove et al. 1994). This returns to the risk factors of Fontan operations stated previously and whether or not the BDG is an effective procedure.

Another major concern with staging procedures is the time between the first stage and the complete Fontan. During this time, blood flow from the SVC is obligated to the right lung. Therefore, the right lung does not contain hepatic venous blood. Investigators speculate that the absence of hepatic blood contributes to the development of pulmonary atriovenous malformations.

The Norwood procedure, which requires arrest at both stages, is used primarily in high-risk patients. Advantages of the BDG include simplification of the eventual complete Fontan and possible prevention of PA distortion after the PA shunts are in place. Furthermore, the BDG has been performed in increasingly younger patients. Studies have

shown that this procedure can be performed with low to moderate risk in patients as young as one to four months of age (Freedom, Nykanen et al. 1998). Most importantly, the increased survival rates allow the patients to develop physiologically to tolerate the complete Fontan.

Recently, modifications on staging procedures have been developed. A major cause of early death after the Norwood procedure is pulmonary overcirculation through a systemic to pulmonary shunt. A new procedure is being performed as a first stage palliation of HPLH syndrome. Sano and colleagues (Figure 1.10) have been placing a non-valved polytetrafluoroethylene (PTFE) shunt between the right ventricle (RV) and the PA in order to avoid the hemodynamic instability caused by a systemic to pulmonary shunt.

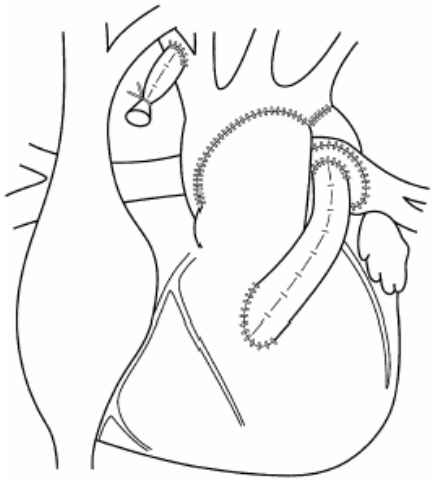

Figure 1.10 Diagram of RV-PA shunt and completion of first stage palliation for high risk patients and patients with HPLH syndrome (Sano, Ishino et al. 2003).

This procedure has produced results markedly different from the traditional Norwood procedure. The RV-PA shunt does not require postoperative management to control pulmonary vascular resistance and provides a stable systemic circulation as well as adequate

pulmonary blood flow. Postoperative management is virtually the same as any other neonatal operation protocol.

1.1.11 Fontan Paradox and Postoperative Complications

Complications, however, do exist. The RV-PA shunt has become obstructive over time, particularly three months after the surgery. Also, the decrease in oxygen saturation and increase in the pressure gradient across the shunt lead to further complications. PA growth is not as developed as with a systemic to pulmonary shunt. Moreover, the RV-PA shunt provides less pulmonary blood flow than a Norwood procedure. The resulting low PVR makes future staging procedures such as a BDG possible. This procedure should be used with low birth weight infants with HPLH syndrome (Sano, Ishino et al. 2003).

As illustrated, many modifications have been implemented since Fontan's original procedure. These modifications have been used to treat numerous CHDs including multiple ventricular septal defects, tricuspid atresia, hypoplastic heart syndrome, or double inlet ventricle. The main factors necessary for an excellent outcome include a well functioning single ventricle, low PVR, normal pulmonary artery physiology, and an unobstructed pathway from the systemic to pulmonary arteries with minimal energy loss (Geggel 1997). Advances in operative technique and postoperative management have been accompanied by an improvement in early survival from 75%-83% in the 1970s to over 90% today (Gentles, Mayer et al. 1997). However, the absence of a subpulmonary pump leads to an increase in central venous pressure, low cardiac output, and a non-pulsatile pulmonary blood flow. Small disturbances in ventricular or pulmonary vascular function, turbulence, and arrhythmias can lead to poor outcomes and either morbidity or mortality of the Fontan patient

(Eicken, Fratz et al. 2003). The modified Fontan circulation in any form has marginal hemodynamics and the greatest risk for failure and complications occurs during the postoperative period. Although management and procedures have improved, numerous complications result from a single ventricle circuit.

Normal circulations having optimal hemodynamics maintain a low caval pressure (less than 10 mm Hg) and a mean PA pressure of at least 15 mm Hg. Fontan circulations do not contain a pulmonary pump and therefore place the systemic circulation in series with the pulmonary circulation. The resulting caval hypertension and pulmonary hypotension creates a paradoxical situation, Figure 1.11, which is believed to be the underlying mechanisms for many complications following a Fontan procedure.

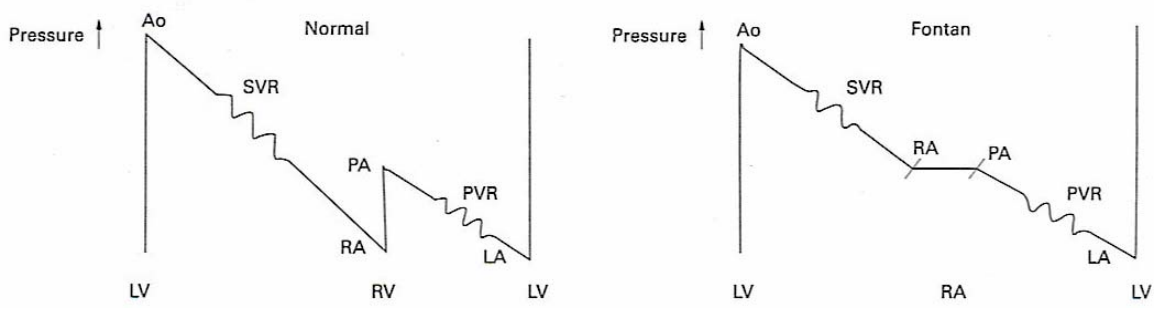

Figure 1.11 The Fontan paradox. Illustration of pressure relations showing normal and Fontan circulations. The absence of the right side of the heart places the systemic circulation in series with the pulmonary circulation creating caval hypertension and/or pulmonary hypotension (Bull 1998).

A successful modification of the classic extracardiac Fontan procedure was performed on a seventeen-year-old patient in Japan by Okano (Okano, Yamagishi et al. 2002). Okano et al are using a Y-shaped bifurcated graft. The cavopulmonary connection consists of one arm of the graft between the IVC and the LPA. The second arm connects the

IVC to the RPA. This modification may be useful in patients with severe MPA defects or when geometries will not allow an unbifurcated graft.

A recent innovative modification of the Fontan circulation has been performed in sheep by Rodefeld (Rodefeld, Boyd et al. 2003). Placement of axial flow pumps in the IVC and SVC percutaneously (Figure 1.12) is performed in order to assist cavopulmonary blood flow. Theoretically, the pumps will reverse the Fontan paradox of caval hypertension and pulmonary hypotension. Moreover, circulation hemodynamics resembling that of a two ventricle physiology are restored.

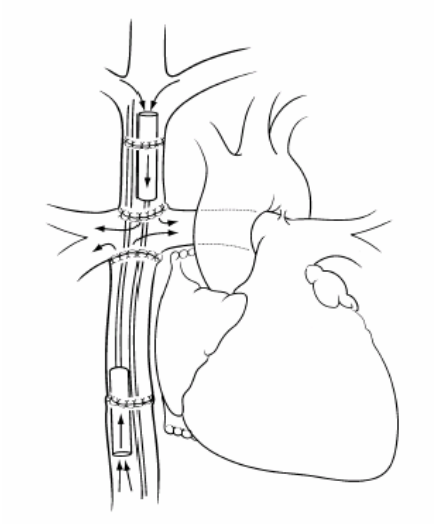

Figure 1.12 Illustration of total cavopulmonary connection with axial flow pumps placed in the inferior vena cava (IVC) and superior vena cava (SVC) to assist cavopulmonary flow (Rodefeld, Boyd et al. 2003).

Early results show great promise in the use of cavopulmonary assist devices. Hemodynamics remained stable for 1 hour and 6 hour durations postoperatively. Systemic venous pressure remained unchanged from normal control circulation conditions. Secondly, pulmonary arterial pressures were maintained in the vicinity of baseline measurements. Although this

study is in its preliminary stages and not currently feasible for clinical use, the use of mechanical or other cavopulmonary assist devices may be a future direction of the modified Fontan circulation. Riemer has also implemented an axial flow pump into a TCPC circuit in large sheep (Riemer et al 2005). The assist device is illustrated in Figure 1.14. Addition of an axial pump resulted in an increase in cardiac output and IVC flow. Furthermore, IVC, MPA, and LA pressures returned to normal values. These examples of flow pumps give direction to future studies in implantable blood flow assist devices for Fontan circulations.

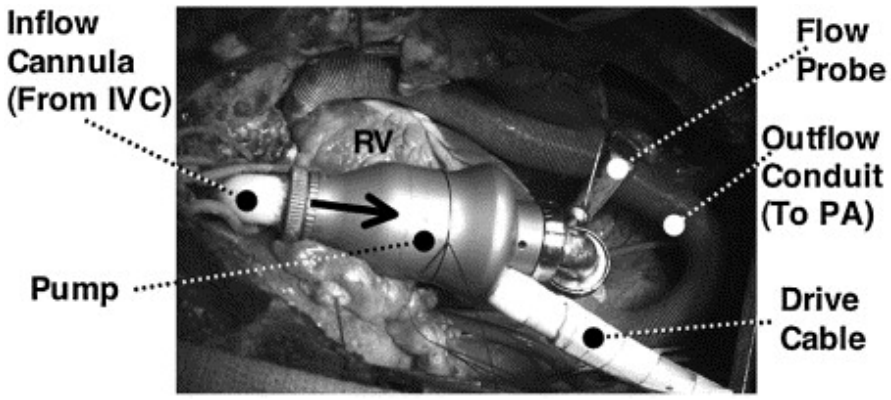

Figure 1.13 Photograph of TCPC ventricular assist device in a sheep. ***Arrow*** **indicates direction of blood flow through the pump.** ***RV*****, Right ventricle. (Riemer et al. 2005)**

A common complication of the Fontan procedure is the chronic elevation of RA pressure. RA pressure along with distortion are causes for supraventricular arrhythmias. In recent models, the lateral tunnel suture line has been shown to provide an electrophysiological substrate that will promote spontaneous atrial flutter. Recent advances such as the extracardiac TCPC that do not require extensive suture lines and bypass the RA completely have significantly lowered the incidence of arrhythmias and atrial flutter.

However, research has shown a prevalence of either arrhythmia or atrial flutter of up to 30% at 5 year follow up (Gandhi, Bromberg et al. 1997).

Another complication concerning Fontan physiology is that the volume burden of the functional single ventricle decreases. As a result, myocardial wall thickness increases, ejection fraction is reduced, hypertrophy occurs, and ventricle size may be reduced. This altered geometry contributes to a diminished cardiac output by affecting systolic and diastolic properties, compliance, passive filling, and the transpulmonary gradient. Another cause of altered ventricular function is a subaortic stenosis (Geggel 1997; Freedom 1998). Recent follow up studies show one-third of patients have a moderate or high reduction in ventricular function. Diuretics have become in increasingly prominent treatment of choice postoperatively (Veldtman, Nishimoto et al. 2001).

Normal pulmonary artery geometry is ideal for a Fontan candidate. Freedom and colleagues have shown that BDG procedures have resulted in a decrease in PA pressure and a decrease in cross-sectional PA area by as much as 32% (Freedom, Nykanen et al. 1998). The decreased area can have a detrimental effect on procedures performed in very young children in which PA growth is necessary.

Thromboembolism is a significant complication post-Fontan and is a major contributor to late morbidity and mortality. Thrombus formation may be related to numerous conditions such as venous stasis, turbulence, and low cardiac output. Thrombosis usually occurs in the right side of the Fontan circuit or the pulmonary arteries. Secondary thromboses can occur as a result of previous formations. Reports have shown that some degree of thrombus development was detected in 65% of patients within the first year after the procedure (Geggel 1997; Coon, Rychik et al. 2001). Prevalence of thrombosis does not

seem to be Fontan modification dependent, but relies on the altered hemodynamics and the Fontan paradox (caval hypertension and pulmonary hypotension).

Chronic conditions that produce high venous pressures and lymph production in the SVC and splanchnic territory are main contributors to a complication resulting from a Fontan circulation. Protein-losing enteropathy (PLE), which is the severe loss of serum proteins into the intestine, is one of the most dangerous complications. Symptoms include diarrhea, vomiting, edema, pleural effusions, and abdominal distention. Onset of PLE occurs approximately six months after the Fontan procedure. As a result, hypoalbuminaemia exists and once a certain level is reached, the cardiovascular physiology begins to fail due to the albumin role of providing oncotic pressure in capillaries (Lemes, Murphy et al. 1998). Studies illustrate that at least 40% of Fontan patients have a raised level of one or more liver enzymes, 25% have a depletion of coagulation factors, and 7% have low serum albumin levels (Bull 1998). Treatment for PLE consists of diuretics, serum albumin infusions, corticosteroid therapy, and a low fat diet. Recent publications have shown a marked decrease in the occurrence of PLE due to surgical management and postoperative treatment.

A dramatic increase in PVR following a modified Fontan procedure is a major cause for early mortality. Extended cardiopulmonary bypass times along with other hemodynamic factors contribute to the high PVR and result in hypoxemia and eventual pulmonary vasoconstriction. As a preventive measure, some clinicians use inhaled nitrous oxide (iNO). iNO is a pulmonary vasodilator in infants and children with CHD. iNO improves oxygenation and can reduce the transpulmonary gradient without a significant effect on systemic arterial pressure (Goldman, Delius et al. 1996).

1.11.2 Research Direction

Although the risk factors and possible complications are numerous, the Fontan procedure or one of its many modifications are a major step in improving the life and treatment of children born with CHD resulting in a univentricular heart. As shown, these procedures have significant morbidity, but without a better alternative, they are the only palliative procedure available today in lieu of a heart transplant. The need for further knowledge, refinements, patient databases, and clinical research is necessary in order to help these patients have an opportunity to live a normal life span with a reasonable quality of life. Today, more than 90% of Fontan patients perceived their state of health to be good and were able to participate in most daily activities. Cardiac medication is common and there is a need for further reinterventions in order to alleviate complications as the understanding of Fontan circulations increases (Gentles, Gauvreau et al. 1997).

These defects occur in one percent of all live births. As seen, factors such as the type of CHD, severity of the CHD, vascular geometry, hemodynamic parameters, age (anatomic and physiological development) of the patient, and postoperative complications are used to help determine if the patient meets Fontan procedure criteria and the modification used.

1.2 Problem Statement

Right heart bypass (Fontan) modifications, although progressive, need extensive additional research in order to establish novel surgical therapeutics, peri- and postoperative

management strategies, and procedural protocol in order to increase life expectancy and reduce attrition.

1.3 Hypothesis and Specific Aims

Hypothesis: Investigation of various Fontan modifications, not available via computer simulation or in vitro experimental protocol, through implementation of surgical designs in-vivo will help improve surgical design, operative therapeutics, pre, peri- and postoperative management strategies. Results will lead to new insights in reduction of operative complications.

Specific Aims: To support this hypothesis, the following specific aims were proposed:

(1) Investigate the effects of ventilation parameters on hemodynamics under normal and various Fontan modifications.
(2) Determine power losses of various Fontan circulations under varying physiological parameters.
(3) Determine time offsets regarding positive pressure ventilation (PPV) for implementation in an electrical computer simulation model.
(4) Determine feasibility and establish protocol at the University of North Carolina at Chapel Hill for geometry and velocity mapping via MRI.

1.4 Organization

This dissertation has been subdivided into individual chapters, each with an emphasis on a specific aim. Chapter 2 describes the universal methods used throughout the project. Surgical procedures are described and ventilation protocol outlined. Also included in Chapter 2 are the descriptions of software programs used to acquire, process, and analyze the animal data. Source code for database storage and visualization graphical user interface (GUI) programs are available in Appendix V and Appendix VI.

Chapter 3 focuses on Specific Aim 1: Investigate the effects of ventilation parameters on hemodynamics under normal and various Fontan modifications.

Chapter 4 focuses on Specific Aim 2: Determine power losses of various Fontan circulations under varying physiological parameters.

Chapter 5 focuses on Specific Aim 3: Determine time offsets regarding positive pressure ventilation (PPV) for implementation in an electrical computer simulation model.

Chapter 6 includes general discussion, conclusions, and future work of this research project.

Appendices I, II, and III are manuscript drafts that have been submitted to their appropriate journals.

Appendix IV focuses on Specific Aim 4: Determine feasibility and establish protocol at the University of North Carolina at Chapel Hill for geometry and velocity mapping via MRI.

As mentioned, Appendices V and VI are Matlab™ source code for GUI development instrumental in database organization and data observation and analysis.

Additional manuscripts are in progress that will describe in a more detailed and concise manner the overall findings of this dissertation. Additional research into the hemodynamic differences between inspiration and expiration is in progress and results will be submitted to their appropriate journals. The projected submission date for these manuscripts is August 2006.

CHAPTER II

METHODS

2.1 Animals Studies

In-vivo animal experiments were performed in lambs one to three months in age, ranging from 10.0 to 30.0 kilograms. Lambs in this weight range were chosen in order to closely approximate the anatomy and vessel geometries of children ranging from one month to three years old. All animals were cared for in accordance with the "Guide for the Care and Use of Laboratory Animals" (NIH Publication No. 86-23, revised 1985) and were in accordance with the standards of the Institutional Animal Care and Use Committee of the University of North Carolina at Chapel Hill.

2.2 Surgical Procedure

The animal was sedated using ketamine (30 mg/kg) intramuscularly and then administered isoflurane and oxygen throughout the procedure. Once sedated, the lamb was positioned on the table and its chest, right flank, thorax, and neck were shaved. Endotracheal intubation of the animal took place using an appropriately sized tube with a balloon and stilette. The tidal volume administered was 10 – 15 ml / kg without any positive end expiratory pressure or adjusted accordingly to maintain optimal arterial blood gas tensions. Measurements of respiration rate, carbon dioxide (CO_2) return, and pulse oximetry (placed on the tongue) were monitored. Next, a cut down on the internal jugular was performed and

a double lumen catheter was inserted. This allowed for intravenous fluid and pharmaceutical administration throughout the procedure. Once this was completed, the carotid artery was identified and a Millar Mikro-Tip Catheter (MPC-500, Millar Instruments, Houston, TX) pressure transducer was introduced (Figure 2.1). This transducer was positioned as close to the aortic arch as possible in order to record and observe arterial pressure (AOP). A mid-sternotomy was performed that started at approximately the sixth interspace. Exposure was from the superior azygous vein to the diaphragm. The superior vena cava (SVC) was cleared and the azygous vein, if present, was tied off. The same was done for the inferior vena cava (IVC). The aorta (AO) was then dissected and cleaned and the pulmonary arteries were exposed. The pericardium was opened and as much as possible was preserved in case a pericardial patch was needed during the operation. The ventilation protocol was administered and the control measurements were acquired. Once control data were collected, all pressure and flow transducers were removed except the arterial and air pressure monitors. Cardiopulmonary bypass was then performed using a bi-caval cannulation and arterial cannulation at the aortic arch. Once on bypass, one of the Fontan modification procedures was performed. Upon procedure completion, the animal was taken off bypass and the Fontan circulation was created. All pressure and flow transducers were inserted and the same ventilation protocol was performed. Arterial blood gases were closely monitored throughout the procedure and pharmaceutical adjustments were provided when needed. Blood gases were measured by an iSTAT analyzer (Abbott Laboratories, IL). Parameters monitored included hematocrit, hemoglobin, sodium, potassium, pH, PCO_2, PO_2, Calcium, O_2 saturation, bicarbonate, and base excess.

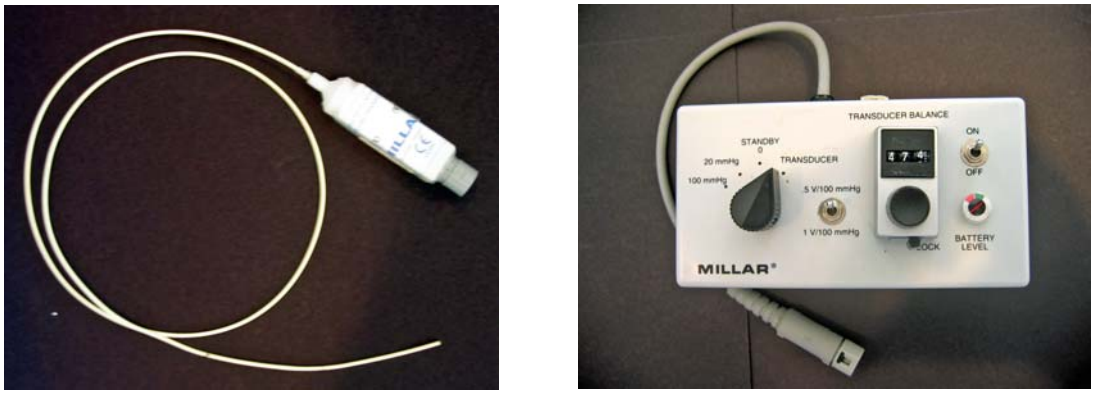

A **B**

Figure 2.1 Photographs of a Millar™ Mikro-Tip intravascular A) pressure transducer catheter and B) control box.

2.3 Data Acquisition

Before cardiopulmonary bypass and the Fontan modification procedure, multiple pressure and flow transducers were introduced. A Validyne pneumotachometer (Validyne Engineering, Northridge, CA) was introduced into the air circuit in order to monitor and record air flow. Also in the air circuit, a fluid filled polypropylene catheter was inserted and connected to a Statham P23Gb transducer (Statham Transducer P23Gb, Siemens) to measure airway pressure. Millar pressure transducers were placed in the aorta (AO), main pulmonary artery (MPA), SVC, IVC, right atria (RA), left atria (LA), and left ventricle (LV). To record blood flow, Transonic T206 Small Animal Blood Flow probes (Transonic Systems Inc., Ithaca, NY) were positioned around the LPA, MPA, SVC, IVC, and aorta (Figure 2.2).

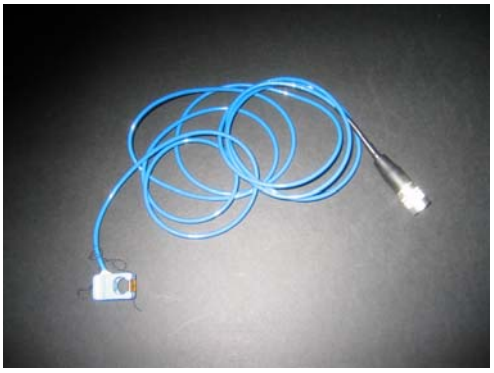

A **B**

Figure 2.2 Photographs of A) Transonic™ transit-time flow probe and B) Transonic™ T206 small animal flow control unit.

Conductive gel was placed between the vessel and transducer in order to improve the signal quality. Acquisition programs were developed using LabVIEW (National Instruments, Austin, TX). Data were recorded at a rate of 200 Hertz for individual episodes of 5.12 seconds or 1024 data points/episode. Illustrations of data acquisition schematics and graphical user interfaces (GUI) for calibration, monitoring, and acquisition are shown in Figure 2.3 and Figure 2.4.

A)

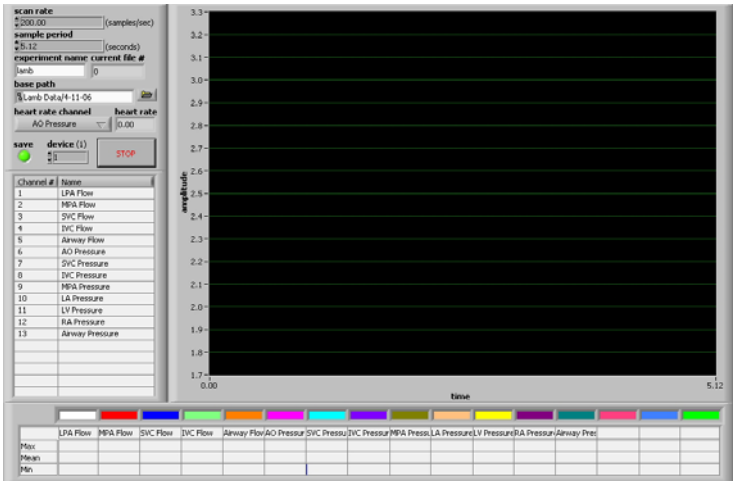

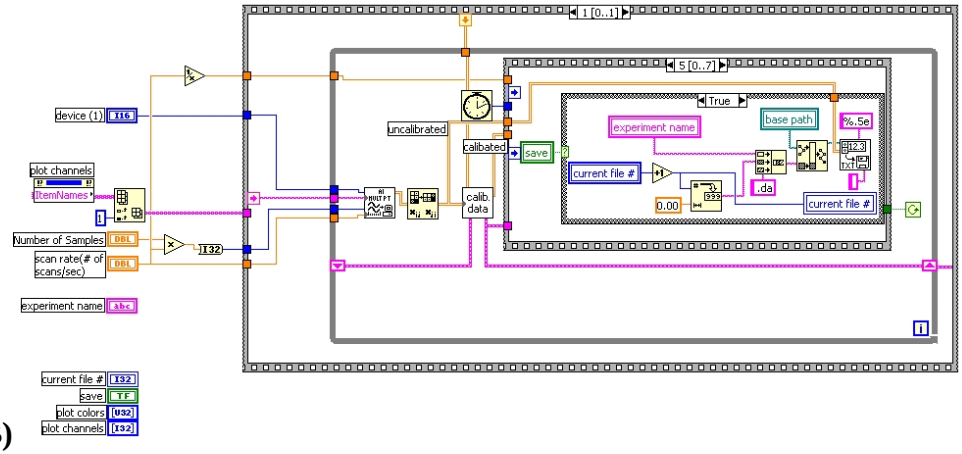

B)

Figure 2.3 Schematics showing A) hemodynamic data monitoring and acquisition GUI and B) program diagram example.

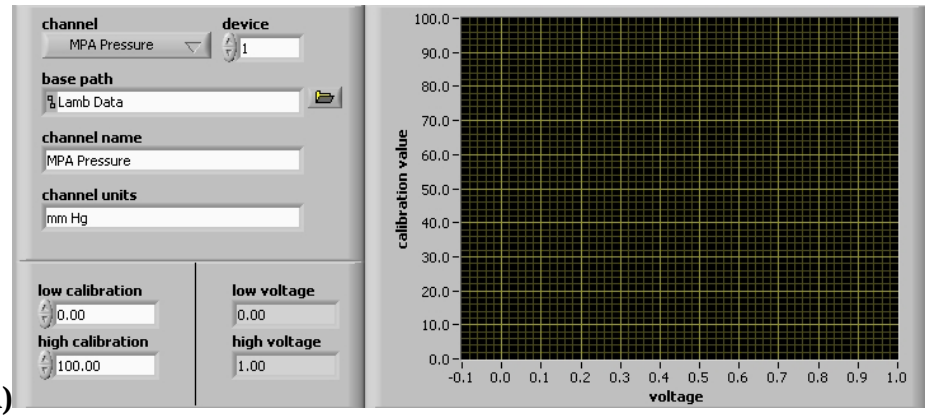

A)

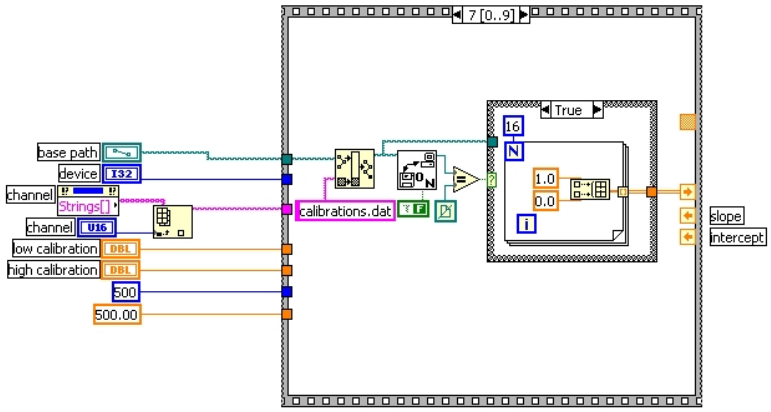

B)

Figure 2.4 Schematics showing A) hemodynamic data channel calibration GUI and B) program diagram example.

An acquisition cart was constructed that housed all equipment necessary to monitor and acquire the experimental data. This was required because the acquisition equipment had to be mobile due to experiments being performed away from the lab in an approved University of North Carolina animal surgical suite.

2.4 Ventilation Protocol

The ventilation protocol was administered under both normal and Fontan circulations. While maintaining a constant ventilation rate at 13 breaths/min, stroke volumes were varied in 100 mL intervals from 300 to 700 mL/breath. Next, while maintaining a constant stroke volume at 400 mL/breath, the ventilation rate was varied in 5 breaths/minute intervals from 8 to 23 breaths/minute. Furthermore, keeping air flow rate constant at 5200 mL/minute, all combinations of ventilatory rates (8,13,18, and 23 breaths/min) and stroke volumes (650, 400, 290, and 225 mL/breath) were performed. Multiple episodes of each parameter setting were recorded.

2.5 Surgical Procedures Investigated

Normal circulations as well as three modifications of the classical Fontan procedure were investigated and illustrated in Figure 2.5. The AP connection consisted of a graft connected to the RA appendage. The graft was connected to the MPA by an end-to-side anastomosis. The tricuspid valve was closed using a pursestring suture.

The TCPC connection: The IVC was transected and connected to the transected MPA via an end-to-end anastomosis. The SVC was subsequently attached to the RPA via an end-

to-side anastomosis. This connection used native vessels for the Fontan connection. No synthetic graft was used.

The TCPX connection: The IVC was connected to the extracardiac graft using an end-to-end anastomosis. The graft was then connected to the inferior side of the RPA via an end-to-side anastomosis. The SVC was attached to the superior side of the RPA by and end to side anastomosis.

The TCPY connection: The IVC was connected to the graft using an end-to-end anastomosis. The SVC was connected to the graft using an end-to-side anastomosis. The MPA was attached to the graft using an end-to-end anastomosis.

The AP connection incorporated the RA into the Fontan circulation whereas the TCPC, TCPX, and TCPY bypassed the right heart completely. In all connections, an atrial septectomy was performed to allow perfusion.

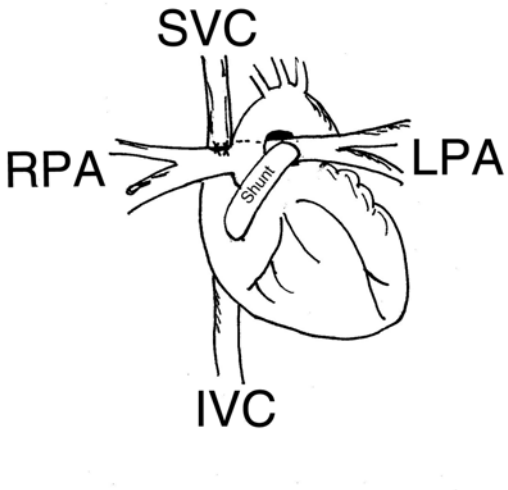

A) Atriopulmonary connection (AP).

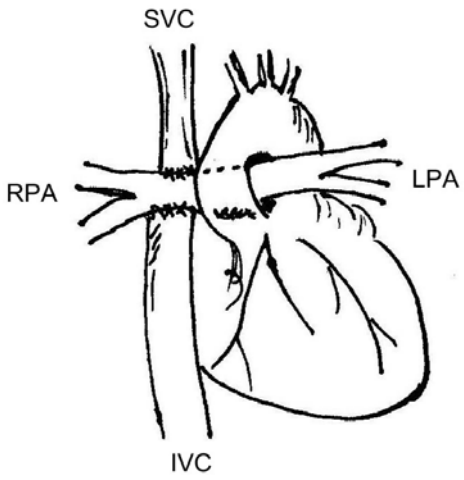

B) Schematic of total cavopulmonary connection without use of synthetic graft (TCPC).

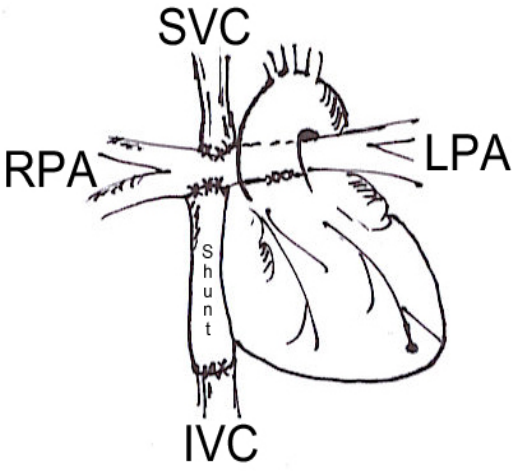

C) Schematic of total cavopulmonary connection with extracardiac graft (TCPX).

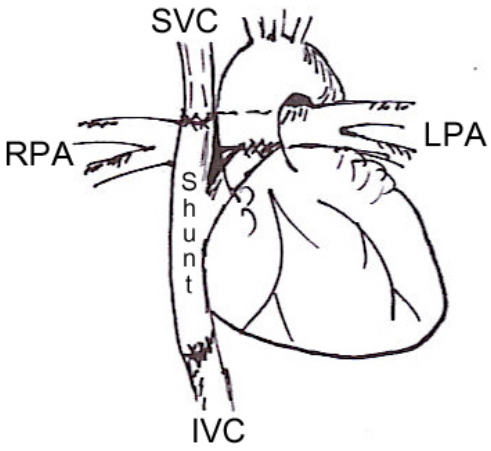

D) Schematic of modified total cavopulmonary connection (TCPY).

Figure 2.5 Schematic drawings of the A) AP, B) TCPC, C) TCPX, and D) TCPY Fontan modifications.

To date, we have had eleven successful AP procedures, four successful TCPC procedures, four successful TCPX procedures, and six successful TCPY procedures. Normal lamb anatomy with pressure and flow transducers inserted is pictured in Figure 2.7.

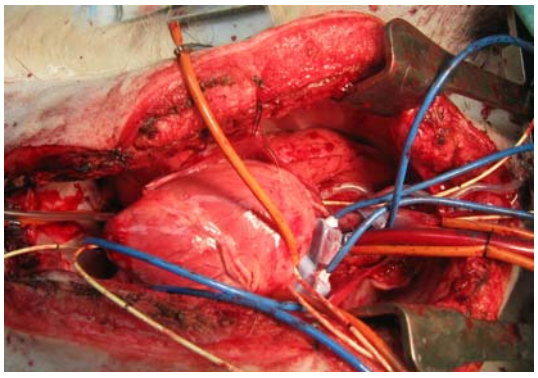

Figure 2.6 Photograph of in-vivo normal anatomy of a lamb with pressure and flow transducers inserted.

As stated, the ventilation protocol was performed for the normal circulation in order to acquire baseline measurements for comparison. Once acquired, one of the Fontan modification procedures was performed. An illustration of an AP connection in a lamb is shown in Figure 2.7.

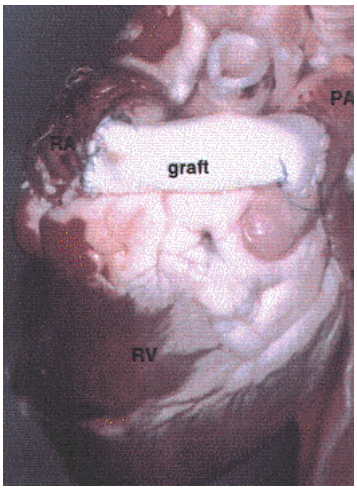

Figure 2.7 Photograph of atriopulmonary (AP) anatomy created in a lamb. A graft was used to connect the right atrial (RA) appendage to the main pulmonary artery (PA). A suture was placed around the tricuspid valve to separate the right ventricle (RV) from the circulation.

A novel procedure examined in this study was the TCPY. This allowed for a better connection due to the short branching right pulmonary arteries. Figure 2.8 illustrates a completed TCPY connection in a lamb. A closer examination of the anastomoses is pictured in Figure 2.9.

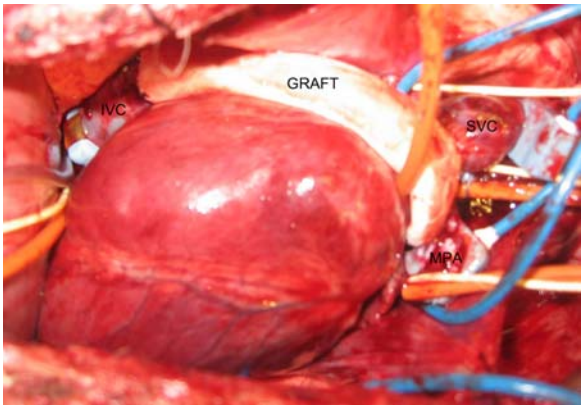

Figure 2.8 Photograph of total cavopulmonary connection (TCPY) anatomy created in a lamb. Vessels of interest labeled include the inferior vena cava (IVC), superior vena cava (SVC), and main pulmonary artery (MPA).

A)

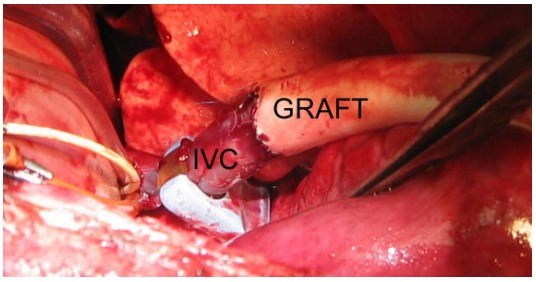

B)

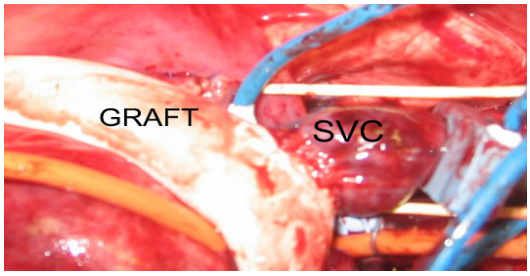

C) 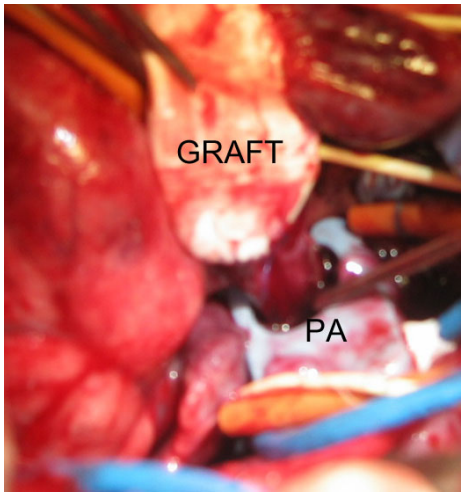

Figure 2.9 Close-up inspections of the A) inferior vena cava (IVC) B) superior vena cava (SVC) and C) pulmonary artery (PA) anastamoses in a total cavopulmonary connection (TCPY) performed in a lamb.

Cardiopulmonary bypass times averaged approximately 90 minutes. Bypass pump rates were set at approximately one-third of normal cardiac output to maintain proper perfusion. Central venous pressure was monitored in order to assess and maintain blood volume while on bypass. Steroids were given prior to going on bypass. Blood gases were taken approximately every five minutes to control hemodynamic stability. Ventilation of the lungs was performed occasionally while on bypass in order to prevent fluid buildup in the lungs. Additional blood from a donor animal was heated to 37 degrees Celsius and then hemoconcentrated using an Minimax Plus (Medtronic Inc., Minneapolis MN) oxygenator system. Surviving lambs were euthanized with a lethal dose of concentrated potassium.

2.6 Data Analysis GUI Development

To date, forty-eight lamb studies have been completed. With each study, multiple episodes of data were acquired and stored. Data files were transferred from the experimental

cart to a workstation. Data were then converted from voltage readings to pressure and flow units using the calibration measurements in a Matlab™ (The Mathworks Inc., Natick, MA) subroutine. Large quantities of data under multiple experiments required the development of a standardized database and file allocation system. The database enabled multiple programs access to a universally formatted storage system. In the process, multiple GUIs were developed.

2.6.1 Data Structure Development

Data were stored in a structure containing experiment information. A GUI was constructed for entering the experiment name, date, Fontan connection procedure, weight, and sex. Additionally, the number of data episodes, beginning episode, maximum number of episodes, and the episode in which the Fontan connection begins were entered. The number of data channels acquired was also needed in order to set up an array containing the channel number for each hemodynamic variable measured. The initial GUI panel is shown in Figure 2.10. A message board and help files were implemented in order to facilitate use.

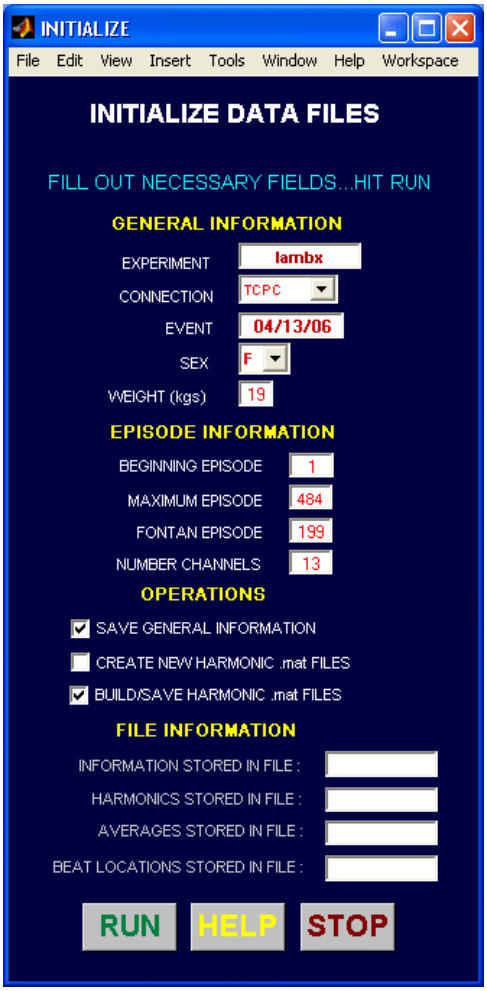

Figure 2.10 Matlab™ developed GUI panel for entry and creation of data structure of initial experimental data information. All operations were performed using text entry, pull-down menus, and control buttons.

2.6.2 Channel Array GUI

Execution of the "INITIALIZE DATA FILES" GUI created of an array for channel number storage. This GUI enabled the user to specify from a pull-down menu the hemodynamic variable measured. If the same channel was used throughout the experiment, the radio button labeled "All" was depressed. Next, a pull-down menu for channels numbered 1-16 was used to select the appropriate channel. If a channel was changed during the experiment due to transducer malfunction, surgeon preference, or surgical complications,

the beginning and ending episodes were entered into bracketed text boxes for each channel. Subsequently, the first and second channel numbers were selected from pull-down menus. Figure 2.11 shows an example using the airway flow (AIRQ) hemodynamic parameter being measured on channel 5 from episodes 1 to 199 and then measured on channel 14 from episodes 200 to 486. All other hemodynamic parameters are shown using the same channel throughout the experiment. Once completed, the "Finished" button, which calls subroutines to store the channel information in an array as well as include the array in the data structure, was "pressed". This concludes the storage of general information for each experiment.

Figure 2.11 Channel specification GUI developed for channel number array creation. An example using multiple channels for airway flow (AIRQ) is illustrated. Pull-down menus allow for hemodynamic variable and channel number selection. Text boxes create array indices.

2.6.3 Bad Data File Elimination

Once the information and channel arrays were stored into a data structure, data analysis followed. A subroutine first loads each data file to check for errors. If the file did not contain enough points, was corrupted, or if the user specifies that it contained bad data, the episode number was stored into an array. Once identified, bad files were omitted from any future data processing and analysis.

2.6.4 Average Beat Determination

Data processing began by loading each episode of 1024 points sampled at 200 Hertz (Hz). The arterial pressure (AOP) was used as the standard for the heartbeat. The mean was removed and a fast Fourier transform (FFT) of the data padded with zeros to improve resolution was performed. From the FFT, the number of beats per episode was determined. Also, the number of data points per beat was determined.

Next, a differential filter was applied to determine starting locations of subsequent heartbeats. The peaks provided index locations for dividing the data episode into individual heartbeats. The subroutine cycled through the episode returning individual beats for all hemodynamic parameters. A time based average of all the beats was then calculated. This process is illustrated in Figure 2.12. Furthermore, averages for all channels for each episode were calculated and stored in a separate file within the data structure.

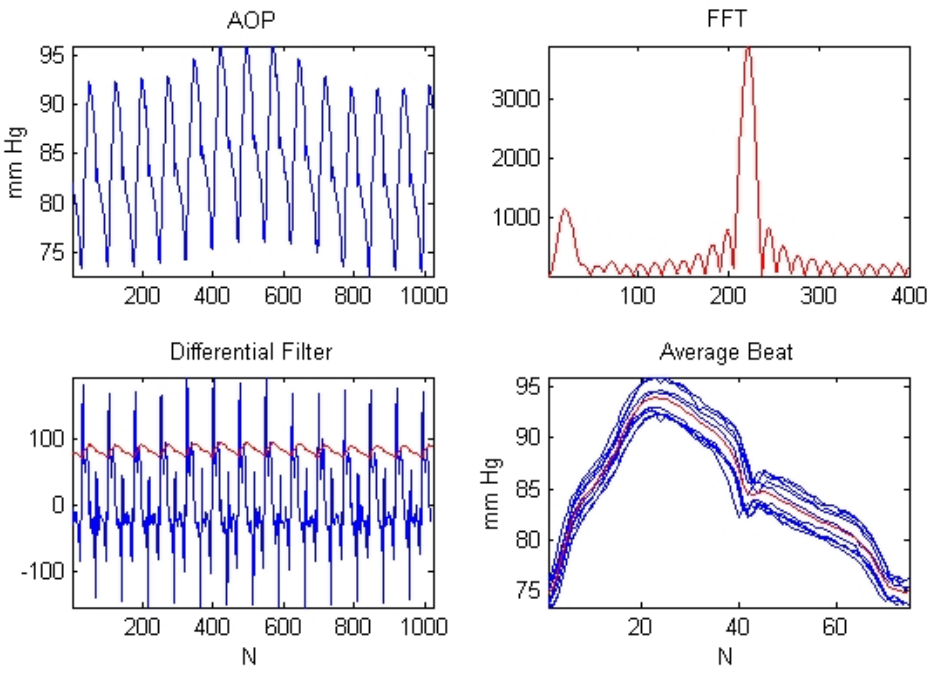

Figure 2.12 Matlab GUI window showing a) arterial pressure (AOP) b) fast Fourier transform (FFT) of arterial pressure (AOP) with mean subtracted c) AOP (red) and differential filter (blue) and d) individual beats (blue) with average beat (red).

2.6.5 .mat File of Average Beat

Once the average beat was calculated for each hemodynamic variable, an FFT was performed. For reconstruction purposes, the mean and first twenty harmonics were stored in .mat files. Each .mat file contained average information for all channels and fifty episodes. This allows quick access and analysis to be performed. A file containing starting beat locations for each episode was also stored within the data structure.

2.7 Hemodynamic Examination GUI

For close examination of individual hemodynamic variables or to compare variables, a data observation GUI was developed. The main menu gave options of viewing one, two, or multiple channels. The user was given the choice to either view the episode in its entirety or to view the average beat of an episode. Text boxes allowed for labeling of the graph title and x and y axes for each graph. Another plot option was to make an .avi movie file from multiple data files to show waveform transitions. Figure 2.13 shows the main plot menu in addition to one and two channel GUI options.

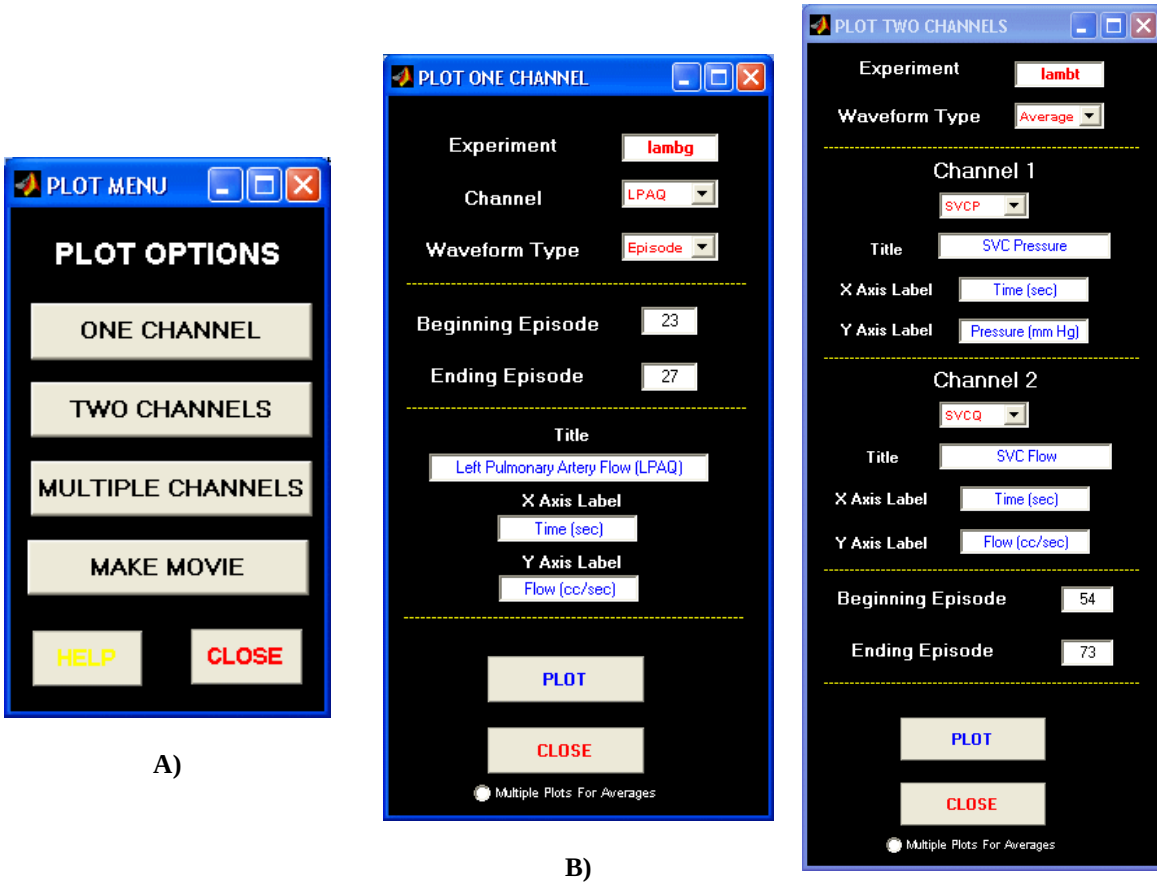

Figure 2.13 Matlab GUI for hemodynamic examination. A) Main GUI menu B) GUI for examination of one variable and C) GUI for examination of two variables.

Figure 2.14 illustrates multiple channels plotted along with its associated graph.

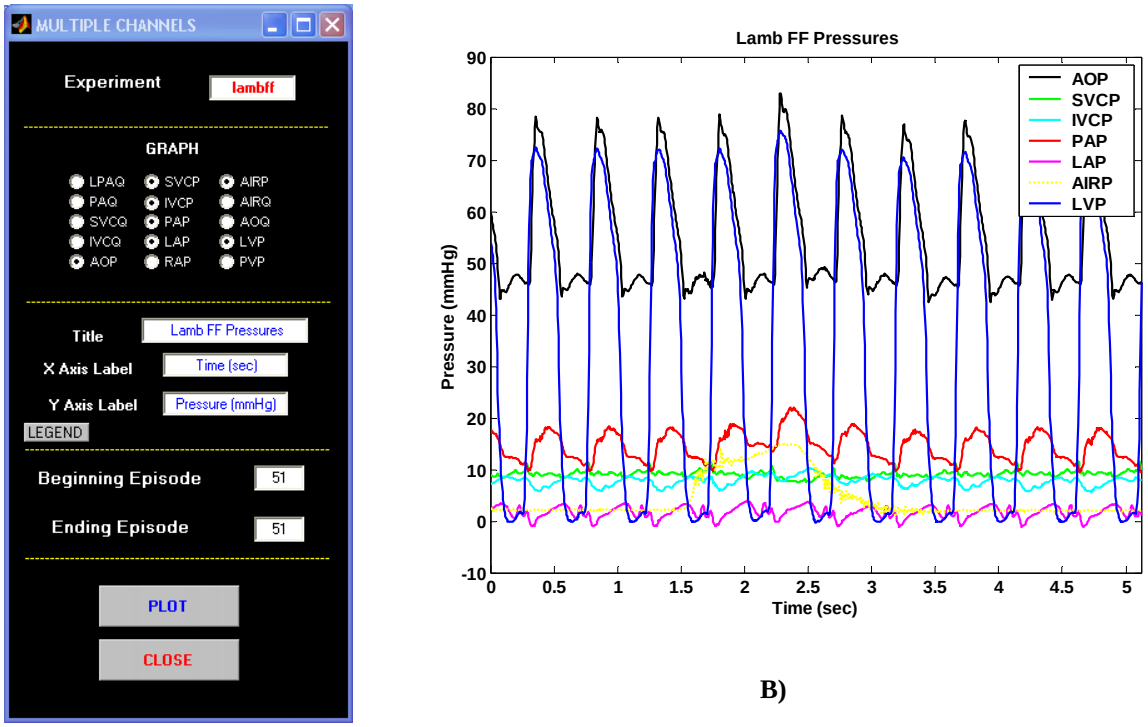

Figure 2.14 Matlab GUI display for multiple channel examination as well as its calculated graph. For illustrative purposes, A) the GUI menu and B) graph showing pressures for experiment are displayed.

The program source codes as well as callback subroutines for the INITIALIZE DATA FILE GUI are provided in Appendix V. Source code and subroutines for the DATA EXAMINATION GUI are located in Appendix VI. Additional GUIs have been developed for data analysis and postprocessing in Chapters 3 through 5. Their source code has not been included because the GUI was focused on the specific aim and not on general hemodynamic and data analysis.

2.8 Section Methodology

The methodology presented above is universal and used throughout this dissertation. Additional methods focused on individual specific aims are presented in their appropriate chapters. Ventilation protocol and surgical procedures will be referred to throughout the text.

CHAPTER III

IN-VIVO HEMODYNAMIC ANALYSIS

3.1 Abstract

Background. Respiration manipulations and management are vital for infants with a univentricular heart. Positive pressure ventilation (PPV) has been shown to have a deleterious effect on blood flow in patients with a univentricular physiology. Postoperative length of stay in the intensive care unit is predominantly determined by need for mechanical ventilation and respiratory insufficiency. With a passive pulmonary physiology and with the pulmonary and systemic circulations now connected in series, keeping the pulmonary vascular resistance (PVR) and systemic vascular resistance (SVR) as low as possible is vital. However, endotracheal intubation and PPV promote increased PVR. Management is dependent on adequate ventilation. To date, management strategies are decided by individual institutions. This study examines the effect of positive pressure ventilation (PPV) on hemodynamic parameters in normal and Fontan circulations. The overall hypothesis for this research is that a fundamental understanding of the AP and various TCPC geometries will lead to improved surgical planning and designs and thus the potential for improved long term outcomes in patients. In order to address this hypothesis, investigation will occur for the following specific aims: (1) Qualitative and quantitative assessment of Fontan flow dynamics for different AP and TCPC anatomic geometries and physiological conditions through in-

vivo animal studies performed in lambs. (2) Examine the effect of PPV on hemodynamic variables both in normal and Fontan circulations.

Methods. In-vivo experiments were performed in lambs. Normal and four Fontan modification procedures have been examined. These are the atriopulmonary connection (AP), total cavopulmonary connection without a synthetic graft (TCPC), extracardiac total cavopulmonary connection (TCPX), and the total cavopulmonary connection using a Y-shaped graft (TCPY). Multiple pressure and flow transducers were introduced. Ventilation manipulation varying ventilation rate, stroke volume, and minute ventilation was performed under both normal and Fontan circulations. Data were recorded at 200 Hertz. Data analysis was performed using MATLAB^{TM}. Hemodynamic changes and systemic and vascular resistances were calculated.

Results. AP. A reduction in cardiac output (CO) amounting to 63% was observed between normal and AP conditions. SVR increased by 54% and PVR increased 137% between circulations. SVR increased significantly as respiration rate increased. No significant changes occurred in pressure and flows with varying ventilation rate. Also, no significant changes occurred with varying stroke volume. SVR showed a decreasing trend as stroke volume increased. No significant changes occurred in IVCQ, SVCQ, and PAQ with varying minute ventilation. Vascular resistances remained statistically unchanged with varying minute ventilation. TCPC. CO decreased by 61% between normal and TCPC circulations. PVR increased by 136% to 736.2±54.1 dyne•sec•cm-5. Respiration rate had little effect on hemodynamic variables. Statistically significant decreases in pressure occurred for all parameters as stroke volume increased. Extremely low and high stroke volumes decreased the flow by 47% from middle range stroke volumes. Stroke volume had no significant

difference on LPAQ or SVCQ. No significant changes occurred in vascular resistance with changing stroke volumes. Pressure waveforms showed minimal change throughout the constant minute ventilation range. TCPX. Normal flow contributions, IVC (74%), SVC (26%), and LPA (41%), are present in the TCPX circulation [IVC (72.4%), SVC (27.6%), and LPA (48.4%)]. Extremely high vascular resistances were created. The SVR was 4579.8±1603.5 dyne•sec•cm-5 and the PVR was 45.8±16.8 dyne•sec•cm-5. A 68% decrease in CO from 32.0±2.5 cc/sec under normal circulation to 10.2±5.4 cc/sec under TCPX circulations were a result of the high resistances. Mean pressures for the IVC, SVC, and PA were 25.2±5.3 mm Hg, 24.0±4.6 mm Hg, and 28.9±4.3 mm Hg respectively. No significant effects were observed with varying respiration rate. CO showed a decreasing trend as rate increased. SVR decreased when high rates were imposed. Significant increases in pressure occurred at low stroke volumes (300-400 mL). No changes were seen in SVR across varying stroke volumes. TCPY. PVR increased 26% from 543.8±303.6 dyne•sec•cm-5 to 688.5±267.8 dyne•sec•cm-5. SVR increased 4% from 27.3±3.7 dyne•sec•cm-5 to 26.1±17.6 dyne•sec•cm-5. Flow contributions remained similar, with LPA flow comprising of 39% of the flow under normal conditions to 32% in TCPY conditions. IVC flow was 79% of systemic flow under normal circulation to 78% in the TCPY circulation. Cardiac output decreased 51% between circulations. All pressures increased significantly with increasing respiratory rates keeping stroke volume constant. However, IVC flow increased as respiration increased. Furthermore, SVC and LPA flows significantly increased at a lower rate as respiration increased. PVR increased with respiration rate. At low stroke volumes, SVR decreased sharply as rate increased. PVR significantly increased as stroke volume

increased at various rates. SVR decreased as volume increased for low rates and increased as stroke volume increased for high rates.

Conclusions. Significant hemodynamic changes occurred between anatomic Fontan connections. Systemic and vascular resistances differed according to procedure. Overall, stroke volume and ventilation rate had a predominantly instantaneous effect on hemodynamics, but minimal effects on averages. Promising hemodynamics were observed in the novel TCPY procedure. Flow ratios, flow distribution, and resistances approached normal circulation values for the TCPY circulation. However, systemic pressures remained high that may lead to postoperative complications. To improve recovery time and perfusion efficiency, ventilation management may be beneficial if prescribed dependent on Fontan procedure. Limitations to this study are the acute, open chest study performed on an animal with previously normal circulation. Hemodynamic adaptations are not available.

3.2 Introduction

Approximately two out of every thousand children in the United States are born with congenital heart defects that impair the right heart and atriopulmonary pathway. As a result, there is only a single effective ventricle. Surgical treatment for these defects, termed "Fontan" repairs, consist of bypassing the right side of the heart and connecting the systemic and pulmonary circulations in series with the univentricular pump. However, these surgical repairs are palliative, not curative. Cardiologists report that patient populations with these defects comprise 20% of their caseload and at least 50% of their time. Surgical repairs severely alter the systemic and pulmonary hemodynamics. Also, the creation of a low-pressure system further leads to numerous postoperative complications (e.g. venous

hypertension, liver failure, and/or pulmonary hypotension) requiring lifelong, intensive medical attention. Standardization of repair designs that are specific for different anatomical and physiological variations has not been developed. Therefore, it is necessary to optimize the surgical pathway as well as develop pre-, peri-, and postoperative management methods to understand the precise hemodynamic changes following implementation of the Fontan circulation. The surgical design will always be the starting point of functional outcome studies. In order to develop adequate surgical therapeutics and peri- and postoperative management strategies, a study of the acute changes from normal to various Fontan anatomies and the resulting changes in hemodynamic variables produced by the new circulation is necessary.

3.3 Problem Statement

Respiration manipulations and management are vital for infants with a univentricular heart. Positive pressure ventilation (PPV) has been shown to have a deleterious effect on blood flow in patients with a univentricular physiology. (Lofland, 2001). Postoperative length of stay in the intensive care unit is predominantly determined by need for mechanical ventilation and respiratory insufficiency. With a passive pulmonary physiology and with the pulmonary and systemic circulations now connected in series, keeping the pulmonary vascular resistance (PVR) and systemic vascular resistance (SVR) as low as possible is vital. However, endotracheal intubation and PPV promote increased PVR. Management is dependent on adequate ventilation. To date, management strategies are decided by individual institutions. This study examines the effect of positive pressure ventilation (PPV) on hemodynamic parameters in normal and Fontan circulations.

Furthermore, in-vitro models and computer simulations depend on input parameters and boundary conditions such as instantaneous pressures and flows, flow ratios, vascular resistances, and respiration that are obtained by in-vivo examination not available in humans. Also, respiration is usually not taken into consideration in present magnetic resonance studies due to respiratory and cardiac gating.

3.4 Specific Aims

The overall hypothesis for this research is that a fundamental understanding of the AP and various TCPC geometries will lead to improved surgical planning and designs and thus improve long term outcomes in patients. In order to address this hypothesis, investigations will address the following specific aims:

1) Qualitative and quantitative assessment of Fontan flow dynamics for different AP and TCPC anatomic geometries and physiological conditions through in-vivo animal studies performed in lambs.
2) Examination of the effect of PPV on hemodynamic variables in normal and Fontan circulations.

3.5 Data and Statistical Analysis

Data analysis was performed using MATLAB^{TM} (The Mathworks Inc., Natick, MA). All values were expressed as mean ± SD. Univariate and repeated measures analysis of variance were used to determine statistical significance. A p-value < 0.05 was regarded as significant. The post hoc Bonferroni test was used in order to compensate for type I error

with multiple comparisons and the Tukey honestly significant difference test was used for multiple comparison tests across experimental groups.

For percent change calculations, reference parameters used were minimum parameter settings: rate of 8 breaths/min, a stroke volume of 400 mL, and a constant minute ventilation combination of 8 breaths/min and 650 mL stroke volume (see ventilation protocol section in Chapter 2 for more detail).

3.6 Vascular Resistance Calculations

Systemic vascular resistance and pulmonary vascular resistance were calculated.

For normal and AP connections,

$$SVR\ (dyne \bullet \sec \bullet cm^{-5}) = 80 * \frac{(\overline{AOP} - \overline{RAP})mmHg}{CO\ (L * \min^{-1})}$$

where AOP is mean arterial pressure, RAP is mean right atrial pressure and CO is mean cardiac output.

For TCPC, TCPX, and TCPY connections, SVR was calculated by:

$$SVR\ (dyne \bullet \sec \bullet cm^{-5}) = 80 * \frac{(\overline{AOP} - \overline{PAP})mmHg}{CO\ (L * \min^{-1})}$$

$$SVR\ (HRU) = \frac{(\overline{AOP} - \overline{PAP})mmHg}{CO\ (L * \min^{-1})}$$

where PAP is mean pulmonary artery pressure. Pulmonary artery pressure was used because the right atria was eliminated from the circulation. Pulmonary vascular resistance was calculated by:

$$PVR\ (dyne \bullet \sec \bullet cm^{-5}) = 80 * \frac{(\overline{PAP} - \overline{LAP})mmHg}{CO\ (L * \min^{-1})}$$

$$PVR\,(HRU) = \frac{\overline{(PAP} - \overline{LAP)}mmHg}{CO\,(L * \min^{-1})}$$

HRU represents the commonly used in practice Hybrid Resistance Units or Wood Units.

3.7 Normal Circulation

For comparison purposes, normal circulation baseline measurements were acquired. This allowed for examination of the changes between normal and different modified Fontan connections. In order to normalize between lamb studies, control data were only analyzed with its associated Fontan modification and not used for comparison across Fontan connections. Also, percent changes were calculated in order to normalize between lambs of different size and weight and summarize hemodynamic variable transitions between ventilation parameters. Multiple episodes were acquired and averaged to minimize outliers. Figure 3.1 illustrates normal circulation data for the IVC over the ventilation protocol settings. Changes in pressures and flows were observed during ventilation cycles. In order to concisely present the data, control data will be presented along with its appropriate Fontan connection.

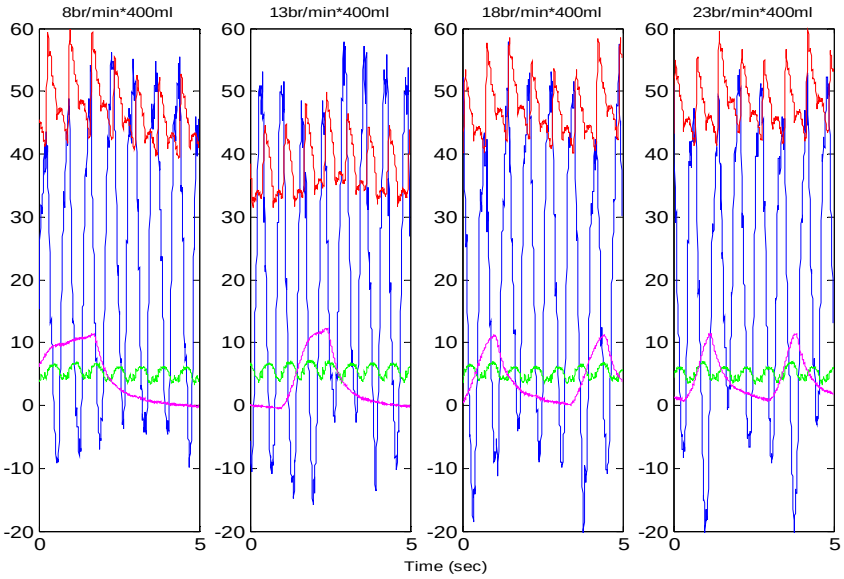
8br/min*400ml
13br/min*400ml
18br/min*400ml
23br/min*400ml
Time (sec)

A

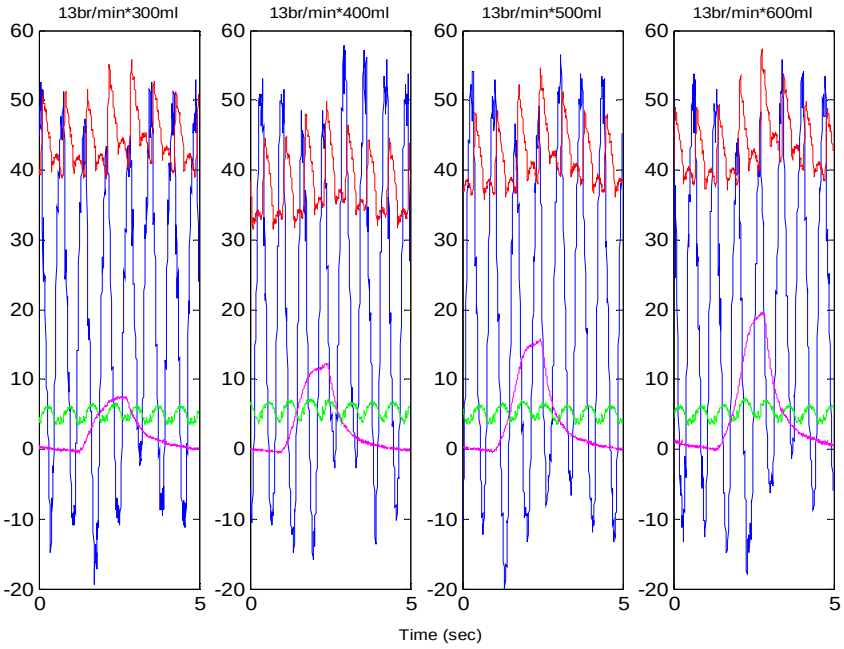
13br/min*300ml
13br/min*400ml
13br/min*500ml
13br/min*600ml
Time (sec)

B

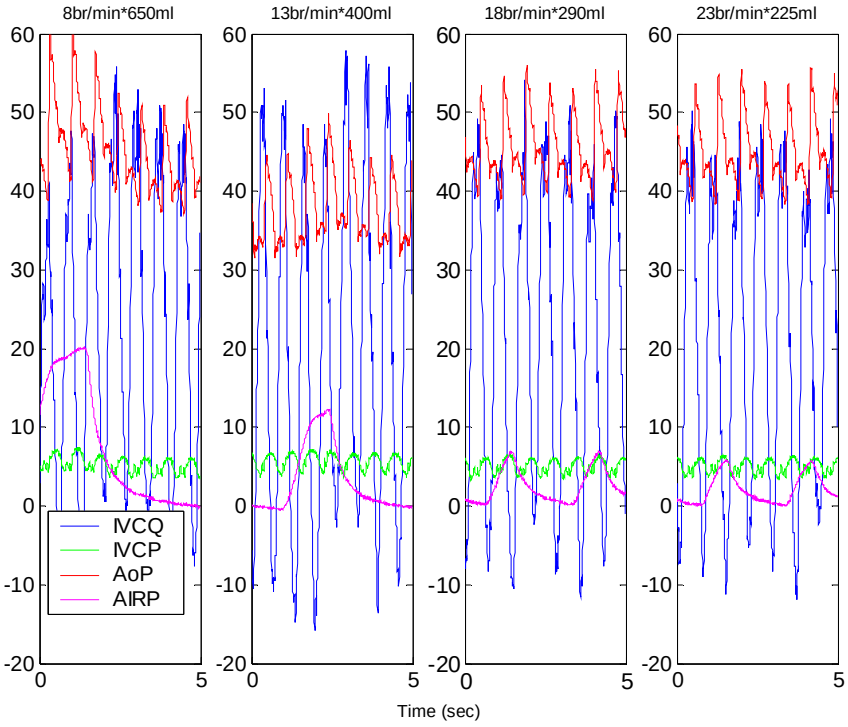

C

Figure 3.1 A representative example of ventilation protocol under normal circulation. Inferior vena cava flow (IVCQ), pressure (IVCP), arterial pressure (AOP), and airway pressure (AIRP) at A) various stroke volumes keeping ventilation rate constant at 13 breaths/min B) varying ventilation rates keeping stroke volume constant and B) combinations of rate and stroke volume keeping minute ventilation constant.

3.8 AP Connection Results

3.8.1 Waveform Analysis for AP Connection

The AP connection is unique in that transitions from normal to Fontan circulation are possible within the animal study. To transition from normal to the Fontan circulation, the RA to PA shunt was unclamped with subsequent closure of the pursestring suture around the

tricuspid valve to eliminate the right ventricle. Waveform transitions were examined between the two circulations. Figures 3.2, 3.3, and 3.4 illustrate changes in systemic and pulmonary circulations between normal and AP conditions. Table 3.1 summarizes overall hemodynamic changes between circulations.

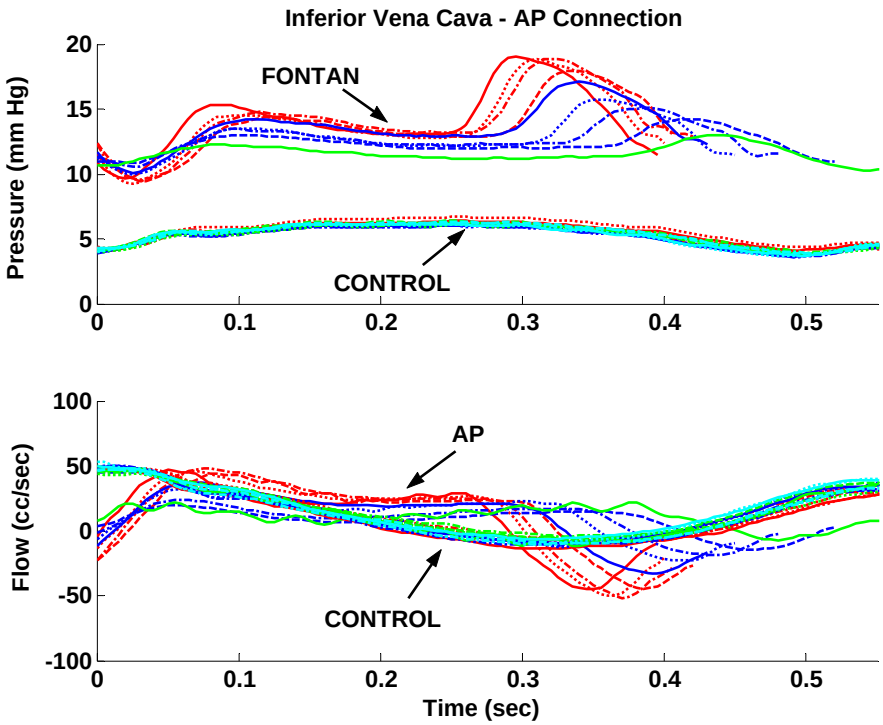

Figure 3.2 Multiple average beats of pressure and flow waveform transitions of the inferior vena cava (IVC) between normal and atriopulmonary (AP) circulations.

As illustrated in Figure 3.2, eliminating the right ventricle and thus increasing the vascular resistance increased the backflow of the IVC. IVC flow decreased significantly from 23.3 ± 6.3cc/sec in normal circulation to 7.7 ± 4.1cc/sec under AP conditions. With increased resistance, IVC pressures increased from 8.1 ± 6.3 mm Hg to 19.6 ± 5.4 mm Hg.

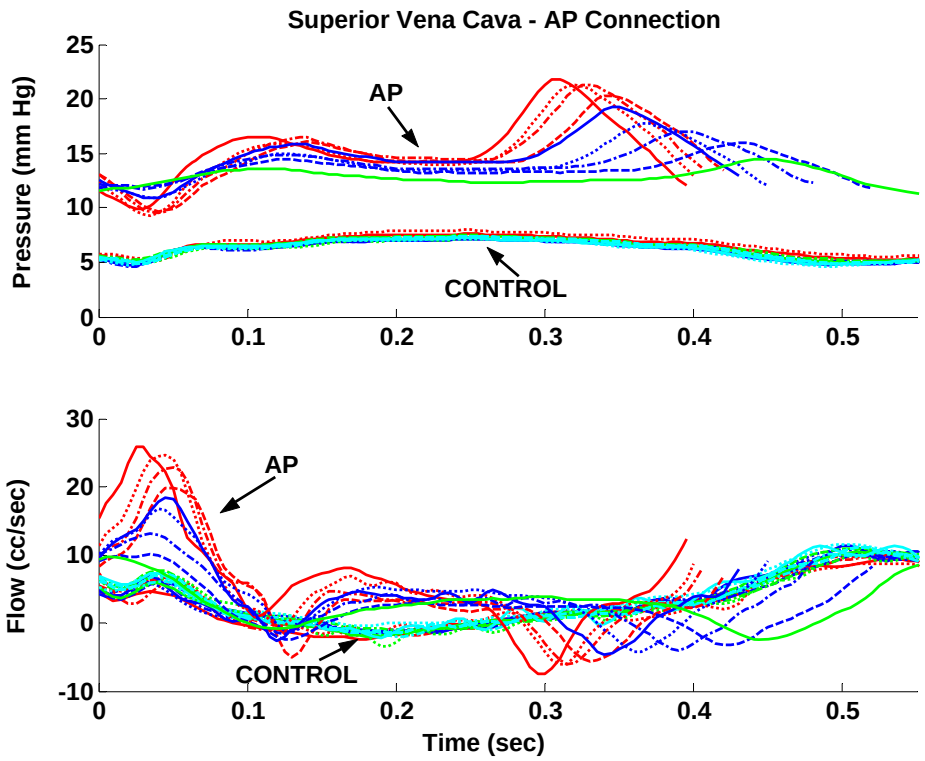

Figure 3.3 Multiple average beat analysis of pressure and flow waveform transitions of the superior vena cava (SVC) between normal and atriopulmonary (AP) circulations.

SVC flow is significantly reduced by approximately 43 % from normal conditions (5.1 ± 1.7 cc/sec) to AP (2.9 ± 1.7 cc/sec). Increased backflow is also present during atrial contraction. Pressures increased significantly from 8.7 ± 2.0 mm Hg to 19.0 ± 2.8 mm Hg. SVC pressure "a" waves are much more pronounced under AP conditions with the increase in RA pressure.

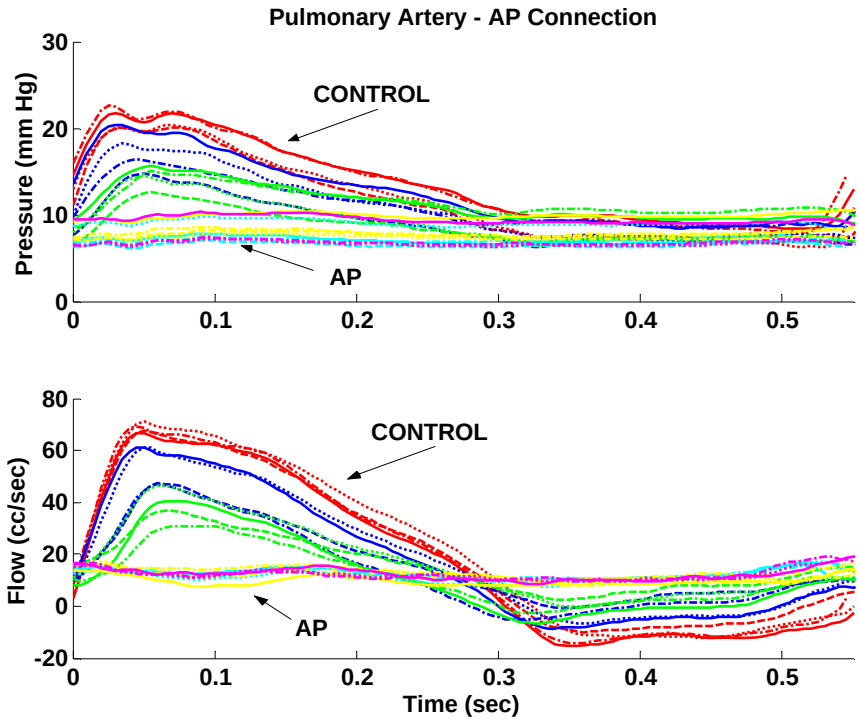

Figure 3.4 Multiple average beat analysis of pressure and flow waveform transitions of the main pulmonary artery (MPA) between normal and atriopulmonary (AP) circulations.

Fig. 3.4 illustrates the removal of the pulsatility between the normal and AP connection in the MPA pressure by removal of the right ventricle. Elimination of PA pulsatility has been linked to numerous postoperative complications including patency and growth problems. PA pressure decreased significantly from 21.5 ± 5.3 mm Hg to 17.0 ± 2.9 mm Hg. This is due to lack of driving force and a significant decrease in cardiac output. Pulmonary artery waveforms maintain some pulsatility, but studies have observed the RA to be deleterious in aiding pulmonary blood flow (Chapter I).

Vascular resistance increased with removal of the right ventricle and the subsequent RA to MPA shunt. Right atrial (RA) pressure significantly increased from 6.2 ± 3.2 mm Hg to

15.7 ± 6.1 mm Hg. The RA pressure values maintained a close proximity to the mean PA pressure.

3.8.2 Overall Resistance Analysis of AP Connection

Pulmonary vascular resistance increased significantly from 6.7 ± 4.2 Wood Units under normal circulation to 15.9 ± 5.4 Wood Units under AP conditions. This 136% increase is due to the reduction in cardiac output. Cardiac output decreased from 31.3 ± 11.6 cc/sec to 11.3 ± 4.1cc/sec. This 64% reduction in flow dominated the decreases in PA pressure and increases in RA pressure. Even with reduction in flow and altered geometry, flow ratios to the left pulmonary artery and the percentage of flow from the IVC and SVC remained within normal ranges. However, significant differences occurred between AP and normal values.

	Normal Mean ± SD n=493	AP Connection Mean ± SD n=532
Pressures (mm Hg)		
AOP	46.7 ± 6.3	43.5 ± 17.0*
PAP	21.5 ± 5.3	17.0 ± 2.9*
SVCP	8.7 ± 2.0	19.0 ± 2.8*
IVCP	8.1 ± 6.3	19.6 ± 5.4*
LAP	8.1 ± 2.8	6.5 ± 2.6*
RAP	6.2 ± 3.2	15.7 ± 6.1*
Flows (cc/sec)		
PAQ	29.7 ± 10.9	9.3 ± 3.7*
SVCQ	5.1 ± 1.7	2.9 ± 1.7*
IVCQ	23.3 ± 6.3	7.7 ± 4.1*
LPAQ	12.1 ± 4.3	4.3 ± 2.3*
CO	31.3 ± 11.6	11.3 ± 4.1*
% LPAQ	42.2 ± 9.1	52.4 ± 9.7
% SVCQ	18.1 ± 5.2	27.9 ± 5.3
% IVCQ	81.9 ± 5.2	72.1 ± 5.3
Vascular Resistance		
PVR		
dyne·sec·cm^{-5}	536 ± 333.7	1270 ± 434.4*
Wood Units	6.7 ± 4.17	15.9 ± 5.4*
SVR		
dyne·sec·cm^{-5}	1987.1 ± 358.1	3065.6 ± 1550.3*
Wood Units	24.8 ± 4.5	38.4 ± 19.3*

Table 3.1 Overall hemodynamic values under normal and atriopulmonary (AP) circulations. AOP, arterial pressure; PAP, pulmonary artery pressure; SVCP, superior vena cava pressure; IVCP, inferior vena cava pressure; LAP, left atrial pressure; RAP, right atrial pressure; PAQ, main pulmonary artery flow; SVCQ, superior vena cava flow; IVCQ, inferior vena cava flow; LPAQ, left pulmonary artery flow; CO, cardiac output; PVR, pulmonary vascular resistance; SVR, systemic vascular resistance. *Statistically significant differences with a $p<0.05$ as indicated.

Statistically different ($p<0.05$) values occurred for all hemodynamic variables measured between the normal and AP modification. Substantial differences occurred in SVC and IVC pressures that increased at 118% and 142% respectively. The increase in RA pressure that increased 153% from 6.2±3.2 mm Hg to 15.7±6.1 mm Hg has deleterious effects on postoperative complications and cardiac function. A reduction in cardiac output of 63% occurred between circulations. SVR increased by 54% and PVR increased 137% between circulations.

3.9 AP Ventilation Effects

3.9.1 Varying Ventilation Rate

Varying respiration rate keeping stroke volume constant (Figure 3.5) had a significant effect at the highest measured rate of 23 breaths/min. No significant changes occurred at low rates. This change at high rates increased the AOP, thereby increasing CO and SVR.

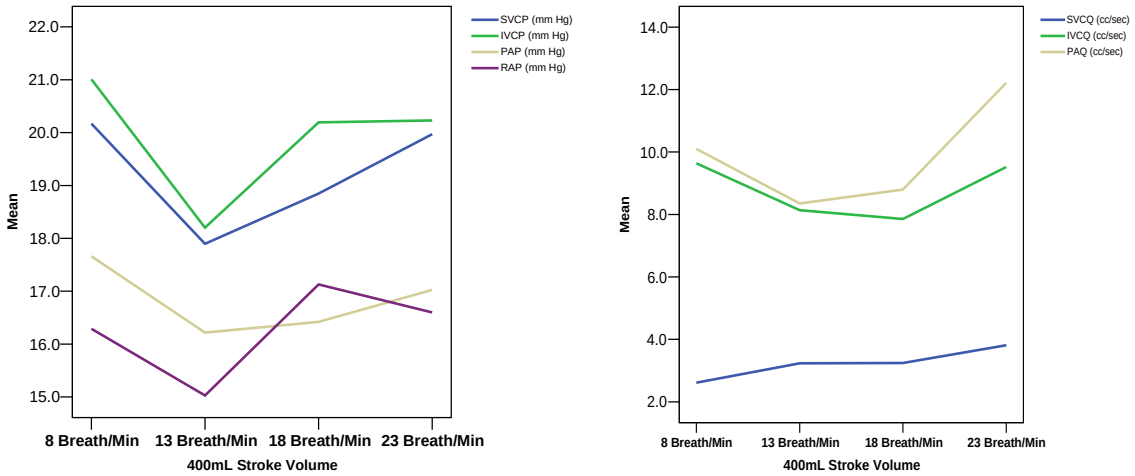

A **B**

Figure 3.5 Mean values for the atriopulmonary (AP) connection illustrating A) pressures (P) and B) flows (Q) for superior vena cava (SVC), inferior vena cava (IVC), pulmonary artery (PA), and right atria (RA) varying ventilation rates keeping stroke volume constant.

Even though individual parameters were not drastically affected by varying respiration rate, SVR illustrated significant changes (Figure 3.6). SVR increased significantly from 1145.1 ± 307.2 dyne·sec·cm^{-5} to 1293.6 ± 457.8 dyne·sec·cm^{-5} as ventilation rate increased. No significant changes occurred in pressure and flow in the 8 to 18 breaths/min ventilation range. PVR did not change significantly over varying respiration rates. Vascular resistances are shown in Figure 3.6.

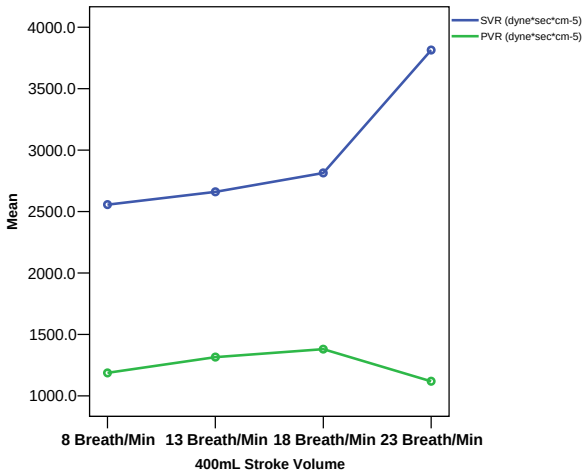

Figure 3.6 Systemic vascular resistance (SVR) and pulmonary vascular resistance (PVR) for the atriopulmonary (AP) circulation under varying ventilation rates keeping stroke volume constant at 400 mL.

3.9.2 Varying Stroke Volume

Holding ventilation rate constant at 13 breaths/min, stroke volume was incremented by 100 mL from 300mL to 600mL. No significant differences were observed (Figure 3.7) in any hemodynamic variable measured over various stroke volumes.

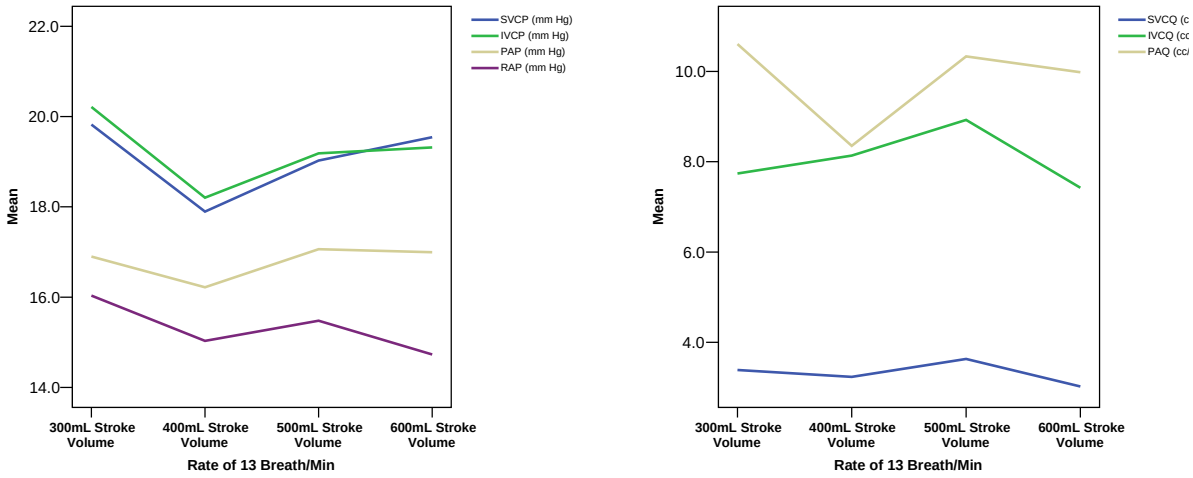

A **B**

Figure 3.7 Mean values for the atriopulmonary (AP) connection illustrating A) pressures (P) and B) flows (Q) for superior vena cava (SVC), inferior vena cava (IVC), pulmonary artery (PA), and right atria (RA) varying stroke volume keeping ventilation rate constant at 13 breaths/min.

SVR decreased as stroke volume increased. There were no significant changes in PVR. SVR was significantly different between volumes of 300mL and 400mL and from 500mL to 600mL shown in Figure 3.8. SVR decreased from 3772.7 ± 1478.7 dyne·sec·cm^{-5} to 2656.1 ± 1406.3 dyne·sec·cm^{-5}.

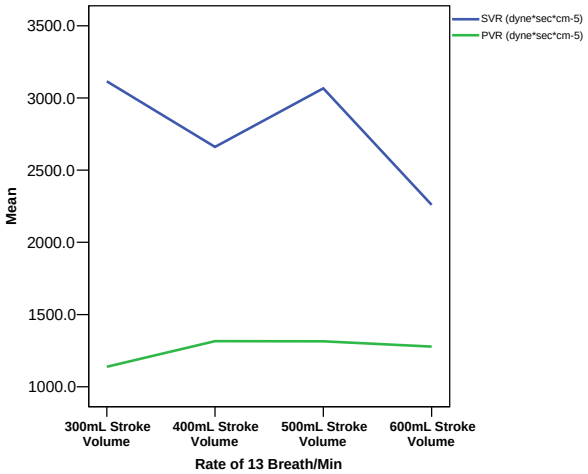

Figure 3.8 Systemic vascular resistance (SVR) and pulmonary vascular resistance

(PVR) for the atriopulmonary (AP) circulation under varying stroke volumes keeping ventilation rate constant at 13 breaths/min.

3.9.3 Constant Minute Ventilation

Examination of combinations of various ventilation rates and stroke volumes was examined with an overall minute ventilation of 5200 mL/min. Combinations observed were 8 breath/min at a stroke volume of 650 mL, 13 breaths/min at a stroke volume of 400 mL, 18 breaths/min at a stroke volume of 290 mL, and 23 breaths/min at a stroke volume of approximately 225 mL. Significant changes occurred at the rate of 13 breaths/min and 400mL for AOP, SVCP, IVCP, PAP, and LPAQ and have a trough at 400 mL followed by a leveling trend as rates increased and stroke volumes decreased.

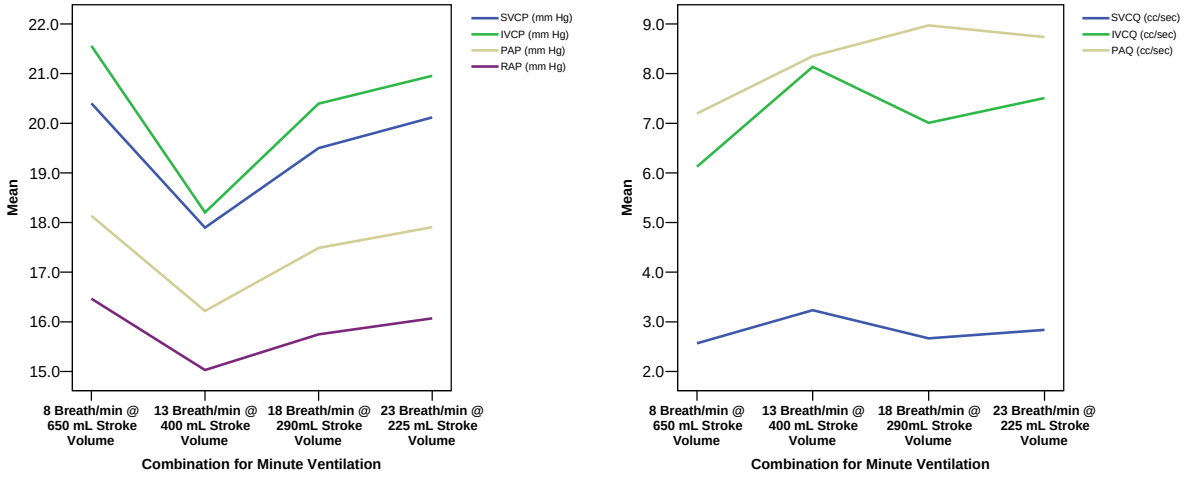

A **B**

Figure 3.9 Mean values for the atriopulmonary (AP) connection illustrating A) pressures (P) and B) flows (Q) for superior vena cava (SVC), inferior vena cava (IVC), pulmonary artery (PA), and right atria (RA) keeping minute ventilation (mL/min) constant at 5200 mL.

PVR decreased significantly from 1546.4 ± 535.4 dyne·sec·cm^{-5} to 1169.8 ± 335.7 dyne·sec·cm^{-5} across minute ventilation combination range. Alternatively, SVR increased as respiration rate increased and stroke volume decreased from 2943.1 ± 1326.3 dyne·sec·cm^{-5} to 3221.7 ± 1325.9 dyne·sec·cm^{-5}. No significant changes occurred in IVCQ, SVCQ, and PAQ.

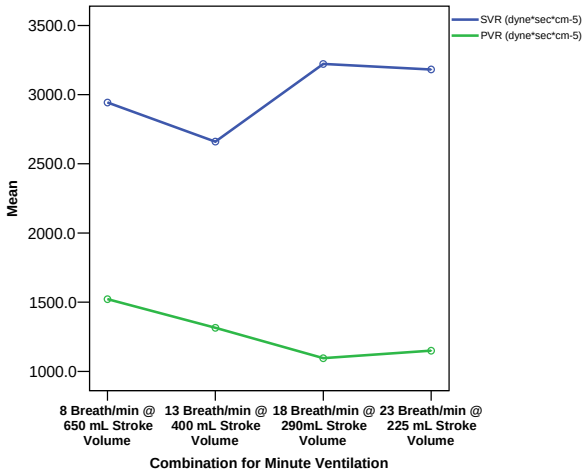

Figure 3.10 Systemic vascular resistance (SVR) and pulmonary vascular resistance (PVR) for the atriopulmonary (AP) circulation under constant minute ventilation (5200 mL/min).

3.9.4 AP Circulation Discussion

Percent changes between ventilation protocol parameters were calculated (Table 3.2). This facilitated a normalized comparison between lambs regardless of weight, body size, and cardiac output. An advantage of the AP circulation was the maintenance of normal blood flow distribution to the lungs postoperatively. Pulmonary artery pulsatility remained, decreasing the probability of impatency and growth complications. Pulsatility may also help lower the vascular resistance via the additional shear stresses applied to vessel walls.

Regardless of ventilation protocol, PAP had minimal changes. PVR decreased as rates were increased and stroke volume decreased. The PVR decrease mirrored the increase

in CO. LAP increases were also associated with decreased PVR. Between normal ventilation ranges, increases in SVC and IVC flow were related to the decrease in SVR. At high rates, SVR increased as observed through a combined increase in AOP pressure and decrease in CO. Higher stroke volumes presumably decreased pulmonary arteriole resistance by opening up additional lung units. Throughout the ventilation protocol, volume and rate manipulations had minimal effect on both systemic and pulmonary pressures. However, volume and rate changes affected the flow from the lungs to the heart. This resulted in increased LAP for either stroke volume or rate increases. As illustrated in Table 3.2, high rates and high stroke volumes that simulate exercise conditions had a deleterious effect on CO.

AP Hemodynamic Variable Percent Change

	LPAQ	PAQ	SVCQ	IVCQ	AOP	SVCP	IVCP	PAP	LAP	RAP
Stroke Volume (mL)										
300	0	0	0	0	0	0	0	0	0	0
400	-4	-13	28	6	-5	-6	-6	10	20	8
500	16	-11	30	28	-3	0	1	8	20	12
600	-16	-10	0	-15	-12	-2	-2	1	5	-2
Rate (Breath/min)										
8	0	0	0	0	0	0	0	0	0	0
13	23	-7	-101	22	-4	-7	-7	5	10	12
18	29	2	-67	25	4	-7	-7	0	7	7
23	22	13	-33	-3	45	4	5	1	-17	7
Combination (br/min*mL)										
8*650	0	0	0	0	0	0	0	0	0	0
13*400	37	51	213	153	1	-14	-15	5	44	20
18*290	15	30	55	20	6	-7	-8	-5	19	-4
23*225	14	17	-5	26	9	-4	-4	-3	10	-1

Table 3.2 Percent change in measured hemodynamic variable in the atriopulmonary (AP) connection. Low parameter settings (300 mL stroke volume, 8 breath/min ventilation rate, and constant minute ventilation at 8 breaths/min at a stroke volume of 650 mL) were used as the reference.

3.10 TCPC Circulation Results

3.10.1 Waveform Analysis for TCPC Connection

The total cavopulmonary connection (TCPC) is unique in that no synthetic material was used to bypass the right side of the heart. Instead, the IVC was transected and sutured to the RPA in an end to side anastomosis. The MPA was transected and connected to the SVC via an end-to-end anastomosis. This connection allows for hemodynamic observations without energy losses or compliance concerns associated with a synthetic graft. With elimination of the right atria, pulsatility was essentially removed from the system. Also, ventilation had a much larger effect on instantaneous pressure and flow waveforms. Normal and TCPC waveforms for the IVC and SVC are illustrated in Figures 3.11 and 3.12. Overall hemodynamic changes are summarized in Table 3.3.

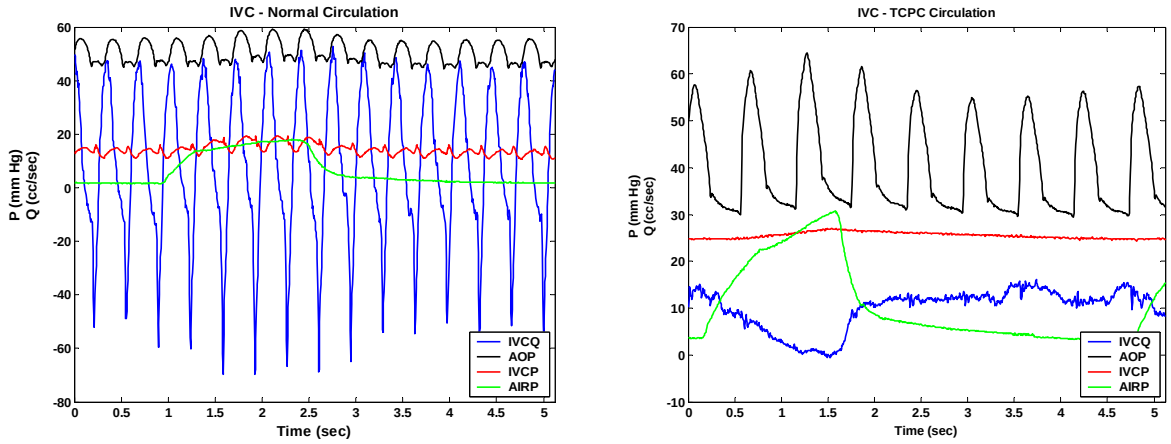

A **B**

Figure 3.11 Representative waveforms depicting pressure (P) and flow (Q) of the inferior vena cava (IVC) under A) normal circulation and B) TCPC circulations. Arterial pressure (AOP) and airway pressure (AIRP) are shown for reference.

IVCP, now in series with the vascular resistance, significantly increased, doubling from 12.1 ± 2.7 mm Hg to 24.2 ± 4.2 mm Hg. Ventilation effects were dominant under TCPC

anatomy. During inspiration, pressure increased and flow decreased markedly, often approaching zero mL/sec. Pulsatility was essentially removed from the IVC pressure tracing except for ventilation artifacts. IVC flow decreased from 24.3 ± 12.9 ccs/sec to 12.6 ± 6.0 ccs/sec.

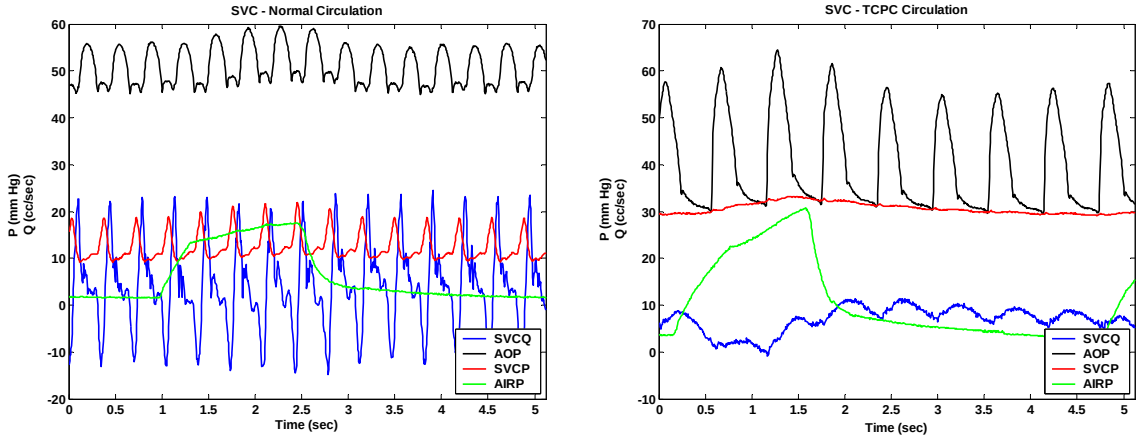

A **B**

Figure 3.12 Representative waveforms depicting pressure (P) and flow (Q) of the superior vena cava (SVC) under A) normal circulation and B) TCPC circulations. Arterial pressure (AOP) and airway pressure (AIRP) are shown for reference.

As with the IVC, placing the SVC in series with the pulmonary vasculature significantly increased the pressure from 14.1 ± 1.8 mm Hg to 29.5 ± 3.7 mm Hg. Pulsatility was removed with elimination of the right atria and complete bypass of the right side of the heart. Ventilation effects were observed in the TCPC waveforms that produced increased pressures and decreased flows during inspiration. SVC flow decreased from 10.5 ± 8.4 cc/sec to 6.7 ± 1.0 ccs/sec under TCPC conditions. During inspiration (Figure 3.13), flow was essentially zero where pressures had minimal change. MPA flows decreased by 81% and pressures increased by 22%. Pulsatility was now absent in the pulmonary arteries, which may lead to postoperative complications (Chapter I).

	Normal Mean ± SD n=239	TCPC Connection Mean ± SD n=196
Pressures (mm Hg)		
AOP	56.7 ± 8.9	33.9 ± 6.32*
PAP	15.6 ± 2.4	20.0 ± 5.5*
SVCP	14.1 ± 1.8	29.5 ± 3.7*
IVCP	12.1 ± 2.7	24.2 ± 4.2*
LAP	13.0 ± 1.3	9.9 ± 4.6*
Flows (cc/sec)		
SVCQ	10.5 ± 8.4	6.7 ± 1.0
IVCQ	24.3 ± 12.9	12.6 ± 6.0
LPAQ	10.9 ± 3.2	3.9 ± 0.8*
CO	38.8 ± 12.3	15.2 ± 3.3*
% LPAQ	44.2 ± 14.0	28.4 ± 5.8*
% SVCQ	24.6 ± 10.7	44.7 ± 7.3*
% IVCQ	75.4 ± 10.7	55.3 ± 7.3*
Vascular Resistance		
PVR		
dyne·sec·cm^{-5}	314.4 ± 129.9	736.4 ± 54.1*
Wood Units	3.93 ± 1.6	9.2 ± 0.7*
SVR		
dyne·sec·cm^{-5}	2523.5 ± 1452.1	2137.5 ± 423.1
Wood Units	31.5 ± 18.2	26.7 ± 5.3

Table 3.3 Overall hemodynamic values under normal and total cavopulmonary connection (TCPC) circulations. AOP, arterial pressure; PAP, pulmonary artery pressure; SVCP, superior vena cava pressure; IVCP, inferior vena cava pressure; LAP, left atrial pressure; RAP, right atrial pressure; PAQ, main pulmonary artery flow; SVCQ, superior vena cava flow; IVCQ, inferior vena cava flow; LPAQ, left pulmonary artery flow; CO, cardiac output; PVR, pulmonary vascular resistance; SVR, systemic vascular resistance.

***Statistically significant differences with a $p<0.05$ as indicated.**

3.10.2 Overall Resistance Analysis of TCPC Connection

The TCPC connection eliminated the right side of the heart placing the systemic and vascular resistances in series. This connection enabled examination of the Fontan circulation without use of a synthetic graft. Significant differences, mean increases in pressure and mean decreases in flow, occurred in all parameters except for SVCQ and SVR. CO decreased by 61% from 38.8±12.3 cc/sec to 15.2±3.3 cc/sec between normal and TCPC circulations. PVR increased by 136% to 736.2±54.1 dyne·sec·cm^{-5}.

3.11 TCPC Respiration Effects

3.11.1 Varying Ventilation Rate

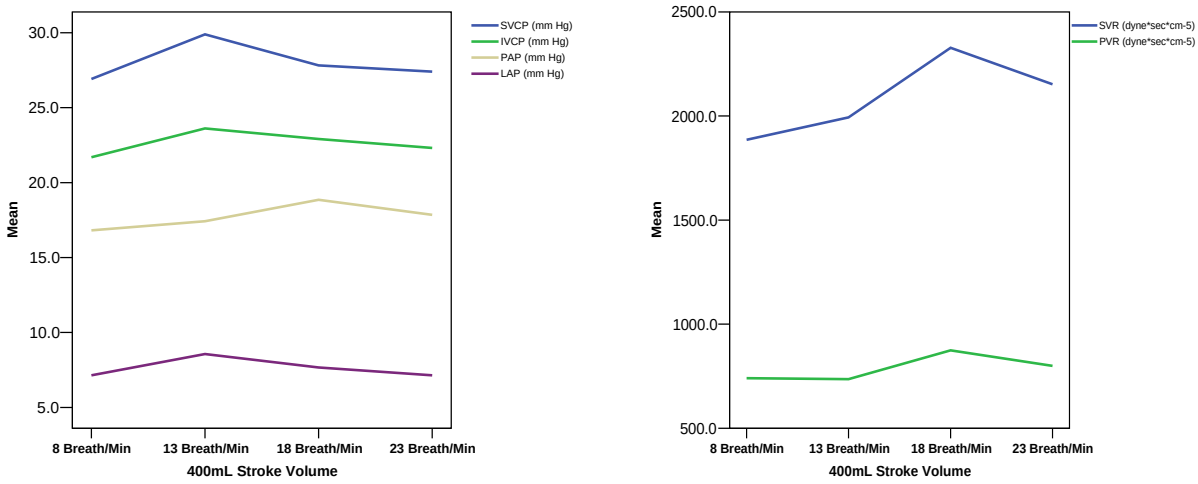

A **B**

Figure 3.13 Mean values for the total cavopulmonary connection (TCPC) illustrating A) pressures (P) of superior vena cava (SVC), inferior vena cava (IVC), pulmonary artery (PA), and left atria (LA) and B) systemic (SVR) and pulmonary (PVR) vascular resistance varying respiration rates keeping stroke volume constant at 400 mL.

Ventilation rate had minimal effect on all hemodynamic variables. No significant differences were observed keeping stroke volume constant. SVR and PVR increased slightly as rates increased.

3.11.2 Varying Stroke Volume

Varying stroke volume keeping respiration rate the same for the TCPC connection is illustrated in Figures 3.14 and 3.15.

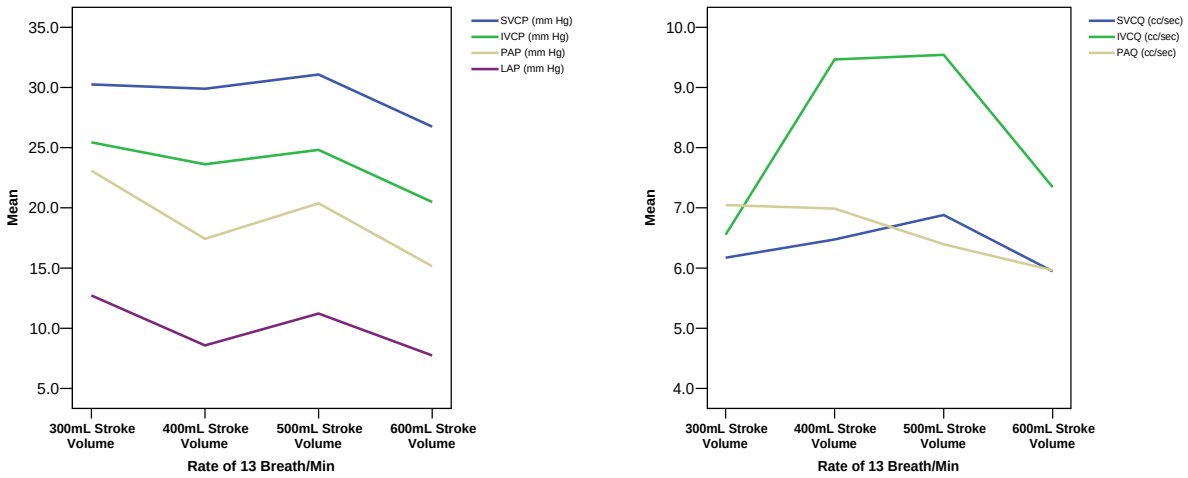

A **B**

Figure 3.14 Mean values for the total cavopulmonary connection (TCPC) illustrating A) pressures (P) and B) flows (Q) for superior vena cava (SVC), inferior vena cava (IVC), pulmonary artery (PA), and left atria (LA) varying stroke volume keeping respiration rate constant at 13 breaths/min.

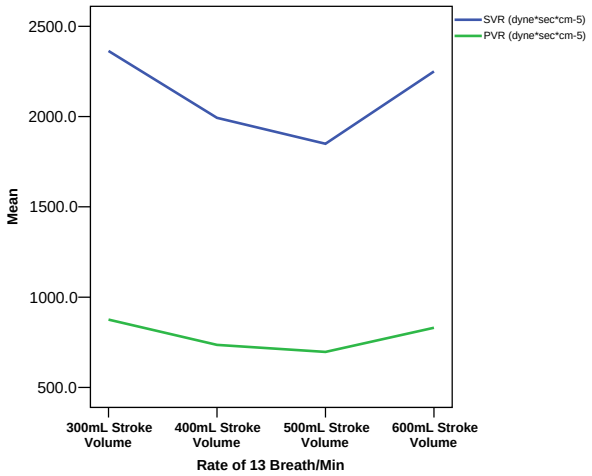

Figure 3.15 Systemic vascular resistance (SVR) and pulmonary vascular resistance (PVR) for the total cavopulmonary (TCPC) circulation under varying stroke volumes keeping respiration rate constant at 13 breaths/min.

Pressure significantly decreased for all parameters as stroke volume increased. A stroke volume of 600 mL produced the largest pressure decrease. IVCP decreased from 25.4±3.2 mm Hg at a stroke volume of 300 mL to 20.5±3.8 mm Hg at a stroke volume of 600mL, a difference of 19%. SVCP decreased 12%, PAP by 34%, and LAP by 39%. Stroke volume had a pronounced effect on IVCQ at various stroke volumes. Extremely low and high stroke volumes decreased the flow by 47% from middle range stroke volumes. Stroke volume had no significant difference on LPAQ or SVCQ. No significant changes occurred in vascular resistance.

3.11.3 Constant Minute Ventilation

Combinations of ventilation rate and stroke volume keeping minute ventilation constant are illustrated in Figures 3.16.

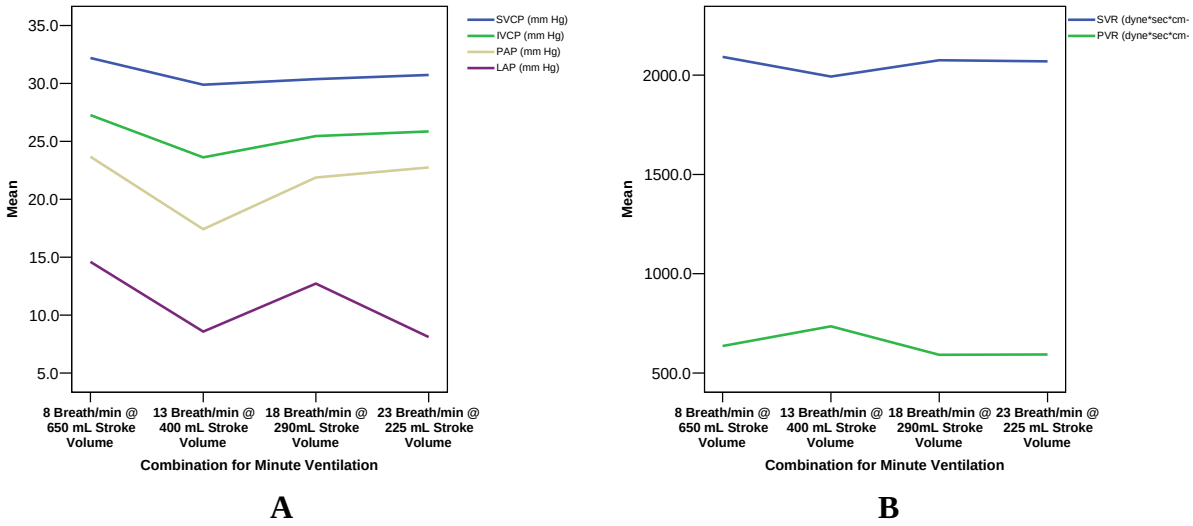

A **B**

Figure 3.16 Mean values for the total cavopulmonary connection (TCPC) illustrating A) pressures (P) of superior vena cava (SVC), inferior vena cava (IVC), pulmonary artery (PA), and left atria (LA) and B) systemic (SVR) and pulmonary (PVR) vascular resistance keeping minute ventilation constant at 5200 mL/min.

No significant changes occurred over minute ventilation combinations. SVCQ increased at the maximum rate value (23 breath/min at 225 mL stroke volume). Alternately, IVCQ decreased at high rates and low stroke volumes. No changes occurred in systemic or pulmonary vascular resistance. Pressure waveforms maintained stable throughout.

3.11.4 TCPC Circulation Discussion

Significant differences were observed between the normal and TCPC circulations. Only SVCQ and SVR remained within normal ranges. Varying stroke volume and ventilation frequency did not produce significant effects within the range examined. Minimal effects occurred in pressure measurements (Table 3.4). Minimal changes occurred in PVR and SVR throughout the ventilation protocol except for minimum and maximum experimental stroke volumes. As with the AP connection, high stroke volumes produced

negative changes in pulmonary and systemic flows. Largest percent change increases occurred with varying stroke volume within normal ranges.

	TCPC Hemodynamic Variable Percent Change								
	LPAQ	PAQ	SVCQ	IVCQ	AOP	SVCP	IVCP	PAP	LA
Stroke Volume (mL)									
300	0	0	0	0	0	0	0	0	0
400	-3	15	41	65	7	10	3	3	-2
500	-1	21	27	-6	8	15	10	11	3
600	-1	-15	7	-8	4	10	8	13	-1
Rate (Breath/min)									
8	0	0	0	0	0	0	0	0	0
13	11	6	24	21	4	9	3	4	1
18	18	17	-4	-8	7	1	3	3	6
23	5	6	2	19	2	0	-1	-1	0
Combination (br/min*mL)									
8	0	0	0	0	0	0	0	0	0
13	-5	53	6	18	-3	-4	-5	-3	-2
18	7	-4	-9	-15	-3	-2	-3	-3	-5
23	13	2	0	-9	1	-1	-1	-1	-2

Table 3.4 Percent change in measured hemodynamic variable in the total cavopulmonary connection (TCPC). Low parameter settings (300 mL stroke volume and 8 breath/min ventilation rate) are used as the reference.

3.12 TCPX Circulation Results

3.12.1 Waveform Analysis for TCPX Connection

The TCPX connection is a Fontan modification commonly used in practice today. An extracardiac shunt connected the IVC to the RPA via an end-to-end anastomosis. The SVC was attached to the RPA via an end-to-end anastomosis. This connection differs from the previously discussed TCPC connection via the inclusion of a synthetic graft. This non-compliant graft has significant effects on overall hemodynamics. Figures 3.17, 3.18, and 3.19 illustrate the changes in systemic and pulmonary circulations between normal and TCPX conditions. Overall hemodynamic changes between circulations are summarized in Table 3.5.

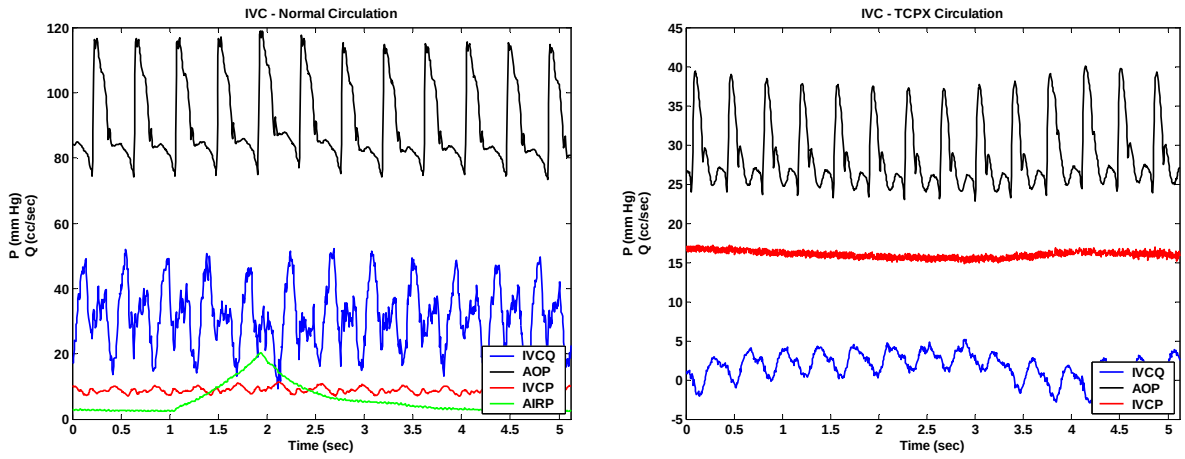

A **B**

Figure 3.17 Representative waveforms depicting pressure (P) and flow (Q) of the inferior vena cava (IVC) under A) normal circulation and B) TCPX circulations. Arterial pressure (AOP) and airway pressure (AIRP) are shown for reference.

Mean IVC pressure increased from 13.6±0.3 mmHg to 25.2±5.3 mm Hg. Pulsatility in the pressure waveform was eliminated except for ventilation effects. A 75% decrease occurs in IVCQ between normal and TCPX circulations. Percent IVC blood flow contribution remained at approximately 73% in both normal and TCPX circulations.

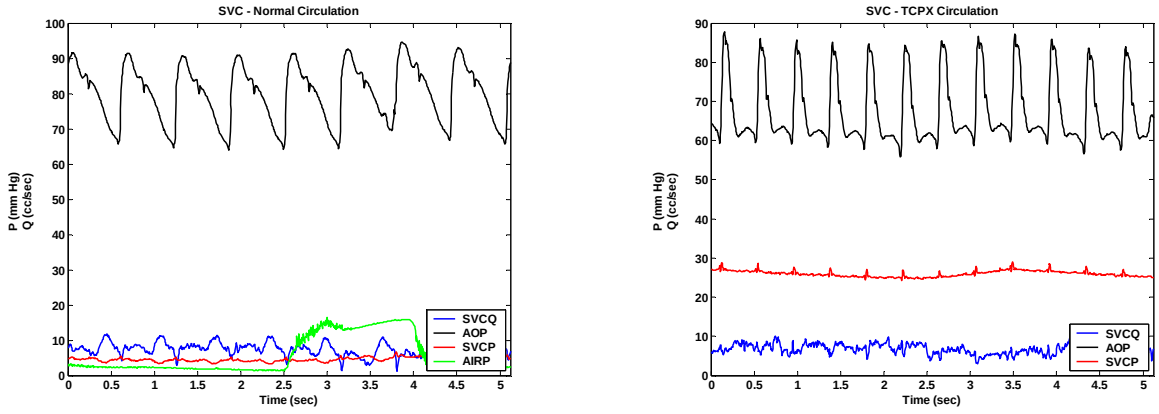

A **B**

Figure 3.18 Representative waveforms depicting pressure (P) and flow (Q) of the superior vena cava (SVC) under A) normal circulation and B) TCPX circulations. Arterial pressure (AOP) and airway pressure (AIRP) are shown for reference.

The SVC displayed similar results as the IVC. SVC pressure increased from 5.9±2.2mm Hg to 24.0±4.6 mm Hg. Pulsatility was removed except for increases in pressure due to ventilation. A 69% decrease in SVCQ occurred between normal and TCPX circulations. SVC flow contributions were maintained at 27.6% in the TCPX compared to 26% under normal conditions.

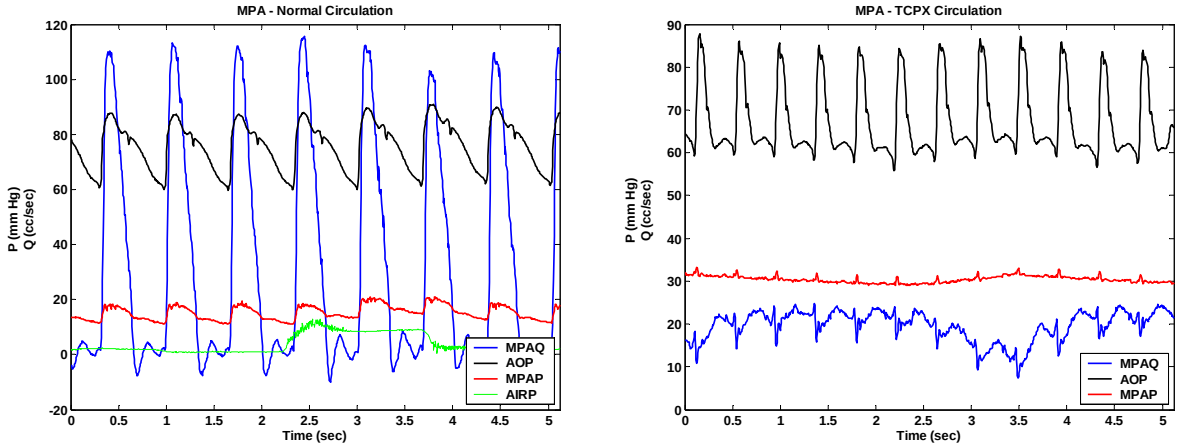

A **B**

Figure 3.19 Representative waveforms depicting pressure (P) and flow (Q) of the main pulmonary artery (MPA) under a) normal circulation and b) TCPX circulations. Arterial pressure (AOP) and airway pressure (AIRP) are shown for reference.

Connecting the pulmonary artery in series with the systemic vessels, PA waveforms displayed similar pressure and flow profiles. Pressure increased from 15.9±1.0mm Hg to 28.9±4.3 mm Hg. Flow is decreased by 66% between circulations.

3.12.2 Overall Resistance Analysis of TCPX Circulation

For TCPX circulation, the SVR was 4579.8±1603.5 dyne·sec·cm^{-5} and the PVR was 3664.4 ± 1343.7 dyne·sec·cm^{-5}. This was consistent with the 68% decrease in CO from 32.0±2.5 ccs/sec under normal circulation to 10.2±5.4 ccs/sec under TCPX circulations.

Increased PA pressures and decreased AO pressures are consistent with the more dramatic PVR increase.

	Normal	**TCPX Connection**
	Mean ± SD	**Mean ± SD**
	n=145	**n=276**
Pressures (mm Hg)		
AOP	77.4 ± 7.7	55.63 ± 18.2*
PAP	15.9 ± 1.0	28.9 ± 4.3*
SVCP	5.9 ± 2.2	24.0 ± 4.6*
IVCP	13.6 ± 0.3	25.2 ± 5.3*
LAP	4.3 ± 0.5	6.5 ± 2.9*
Flows (cc/sec)		
PAQ	32.0 ± 2.5	10.2 ± 5.4*
SVCQ	8.1 ± 0.8	2.4 ± 1.8*
IVCQ	23.0 ± 1.4	5.7 ± 3.1*
LPAQ	12.8 ± 2.1	3.9 ± 2.2*
CO	32.0 ± 2.5	10.2 ± 5.4*
% LPAQ	41.2 ± 6.7	48.4 ± 4.9
% SVCQ	26.0 ± 1.4	27.6 ± 10.1
% IVCQ	74.0 ± 1.4	72.4 ± 10.1
Vascular Resistance		
PVR		
dyne·sec·cm^{-5}	487.1 ± 72.8	3664.4 ± 1343.7*
Wood Units	6.1 ± 0.9	45.8 ± 16.8*
SVR		
dyne·sec·cm^{-5}	3021.4 ± 300.1	4579.8 ± 1603.5*
Wood Units	37.8 ± 3.8	57.3 ± 20.0*

Table 3.5 Overall hemodynamic values under normal and total cavopulmonary with extracardiac shunt (TCPX) circulations. AOP, arterial pressure; PAP, pulmonary artery pressure; SVCP, superior vena cava pressure; IVCP, inferior vena cava pressure; LAP, left atrial pressure; RAP, right atrial pressure; PAQ, main pulmonary artery flow; SVCQ, superior vena cava flow; IVCQ, inferior vena cava flow; LPAQ, left pulmonary artery flow; CO, cardiac output; PVR, pulmonary

vascular resistance; SVR, systemic vascular resistance.

***Statistically significant differences with a p<0.05 as indicated.**

3.13 TCPX Respiration Effects

3.13.1 Varying Ventilation Rate

Hemodynamic changes varying ventilation rate keeping stroke volume constant are illustrated in Figures 3.20 and 3.21.

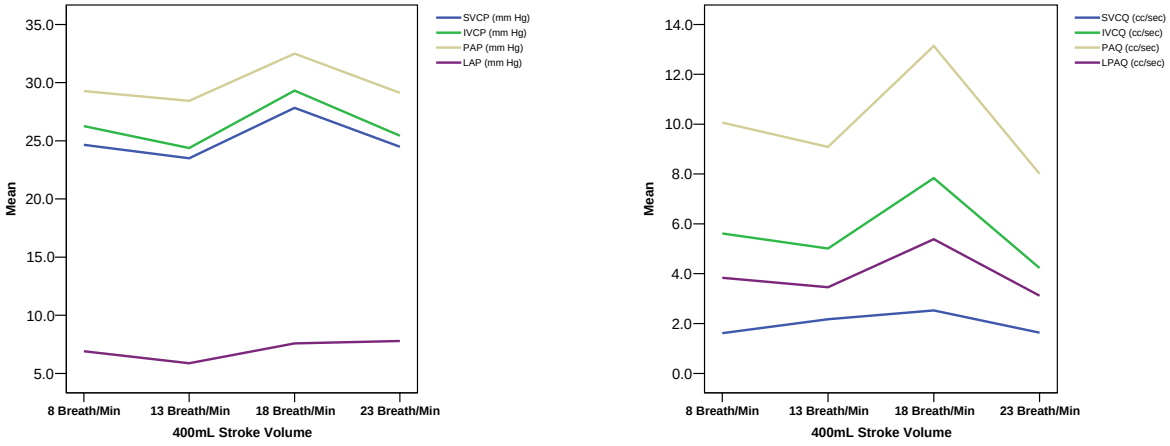

A **B**

Figure 3.20 Mean values for the total cavopulmonary connection with extacardiac shunt (TCPX) illustrating A) pressures (P) and B) flows (Q) for superior vena cava (SVC), inferior vena cava (IVC), pulmonary artery (PA), and left atria (LA) varying respiration rates keeping stroke volume constant at 400 mL.

No significant effects occurred for the hemodynamic variables measured. Pressure and flow differences were not present across ventilation frequencies except at a rate of 18

breaths/min. Increased pressures and flows occurred at this parameter setting. Otherwise, pressures and flow remained stable.

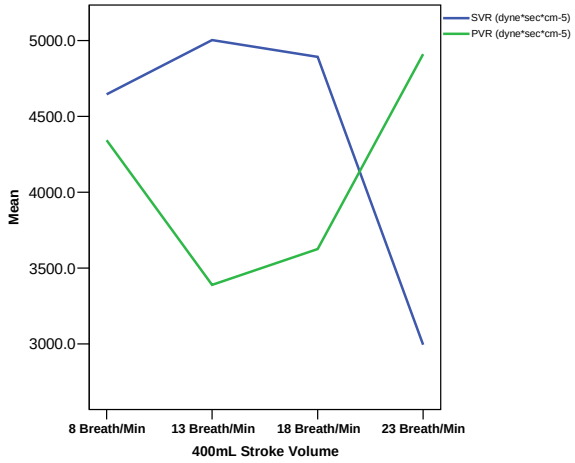

Figure 3.21 Systemic vascular resistance (SVR) and pulmonary vascular resistance (PVR) for the total cavopulmonary circulation with extracardiac shunt (TCPX) under varying respiration rates keeping stroke volume constant at 400 mL.

SVR decreased significantly when high rates were implemented. Conversely, PVR increased between 18 breath/min and 23 breath/min. These changes contributed to the large decrease in CO as rate increased. High rates may contribute to arteriole constriction that may result in the large increase in PVR.

3.13.2 Varying Stroke Volume

Varying stroke volume keeping respiration rate the same for the TCPC connection is illustrated in Figures 3.22 and 3.23.

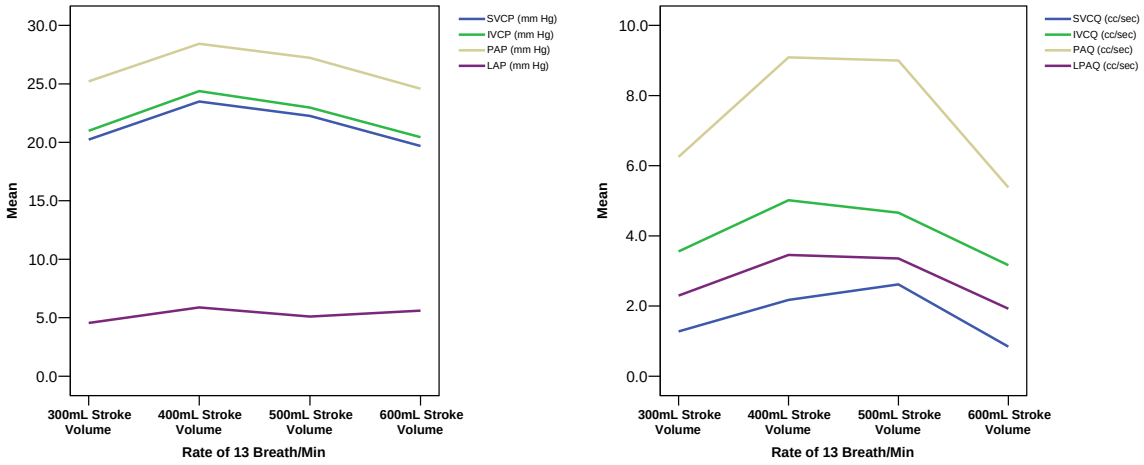

A **B**

Figure 3.22 Mean values for the total cavopulmonary connection with an extracardiac shunt (TCPX) illustrating A) pressures (P) and B) flows (Q) for superior vena cava (SVC), inferior vena cava (IVC), pulmonary artery (PA), and left atria (LA) varying stroke volume keeping ventilation rate constant at 13 breaths/min.

AOP decreased from 51.0±22.2 mm Hg at a stroke volume of 500mL to 39.0±6.5 mm Hg at 600mL. Significant increases in pressure occurred at low stroke volumes (300-400 mL). Flows were less at both the low (300 mL) and high (600 mL) stroke volume settings. SVR had no changes across varying stroke volumes. However, PVR was significantly elevated at low and high stroke volumes.

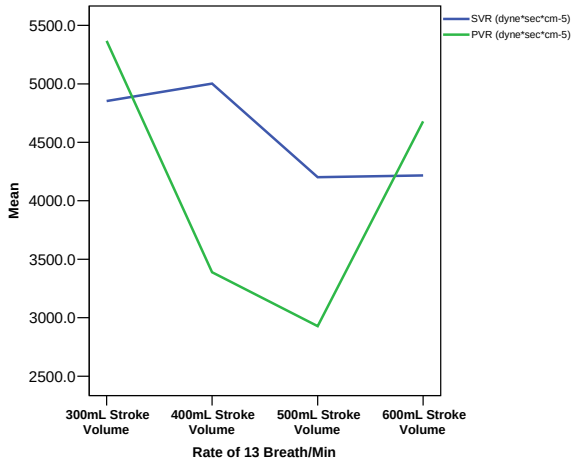

Figure 3.23 Systemic vascular resistance (SVR) and pulmonary vascular resistance (PVR) for the total cavopulmonary with extracardiac shunt (TCPX) circulation under varying stroke volumes keeping ventilation rate constant at 13 breaths/min.

3.13.3 Constant Minute Ventilation

Combinations of respiration rate and stroke volume keeping minute ventilation constant are illustrated in Figures 3.24 and 3.25.

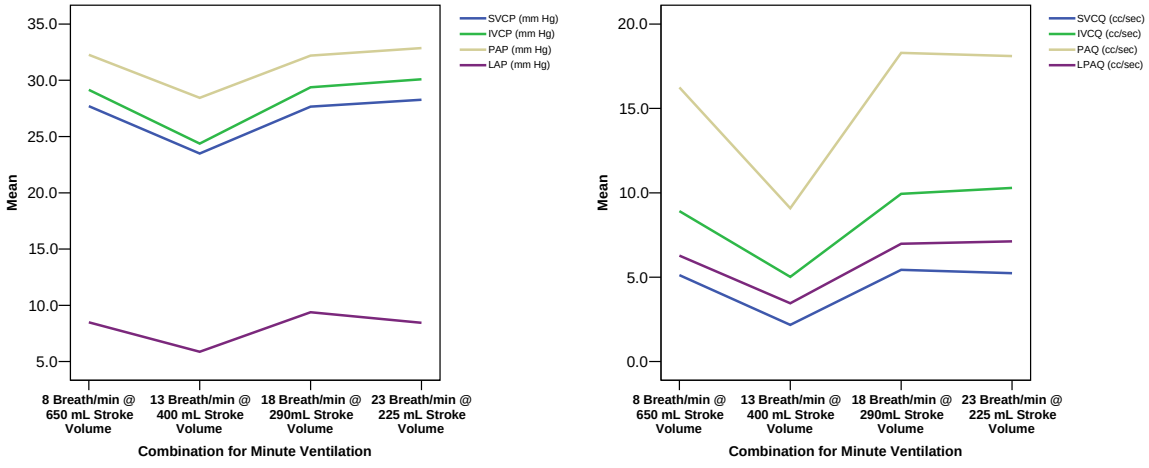

A **B**

Figure 3.24 Mean values for the total cavopulmonary connection with extracardiac shunt (TCPX) illustrating A) pressures (P) and B) flows (Q) for superior vena cava

(SVC), inferior vena cava (IVC), pulmonary artery (PA), and left atria (LA) keeping minute ventilation constant at 5200 mL/min.

Combinations varying respiration rate and stroke volume keeping minute ventilation constant were not significantly different across hemodynamic parameters and vascular resistances. Pressures and flows remained stable throughout the minute ventilation protocol.

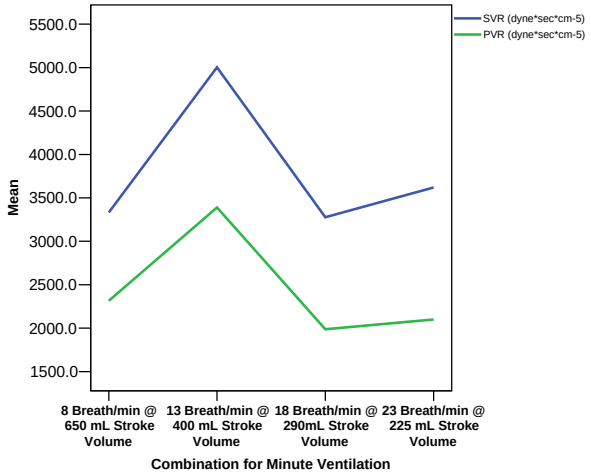

Figure 3.25 Systemic vascular resistance (SVR) and pulmonary vascular resistance (PVR) for the total cavopulmonary connection with extracardiac shunt (TCPX) under constant minute ventilation (5200 mL/min).

3.13.4 TCPX Circulation Summary

Caval and pulmonary pressures were approximately the same in the TCPX circulation. Mean pressures for the IVC, SVC, and PA were 25.2±5.3 mm Hg, 24.0±4.6 mm Hg, and 28.9±4.3 mm Hg respectively. Normal ventilation ranges produced the largest percent increase in the pulmonary and systemic flows. High stroke volumes had a deleterious effect showing decreases in the PAQ, SVCQ, and IVCQ of 17%, 34%, and 15%. Furthermore, high rates produced decreased flows. Percent changes in the TCPX connection

were greater over ventilation protocol ranges than in the TCPC and AP connections. However, ventilation had minimal effect on overall pressures.

TCPX Hemodynamic Variable Percent Change

	LPAQ	PAQ	SVCQ	IVCQ	AOP	SVCP	IVCP	PAP	LAP
Stroke Volume (mL)									
300	0	0	0	0	0	0	0	0	0
400	53	50	74	48	16	18	19	15	31
500	41	39	98	27	3	9	8	7	9
600	-20	-17	-34	-15	-21	-4	-5	-3	17
Rate (Breath/min)									
8	0	0	0	0	0	0	0	0	0
13	-3	-3	41	-5	8	-4	-5	-3	-8
18	32	25	45	31	30	10	9	9	4
23	-19	-21	0	-26	-20	-2	-4	-2	11
Combination (br/min*mL)									
8*650	0	0	0	0	0	0	0	0	0
13*400	-40	-40	-55	-39	-14	-13	-13	-10	-24
18*290	11	13	6	12	5	0	1	0	11
23*225	14	11	2	15	12	2	3	2	0

Table 3.6 Percent change in measured hemodynamic variable in the total cavopulmonary connection with extracardiac shunt (TCPX). Low parameter settings (300 mL stroke volume and 8 breath/min ventilation rate) were used as references.

3.14 TCPY Circulation Results

3.14.1 Waveform Analysis of TCPY Circulation

The TCPY connection is a novel procedure performed due to right pulmonary geometry constraints in the lamb. Either a Y-shaped graft is used or a Y connection is made by connecting the IVC to the MPA via end-to-end anastomosis. Next an end-to-end anastomosis between the SVC and the other bifurcated end of the graft is performed. If a straight graft is used, an end-to-side anastomosis is used to connect the SVC to the graft (Chapter II). Instantaneous ventilation effects were observed in both the normal and TCPY circulations. Overall hemodynamic changes between circulations are summarized in Table 3.7.

An increase in flow occurred in the IVC during inspiration under normal conditions, whereas, a decrease was observed during inspiration under TCPY conditions. Pulsatility was removed from the IVC pressure waveform. IVC pressure increased from 10.9±3.1 mm Hg to 22.8±9.6 mm Hg. IVC flow decreased from 38.4±7.3 cc/sec to 17.9±8.6 cc/sec. As with the TCPX modification, IVC flow contributed 78% in the TCPY compared to 79% in the normal circulation. Representative waveform changes are illustrated in Figures 3.26, 3.27, and 3.28.

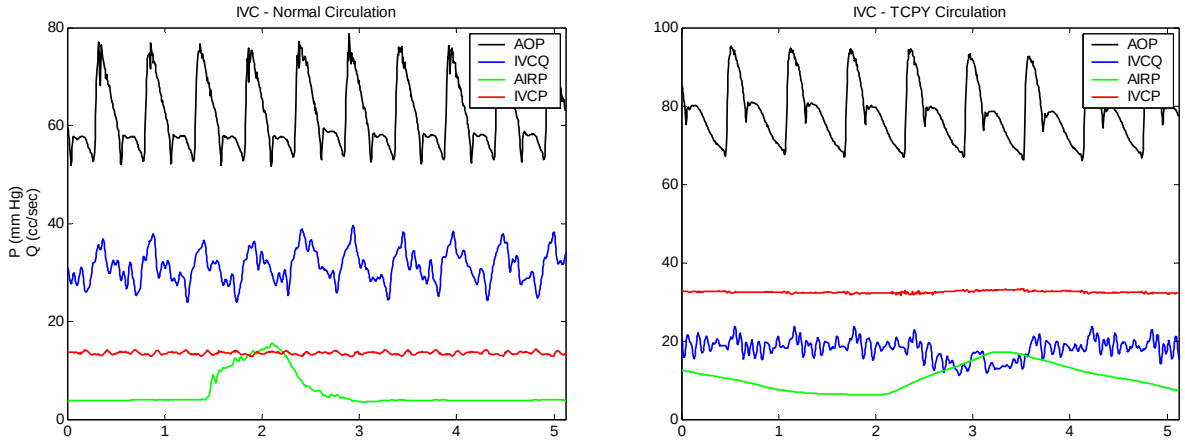

A **B**

Figure 3.26 Representative waveforms depicting pressure (P) and flow (Q) of the inferior vena cava (IVC) under a) normal circulation and b) TCPY circulations. Arterial pressure (AOP) and airway pressure (AIRP) are shown for reference.

SVC blood flow contributions remained stable between normal (21%) and TCPY (22%) circulations. SVC pressure increased to match the IVC and PA pressures at 21.8±5.5 mm Hg. As with the IVC, pulsatility was absent in the SVC pressure waveform except for ventilation artifacts. Flows decreased during inspiration, but did not fall to zero.

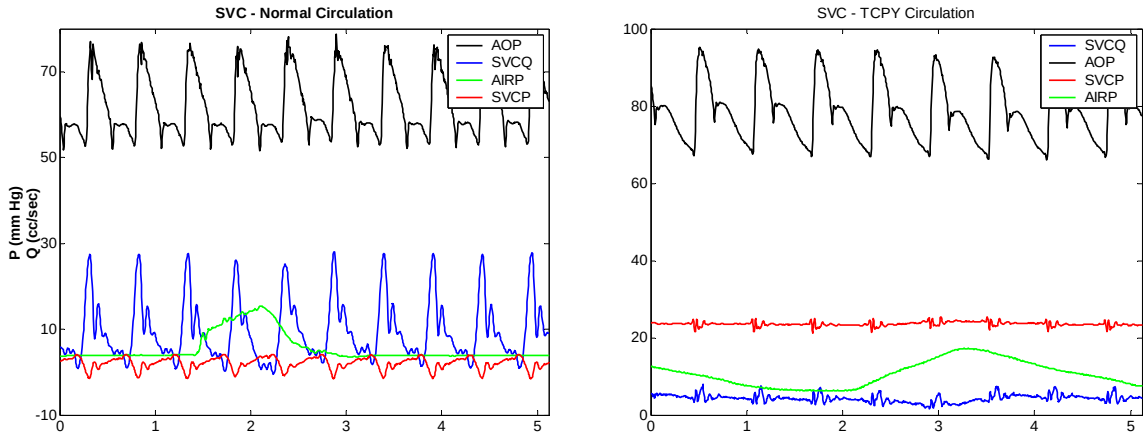

A **B**

Figure 3.27 Representative waveforms depicting pressure (P) and flow (Q) of the superior vena cava (SVC) under a) normal circulation and b) TCPY circulations. Arterial pressure (AOP) and airway pressure (AIRP) are shown for reference.

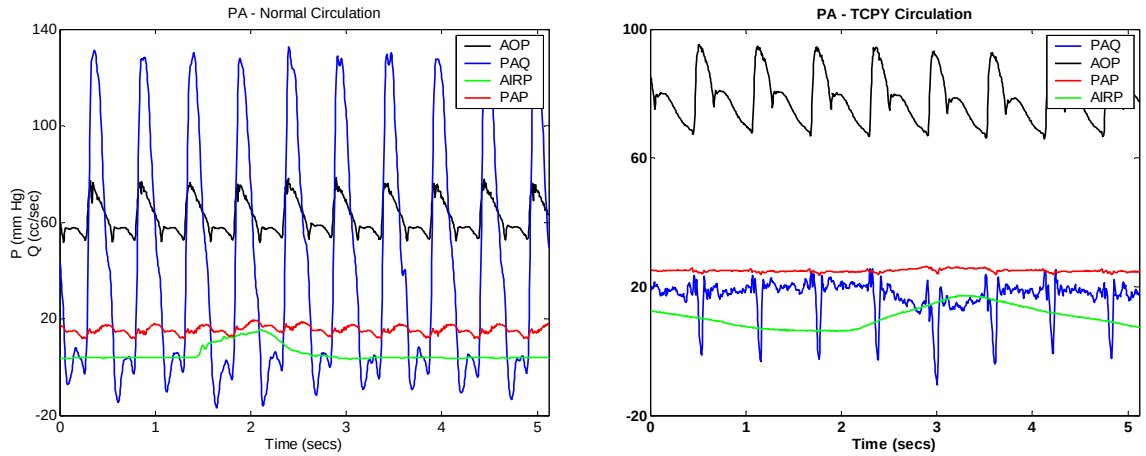

A **B**

Figure 3.28 Representative waveforms depicting pressure (P) and flow (Q) of the main pulmonary artery (MPA) under A) normal circulation and B) TCPY circulations. Arterial pressure (AOP) and airway pressure (AIRP) are shown for reference.

3.14.2 Overall Resistance Analysis of TCPY Circulation

Vascular resistances increased between circulations. However, ranges remained stable between circulations. PVR increased by 26% (6.8±4.8 HRU compared to 8.6±3.7 HRU). Systemic vascular resistance also remained stable measuring 27.3±3.7 HRU under normal conditions and 26.1±17.6 HRU in the TCPY circulation (5% decrease). Cardiac output decreased 51% between circulations. This was significantly less than similar TCPC and TCPX modifications. Also, blood flow was distributed in the same ratios that normal circulation provided.

	Normal **Mean ± SD** **n=369**	**TCPY Connection** **Mean ± SD** **n=2171**
Pressures (mm Hg)		
AOP	68.4 ± 12.6	57.5 ± 21.7*
PAP	18.6 ± 12.6	27.2 ± 8.9*
SVCP	4.6 ± 2.2	21.8 ± 5.5*
IVCP	10.9 ± 3.1	22.8 ± 9.6*
LAP	9.3 ± 5.9	21.4 ± 13.9*
Flows (cc/sec)		
PAQ	47.5 ± 10.3	19.7 ± 10.8*
SVCQ	10.1 ± 1.8	4.6 ± 2.0*
IVCQ	38.4 ± 7.3	17.9 ± 8.6*
LPAQ	19.1 ± 7.1	6.8 ± 3.6*
CO	47.2 ± 7.7	23.0 ± 9.9*
% LPAQ	38.9 ± 11.0	31.9 ± 14.0*
% SVCQ	21.2 ± 3.4	21.8 ± 9.4*
% IVCQ	78.9 ± 3.4	78.2 ± 9.4*
Vascular Resistance		
PVR		
dyne·sec·cm^{-5}	543.8 ± 303.6	688.5 ± 267.8*
Wood Units	6.8 ± 4.8	8.6 ± 3.7*
SVR		
dyne·sec·cm^{-5}	2182.8 ± 299.1	2084.6 ± 1406.1*
Wood Units	27.3 ± 3.7	26.1 ± 17.6*

Table 3.7 Overall hemodynamic values under normal and total cavopulmonary connection with a Y-shaped graft (TCPY) circulations. AOP, arterial pressure; PAP, pulmonary artery pressure; SVCP, superior vena cava pressure; IVCP, inferior vena cava pressure; LAP, left atrial pressure; RAP, right atrial pressure; PAQ, main pulmonary artery flow; SVCQ, superior vena cava flow; IVCQ, inferior vena cava flow; LPAQ, left pulmonary artery flow; CO, cardiac output; PVR, pulmonary vascular resistance; SVR, systemic vascular resistance.

***Statistically significant differences with a $p<0.05$ as indicated.**

3.15 TCPY Respiration Effects

Protocol changes now provide more numerous ventilation parameters. Rate was varied between 8 and 23 breaths/min incrementing stroke volumes by 100 mL between 400 and 800 mL. Stroke volumes were varied from 400 to 800 mL incrementing ventilation rate by 5 breaths/min from 8 to 23 breaths/min.

3.15.1 Varying Ventilation Rate

Pressures and flows for varying ventilation rate at a stroke volume of 400 mL are illustrated in Figures 3.29 and 3.30.

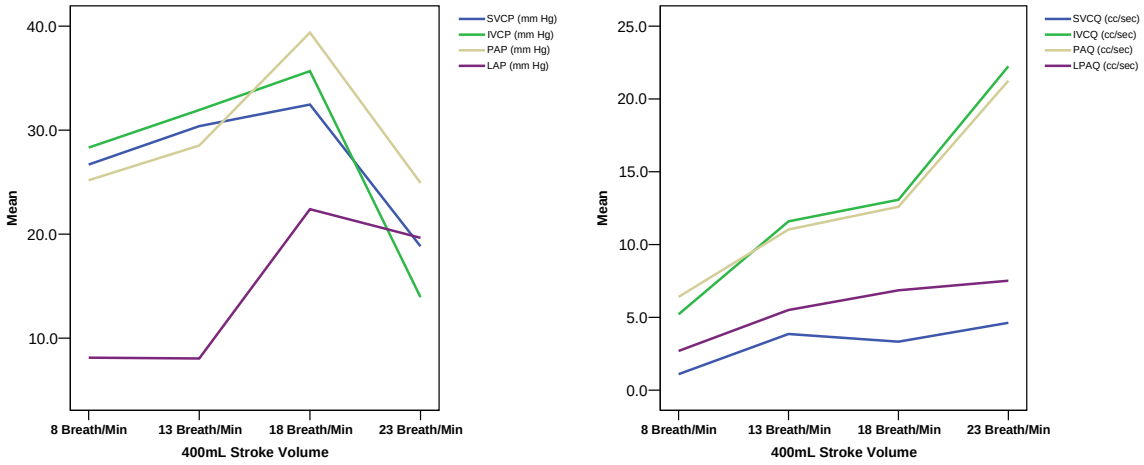

A **B**

Figure 3.29 Mean values for the total cavopulmonary connection with Y-shaped extacardiac shunt (TCPY) illustrating A) pressures (P) and B) flows (Q) for superior vena cava (SVC), inferior vena cava (IVC), pulmonary artery (PA), and left atria (LA) varying ventilation rates keeping stroke volume constant at 400mL.

All pressures increased significantly with increasing respiratory rates keeping stroke volume constant. However, sharp declines occurred at rates over 18 breaths/min (Figure 3.29). IVC flow increased as respiration increased. Furthermore, SVC and LPA flows significantly increased at a lower rate as ventilation increased. LAP pressures increased as rates increased. Hemodynamic variable percent changes with varying ventilation rate are shown in Table 3.8. At a stroke volume of 400mL, SVR and PVR decreased as rate increased. SVCQ, IVCQ, PAQ, and AOQ increased as rate increased. For 500mL stroke volume, SVR and PVR increased as rate increased. At higher stroke volumes, rate increased slightly or had minimal effect on resistances. Cardiac output decreased with rate at higher stroke volumes. Rate had minimal effect on pressures for all stroke volumes examined, except for an increase in pressures at 400 mL as rate increased. LAP increased as rate

increased for all stroke volume settings. Maximum rates produced marked decreases in flows as stroke volumes increased.

Parameter		TCPY HEMODYNAMIC VARIABLE PERCENT CHANGE										
		LPAQ	MPAQ	SVCQ	IVCQ	AOP	SVCP	IVCP	LAP	LVP	MPAP	AOQ
Stroke Volume (mL)	Rate (breath/min)											
500	8	0	0	0	0	0	0	0	0	0	0	0
	13	26	3	-21	5	11	3	1	33	12	3	3
	18	18	3	41	-3	0	-1	0	35	-5	-1	5
	23	-3	-8	14	-2	-8	-3	-3		-8	-3	-4
600	8	0	0	0	0	0	0	0	0	0	0	0
	13	2	2	-30	-1	-5	-5	-5	-6	-6	-6	2
	18	1	-13	18	-10	-15	-4	-3	12	-12	-4	6
	23	-43	-48	-17	-22	-29	-14	-11	-28	-36	-14	-26
700	8	0	0	0	0	0	0	0	0	0	0	0
	13	15	7	-1	0	8	-2	-3	-4	6	-3	6
	18	13	-6	8	-3	-7	-9	-7	0	1	-9	14
	23	-19	-47	-2	-7	-13	-7	-6	-31	-19	-8	-10
800	8	0	0	0	0	0	0	0	0	0	0	0
	13	-9	-8	-20	14	-10	4	3	0	-14	3	-8
	18	2	-1	-9	-1	3	-3	-3	-32	7	-2	-1
	23	-74	-69	14	-40	-37	-27	-17	-18	-53	-25	-37

Table 3.8 Percent change in measured hemodynamic variable in the total cavopulmonary connection with Y-shaped graft (TCPY). A ventilation rate of 8 breaths/min was used for reference.

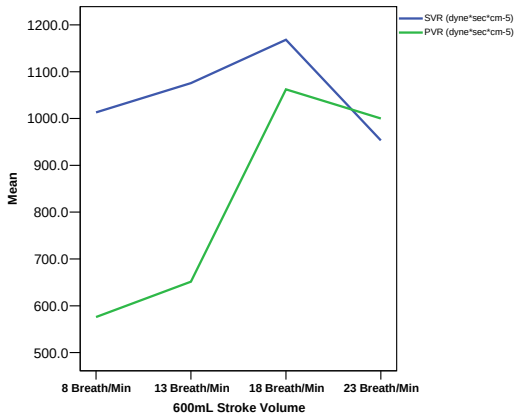

Figure 3.30 Systemic vascular resistance (SVR) and pulmonary vascular resistance (PVR) for the total cavopulmonary circulation with Y-shaped extracardiac shunt (TCPY) under varying respiration rates keeping stroke volume constant.

Pulmonary vascular resistance increased with respiration rate. At low stroke volumes SVR decreased sharply as rate increased. As stroke volume increased, SVR declined less steeply than at lower volumes with increasing rates.

3.15.2 Varying Stroke Volume

Varying stroke volume keeping respiration rate the same for the TCPY connection is illustrated in Figures 3.31 and 3.32.

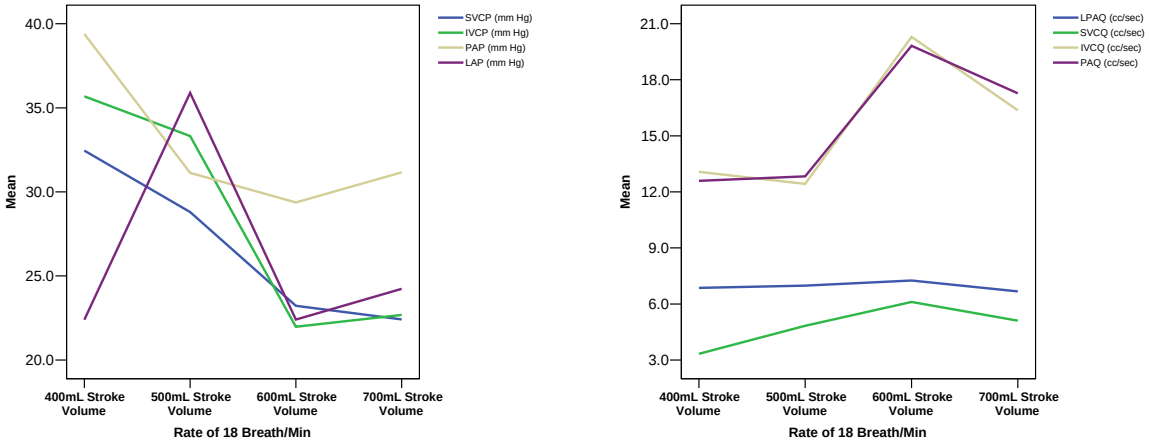

A **B**

Figure 3.31 Mean values for the total cavopulmonary connection with an Y-shaped extracardiac shunt (TCPY) illustrating A) pressures (P) and B) flows (Q) for superior vena cava (SVC), inferior vena cava (IVC), pulmonary artery (PA), and left atria (LA) varying stroke volume keeping respiration rate constant.

All pressures dropped significantly as stroke volume increased from 400 to 700 mL. Flows increased as stroke volume increased until high volumes where a reduction in flow occurred. Hemodynamic variable percent changes with varying stroke volume are shown in Table 3.9.

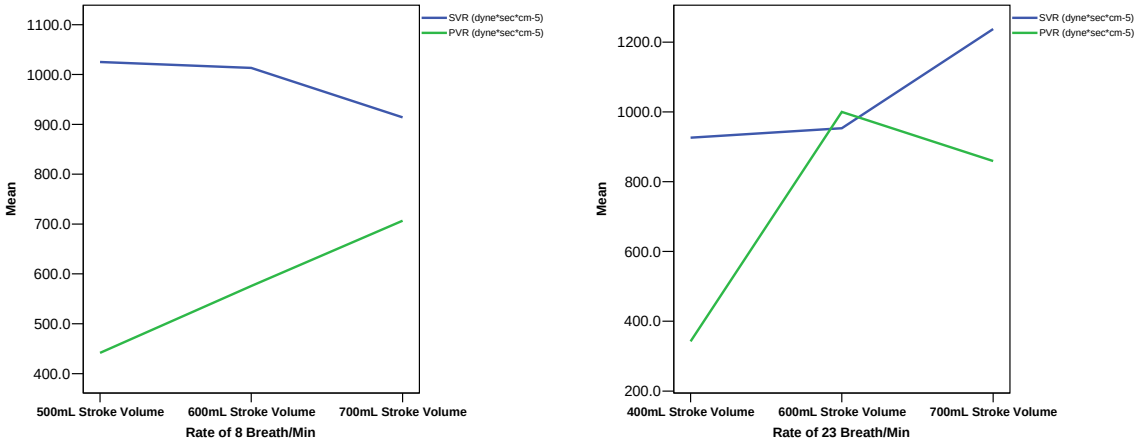

Figure 3.32 Systemic vascular resistance (SVR) and pulmonary vascular resistance (PVR) for the total cavopulmonary with Y-shaped graft (TCPY) circulation under varying stroke volumes keeping ventilation rate constant.

PVR increased significantly as stroke volume increased at various rates. Systemic vascular resistance decreased as volume increased for low rates and increased as stroke volume increased for high rates.

		TCPY Hemodynamic Variable Percent Change										
Parameter		LPAQ	MPAQ	SVCQ	IVCQ	AOP	SVCP	IVCP	LAP	LVP	MPAP	AOQ
Rate (breath/min)	Stroke Volume (mL)											
8	400	0	0	0	0	0	0	0	0	0	0	0
	500	-8	3	33	3	13	-1	0	8	29	0	-9
	600	7	5	44	9	21	6	5	11	23	5	4
	700	24	16	30	24	16	10	8	50	15	10	-3
	800	-20	-20	13	14	15	-7	-5	7	24	-6	3
13	400	0	0	0	0	0	0	0	0	0	0	0
	500	26	3	-21	5	11	3	1	33	12	3	3
	600	2	2	-30	-1	-5	-5	-5	-6	3	-6	2
	700	15	7	-1	0	8	-2	-3	-4	6	-3	6
	800	-9	-8	-20	14	-10	4	3	0	-14	3	-8
18	400	0	0	0	0	0	0	0	0	0	0	0
	500	18	3	41	-3	0	-1	0	35	-5	-1	5
	600	1	-13	18	-10	-15	-4	-3	12	-12	-4	6
	700	13	-6	8	-3	-7	-9	-7	0	1	-9	14
	800	2	-1	-9	-1	3	-3	-3	-32	7	-2	-1
23	400	0	0	0	0	0	0	0	0	0	0	0
	500	-3	-8	14	-2	-8	-3	-3	0	-8	-3	-4
	600	-43	-48	-17	-22	-29	-14	-11	-28	-36	-14	-26
	700	-19	-47	-2	-7	-13	-7	-6	-31	-19	-8	-10
	800	-74	-69	14	-40	-37	-27	-17	-18	-53	-25	-37

Table 3.9 Percent change in measured hemodynamic variables in the total cavopulmonary connection with Y-shaped graft (TCPY) incrementing rate at 5 breaths/min and varying stroke volume. The minimum parameter setting (400 mL stroke volume) was used as the reference.

At a rate of 8 breaths/min, PVR increased with stroke volume. Stroke volume had minimal effect on SVR at both minimum and maximum stroke volume settings. Middle range settings (13 and 18 breaths/min) produced decreases in SVR as stroke volume increased. PVR decreased at a rate of 13 breaths/min as stroke volume increased. At higher rates, PVR increased for low stroke volumes and then stabilized at higher stroke volume settings. All pressures showed minimal changes at higher rates with changing stroke volume. Lower rates decreased the pressures as stroke volume increased.

3.16 Discussion

For a better understanding of overall ventilation effects, comparisons between different Fontan modifications are illustrated in the following figures. Power losses were examined and are discussed in Chapter IV. Previous sections described ventilation parameters within each Fontan modification. This section focuses on the "big picture" as to overall averages at different parameter settings between Fontan modifications.

SVR and PVR for varying stroke volumes are shown in Figure 3.32.

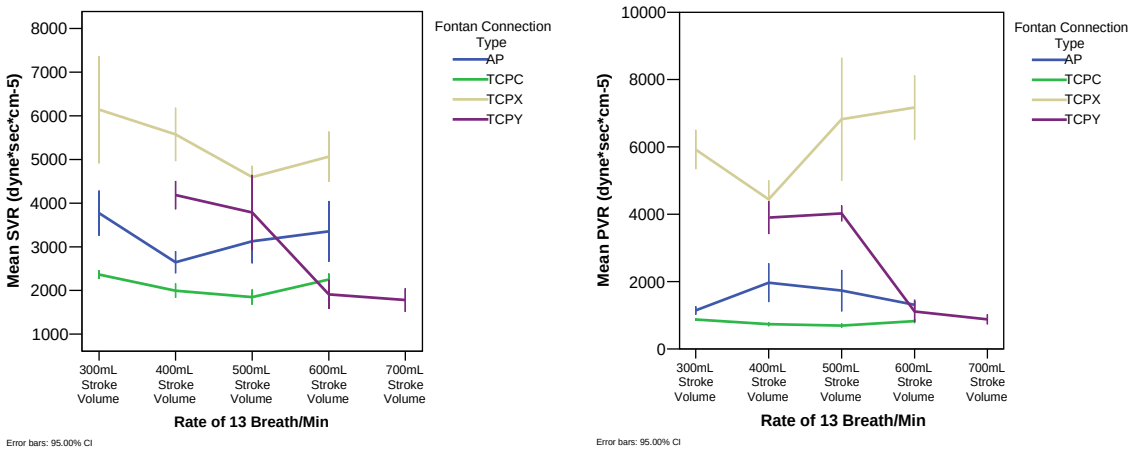

A **B**

Figure 3.33 A) Systemic (SVR) and B) pulmonary vascular resistance (PVR) comparison between Fontan modifications (AP=atriopulmonary; TCPC=extracardiac without shunt; TCPX=extracardiac with shunt; TCPY=extracardiac with Y-shaped connection) varying stroke volume (mL) with constant ventilation rate (breaths/min).

The TCPX connection maintained the highest SVR and PVR for each stroke volume setting. SVR and PVR remained relatively stable with varying stroke volume in the AP, TCPC, and TCPX modifications. As stroke volume increased, TCPY SVR reduced significantly. SVR values between the connections were significantly different from each other. The largest change in SVR and PVR occurred within the TCPY connection with a sharp decrease at higher stroke volumes. Minimal stroke volume effects on SVR and PVR were observed in the AP and TCPC connections. As stroke volume increased, PVR increased in the TCPC connection. Lowest resistances were observed in the AP and TCPC connections. The TCPC does not utilize a synthetic graft and the AP connection utilizes the RA for possible aid in

additional blood flow and pulsatility. Data were not available for the TCPY connection at a stroke volume of 300mL and therefore not displayed.

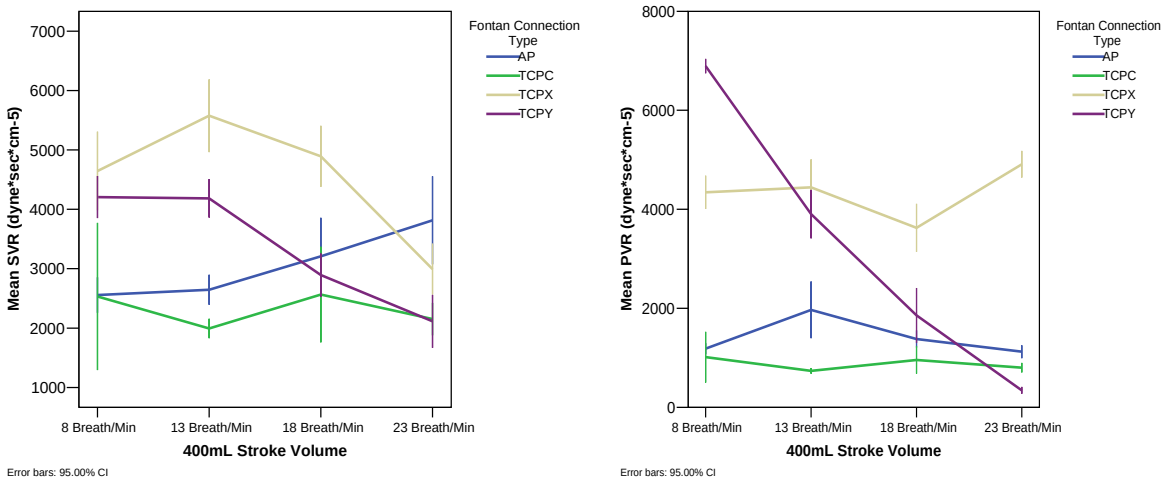

A **B**

Figure 3.34 A) Systemic (SVR) and B) pulmonary vascular resistance (PVR) comparison between Fontan modifications (AP=atriopulmonary; TCPC=extracardiac without shunt; TCPX=extracardiac with shunt; TCPY=extracardiac with Y-shaped connection) varying ventilation rate (breaths/min) with constant stroke volume (400mL).

Similar to varying stroke volume, respiration rates had minimal effect on PVR for the AP and TCPC connections. TCPX had significantly higher PVR and SVR over the ventilation range. TCPY PVR decreased dramatically as the ventilation rate increased. Higher ventilation rates lowered SVR in extracardiac shunt modifications (TCPX and TCPY). Significant differences were observed between all modifications. Higher rates raised SVR in the AP connection. Varying rates caused reductions in both SVR and PVR for the TCPY modification. For comparison, normal values for SVR are approximately 2000 dyne·sec·cm^{-5} for SVR and 500 dyne·sec·cm^{-5} for PVR.

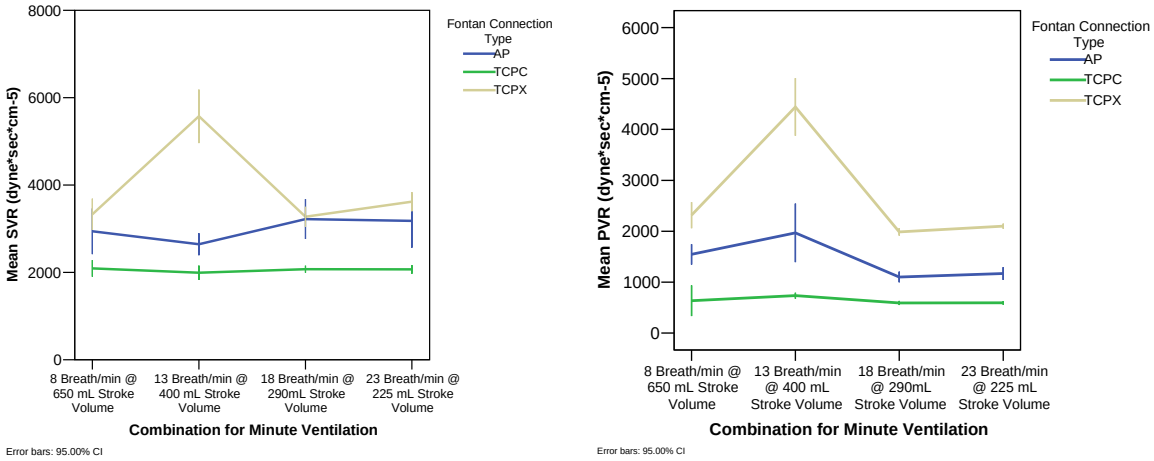

A **B**

Figure 3.35 A) Systemic (SVR) and B) pulmonary vascular resistance (PVR) comparison between Fontan modifications (AP=atriopulmonary; TCPC=extracardiac without shunt; TCPX=extracardiac with shunt; TCPY=extracardiac with Y-shaped connection) varying minute ventilation combinations keeping minute ventilation constant at 5200 mL/min.

Minute ventilation combinations (Figure 3.34) had minimal effects for any Fontan modification examined. Increases at a rate of 13 breaths/min and a stroke volume of 400mL produced increases in both SVR and PVR. Otherwise, resistance remained stable. Significant differences were present between modification types, with TCPX having the largest resistance values.

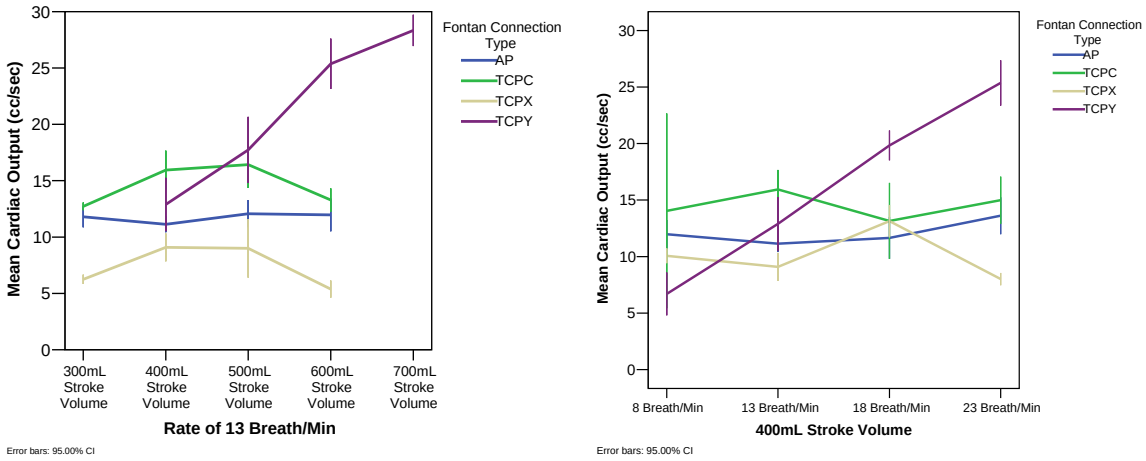

A **B**

Figure 3.36 Cardiac Output comparison between Fontan modifications (AP=atriopulmonary; TCPC=extracardiac without shunt; TCPX=extracardiac with shunt; TCPY=extracardiac with Y-shaped connection) A) varying stroke volume (mL) with constant ventilation rate (breaths/min) and B) varying ventilation rate.

Cardiac output had minimal fluctuations in the TCPC and TCPX connections producing lower CO at minimum and maximum stroke volumes. CO remained stable for AP circulation over both volume and rate ranges. CO increased significantly for the TCPY connection under both increased stroke volumes and increased ventilation rates. As with varying stroke volume, ventilation rate had minimal effect on CO for AP, TCPC, and TCPY modifications.

Blood flow contributions from the caval system as well as blood flow distribution to the right and left lungs has become an area of interest between connections. An ideal connection would minimize power losses and provide normal flow distributions to the right and left lungs. Figure 3.37 illustrates blood flow contributions from the IVC and SVC and percentage of blood flow to the left lung (%LPAQ).

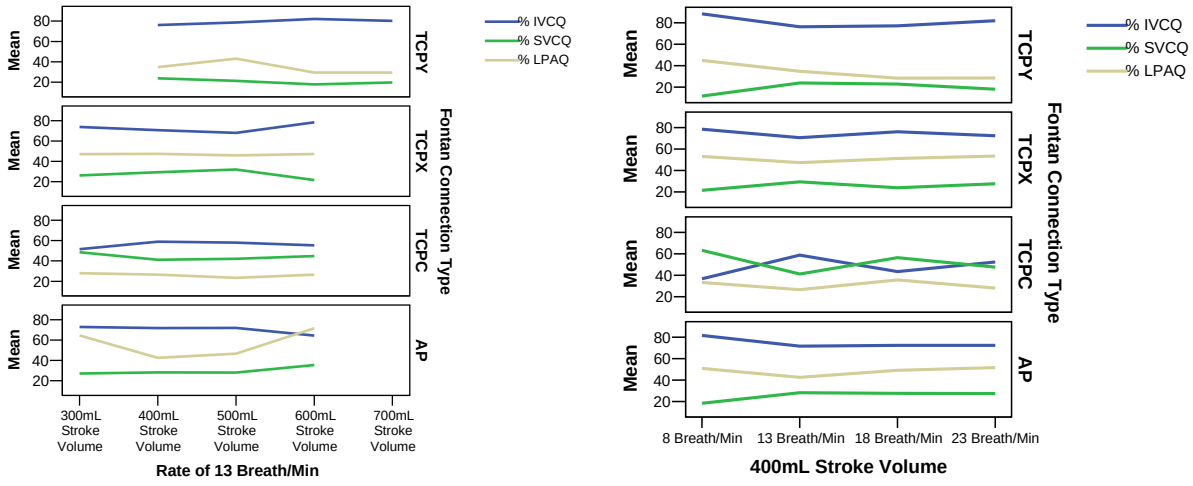

A **B**

Figure 3.37 Blood flow percentage contributions of the inferior vena cava (IVCQ), superior vena cava (SVCQ), and percent of blood flow distributed to the left lung (LPAQ) under different Fontan modifications. AP=atriopulmonary; TCPC=extracardiac without shunt; TCPX=extracardiac with shunt; TCPY=extracardiac with Y-shaped connection for both A) varying stroke volume and B) varying ventilation rate.

IVC blood flow percentage averaged 82%, 75%, 72%, and 78% in the AP, TCPC, TCPX, and TCPY circulation respectively compared to an average normal %IVCQ of 78%. Normal circulation blood flow percentage contributions to the left lung averaged 42%. For the Fontan modifications, %LPAQ averaged 52%, 29%, 48%, and 32% in the AP, TCPC, TCPX, and TCPY circulations. Minimal variations were observed for all flows except for a decreased %LPAQ as ventilation rate increased in the TCPY circulation.

As described in earlier sections, ventilation rate and stroke volume had significant results within the Fontan modifications at specific rates and volumes. Overall, minimal

differences were observed. Figure 3.38 shows average overall pressures and flows for varying ventilation rates between Fontan modifications.

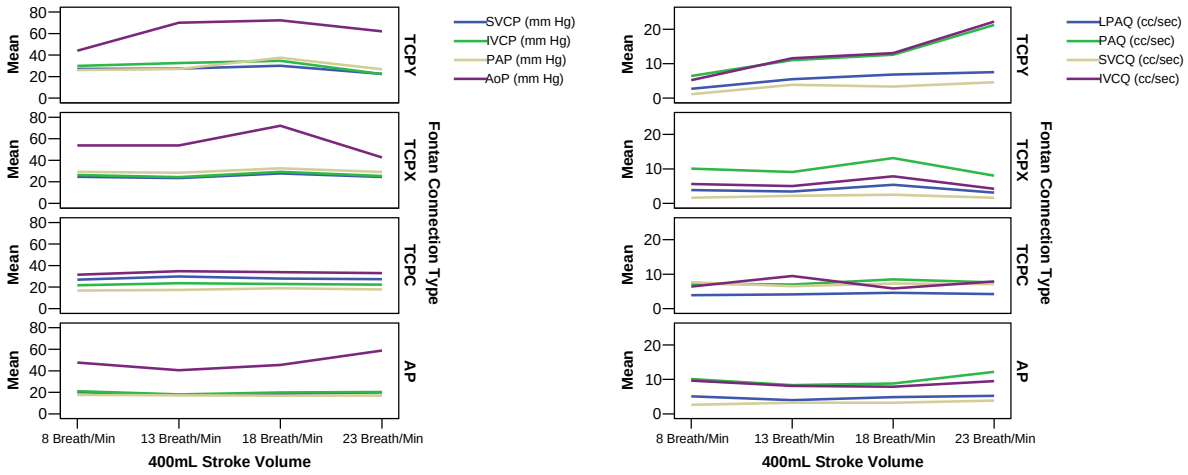

A **B**

Figure 3.38 A) Pressures (P) and B) flows (Q) of the inferior vena cava (IVC), superior vena cava (SVC), main pulmonary artery (PA), and aorta (AO) under different Fontan modifications. AP=atriopulmonary; TCPC=extracardiac without shunt; TCPX=extracardiac with shunt; TCPY=extracardiac with Y-shaped connection for varying ventilation rate.

Minimal changes occurred for all pressures and flows in the TCPC and TCPX circulations. Pressures decreased and flows increased as rate increased for the TCPY connection. AOP increased as rate increased. Results for varying stroke volume are shown in Figure 3.39.

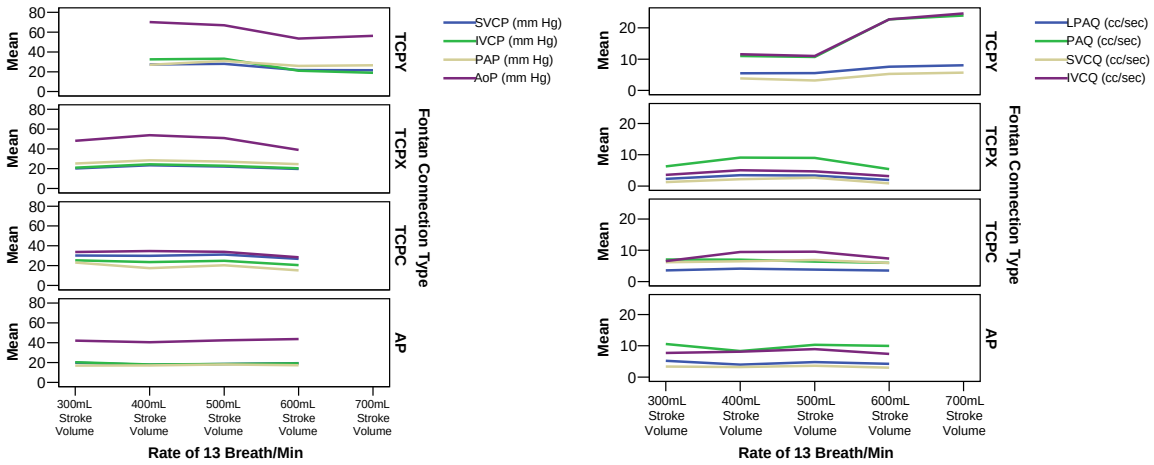

A **B**

Figure 3.39 A) Pressures (P) and B) flows (Q) of the inferior vena cava (IVC), superior vena cava (SVC), main pulmonary artery (PA), and aorta (AO) under different Fontan modifications. AP=atriopulmonary; TCPC=extracardiac without shunt; TCPX=extracardiac with shunt; TCPY=extracardiac with Y-shaped connection for varying ventilation rate.

Similar to varying ventilation rate, stroke volume manipulations did not show marked changes in pressures and flows for Fontan modifications. As with rate, PAQ and LPAQ increased as stroke volume increased.

3.17 Summary

Significant hemodynamic changes occurred between anatomic Fontan connections. Systemic and vascular resistances differed according to procedure. Overall, stroke volume and ventilation rate had a predominantly instantaneous effect on hemodynamics, but minimal effects on averages. Promising hemodynamics were observed in the novel TCPY procedure. Flow ratios, flow distribution, and resistances approached normal circulation values for the

TCPY circulation. However, systemic pressures remained high that may lead to postoperative complications. To improve recovery time and perfusion efficiency, ventilation management may be beneficial if prescribed dependent on Fontan procedure. Limitations to this study are the acute, open chest study performed on an animal with previously normal circulation. Hemodynamic adaptations are not available. Hemodynamics need to be examined on an individual lamb basis in order to rule out variability within the subjects. This research focused on overall hemodynamic measurements. Variability due to lamb weight and CO need to be addressed. See Appendix I for a manuscript draft of summarized results.

CHAPTER IV

ENERGETICS OF POSITIVE PRESSURE VENTILATION IN LAMB FONTAN CIRCULATIONS

4.1 Abstract

Introduction. Approximately two out of every thousand children in the USA are born with congenital heart defects that impair the right heart and atriopulmonary pathway. As a result, there is only a single effective ventricle. Surgical treatment for these defects, termed "Fontan" repairs, consist of bypassing the right side of the heart and connecting the systemic and pulmonary circulations in series with the univentricular pump. However, these surgical repairs are palliative, not curative. Surgical repairs severely alter the systemic and pulmonary hemodynamics. Standardization of repair designs that are specific for different anatomical and physiological variations has not been developed. Positive pressure ventilation (PPV) has been shown to have a deleterious effect on children after undergoing cardiopulmonary bypass and Fontan staging operations. Intensive care duration is critical on removal of PPV. Surgical management strategies and ventilation therapies need to be developed in order to maximize hemodynamic energy and expedite recovery. Computer simulations, in-vitro studies, and computational fluid dynamic analyses that incorporate ventilation parameters will provide a better understanding of Fontan circulations and aid in

management optimization and help prescribe ventilation therapy strategies in operative conditions. In order to provide a more accurate model of Fontan hemodynamics, ventilation parameters need to be instituted in simulation models. The aim of this study is to examine power gains/losses under varying PPV parameters in order to aid in determining an optimal surgical management strategy as well as assist in the development of an accurate computer simulation model. ***Methods.*** In vivo studies were performed in lambs averaging 15 kilograms where a Fontan circulation is created. Four Fontan modification procedures were examined: the atriopulmonary (AP) connection, total cavopulmonary connection without a synthetic graft (TCPC), extracardiac total cavopulmonary connection with graft (TCPX), and the total cavopulmonary connection using a Y-shaped graft (TCPY). Multiple pressure and flow transducers were introduced. Ventilation manipulation varying ventilation rate, stroke volume, and minute ventilation was performed under both normal and Fontan circulations. Data were recorded at a rate of 200 Hertz for episodes of 5.12 seconds or 1024 data points/episode. Data analysis was performed using MATLAB^{TM}. Power gains/losses were calculated throughout multiple respiratory cycles and averaged. Kinetic energy was neglected and an average beat analysis of the mean and the first twenty harmonics was performed. **Results** *AP.* Average power losses were 4.3mW over varying ventilation rate. Systemic power losses were 26% over low ventilation frequencies. Low stroke volumes displayed power losses averaging 13.8%. As stroke volume increased, SVC power gained 15.4% while IVC power had minimal changes. SVC power decreased 12.8% while IVC power gained a maximum of 21.0% over constant minute ventilation manipulation. Neither frequency nor stroke volume had significant effects on MPA power. *TCPC.* Lower rates increased power losses in the SVC and decreased losses in the IVC. The SVC power gained

11.2% as stroke volume was increased. Constant minute ventilation had mild effects on SVC power loss, but as ventilation frequency increased, IVC energy gained increased significantly. Overall power losses were greatest at low rates and high volumes (12.2mW). No significant power losses were present for constant minute ventilation manipulations. *TCPY.* At low rates, increasing stroke volume significantly increased IVC, SVC, and LPA power by 221.3%, 133.4% and 32.0% respectively. As rate increases, increasing stroke volume produced increasing power losses in both systemic and pulmonary vessels. TCPY geometry favored increasing LPA power as stroke volume is increased. Moderate rates in conjunction with high stroke volumes increased systemic power in both the IVC and SVC. Moderate rates with moderate stroke volume increased power losses. Ventilation frequency had a greater effect on power than stroke volume. ***Conclusions.*** Significant differences in power occurred across varying stroke volume and ventilation rate for all Fontan modifications examined. Power losses significantly differ across connection types, emphasizing the importance of procedure geometry and age of operation to prescribing ventilation strategies. Results may provide insight on PPV management and peri- and postoperative therapeutics. A limitation to this study is that this is an open chest acute study, which does not allow the animal to undergo staging procedures to adapt to the new geometry and circulation. Furthermore, vessels were of normal size and compliance and were not preconditioned with an increased pulmonary resistance.

4.2 Introduction

Approximately two out of every thousand children in the United States are born with congenital heart defects that impair the right heart and atriopulmonary pathway. As a result, there is only a single effective ventricle. Surgical treatment for these defects, termed

"Fontan" repairs, consist of bypassing the right side of the heart and connecting the systemic and pulmonary circulations in series with the univentricular pump. However, these surgical repairs are palliative, not curative. Cardiologists report that patient populations with these defects comprise 20% of their caseload and at least 50% of their time. Surgical repairs severely alter the systemic and pulmonary hemodynamics. Also, the creation of a low-pressure system further leads to numerous postoperative complications (e.g. venous hypertension, liver failure, and/or pulmonary hypotension) requiring lifelong, intensive medical attention. Standardization of repair designs that are specific for different anatomical and physiological variations has not been developed. Therefore, it is necessary to optimize the surgical pathway as well as develop pre-, peri-, and postoperative management methods to understand the precise hemodynamic changes following implementation of the Fontan circulation. The surgical design will always be the starting point of functional outcome studies. In order to develop adequate surgical therapeutics and peri- and postoperative management strategies, a study of the acute changes from normal to various Fontan anatomies and the resulting changes in hemodynamic variables produced by the new circulation is necessary.

4.3 Specific Aims

The overall hypothesis for this research is that a fundamental understanding of the AP and various total cavopulmonary (TCP) geometries will lead to improved surgical planning and designs and thus improve long term outcomes in patients. In order to address this hypothesis, investigations will address the following specific aim:

> Determine overall power losses of the atriopulmonary (AP) and various total cavopulmonary (TCP) designs under varying physiological parameters.

4.4 Methods

In-vivo animal experiments are performed in lambs. A detailed description of methods and surgical procedures are described in detail in Chapter II. This study examined the AP, TCPX, and TCPY connections. To recap, illustrations of the Fontan modifications of interest are shown in Figure 4.1

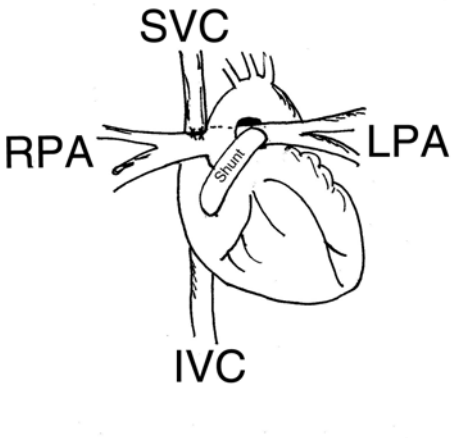

A) Atriopulmonary (AP) connection (AP).

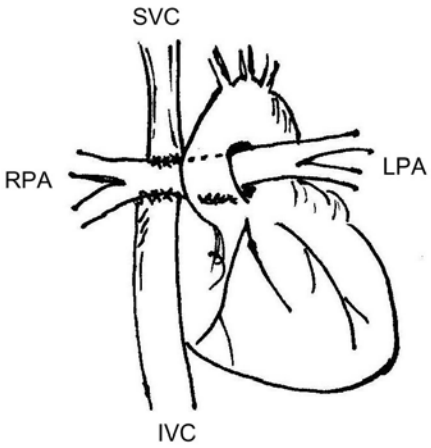

B) Schematic of total cavopulmonary connection without use of synthetic graft (TCPC).

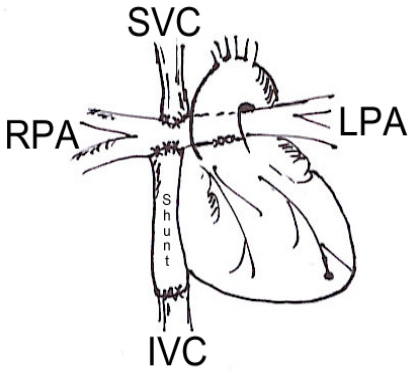

C) Schematic of total cavopulmonary connection with extracardiac graft (TCPX).

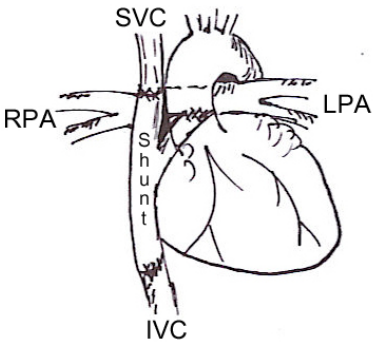

D) Schematic of modified total cavopulmonary connection with a Y-shaped anastomosis (TCPY).

Figure 4.1 Schematics of A) AP, B) TCPC, C) TCPX, and D) TCPY Fontan modifications.

The ventilation protocol (section 2.4) was performed and data recorded. While maintaining a constant respiration rate at 13 breaths/min, stroke volume was varied in 100mL intervals from 300mL to 600mL. Maintaining a constant stroke volume at 400 mL, respiration rate was varied in 5 breaths/minute intervals from 8 to 23 breaths/minute. Furthermore, keeping the air flow rate constant at 5200 mL/minute, four combinations of respiratory rates and stroke volumes were imposed. Multiple episodes of each parameter setting were recorded.

4.5 Power Calculations

Data analysis was performed using MATLAB^{TM} (The Mathworks Inc., Natick, MA). Multiple graphical user interfaces were developed for data analysis. Power gains/losses are calculated throughout multiple respiratory cycles and averaged. Kinetic energy was neglected and an average beat analysis of the mean and the first twenty harmonics was performed via:

$$P = P_o + \Sigma P_k \cos(k\Omega_o t + \theta_k)$$

$$Q = Q_o + \Sigma Q_k \cos(k\Omega_o t + \phi_k) .$$

Where P and Q are pressure and flow respectively, P_o and Q_o are mean pressure and flow, P_k and Q_k are values at each harmonic, and θ_k and ϕ_k are the respective phase angles. Power is divided into its mean and pulsatile terms.

$$\dot{E}_{mean} = P_o * Q_o$$

$$\dot{E}_{pulsatile} = \frac{1}{2}\sum_{k=1}^{20}(P_k * Q_k \cos(\theta_k - \phi_k))$$

Systemic and pulmonary power were calculated via:

$$\dot{E}_{SYS} = \dot{E}_{SVC} + \dot{E}_{IVC}$$

For percent change calculations, minimum parameter settings were used as references: rate of 8 breaths/min, a stroke volume of 300mL, and a constant minute ventilation combination of 8 breaths/min and 650mL stroke volume. Multiple GUIs were developed for data analysis.

4.8 Overall Normal Circulation Energetics

For comparison purposes, normal circulation baseline measurements (ventilation rate of 13 breaths/min at a stroke volume of 400 mL) were acquired. This allowed for overall average examination of the percent changes of different vessels over ventilation parameter settings. Normal circulation results are shown in Figure 4.2. Multiple episodes were acquired and averaged to minimize outliers.

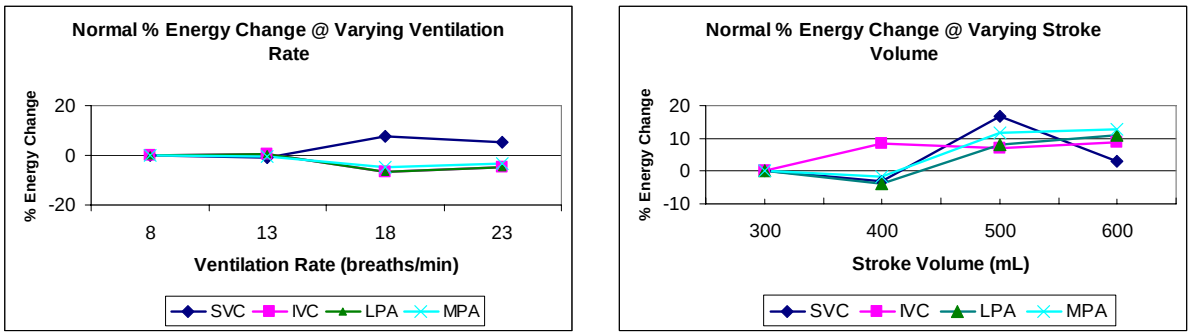

A **B**

Figure 4.2 Percent changes in power in normal circulation under A) varying ventilation rate keeping stroke volume constant at 400 mL and B) varying stroke volume keeping ventilation rate constant at 13 breaths/min. Superior vena cava,

SVC = dark blue; Inferior vena cava, IVC = magenta; Left pulmonary artery, LPA = green; Main pulmonary artery, MPA = cyan. References of a rate of 8 breaths/min and a stroke volume of 300 mL were used.

Minimal power gain/loss variability was shown in the normal circulation with varying ventilation rate. At high rates, power increased in SVC and decreased in IVC and LPA. Stroke volume variations displayed high variability with increased power as stroke volume increased across all vessels. Low stroke volumes had minimal effect on the SVC, LPA, and MPA, but increased the power within the IVC. A summary of findings is in Table 4.1.

Normal Circulation		Ventilation Rate (breath/min)					Stroke Volume (mL)			
% Change in Energy		8	13	18	23		300	400	500	600
SVC		0.0	-0.7	7.6	5.4		0.0	-3.1	16.9	3.1
IVC		0.0	4.8	-2.9	-3.3		0.0	8.5	7.2	8.7
LPA		0.0	0.5	-6.7	-4.9		0.0	2.6	-5.7	-4.7
MPA		0.0	-0.4	-5.0	-3.2		0.0	-4.0	8.0	10.9

Table 4.1 Summary of percent changes in power for normal circulation for superior vena cava (SVC), inferior vena cava (IVC), left pulmonary artery (LPA), and main pulmonary artery (MPA) for varying ventilation rate and stroke volume. A rate of 8 breaths/min and a stroke volume of 300 mL were used for reference.

4.9 Overall AP Circulation Energetics

Overall AP percent changes with varying ventilation rate and stroke volume are shown in Figure 4.3. At ventilation rate of 13 breaths/min, a 22% and 31% decrease in power was observed for the SVC and IVC respectively. At higher rates, MPA energy increased and LPA, SVC, and IVC approached reference values.

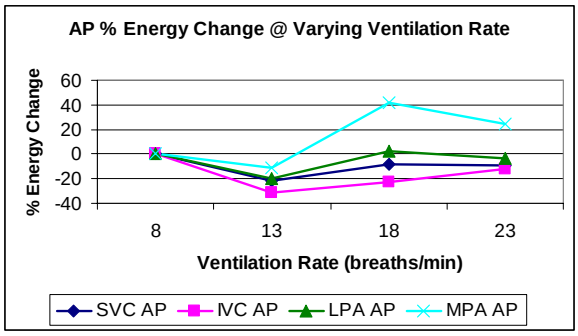

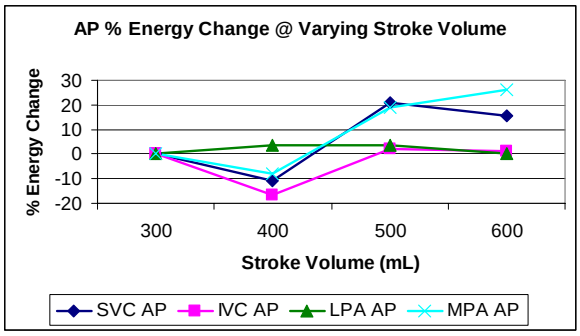

A **B**

Figure 4.3 Percent power changes in atriopulmonary (AP) circulation under A) varying ventilation rate and B) varying stroke volume. Superior vena cava, SVC = dark blue; Inferior vena cava, IVC = magenta; Left pulmonary artery, LPA = green; Main pulmonary artery, MPA = cyan. References used were a rate of 8 breaths/min and a stroke volume of 300 mL.

Stroke volumes displayed an increased in variability. At low volumes, energy decreased by 11%, 16.6%, and 7.8% in the SVC, IVC, and MPA respectively. High stroke volumes increased energy changes in the MPA and SVC. All vessels follow the same trends as both rate and stroke volume increased. Percent change summaries are listed in Table 4.2.

AP Circulation	Ventilation Rate (breath/min)				Stroke Volume (mL)			
% Change in Energy	8	13	18	23	300	400	500	600
SVC	0.0	-22.0	-8.7	-9.4	0.0	-11.0	20.8	15.4
IVC	0.0	-31.1	-22.4	-12.1	0.0	-16.6	2.3	1.2
LPA	0.0	-20.1	2.5	-3.8	0.0	3.6	3.7	0.3
MPA	0.0	-10.7	41.3	24.7	0.0	-7.8	18.8	26.3

Table 4.2 Summary of percent changes in power for the atriopulmonary (AP) circulation for superior vena cava (SVC), inferior vena cava (IVC), left pulmonary artery (LPA), and main pulmonary artery (MPA) for varying ventilation rate and stroke volume. 8 breaths/min and stroke volume of 300 mL were used for reference.

4.10 Overall TCPC Circulation Energetics

Minimal variability occurred as ventilation increased except for an LPA power increase as ventilation rate increased. Similar to AP, a ventilation rate of 13 breaths/min decreased energy in the LPA and MPA. Actual percentage values are summarized in Table 4.3. Stroke volume produced marked changes in power ranging from a decrease in LPA of -15.7% at 500 mL to an increase of 13.2% at a 600 mL stroke volume.

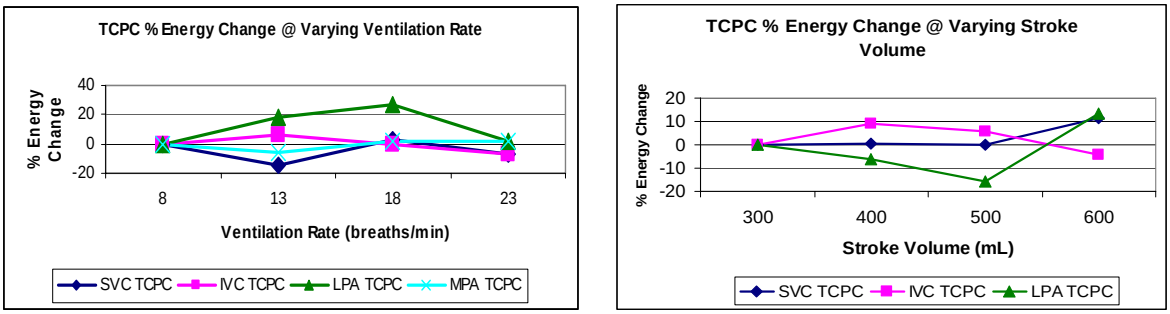

A **B**

Figure 4.4 Percent changes in power for total cavopulmonary connection (TCPC) circulation under A) varying ventilation rate and B) varying stroke volume. Superior vena cava, SVC = dark blue; Inferior vena cava, IVC = magenta; Left pulmonary artery, LPA = green; Main pulmonary artery, MPA = cyan. References of a rate of 8 breaths/min and a stroke volume of 300 mL were used.

IVC showed percent decreases at both high ventilation rates and high stroke volumes. LPA showed inverted results with increased power with ventilation rate and decreased power with increased stroke volume.

TCPC Circulation		Ventilation Rate (breath/min)					Stroke Volume (mL)			
% Change in Energy		8	13	18	23		300	400	500	600
SVC		0.0	-14.8	3.0	-6.5		0.0	0.4	0,2	11.2
IVC		0.0	6.5	-0.3	-7.2		0.0	9.1	5.5	-4.2
LPA		0.0	17.7	27.0	1.7		0.0	-6.3	-15.7	13.2

Table 4.3 Summary of percent power changes for the total cavopulmonary (TCPC) circulation for superior vena cava (SVC), inferior vena cava (IVC), and left pulmonary artery (LPA) for varying ventilation rate and stroke volume. A rate of 8 breaths/min and a stroke volume of 300 mL were used as references.

4.10 Overall TCPX Circulation Energy Changes

Overall TCPX percent energy changes are shown in Figure 4.5.

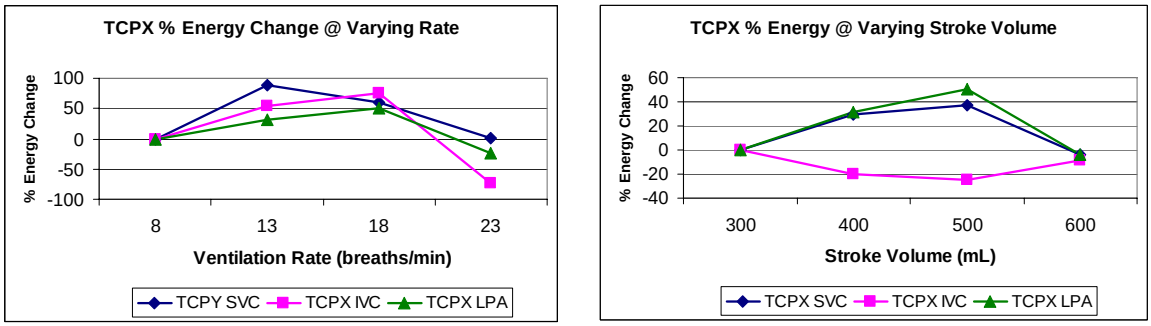

A **B**

Figure 4.5 Percent changes in power for total cavopulmonary connection with extracardiac shunt (TCPX) circulation under A) varying ventilation rate and B) varying stroke volume. Superior vena cava, SVC = dark blue; Inferior vena cava, IVC = magenta; Left pulmonary artery, LPA = green. References of a rate of 8 breaths/min and a stroke volume of 300 mL were used.

Varying ventilation rate had significant results of energy changes in the SVC, IVC, and LPA. As ventilation increased, percent changes increased. At maximum ventilation rates,

energy decreased approximately to baseline values. Similar trends were observed with varying stroke volume. SVC and LPA energy increased with stroke volume. However, IVC decreased by as much as 25% as stroke volume increased. Percentage changes are summarized in Table 4.4.

TCPX Circulation	Ventilation Rate (breath/min)				Stroke Volume (mL)			
% Change in Energy	8	13	18	23	300	400	500	600
SVC	0.0	88.4	60.9	1.5	0.0	29.1	37.0	-3.6
IVC	0.0	54.5	75.1	-74.1	0.0	-19.7	-24.9	-8.7
LPA	0.0	30.6	49.6	-23.1	0.0	31.9	50.3	-4.2

Table 4.4 Summary of percent power changes for the total cavopulmonary with extracardiac shunt (TCPX) circulation for superior vena cava (SVC), inferior vena cava (IVC), and left pulmonary artery (LPA) for varying ventilation rate and stroke volume. A rate of 8 breaths/min and a stroke volume of 300 mL were used as references.

4.11 Overall TCPY Circulation Energy Changes

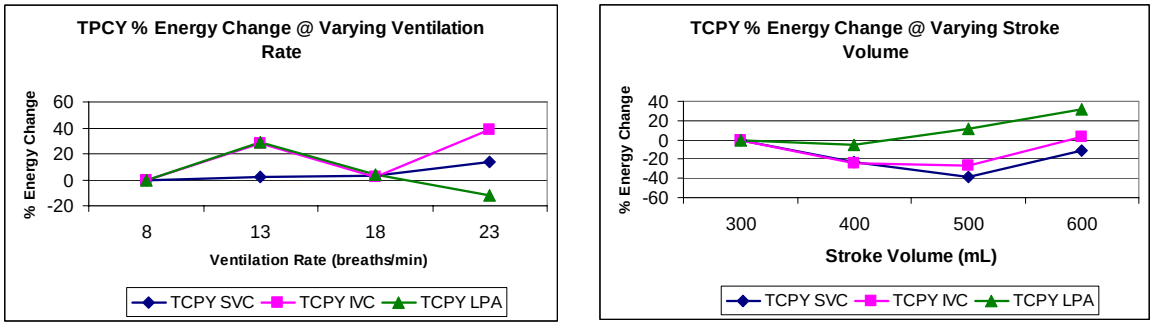

A **B**

Figure 4.6 Percent changes power for total cavopulmonary connection with Y-shaped extracardiac shunt (TCPY) circulation under A) varying ventilation rate and B) varying stroke volume. Superior vena cava, SVC = dark blue; Inferior vena cava,

IVC = magenta; Left pulmonary artery, LPA = green. References of a rate of 8 breaths/min and a stroke volume of 300 mL were used.

A ventilation rate of 13 breaths/min produced increased power in both the IVC and LPA of approximately 28%. At high ventilation rates, variability occurred, producing different results for all vessels (increases in IVC and SVC and a decrease in LPA). Similar trends were observed in the TCPY for varying stroke volume. Decreased power occurred for a stroke volume of 400 mL for the SVC, IVC, and LPA. As stroke volume increased, percent changes in power remained at a decreased rate from baseline for both the SVC and IVC. LPA percent power increased as stroke volume increased. Percent changes are summarized in Table 4.5.

TCPY Circulation	Ventilation Rate (breath/min)				Stroke Volume (mL)			
% Change in Energy	8	13	18	23	300	400	500	600
SVC	0.0	2.0	3.4	13.5	0.0	-23.4	-38.3	-11.3
IVC	0.0	28.0	1.8	38.3	0.0	-24.7	-26.7	3.4
LPA	0.0	28.9	3.9	-12.4	0.0	-5.6	11.4	32.0

Table 4.5 Summary of percent changes in power for the total cavopulmonary with Y-shaped extracardiac shunt (TCPY) circulation for superior vena cava (SVC), inferior vena cava (IVC), and left pulmonary artery (LPA) for varying ventilation rate and stroke volume. A rate of 8 breaths/min and a stroke volume of 300 mL were used as references.

4.11 Power Comparison Between Fontan Modifications

4.11.1 Left Pulmonary Artery Energy Transfer

To analyze the amount of power transferred through the Fontan connection, a ratio of the amount of total power transferred to the left pulmonary artery was calculated. This was calculated.

$$\dot{E}_{LPA}\ (E\ Ratio) = \frac{\dot{E}_{LPA}}{\dot{E}_{SYS}}$$

$$\dot{E}_{SYS} = \dot{E}_{SVC} + \dot{E}_{IVC}$$

Where total systemic power is the addition of SVC and IVC power. Power values were calculated by methods described in section 4.5. Results give a better understanding of the percentage of power distributed to the left lung. Results for varying stroke volume at a ventilation rate of 13 breaths/min are shown in Figure 4.7.

A comparable RPA ratio could not be calculated as placement of a flow probe around the right pulmonary artery was not possible after the Fontan circulation was implemented. The vessel is the main site of the cardiopulmonary anastomoses and the downstream length before the vessel branches into the upper and lower lobes is too short. Given the goals of the study, however, a rough estimation of total power conserved across the connection geometry was needed. Based on available data, equations 7 and 8 were used.

4.11.2 Varying Stroke Volume

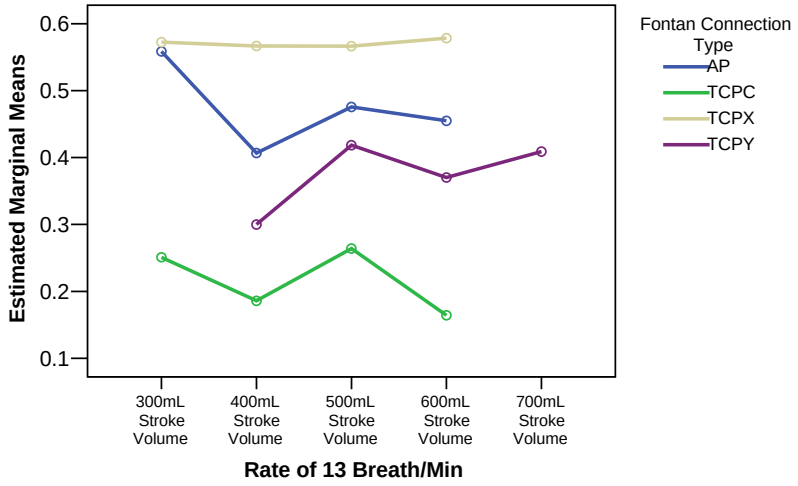

Figure 4.7 Ratio of left pulmonary artery power to total systemic power over varying stroke volumes for the atriopulmonary (AP), total cavopulmonary (TCPC), TCPC with extracardiac shunt (TCPX), and TCPC with Y-shaped graft (TCPY).

Minimal variability with no statistical differences within the connections was observed except for at low volumes in the AP connection. The TCPC connection was the least efficient, transferring an average of 22.6 ± 9.8% of the total power to the right lung. The TCPX delivered the highest power percentage to the left lung at an average of 57.0 ± 5.7%. AP and TCPY averaged 45.0 ± 9.2% and 39.0 ± 9.9% respectively for varying stroke volumes.

4.11.3 Varying Ventilation Rate

LPA energy ratios for varying ventilation rate are shown in Figure 4.8.

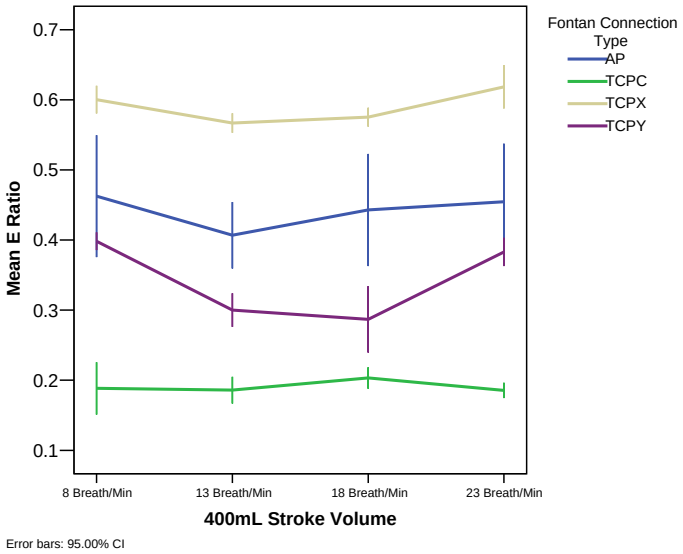

Figure 4.8 Ratio of left pulmonary artery power to total systemic power over varying ventilation rates for the atriopulmonary (AP), total cavopulmonary (TCPC), TCPC with extracardiac shunt (TCPX), and TCPC with Y-shaped graft (TCPY).

Similar to varying stroke volumes, minimal variability occurred within connection type. Statistical differences were observed over middle range stroke volumes for the TCPY connection. Average power transferred to the left lung was 42.7 ± 27.9%, 19.0 ± 4.1%, 58.0 ± 5.8%, and 34.5 ± 11.6% for AP, TCPC, TCPX, and TCPY modifications respectively.

4.11.4 Minute Ventilation Combinations

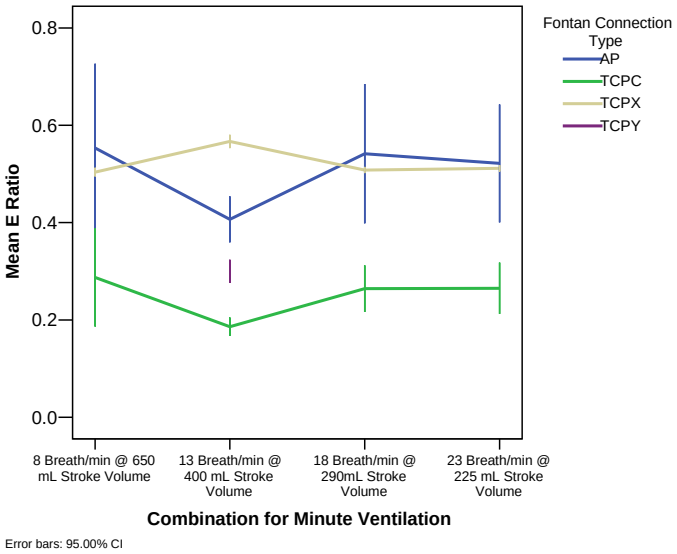

Figure 4.9 Ratio of left pulmonary artery energy to total systemic energy over constant minute ventilation combinations for the atriopulmonary (AP), total cavopulmonary (TCPC), and TCPC with extracardiac shunt (TCPX). Data was not available for TCPY connection.

Statistical differences occurred between the TCPC connection and both AP and TCPX connections. Insufficient data were available for the TCPY comparison. Within each modification, minimal changes occurred over the constant minute ventilation spectrum. Similar left heart powers were observed when varying ventilation rate and stroke volumes were compared. Mean percent transfers were 36.4 ± 3.75%, 23.8 ± 10.3% and 54.7 ± 5.7% for AP, TCPC, and TCPX modifications.

Regardless of rate, stroke volume, and minute ventilation combination, minimal variability was observed within each modification. Furthermore, power transferred to the left lung remained stable within modifications, but were statistically different between modifications. This will require further examination within individual animals studied to help predict transfer ratios based on modification, weight, and cardiac output. For better

energy transfer analysis, a flow probe needs to be implemented on the right pulmonary artery for accurate pressure losses and energy distribution. However, the techniques described above give a good approximation to energy distribution across Fontan modification regions.

4.12 Power losses between Fontan modifications

To examine power losses across various Fontan modifications, a ratio of power leaving the connection to power entering the system was calculated. This was calculated via:

$$\frac{\dot{E}_{OUT}}{\dot{E}_{SYS}}$$

$$\dot{E}_{OUT} = \overline{PAP} * \overline{CO}$$

PAP and CO are expressed as means. These variables have been normalized such that a value of 1 implies complete conservation within the connection to a value of zero being complete power loss across the Fontan connection site.

4.12.1 Varying Stroke Volume

Power conservation ratios for varying stroke volume are shown in Figure 4.10.

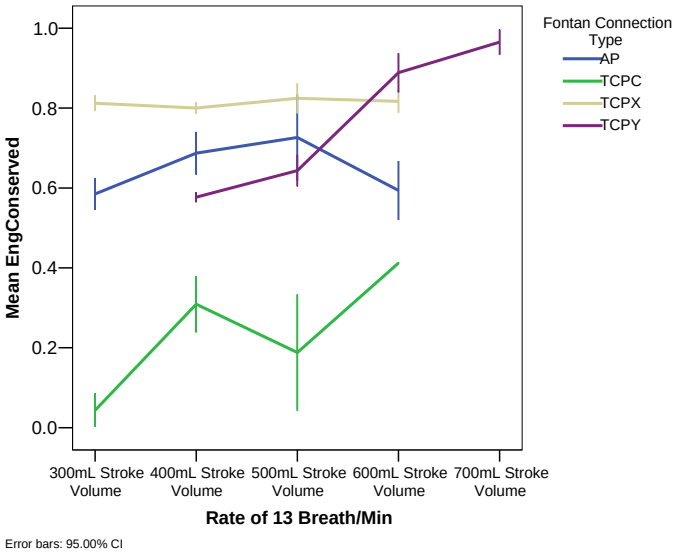

Figure 4.10 Ratio of power leaving Fontan modification connection site to power entering connection site (EngConserved) for the atriopulmonary (AP), total cavopulmonary (TCPC), and TCPC with extracardiac shunt (TCPX). Results are shown for varying stroke volumes at a rate of 13 breaths/min.

High variability with increasing stroke volume was observed for the TCPC and TCPY connections. The TCPX connection preserved the most power throughout the volume spectra except for at high volume where the TCPY connection was more efficient. The AP and TCPX remained relatively consistent over the ventilation range. Efficiencies increased with stroke volume for the TCPY modification.

4.12.2 Varying Ventilation Rate

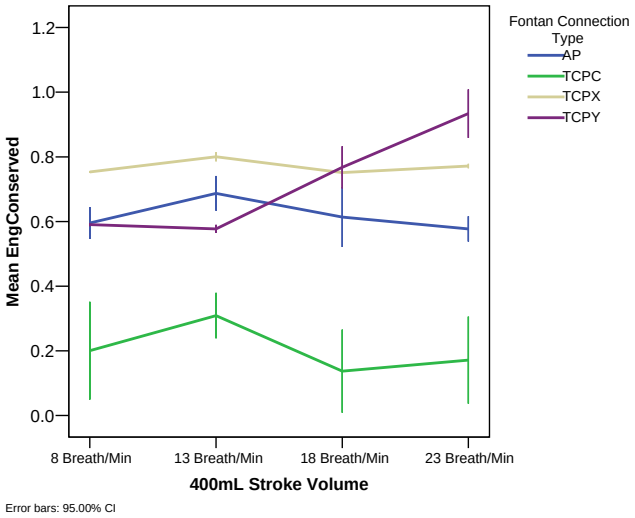

Figure 4.11 Ratio of power leaving Fontan modification connection site to power entering connection site (EngConserved) for the atriopulmonary (AP), total cavopulmonary (TCPC), and TCPC with extracardiac shunt (TCPX). Results are shown for varying ventilation rates.

Energy conservation increased with ventilation rate for the TCPY connection. All other connections maintained consistent power losses over the ventilation rate spectra. Average energy preserved was 61.8%, 20.4%, 76.9%, and 71.7% for the AP, TCPC, TCPX, and TCPY connections. Maximum power conservation occurred in the TCPY connection of 93.4% at a rate of 23 breaths/min.

4.12.3 Constant Minute Ventilation

Minimal variability was observed for all Fontan connection over constant minute ventilation ranges. Data were not available for the TCPY connection. Statistical differences occurred at a rate of 13 breaths/min and a stroke volume of 400mL. The highest energy efficiency observed was the TCPX connection with a 77% energy conservation. The AP was slightly less at an average power loss of 38%. The TCPC had the highest power losses averaging 85%.

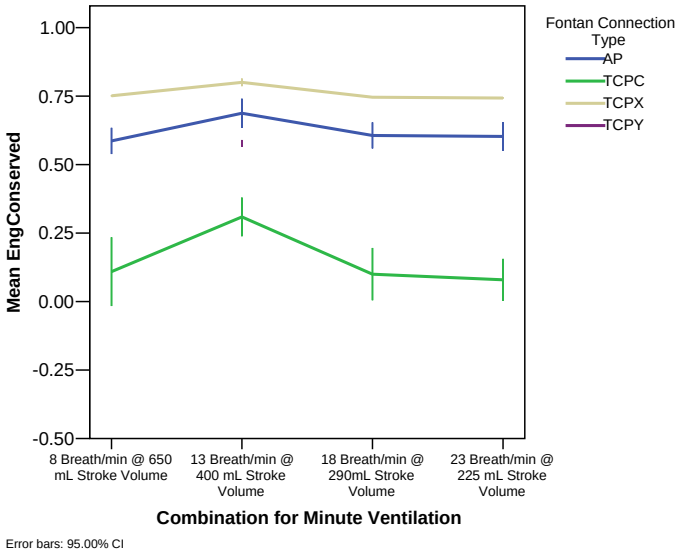

Figure 4.12 Ratio of power leaving Fontan modification connection site to power entering connection site (EngConserved) for the atriopulmonary (AP), total

cavopulmonary (TCPC), and TCPC with extracardiac shunt (TCPX). Results are shown for constant minute ventilation combinations.

4.13 Energetic Summary

Though the number of studies is relatively small, these results demonstrate that our lamb models of Fontan circulations exhibit the expected increased sensitivity to respiration parameters. All models showed increased responsiveness relative to the normal circulation. Furthermore, though the mechanisms are not readily apparent, different connection geometries and materials, even in this simpler open-chest preparation appeared to react differently. The following are examples of generalizations relative group patterns observed. 1) With the exception of the TCPY connections, assuming that higher powers are preferable, results imply that all subjects might have fared better had stroke volumes increased to 500 ml and/or baseline ventilations rates were increased to 18 breathes/minutes. This should have been expected as anesthesiologists prefer to under ventilate and under perfuse during the operative period. 2) With the exception of TCPX, SVC and IVC power appears to go up and down in concert, contrary to the hypothesis that the SVC, which serves the head, is more isolated from respiration influences than the IVC. 3) Likewise, the TCPX appeared to be the most compromised by unusually high or low rates and stroke volumes.

Findings support the concept that ventilation protocols could be designed to specifically improve the peri-operative care of Fontan patients. Rates and stroke volumes could be altered to maximize an appropriate power measurement, assuming such could be monitored. The resolution for this study was relatively large, with step sizes of 5 breaths/minute and 100 ml stroke volumes. Fifty percent power changes were often observed during one step in either direction, indicating that a finer resolution would be helpful. A

logical next step in this direction would be to develop a technique for moving settings up or down based on real-time measurements of power levels. The technique would be evaluated against other protocols used by anesthesiologists and respiration therapists. Our Fontan animal models provide an ideal test bed for a new protocol.

Results presented in this report focus on group findings relative to the effects of ventilation parameters on different Fontan connection geometries. Of perhaps more interest, as has been true for patient studies, will be a more detailed analysis of individual animal data. Waveforms will be subjected to transfer function and correlation analyses to tease out the different influence pathways. Findings will be used to improve lumped parameter models of the entire circulation.

Various labs have reported animal models of the Fontan circulation, but no other lab, to the best of our knowledge, has actually created the single ventricle physiology in animals approximating the size of a child or used the models to investigate the effects of respiration. In vitro and CFD studies, however, have been used extensively to study power losses across different Fontan geometries, focusing particularly on the effects of offset diameter, flaring, nonplanar geometry, compliance mismatch, etc. In general, all studies confirm that caval offsets and flaring decrease energy losses. No attempt was made to control flaring in our animal models. Due to lamb anatomy, TCPC and TCPX configurations had little if any caval offset. The TCPY geometry, however, is somewhat more analogous to a recently described "optiflow" model in which power losses are minimized by avoiding direct impact of SVC and IVC flows.

Using MRI obtained velocity measurements and a viscous dissipation function, power losses across geometries can be estimated in humans. The technology is being used to assess

exercise tolerance in patients with Fontan circulations. Again, due to lack of pressure measurements, power available can not be measured using this technique.

The major advantage of the in vivo studies in lambs is the capability of measuring both pressure and flow waveforms needed for measuring power at input and output locations across the Fontan geometry, which is not yet possible via MRI studies in humans. The major disadvantage, particularly compared to in vitro and CFD studies, is the inability to control parameters. Our power loss percentages ranged from 10% to 70%. These values, however, appeared to be a function of cardiac output, which is perhaps the most important variable for optimization.

CHAPTER V

DETERMINATION OF TIME OFFSETS BY TRANSFER FUNCTION ANALYSIS

5.1 Abstract

Background. Literature has suggested the increased role of respiration and its influences on the hemodynamics of various Fontan circulations. Approximately 1/3 of Fontan hemodynamic energy and blood flow can be contributed to respiration. However, little experimental research has been performed in order to help model the respiration effects on various aspects of Fontan circulations both pre- and postoperatively. Positive pressure ventilation (PPV) is known to have a deleterious effect on children after undergoing cardiopulmonary bypass and Fontan staging operations. Removal of PPV and endotracheal intubation is necessary for leaving the Intensive Care Unit thereby decreasing hospital stay. Surgical management strategies and ventilation therapies need to be developed in order to maximize hemodynamic energy and expedite recovery. Computer simulations, in-vitro studies, and computational fluid dynamic analyses that incorporate ventilation parameters will provide a better understanding of Fontan circulations. Furthermore, ventilation parameter studies will aid in management optimization and help prescribe ventilation therapy strategies in operative conditions. The purpose of this research is to investigate the input/output relationships between the airway pressure and numerous blood vessels of interest in Fontan circulations and to explore the time offsets that occur due to various

ventilation parameters on the pulmonary and systemic circulations. To achieve this, a transfer function analysis is performed. ***Methods.*** In-vivo experiments were performed in lambs. Multiple pressure and flow transducers were introduced. Ventilation manipulations varying ventilation rate, stroke volume, and minute ventilation were performed under both normal and Fontan circulations. Data were recorded at 200 Hertz. Transfer function relationships were investigated using airway pressure as input and aortic pressure (AOP), superior vena cava (SVC) pressure, inferior vena cava (IVC) pressure, and main pulmonary artery (PA) pressure as outputs. Representative time series waveforms along with their associated spectra were computed. Results of normal and three different Fontan circulations were investigated. ***Results.*** Marked changes occurred in driving waveforms between normal and Fontan circulations. Pulsatility was removed corresponding with the removal of the right atria between the atriopulmonary (AP) connection and the various total cavopulmonary (TCP) procedures. Respiration effects with an increase in backflow of the IVC and a subsequent increase in pressures during inspiration. *Normal.* Under normal circulation, varying stroke volume and ventilation rate had minimal effect on the MPA and IVC. Stroke volume had a significant effect ($p < 0.05$) on the SVC, with an increase in stroke volume leading to an increase in time offset. Time offsets averaged -0.15±0.01 secs for the IVC, -0.21±0.01 secs for the SVC, and -0.09±0.02 sec for the MPA. AO delays increased as rates increased for varying ventilation rate and for combinations with high ventilation rates and low stroke volumes. AO delays averaged -0.30 secs. *AP.* For AP conditions, low stroke volume, low ventilation rate, and combinations with low rates and high stroke volume had a significant effect on the IVC, producing greater offsets. Stroke volume had no effect on SVC offset. Low ventilation frequency increased SVC offset. MPA showed no significant changes with

varying frequency or minute combinations. As stroke volume increased, offsets increased for the MPA. Average offset for the AP circulation were -0.35 secs for the IVC, -0.29 secs for the SVC, and -0.11 secs for the MPA. No significant changes occurred in the AO over all ventilation parameters. An average AO delay of -0.33 secs was observed. *TCPX*. Under TCPX conditions, low stroke volume had a significant effect on the IVC, SVC, and MPA creating larger offsets. With varying ventilation rate, low and high frequency extremes had a lesser effect than middle range frequencies producing a larger offset. Constant minute ventilation had minimal effect on the IVC and MPA. Higher rate combinations produced a significantly larger offset in the SVC. Average offsets were -0.77±0.04 secs for the IVC, -0.70±0.11 secs for the SVC, and -0.60±0.03 secs for the MPA. No significant changes occurred in the AO over all ventilation parameters. An average AO delay of -0.29 secs was observed. *TCPY*. For TCPY conditions, the IVC showed no significant differences with varying stroke volumes. Higher stroke volumes significantly decreased the time delay in the SVC. Low stroke volumes produced larger offsets for the MPA. Ventilation frequency had minimal effect on IVC offset. Greater delays were observed in the SVC at low rates than at higher rates. As rate increased, offsets remained unchanged for the MPA. Offsets averaged -0.35 secs for the IVC, -0.27 secs for the SVC, and -0.15 secs for the MPA. Varying ventilation parameters had minimal effect on AO time delays. TCPY average delays were 0.1 sec longer than other Fontan modifications. Overall average AO delays for the TCPY was -0.40 secs. ***Conclusions.*** Instantaneous measurements in animal models enabled the observation and quantification of normal and Fontan circulations not available in humans. Time offsets were determined for the IVC, SVC, PA and AO. Results provide great insight on future directions needed to optimize surgical protocol and reduce power losses. Both

stroke volume and ventilation frequency have significant effect on time offsets between airway pressure and systemic and pulmonary vessels. Furthermore, time offsets are significant across different Fontan geometries, increasing the need to implement them into computer simulation models. The TCPX connection shows the largest time offset. TCPY and AP connections have smaller offsets and display trends similar to normal circulation. A limitation of this study is the open chest acute preparation, which does not allow the animal to undergo the staging procedures experienced by patients to adapt to the new geometry and circulation. In addition, a normal four-chamber heart is being altered. The single ventricle geometry created is not preconditioned with an increased vascular resistance and afterload. In-vivo studies also need to be compared to three-dimensional magnetic resonance images of human patients to determine the accuracy of the flow field and pressure distributions. Parallel studies are being performed that implement these time offsets into an electrical computer model in order to more accurately describe Fontan hemodynamics and aid in determining the optimal surgical pathway.

5.2 Introduction

Positive pressure ventilation (PPV) is known to have a deleterious effect on children after undergoing cardiopulmonary bypass and Fontan staging operations. Removal of PPV and endotracheal intubation is critical to minimizing time in the Intensive Care Unit. Surgical management strategies and ventilation therapies need to be developed in order to maximize hemodynamic energy and expedite recovery. Computer simulations, in-vitro studies, and computational fluid dynamic analysis that incorporate ventilation parameters will provide a better understanding of Fontan circulations. Furthermore, ventilation

parameter studies will aid in management optimization and help prescribe ventilation therapy strategies in operative conditions.

Literature has suggested the increased role of respiration and its influences on the hemodynamics of various Fontan surgical modifications performed in children born with a univentricular heart. Recently, research has shown that approximately one-third of hemodynamic energy and blood flow can be contributed to respiration. However, little experimental research has been performed in order to help model the respiration effects on various aspects of Fontan circulations. This study investigates the input/output relationships between the airway pressure and numerous blood vessels under normal circulation conditions and under three Fontan modification procedures. It is generally accepted that venous return to the heart increases during inspiration and decreases during expiration under normal physiological conditions. This is achieved by the decrease in intrathoracic pressure during inspiration that in turn creates an increase in the pressure difference between the peripheral vessels and the right atrium. Subsequently, this pressure difference facilitates blood flow into the vessels of the chest cavity. Respiration also influences blood flow to the chest via the descent of the diaphragm on the visceral organs during inspiration. The movement of the diaphram physically forces blood motion toward the inferior vena cava during inspiration. With PPV, the opposite effect is observed. Pressures increase and flows decrease during inspiration.

5.3 Specific Aim

The specific aim of this research is to determine the time offsets that occur due to various ventilation parameters on the pulmonary and systemic circulations. Normal and

three modified Fontan circulations were examined and transfer function analyses were performed.

5.4 Surgical Procedures and Ventilation Protocol

Normal circulations and three modifications of the classical Fontan procedure were investigated. The modifications are described in detail in Chapter II. This study examined the AP, TCPX, and TCPY connections. To recap, illustrations of the Fontan modifications of interest are shown in Figure 5.1.

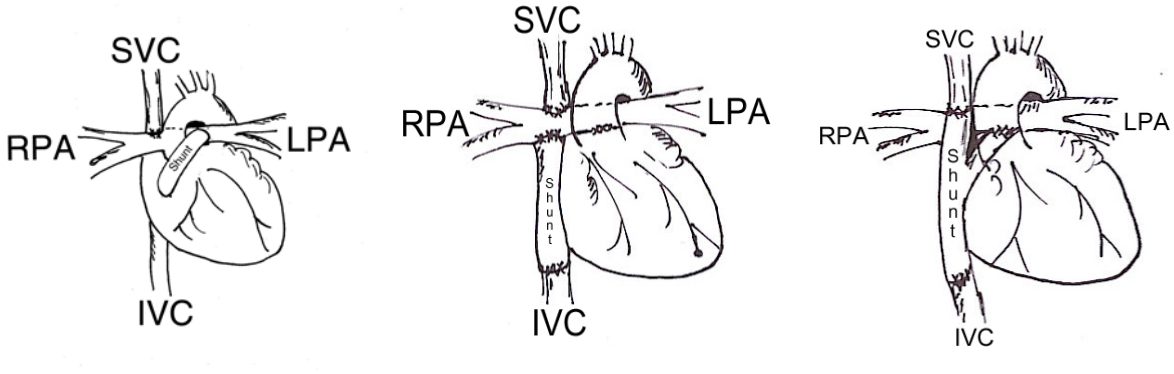

A) Atriopulmonary connection (AP).

B) Schematic of total cavopulmonary connection with extracardiac graft (TCPX).

C) Photograph of modified total cavopulmonary connection (TCPY).

Figure 5.1 Illustrations of the A) AP, B) TCPC, and C) TCPY Fontan modifications.

The ventilation protocol (section 2.4) was administered under both normal and Fontan circulations. While maintaining a constant ventilation rate, stroke volume is varied in 100 mL intervals from 300 to 700 mL/breath. Next, while maintaining a constant stroke volume, the ventilation rate is varied in 5 breaths/minute intervals from 8 to 23 breaths/minute. Furthermore, keeping air flow rate constant at 5200 mL/minute, all combinations of ventilation rates and stroke volumes are performed. Multiple episodes of each parameter setting are recorded.

5.5 Data and Statistical Analysis

Data analysis was performed using MATLAB (The Mathworks Inc., Natick, MA). Multiple graphical user interfaces were developed for data analysis. Statistical analysis was performed using the SPSS (SPSS Inc., Chicago, Illinois) software package. All values were expressed as mean ± SD. The univariate and repeated measures analysis of variance was used to determine whether group-average time offsets (determined from the transfer function phase angles) were significantly different at each of the varying tidal (stroke) volumes and at each breathing frequency. A p-value < 0.05 was regarded as significant. The post hoc Bonferroni test was used in order to compensate for type I error with multiple comparisons and the Tukey honestly significant difference test was used for multiple comparison tests across experimental groups.

Transfer function analysis is a widely used technique for determining relationships between cardiovascular signals and respiration. Input/output transfer function relationships were investigated using the airway pressure (AIRP) as input and aortic pressure (AOP), superior vena caval pressure (SVCP), inferior vena caval pressure (IVCP), and main pulmonary artery pressure (MPAP) as outputs. Representative time series along with their associated spectra were computed. Complex transfer functions, H (*f*), were computed for normal and Fontan circulations according to the respiration protocol described and calculated via:

$$H(f) = \frac{G_{IO}(f)}{G_{II}(f)}$$

where I is the input, O is the output, G_{IO} is the cross-spectra, and G_{II} is the auto-spectra for each relationship. The resulting frequency response phase angles $\theta(f)$ were estimated using:

$$\theta(f) = \tan^{-1}[\frac{H_{imaginary}(f)}{H_{real}(f)}]$$

Negative phase values, characterized as “phase lag”, indicate that changes in the input precede changes in the output. When changes in the output precede changes in the input, phase values are positive and are characterized as “phase lead”. The corresponding phase values at the respiration rates investigated were converted to time offsets. Offsets are the time it takes for one physiological signal to respond to a change in another signal. Negative time offsets indicate peaks in input preceding peaks in output. Positive offsets indicate peaks in output preceding peaks in input. Group averaging at each respiration parameter was performed.

5.6 Normal Circulation Results

For comparison, the normal circulation ventilation protocol was performed and time offsets were calculated. Systemic and pulmonary waveforms are illustrated along with AIRP to demonstrate respiration effects (Figure 5.2).

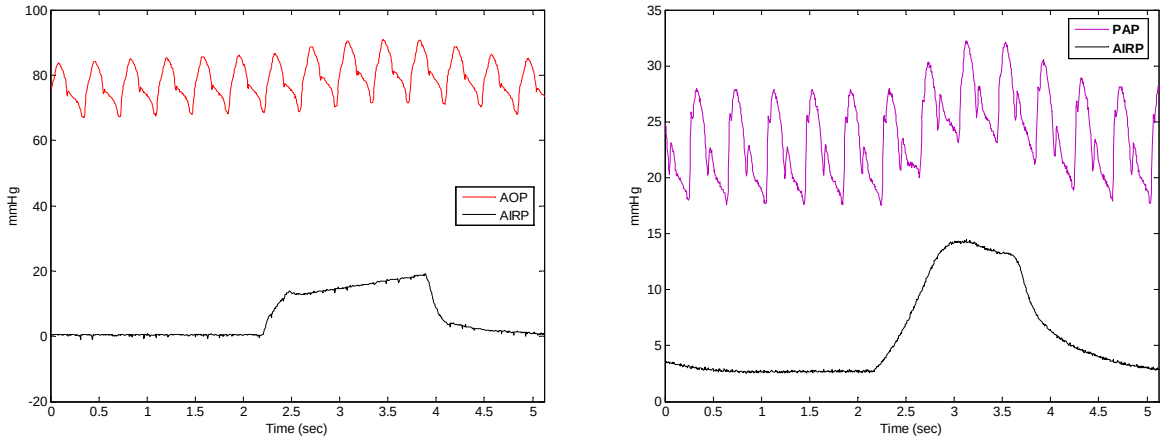

A **B**

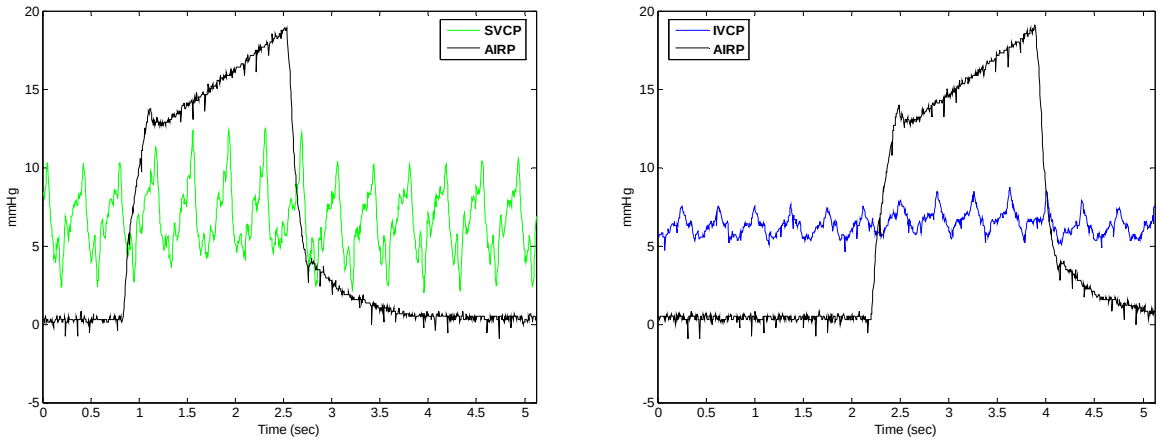

C **D**

Figure 5.2 Representative waveforms showing respiration effects of normal circulation on the A) arterial pressure (red); AOP B) pulmonary artery pressure (purple); PAP C) superior vena cava pressure (green); SVC and D) inferior vena cava pressure (blue); IVC. Airway pressure (AIRP) is shown for reference in black.

5.6.1 Varying Stroke Volume

An average time lag offset of -0.15±0.01secs occurred between respiration and IVCP. Significant differences did not occur between stroke volume settings. The time lag offset between respiration and the SVCP averaged -0.21±0.01sec with varying stroke volumes. Statistical differences occur with SVC time offset increasing as the stroke volume increases (Figure 5.3).

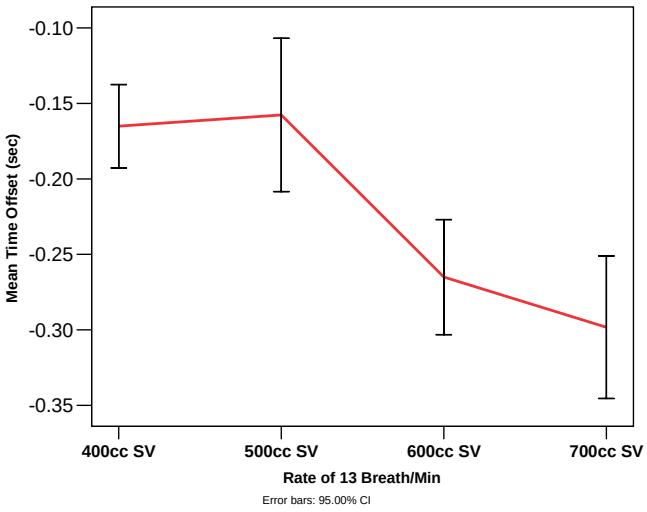

Figure 5.3 Mean time offset (sec) analysis for superior vena cava (SVC) under normal circulation with varying stroke volumes (SV). Error bars show 95% confidence intervals.

Varying stroke volume had no effect on time offsets of the main pulmonary artery. Pure time delays ranged from -.09±0.02secs to 0.08±0.03secs with an average of zero delay. No significant changes in offset occurred for the AOP. An average delay of -0.29 ± 0.20 secs was observed.

5.6.2 Varying Ventilation Rate

As rate increased, time lag offsets for the IVC decreased from -0.12 ± 0.03 secs to a delay of -0.01±0.03secs. Varying respiration frequency had little or no effect on time offsets of the SVC. Regardless of parameter setting, offsets averaging -0.1 seconds occurred. Differences were significant between 13 and both 18 and 23 breaths/min. As with stroke volumes, respiration frequency had no effect on time offsets of the MPA. A -0.01±0.03 secs delay averaged across all settings. Significant differences were observed in the AOP waveforms (Figure 5.4). As ventilation rate increased, time delays increased. A delay of -

0.26 ± 0.15 secs was observed at a rate of 8 breaths/min increasing to a delay of -0.47 ± 0.55 secs at a rate of 23 breaths/min.

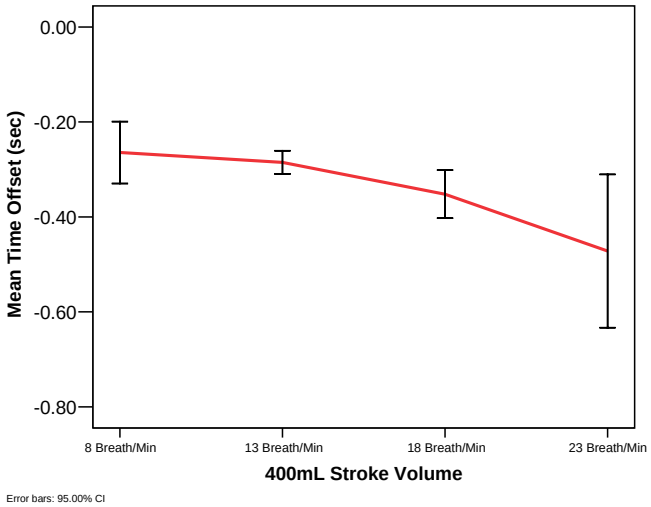

Figure 5.4 Mean time offset (sec) analysis for aortic pressure (AOP) under normal circulation with varying ventilation rate. Error bars show 95% confidence intervals.

5.6.3 Constant Minute Ventilation

Keeping minute ventilation constant, an average delay of -0.1 ± 0.04 secs was observed in the IVC. Constant minute ventilation combinations with lower ventilation rates and higher stroke volumes produced larger delays (-0.16 ± 0.02 secs and -0.12 ± 0.01 secs for 8 and 13 breaths/min combinations). Results showed statistical differences between the extremes of 8 and 23 breaths/min combinations. The results for the SVC showed the same trend as with varying rate and stroke volume. Across multiple combinations, a -0.1 sec time delay was observed. Lower rate combinations with higher tidal volumes had a greater effect on time offsets. Minimal delay (-0.01 ± 0.0 secs) and no significant differences in the MPA were observed. This is consistent with the other respiratory parameters examined. As with

varying ventilation rate, figure 5.5 illustrates significant AOP time delay differences as combinations are incremented increasing rate and decreasing stroke volumes. An average delay of -0.31 ± 0.20 secs was observed for constant minute ventilation combinations.

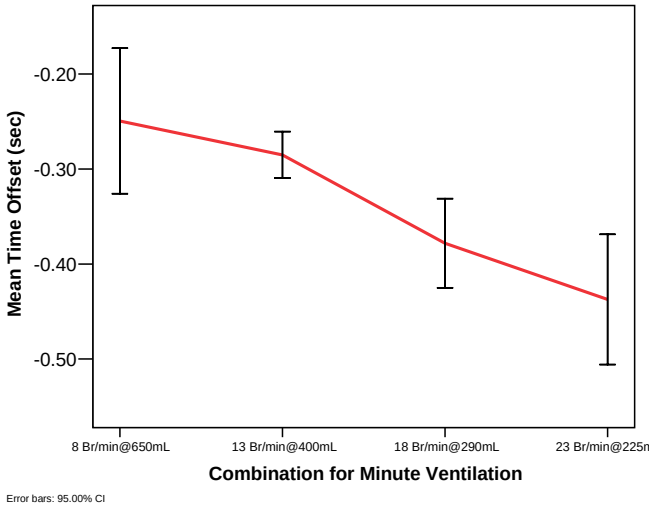

Figure 5.5 Mean time offset (sec) analysis for aortic pressure (AOP) under normal circulation with constant minute ventilation. Error bars show 95% confidence intervals.

5.6.4 Normal Circulation Summary

Time offsets are summarized in Tables 5.1 and 5.2. Overall trends of time delay on the vessels of interest observed were:

IVC

Regardless of respiration rate or stroke volume, IVCP had an average lag offset of approximately -0.1 sec. As frequency and stroke volume increased, a decreasing trend to minimal or no delay was observed. Varying ventilation or stroke volume seemed to have very little effect on the overall delay.

SVC

As with the IVC, an overall time offset of -0.1sec occurs with varying respiration rate and combinations maintaining constant minute volume. However, stroke volume had a direct effect on time delay. The average delay was approximately -0.2 sec with lower volumes and increased as volume increased. As expected, under normal physiology, respiration had an effect, but compensation is quick to respond to altered respiratory states.

PAP

Ventilation parameters examined had no significant effects on the time delays in the pulmonary artery.

Stroke Volume (cc) @ 13 Breath/min	300	400	500	600	Average
MPA Offset (sec)	0.1	0.0	0.0	-0.1	0.0
IVC Offset (sec)	-0.2	-0.1	-0.1	-0.2	-0.1
SVC Offset (sec)	-0.2	-0.2	-0.2	-0.3	-0.2
Ventilation Rate @ 400 cc Stroke Volume	8	13	18	23	Average
MPA Offset (sec)	0.0	0.0	0.0	-0.1	0.0
IVC Offset (sec)	-0.1	-0.1	-0.1	0.0	-0.1
SVC Offset (sec)	-0.1	-0.2	-0.1	-0.1	-0.1
Constant Minute Ventilation	8breath/min*650cc	13breath/min*400cc	18breath/min*290cc	23breath/min*225cc	Average
MPA Offset (sec)	0.1	0.0	0.0	-0.1	0.0
IVC Offset (sec)	-0.2	-0.1	-0.1	0.0	-0.1
SVC Offset (sec)	-0.1	-0.2	-0.1	-0.1	-0.1

Table 5.1 Summary table of average time offset (sec) in the normal circulation of the main pulmonary artery (MPA), inferior vena cava (IVC), and superior vena cava (SVC). Results are shown for varying stroke volumes, ventilation rate, and combinations of stroke volume and rate with constant minute ventilation.

AOP

Varying stroke volume had little effect on overall delays. Time delays increased as both ventilation rates increased and as respiration rate increased keeping constant minute ventilation. An average overall delay of -0.3 sec was determined for normal circulation conditions.

Stroke Volume (cc) @ 13 Breath/min	300	400	500	600	Average
AOP Offset (sec)	-0.3	-0.3	-0.3	-0.3	-0.3
Ventilation Rate @ 400 cc Stroke Volume	8	13	18	23	Average
AOP Offset (sec)	-0.3	-0.3	-0.4	-0.5	-0.4
Constant Minute Ventilation	8breath/min*650cc	13breath/min*400cc	18breath/min*290cc	23breath/min*225cc	Average
AOP Offset (sec)	-0.2	-0.3	-0.4	-0.4	-0.3

Table 5.2 Summary table of average time offset (sec) in the normal circulation of the aortic pressure (AOP). Results are shown for varying stroke volumes, ventilation rate, and combinations of stroke volume and rate with constant minute ventilation.

5.7 AP Circulation Results

Figure 5.6 illustrates the respiration effects on the AP circulation. Illustrated are the systemic and pulmonary waveforms along with AIRP.

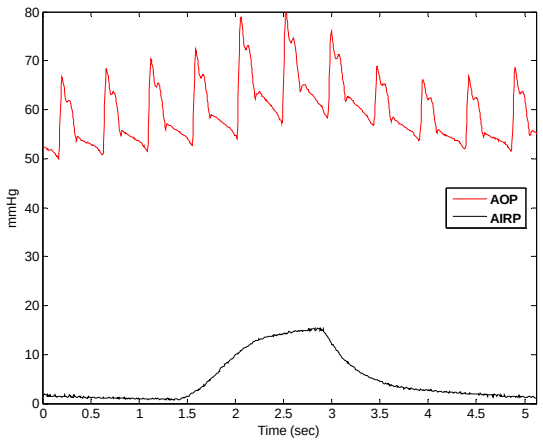

A

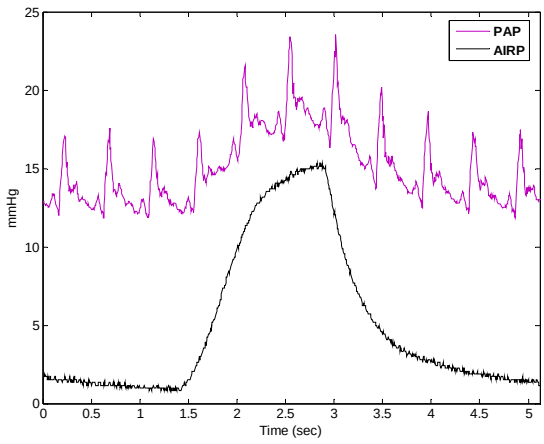

B

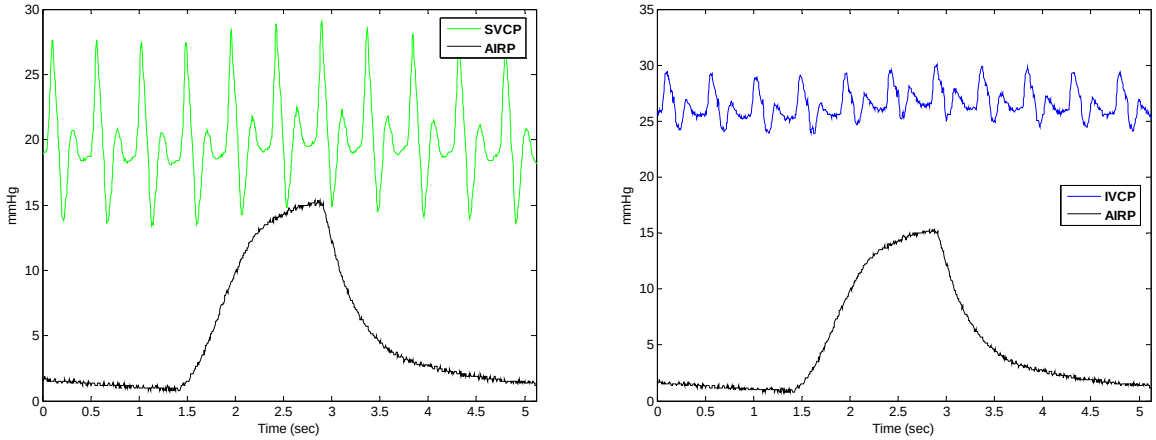

C **D**

Figure 5.6 Representative waveforms showing respiration effects of atriopulmonary (AP) circulation on the A) arterial pressure (red); AOP B) pulmonary artery pressure (purple); PAP C) superior vena cava pressure (green); SVC and D) inferior vena cava pressure (blue); IVC. Airway pressure (AIRP) is shown in black.

5.7.1 Varying Stroke Volume

Time offsets averaged -0.45 secs in the IVC with varying stroke volume. Differences were significant between 300cc and 400cc, with delays of -0.53 ± 0.04 secs and -0.36 ± 0.02 secs respectively. For the SVC, there were no statistically significant differences with varying stroke volume. An average time delay of -0.38secs was observed. A -0.16sec delay occurred in the MPA over various stroke volumes. As stroke volume increased, time delays increased also. The highest delay observed, -0.28 ± 0.04 secs, occurred at a stroke volume of 600 cc. Significant differences were observed between 600 cc and all other settings. MPA delays for the AP circulation are illustrated in Figure 5.7.

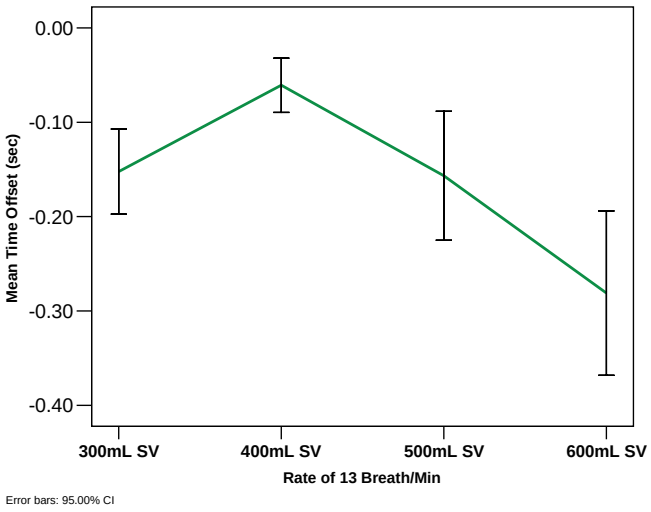

Figure 5.7 Mean time offset (sec) for main pulmonary artery (MPA) in the AP circulation with varying ventilation stroke volumes (SV). Significant increases in offset occur as SV increases. Error bars indicate 95% confidence interval.

No significant changes occurred for the AOP with varying stroke volume. An average delay of -0.31 ± 0.64 secs was observed.

5.7.2 Varying Ventilation Rate

Statistical differences occurred in the IVC with lower respiration rates having larger delays than higher rates. Offsets for low ventilation rates (8 and 13 breath/min) had offsets of -0.38±0.04secs and -0.36±0.02secs whereas at higher rates (18 and 23 breath/min), the offset decreased significantly (-0.28±0.04 and -0.22±0.04sec respectively). Overall, the average offset over the respiration rate spectra for the IVC was -0.31secs. For the SVC, the average offset over the respiration rate spectra was -0.26 sec. The least delay, -0.17±0.03 secs, was observed at 23 breaths/min. Lower rates (8 and 13 breath/min) were significantly different from higher rates (18 and 23 breath/min) and averaged a greater delay of -0.31 secs.

IVC and SVC offsets are shown in Figure 5.8. Time delays for the MPA were -0.10secs throughout the experiment, with no consistent changes observed with varying rates.

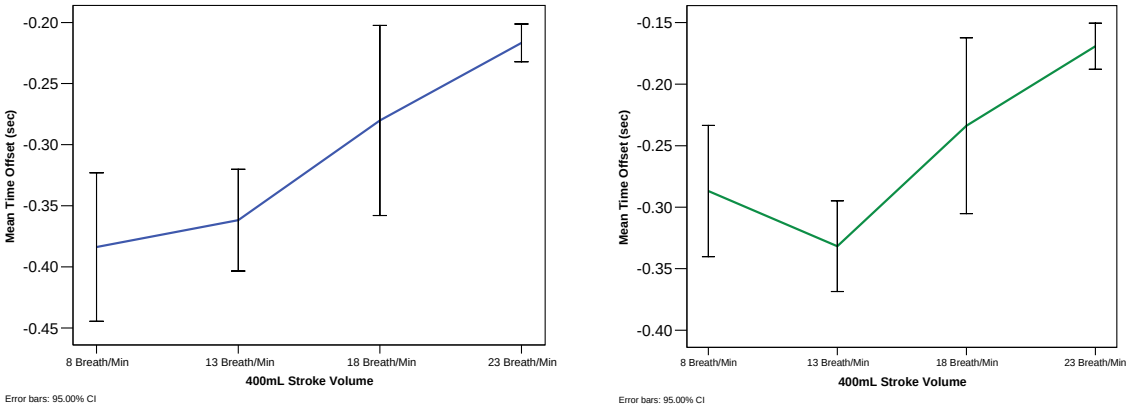

A **B**

Figure 5.8 Systemic venous time offsets (sec) of the A) inferior vena cava (IVC) and B) superior vena cava (SVC) in the AP circulation under varying ventilation rates.

As with varying stroke volume, no consistent changes were observed with increased ventilation rate in the AOP. As rates increased, the delay decreased, but not by significant amounts. An average delay of -0.33 ± 0.7 secs was observed.

5.7.3 Constant Minute Ventilation

As with varying respiration rates, IVC offsets showed significant differences: offset times decreased as rate increased and stroke volume decreased while maintaining minute ventilation constant. The offset at 8 breaths/min was -0.31±0.04secs; the offset at 23 breath/min was -0.21±0.05secs. As with varying rates, low minute ventilation combinations produced a -0.3sec delay in the SVC. Higher respiration rate minute ventilation combinations decreased the offset to -0.16±0.05sec. Essentially no time offset variation was

present with varying minute ventilation combinations in the MPA. Average delays were -0.07sec. Time delays for the AOP keeping minute ventilation constant is shown in Figure 5.9. An average delay of -0.34 ± 0.77 secs occurred in the AOP. There were no significant differences between parameters.

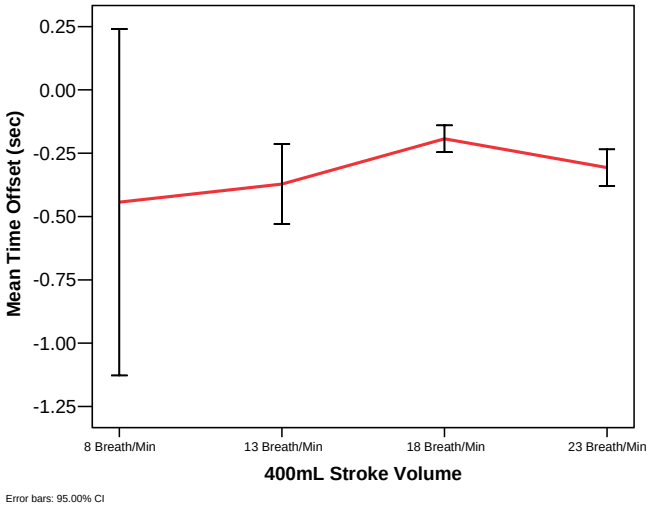

Figure 5.9 Time offsets (sec) of the aorta (AOP) with an AP circulation at different constant minute ventilation combinations.

5.7.4 AP Circulation Summary

Time offsets are summarized in Tables 5.3 and 5.4. Overall trends of time delay on the vessels of interest observed were:

IVC

Stroke volume changes had a larger effect on time offsets. Average IVCP delays were -0.45secs. Rate changes and minute ventilation changes produced a delay, but to a lesser degree, averaging -0.3secs. Lower stroke volumes, lower rates, and combinations with the lower rates and higher volumes produced a greater delay.

SVC

There were no statistically different time delays when varying stroke volume while maintaining a constant ventilation rate. The delay averaged -0.38secs throughout the volume spectra. With varying respiratory rates and with varying minute ventilation combinations, lower rates (8 and 13 breath/min) produced a significant delay (-0.31sec), whereas delays decreased as rates increased (-0.17secs).

PAP

No significant delays were observed with both varying ventilation rate and varying minute ventilation combinations. As stroke volume increased time delays increased to -0.2 sec. Otherwise, an average delay of -0.1 sec was present.

Stroke Volume (cc) @ 13 Breath/min	300	400	500	600	Average
MPA Offset (sec)	-0.2	-0.1	-0.2	-0.3	-0.2
IVC Offset (sec)	-0.5	-0.4	-0.4	-0.5	-0.5
SVC Offset (sec)	-0.4	-0.3	-0.4	-0.4	-0.4
Ventilation Rate @ 400 cc Stroke Volume	8	13	18	23	Average
MPA Offset (sec)	-0.2	-0.1	-0.1	-0.1	-0.1
IVC Offset (sec)	-0.4	-0.4	-0.3	-0.2	-0.3
SVC Offset (sec)	-0.3	-0.3	-0.2	-0.2	-0.3
Constant Minute Ventilation	8breath/min*650cc	13breath/min*400cc	18breath/min*290cc	23breath/min*225cc	Average
MPA Offset (sec)	-0.1	-0.1	-0.1	0.0	-0.1
IVC Offset (sec)	-0.3	-0.4	-0.2	-0.2	-0.3
SVC Offset (sec)	-0.3	-0.3	-0.2	-0.2	-0.2

Table 5.3 Summary table of average time offsets under atriopulmonary (AP) circulation of the main pulmonary artery (MPA), inferior vena cava (IVC), and superior vena cava (SVC). Results are shown for varying stroke volumes, ventilation rate, and combinations of stroke volume and rate with constant minute ventilation.

AOP

No consistent changes were present for any parameter manipulation measured. Average delays for all three subgroups was -0.3 secs.

Stroke Volume (cc) @ 13 Breath/min	300	400	500	600	Average
AOP Offset (sec)	-0.2	-0.4	-0.2	-0.2	-0.3
Ventilation Rate @ 400 cc Stroke Volume	8	13	18	23	Average
AOP Offset (sec)	-0.4	-0.4	-0.2	-0.3	-0.3
Constant Minute Ventilation	8breath/min*650cc	13breath/min*400cc	18breath/min*290cc	23breath/min*225cc	Average
AOP Offset (sec)	-0.4	-0.4	-0.2	-0.3	-0.3

Table 5.4 Summary table of average time offset (sec) in the atriopulmonary (AP) circulation of the aortic pressure (AOP). Results are shown for varying stroke volumes, ventilation rate, and combinations of stroke volume and rate with constant minute ventilation.

5.8 TCPX Circulation Results

Complete elimination of the right heart produced marked changes in pressure waveforms. Pulsatility was essentially removed within the passive system. Representative waveforms showing ventilation effects are shown in Figure 5.10.

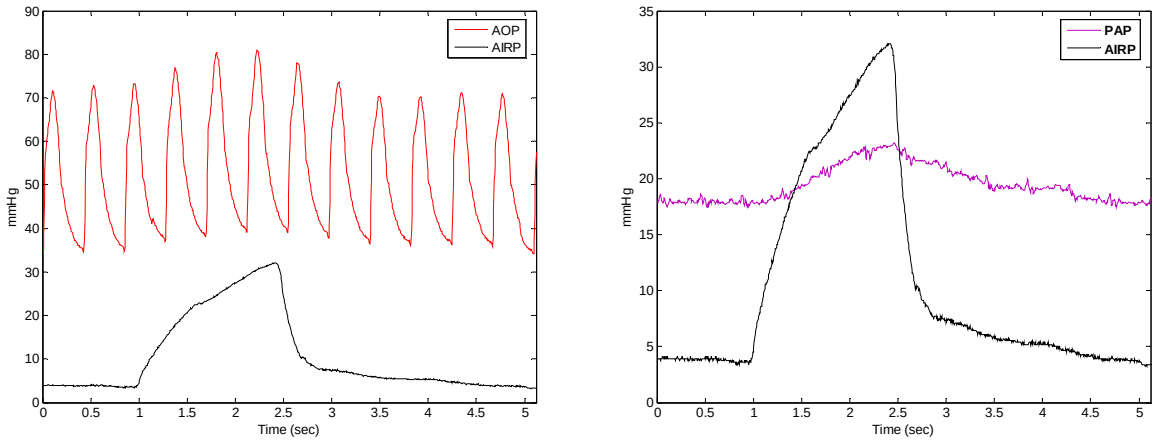

A **B**

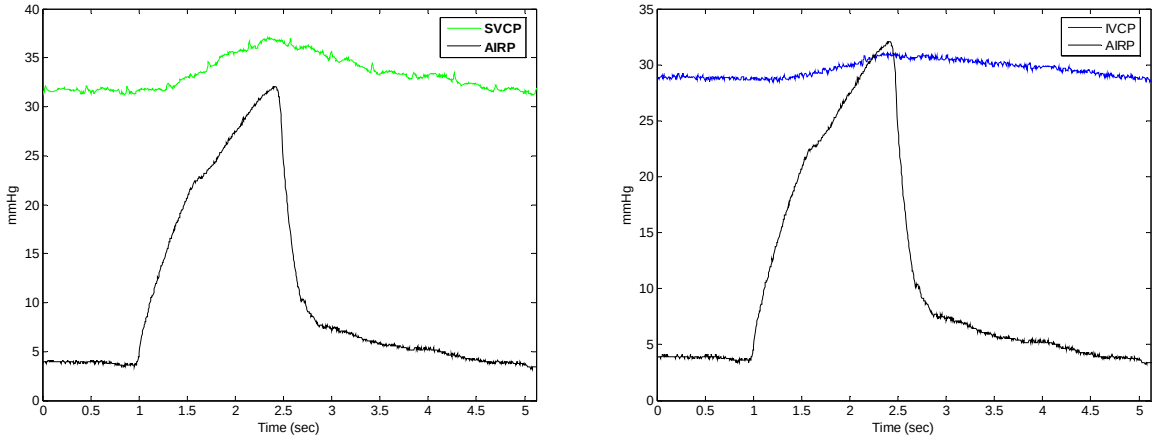

C **D**

Figure 5.10 Representative waveforms showing respiration effects of TCPX circulation on the A) arterial pressure (red); AOP B) main pulmonary artery pressure (purple); PAP C) superior vena cava pressure (green); SVC and D) inferior vena cava pressure (blue); IVC.

Airway pressure (AIRP) is shown in black.

5.8.1 Varying Stroke Volume

The average IVC time delay was -0.83 secs. Significant differences occurred between all stroke volume settings. As stroke volume increased from 300cc to 600cc, the time delay decreased from -1.05±0.04 secs to -0.63±0.06 secs. The SVC time delay averaged -0.79 sec over the stroke volume range. The maximum delay of -0.92±0.04 secs occurred at a stroke volume of 300cc. As stroke volume increased, delays stabilize at approximately -0.75 sec. A stroke volume of 300cc created an MPA delay of -0.87±0.04 secs. All other parameter settings created a delay averaging -0.59 sec. Significant differences occurred between 300cc and all other settings. IVC and SVC offsets with varying tidal volume are shown in Figure 5.11.

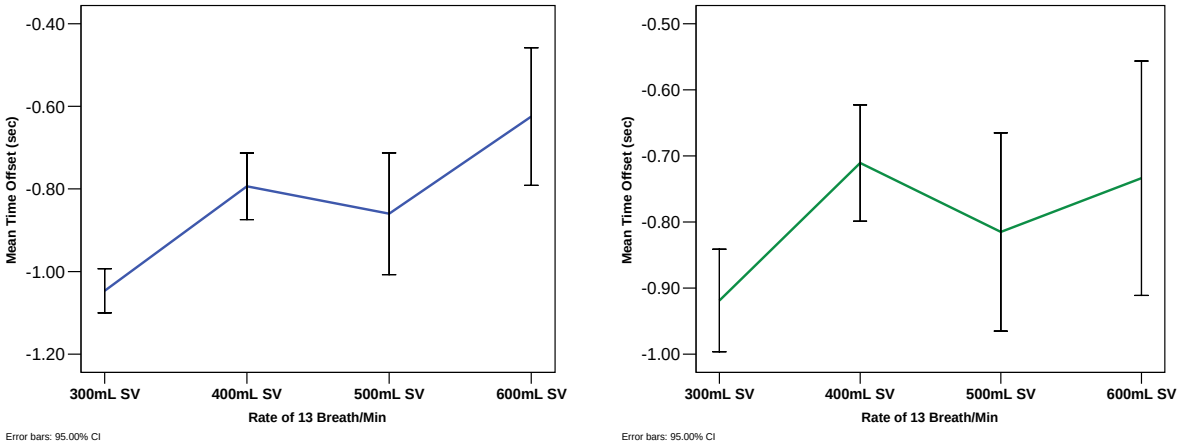

A **B**

Figure 5.11 Systemic venous time offsets (sec) of the A) inferior vena cava (IVC) and B) superior vena cava (SVC) in the TCPC circulation under varying ventilation rates. Error bars depict 95% confidence intervals.

As stroke volume increased, time delays for the AO increased from -0.28 ± 0.24 secs at a 300 cc stroke volume to -0.47 ± 0.25 secs at 600 cc.

5.8.2 Varying Ventilation Rate

Frequencies of 8 and 23 breath/min produced the smallest time delays in the IVC (-0.5 secs). Middle range frequencies of 13 and 18 breath/min produced higher delays of -0.79±0.05 secs and -0.92±0.09 secs respectively. For the SVC, a -0.63 sec time delay over the frequency range was observed. Low and higher rates maintained a lesser delay (-0.55 secs and -0.43 secs) than middle range frequencies (-0.71 secs and 0.83 secs). The MPA had a -0.51 sec delay over the frequency range. Low and high rates created smaller delays (-0.38secs and -0.37secs) than middle range frequencies (-0.62 secs and -0.69 secs). The MPA, SVC, and IVC followed the same trend. Statistically significant differences were observed across respiration rates with middle ranges differing from extreme low and high

rates. No marked changes occurred over varying ventilation rates for the AOP with an average delay of -0.28 ± 0.23 secs.

5.8.3 Constant Minute Ventilation

No significant differences were observed in the IVC or MPA across minute ventilation combinations. Time delays for the IVC and MPA averaged -0.76 secs and -0.62 secs respectively. The SVC time delay averaged -0.68 secs. Statistical differences were observed between 18 and 23 breath/min combinations. The AO had no significant differences with an average delay of -0.28 ± 0.28 secs.

5.8.4 TCPX Circulation Summary

Time offsets are summarized in Tables 5.5 and 5.6. Overall trends of time delay on the vessels of interest observed were:

IVC

Regardless of parameter or setting, time delays remained at approximately -0.75 secs. However, significant differences occurred with low tidal volumes and middle range respiration rates creating a larger delay.

SVC

Regardless of parameter or setting, time delays averaged at -0.7 secs. The SVC displayed the same trends as with IVC.

PAP

An average time delay across all parameters was -0.6 secs. The MPA displayed the same trends as the IVC and SVC.

Stroke Volume (cc) @ 13 Breath/min	300	400	500	600	Average
MPA Offset (sec)	-0.9	-0.6	-0.7	-0.5	-0.7
IVC Offset (sec)	-1.0	-0.8	-0.9	-0.6	-0.8
SVC Offset (sec)	-0.9	-0.7	-0.8	-0.7	-0.8
Ventilation Rate @ 400 cc Stroke Volume	8	13	18	23	Average
MPA Offset (sec)	-0.4	-0.6	-0.7	-0.4	-0.5
IVC Offset (sec)	-0.6	-0.8	-0.9	-0.5	-0.7
SVC Offset (sec)	-0.5	-0.7	-0.8	-0.4	-0.6
Constant Minute Ventilation	8breath/min*650cc	13breath/min*400cc	18breath/min*290cc	23breath/min*225cc	Average
MPA Offset (sec)	-0.6	-0.6	-0.8	-0.5	-0.6
IVC Offset (sec)	-0.7	-0.8	-0.9	-0.6	-0.8
SVC Offset (sec)	-0.7	-0.7	-0.8	-0.5	-0.7

Table 5.5 Summary table of average time offsets under total cavopulmonary with extracardiac shunt (TCPX) circulation of the main pulmonary artery (MPA), inferior vena cava (IVC), and superior vena cava (SVC). Results are shown for varying stroke volumes, ventilation rate, and combinations of stroke volume and rate with constant minute ventilation.

AOP

With varying stroke volume, the largest delay of -0.47 ± 0.25 secs occurred at a stroke volume of 600 cc. Combinations with constant minute ventilation showed similar results with the largest delay of -0.44 ± 0.13 secs at a rate of 23 breaths/min and a stroke volume of 225 cc. Varying ventilation rate had no effect on time delays with an average delay of -0.28 ± 0.23 secs. Overall, delays had no consistent changes regardless of ventilation parameter setting. Ventilation protocol produced an overall AO delay of -0.29 ± 0.25 secs.

Stroke Volume (cc) @ 13 Breath/min	300	400	500	600	Average
AOP Offset (sec)	-0.3	-0.3	-0.4	-0.5	-0.3
Ventilation Rate @ 400 cc Stroke Volume	8	13	18	23	Average
AOP Offset (sec)	-0.2	-0.3	-0.3	-0.3	-0.3
Constant Minute Ventilation	8breath/min*650cc	13breath/min*400cc	18breath/min*290cc	23breath/min*225cc	Average
AOP Offset (sec)	-0.3	-0.3	-0.2	-0.4	-0.3

Table 5.6 Summary table of average time offset (sec) in the total cavopulmonary with extracardiac shunt (TCPX) of the aorta (AO). Results are shown for varying stroke volumes, ventilation rate, and combinations of stroke volume and rate with constant minute ventilation.

5.9 TCPY Circulation Results

The TCPY connection is similar to the TCPX connection except the SVC in connected to a synthetic graft instead of to the RPA. The SVC was connected to the graft via an end-to-side anastomosis or connected to a Y-shaped graft via an end-to-end anastomosis. Waveforms are similar to the TCPX and are illustrated in Figure 5.12.

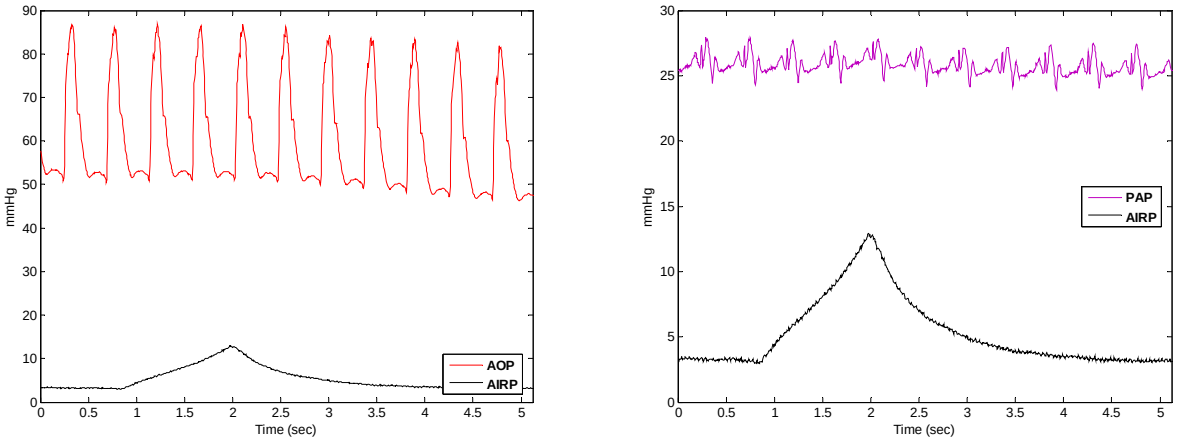

A **B**

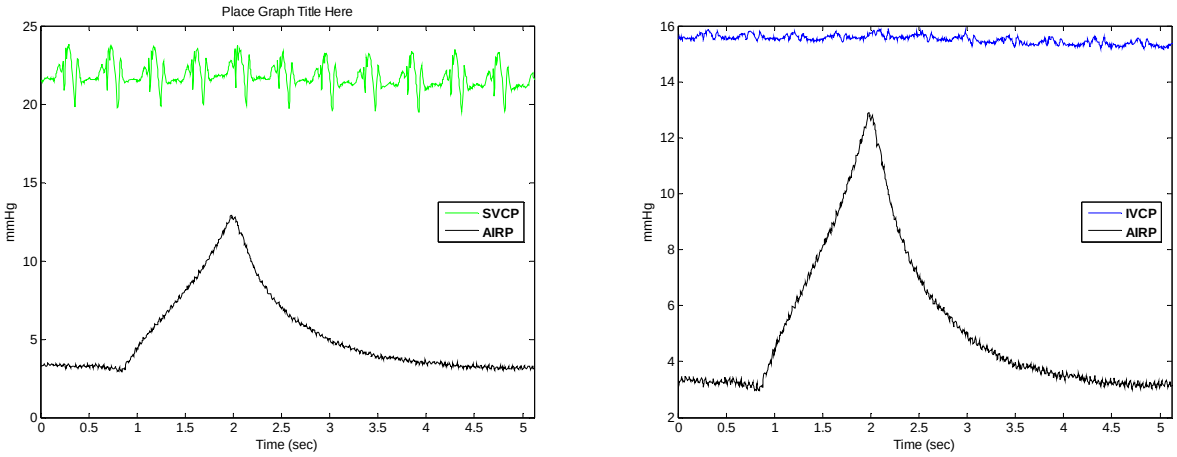

C **D**

Figure 5.12 Representative waveforms showing respiration effects of TCPY circulation on the A) arterial pressure (red); AOP B) main pulmonary artery pressure (purple); PAP C) superior vena cava pressure (green); SVC and D) inferior vena cava pressure (blue); IVC. Airway pressure (AIRP) is shown in black.

5.9.1 Varying Stroke Volume

For closer examination and better operative management, respiratory protocol changes were implemented for varying tidal volumes at four different ventilation frequencies. Stroke volumes were varied from 400 ccs to 700 ccs while rates were held constant from 8 to 23 breaths/min in 5 breath/min increments. For varying ventilation rate, stroke volumes were held constant at increments of 400 ccs to 700 ccs while rate was incremented from 8 to 23 breaths/min. Systemic circulation results for varying stroke volume are presented in Figure 5.13.

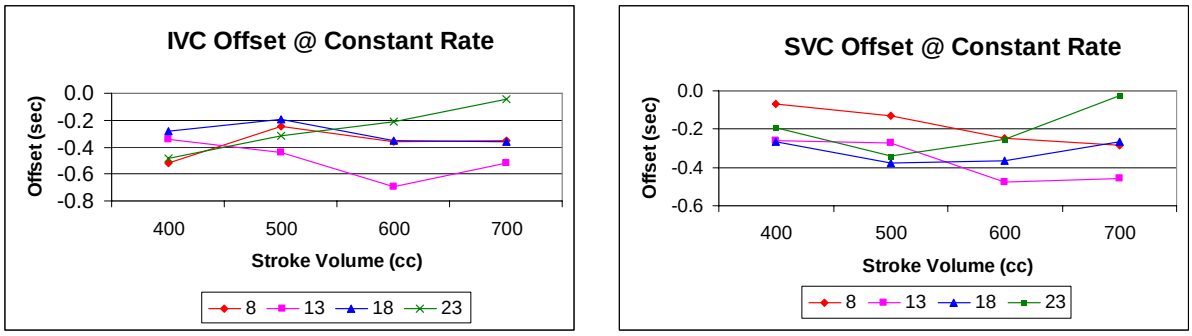

A **B**

Figure 5.13 Total cavopulmonary connection with a Y-shaped anastomosis (TCPY) time offsets (sec) for the A) inferior vena cava (IVC) and B) superior vena cava (SVC) with varying stroke volume incrementing ventilation rate by 5 breaths/min.

IVC

At a ventilation rate of 8 breaths/min, an average delay of -0.33sec was observed while varying stroke volume from 400ccs to 700ccs. Statistical differences only occurred between 400ccs and all other parameter settings (500ccs-700ccs). The greatest delay occurred at 400ccs with a value of -0.52±0.2 secs. At 13 breaths/min, higher stroke volumes produced greater time offsets, with 600ccs having the greatest delay of -0.69±0.05 secs. The time delay averaged -0.50 secs. No significant differences were observed between settings. At 23 breaths/min, the time delay decreased as the stroke volume increased. The maximum delay (corresponding to 400ccs) was -0.49±0.12 secs. The minimum delay (700ccs) was -0.04±0.04 secs. The average delays across parameter settings was -0.26 secs.

SVC

Except for the 23 breaths/min rate, as stroke volume increased, time offsets also increased. At 23 breaths/min, the time offset decreased from -0.19±0.04 secs at stroke volume of 400ccs to an offset of -0.03±0.04 secs at a stroke volume of 700ccs. An average delay of -0.27 secs was observed over varying stroke volumes. Statistical differences

occurred between 400ccs and 700ccs for 8 breaths/min, between 500ccs and 700cc for 13 breaths/min, and between 700ccs and all other settings for 23 breaths/min.

PAP

Small changes in time delays occurred across varying stroke volumes as illustrated in Figure 5.11. The average delay was -0.15secs. Low rates and low volumes created the largest delays. Statistical differences occurred at 500ccs for 13 breaths/min and at 700ccs for 23 breaths/min.

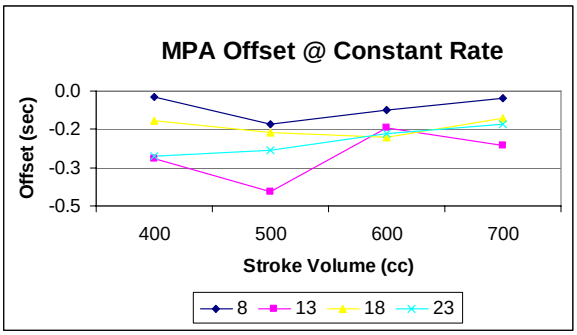

Figure 5.14 Total cavopulmonary connection with a Y-shaped anastomosis (TCPY) time offsets (sec) for the main pulmonary artery (MPA) varying stroke volume incrementing ventilation rate by 5 breaths/min from 8 to 23 breaths/min.

AOP

Time offsets for the AO while varying stroke volume with ventilation rate held constant are shown in Figure 5.15. No statistical differences occurred for varying stroke volume at rates of 8 and 18 breaths/min with average delays of -0.40 ± .30 secs and -0.34 ± .22 secs respectively. For rates of 13 and 23 breaths/min, differences occurred between middle range stroke volumes (500ccs and 600ccs) and maximum and minimum rates (500ccs and 600ccs). An overall average delay for the AO at different stroke volumes keeping rate constant was -0.40 secs

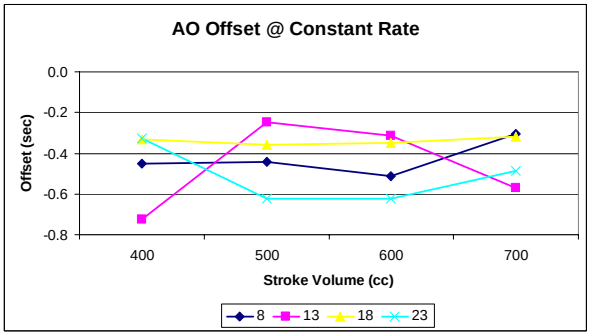

Figure 5.15 Total cavopulmonary connection with a Y-shaped graft (TCPY) time offsets (sec) for the aorta (AO) varying stroke volume (ccs) incrementing ventilation rate by 5 breaths/min from 8 to 23 breaths/min.

5.9.2 Varying Ventilation Rate

IVC

Varying respiration rate showed little statistically significant effect over the entire stroke volume spectra. However, at high stroke volumes (600cc and 700cc), the time offset decreases as rate increases. An average time delay of -0.33 sec was observed for all stroke volumes.

SVC

An average delay of -0.28 secs was observed over varying respiration rates. A significant increase in time delay occurred between 8 breaths/min and higher rates for all stroke volumes examined. Time delays tended to stabilize as rate increased until very high rates were achieved. At very high rates, delays shortened as stroke volume increased. Statistical differences occurred for 400ccs between 8 and 23 breaths/min, for 500ccs between 8 and 18 breaths/min, for 600ccs between 13 and 23 breaths/min, and for 700ccs between 13 and 23 breaths/min.

IVC and SVC offset means for varying ventilation rate are seen in Figure 5.16.

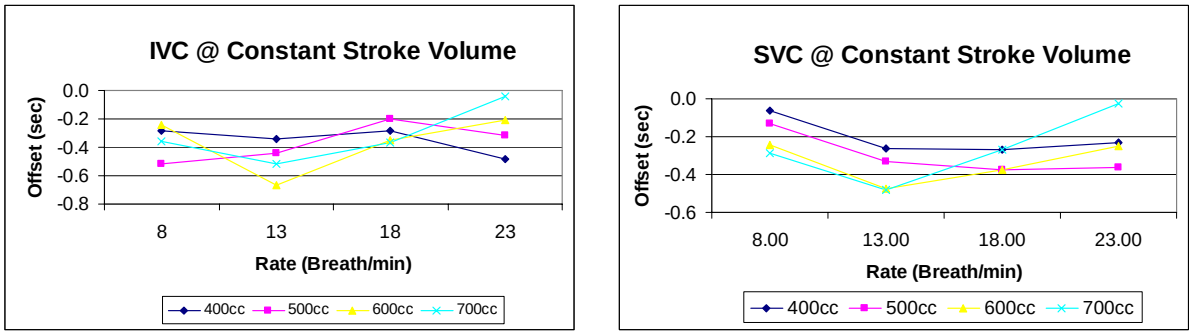

A **B**

Figure 5.16 Total cavopulmonary connection with a Y-shaped anastomosis (TCPY) time offsets (sec) for the A) inferior vena cava (IVC) and B) superior vena cava varying ventilation rate incrementing stroke volume by 100ccs from 400ccs to 700ccs.

PAP

A stroke volume of 500ccs accounted for the largest offsets with increasing ventilation rate. An overall delay of -0.18secs was observed. Significant differences occurred at a stroke volume of 500cc at low frequencies (8 and 13 breaths/min) as shown in Figure 5.17. At high ventilation rates, all volumes maintained an offset of approximately -0.24 secs.

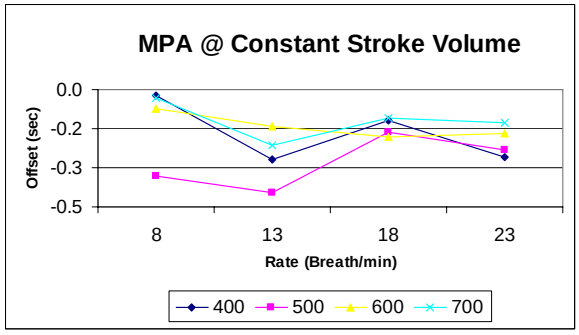

Figure 5.17 Total cavopulmonary connection with a Y-shaped anastomosis

(TCPY) time offsets (sec) for the main pulmonary artery (MPA) varying ventilation rate incrementing stroke volume by 100ccs from 400ccs to 700ccs.

AOP

Varying ventilation rate keeping stroke volume constant for middle range values (500cc and 600cc) produced similar results. No statistical differences were observed except for the maximum rate of 23 breaths/min at a stroke volume of 600ccs. Average delays for 500ccs and 600ccs were -0.38 ± 0.27 secs and -0.37 ± 0.25 secs respectively. For low and high stroke volumes, 400ccs and 700ccs, similar results produced average delays of -0.40 ± 0.28 secs and -0.41 ± 0.25 secs. Statistical differences between ventilation rates were observed. Results varying ventilation rate incrementing stroke volume are shown in Figure 5.18.

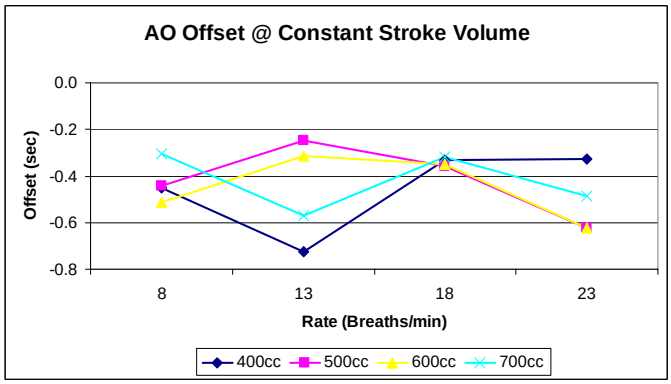

Figure 5.18 Total cavopulmonary connection with a Y-shaped graft (TCPY) time offsets (sec) for the aorta (AO) varying ventilation rate incrementing stroke volume by 100ccs from 400ccs to 700ccs.

5.9.3 TCPY Circulation Summary

Time offsets are summarized in Tables 5.7. Overall trends of time delay on the vessels of interest observed were:

	Varying Stroke Volume (400cc - 700cc)				
		RATE (Breath/min)			AVERAGE
Parameter	8	13	18	23	
IVC Offset (sec)	-0.35	-0.50	-0.30	-0.26	-0.35
SVC Offset (sec)	-0.18	-0.37	-0.32	-0.20	-0.27
MPA Offset (sec)	-0.06	-0.25	-0.14	-0.13	-0.15
AO Offset (sec)	-0.4	-0.42	-0.34	-0.45	-0.4

A

	Varying Rate (8 - 23 Breath/min)				
		STROKE VOLUME (cc)			AVERAGE
Parameter	400	500	600	700	
IVC Offset (sec)	-0.35	-0.37	-0.37	-0.32	-0.35
SVC Offset (sec)	-0.21	-0.30	-0.34	-0.27	-0.28
MPA Offset (sec)	-0.17	-0.28	-0.14	-0.12	-0.18
AO Offset (sec)	-0.4	-0.38	-0.37	-0.41	-0.39

B

Table 5.7 Time offsets for total cavopulmonary connection with a Y-shaped graft (TCPY) circulation for the inferior vena cava (IVC), superior vena cava (SVC), and main pulmonary artery (MPA), and aorta (AO) with A) varying stroke volume from 400cc to 700cc incrementing ventilation rate by 5 breaths/min from 8 to 23 breaths/min and B) varying ventilation rate from 8 to 23 breaths/min incrementing stroke volume by 100ccs from 400ccs to 700ccs.

5.10 Comparison between Fontan Circulations

To get a better understanding of the time offset differences, offsets were compared between normal and Fontan circulations. For completeness, individual vessels will be examined.

5.10.1 Inferior Vena Cava

The greatest differences in IVC offset occurred in the TCPX connection. An average delay of -0.77 secs was determined. Also, the TCPX had greater variability across parameters examined, with extreme rate parameters having a significant decreasing effect on offset. The TCPY offset follows the normal circulation closely. Significant differences occurred at a stroke volume of 500ccs, but overall no significant differences were observed (Figure 5.19).

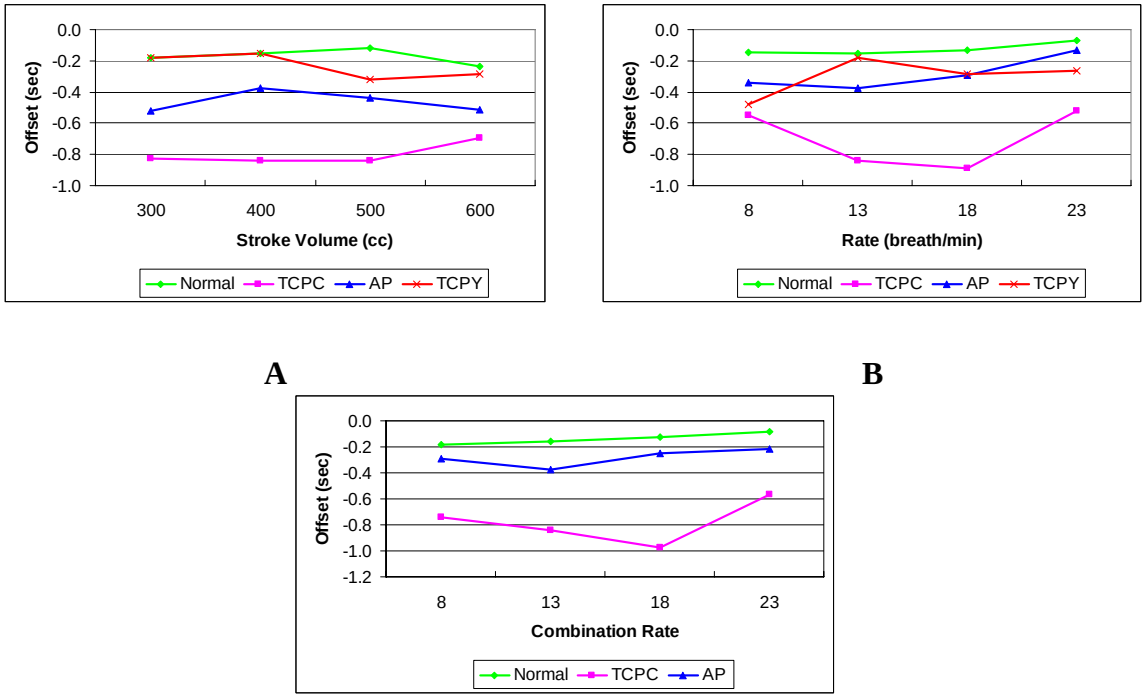

Figure 5.19 Average time offsets (sec) for the inferior vena cava compared between circulations for A) varying stroke volume B) varying ventilation rate and C) constant minute ventilation combinations.

Average offsets for varying stroke volume and ventilation rate were -0.35 secs. The AP connection has the same trend as the normal circulation, except an offset difference averaged -0.24 secs across the stroke volume spectra. As ventilation rate increased, both AP and normal offsets decreased. Average IVC offsets are summarized in Table 5.8.

	NORMAL	AP	TCPC	TCPY
STROKE VOLUME	-0.15	-0.45	-0.83	-0.35
RATE	-0.08	-0.31	-0.70	-0.35
COMBINATION	-0.10	-0.28	-0.76	NA
AVERAGE	-0.11	-0.35	-0.77	-0.35

Table 5.8 Overall average offset (sec) for the inferior vena cava (IVC) under ventilation protocol parameters. NA=data not available.

Although some significant differences occur between rates and volumes, overall offsets remain relatively unchanged. Although connection types differ greatly, average IVC offsets within modifications can be used to simulate delays.

5.10.2 Superior Vena Cava

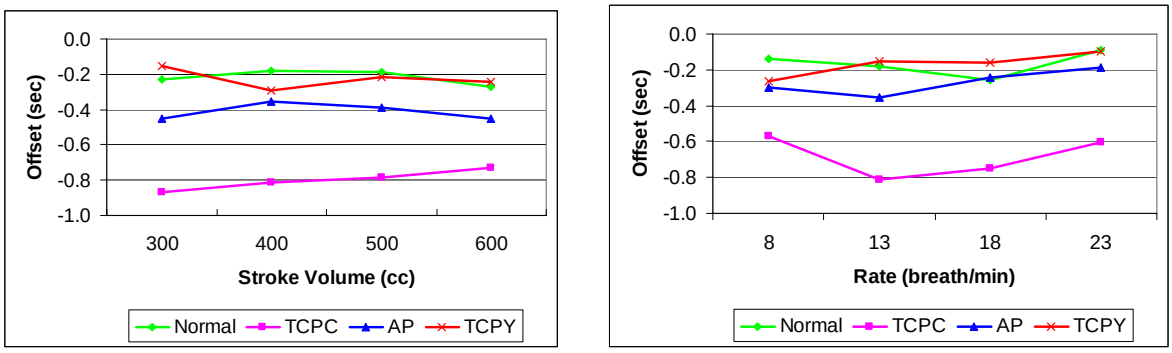

A **B**

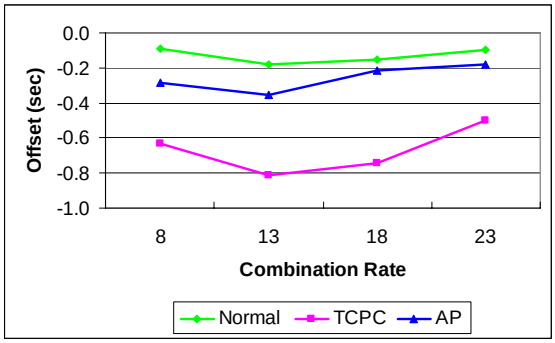

C

Figure 5.20 Average time offsets (sec) for the superior vena cava compared between circulations for A) varying stroke volume B) varying ventilation rate and C) constant minute ventilation combinations.

The TCPX connection is significantly different from the normal circulation and the AP and TCPY circulations for varying stroke volume and varying ventilation rate at all settings (Figure 5.20). TCPX delays were much greater over the entire ranges for all parameters examined. Average SVC offsets were -0.70 secs for the TCPX connection compared to -0.29 secs for the AP connection, -0.28 secs for the TCPY connection, and -0.13 secs for the normal circulation. Extreme conditions decreased the delay, but a significant difference remained between the TCPX and other circulations examined. The AP connection, utilizing the RA, followed the same trends as the normal circulation. However, delays were significantly greater. TCPY offsets were not significantly different from the normal circulation for either varying stroke volume or ventilation rate except at the extremely low ranges of stroke volumes (300ccs) and frequency (8 breaths/min). Average offsets are summarized in Table 5.9.

	NORMAL	AP	TCPC	TCPY
STROKE VOLUME	-0.21	-0.38	-0.79	-0.27
RATE	-0.08	-0.26	-0.63	-0.28
COMBINATION	-0.11	-0.24	-0.68	NA
AVERAGE	-0.13	-0.29	-0.70	-0.28

Table 5.9 Overall average offset (sec) for the superior vena cava (SVC) under ventilation protocol parameters. NA=data not available.

5.10.3 Main Pulmonary Artery

Following the IVC and SVC, the MPA showed a significantly greater offset at all parameters examined for the TCPX connection. As ventilation rate increased, offset differences remained significant; however, differences between connections decreased. Within the connection, variations in stroke volume and respiration had minimal effect, except for a decreasing offset in the AP circulation. Table 5.10 shows average offsets for the MPA.

	NORMAL	AP	TCPC	TCPY
STROKE VOLUME	0.00	-0.16	-0.66	-0.07
RATE	-0.01	-0.10	-0.51	-0.11
COMBINATION	0.01	-0.07	-0.62	NA
AVERAGE	0.00	-0.11	-0.60	-0.09

Table 5.10 Overall average offset (sec) for the main pulmonary artery (MPA) under ventilation protocol parameters. NA=data not available.

5.10.4 Aorta

Regardless of ventilation protocol setting and Fontan modification, average delays were approximately -0.31 secs. The TCPY connection had approximately 0.1 sec longer delays for varying stroke volume and ventilation rate compared to all other Fontan

modifications. Ventilation manipulation had few significant effects for all Fontan connections examined. Results are shown in Table 5.11.

	NORMAL	AP	TCPC	TCPY
STROKE VOLUME	-0.29	-0.31	-0.31	-0.40
RATE	-0.31	-0.33	-0.28	-0.39
COMBINATION	-0.31	-0.34	-0.28	NA
AVERAGE	-0.30	-0.33	-0.29	-0.40

Table 5.11 Overall average offset (sec) for the aorta (AO) under ventilation protocol parameters. NA=data not available.

5.11 Discussion

Instantaneous measurements in animal models allow the observation and quantification of normal and Fontan circulation related parameters not available in humans. Time offsets were determined for the IVC, SVC, and PA. Results have provided insight on future directions needed in order to optimize surgical model simulations. Both stroke volume and ventilation frequency have significant effects on time offsets between airway pressure and systemic and pulmonary vessels. Furthermore, time offsets are significantly different across different Fontan geometries, increasing the need to implement individual models into computer simulations. The TCPX connection shows the largest time offset. TCPX geometry may have an important role in this offset difference. The graft is positioned dorsal to the heart with the lungs having a greater contact area with the graft. This may introduce a physical effect of the lungs compressing the graft producing an offset effect in addition to the lungs compressing the pulmonary arterioles. The TCPY and AP connection grafts are ventral to the heart and positioned mostly away from any physical lung motion except at the IVC anastomosis site. TCPY and AP connections have smaller offsets and display trends similar

to normal circulations. Although significant differences occur among ventilation parameters, overall effects under normal range ventilation rate and volume ranges do not, in general, differ significantly. Therefore, average delays can be used for simulation models for normal conditions. Offsets will have to be altered according to ventilation parameter and Fontan modification to simulate exercise, postoperative complications, or further diseased conditions. In order to accurately predict hemodynamic parameters and outcomes of various physiological conditions, time offsets between respiration and pertinent blood vessels should be applied to future computer simulations and in-vitro research apparatus. Furthermore, this information can be applied to aid in medical management optimization and help prescribe respiration therapy in children in both pre and postoperative conditions.

A limitation to this study is the open chest acute preparation, which does not allow the animal to undergo staging procedures to adapt to the new geometry and circulation. In addition, a normal four-chamber heart is being altered. The single ventricle geometry created is not preconditioned with an increased vascular resistance and afterload. In-vivo studies also need to be compared to three-dimensional magnetic resonance images of human patients to determine the accuracy of the flow field and pressure distributions.

5.12 Future Work

Now that offsets have been determined, the next step is to incorporate the findings into simulations in order to accurately model hemodynamic waveforms. Once the waveforms can be modeled, alterations in geometry and hemodynamic states can be examined. Parallel studies are being performed that implement these time offsets into an electrical computer model. Also, model characteristics will be manipulated in order to help

determine the influence and differences on system hemodynamics by physical lung motion and respiration transit time effects. Illustrated below is the way the results will be used to improve modeling efforts.

The closed loop model under development, which has been implemented in Simulink and described elsewhere, is based on the data obtained from the lamb experiments. The model has pumping atria and ventricles (time varying compliances) and separate pathways for right and left lungs, head, thoracic regions and legs. To model a basic Fontan repair, the RA and RV are simply replaced by an extracardiac conduit linking the caval veins to the pulmonary arteries. Pressure and flow waveform shapes mimic physiological conditions faithfully under both situations.

As a first approximation to the effects of respiration, the treatment used by Rideout et al (1968) was implemented. The resistance of the pulmonary arterioles was varied according to the transmural pressure difference between the airways and the vessels. The changes in waveform shape were consistent with the changes observed in the animal models, including the possible cessation of flow in the IVC and SVC during inspiration. Time offsets, however, were not consistent with those observed in the animals.

Pressure waveforms and their respective offsets for the control model are illustrated in the top row of Fig. 5.21. Regardless of the method used to estimate the offsets, the delays are approximately -.15 secs for the MPA, -.64 secs for the SVC, -.65 secs for the IVC and -1.92 secs for the AO (not shown). While the MPA delay is minimal as expected, the longer delays for the caval veins and AO clearly indicate that this is not the major inspiratory influence on these vessels.

Waveforms and their respective offsets for the Fontan model are illustrated in the bottom row of Fig. 5.21. The delays for the MPA and caval veins are relatively the same magnitude, with the MPA delay lengthening to -.28 secs and the caval vein delays shortening to -.35 secs. The findings are as expected for the computational model as the distance between the pressure measurements is simply the length of the extracardiac conduit. This again is contrary to the experimental results that show little difference in delays in the MPA and longer delays in the caval veins. Again, results indicate that the respiratory effects are multifactorial and likely adhere to different rules in the normal compared to the Fontan circulations. The large inter-animal variability also indicates that the rules are patient specific and may only be well understood by individual rather than collective studies.

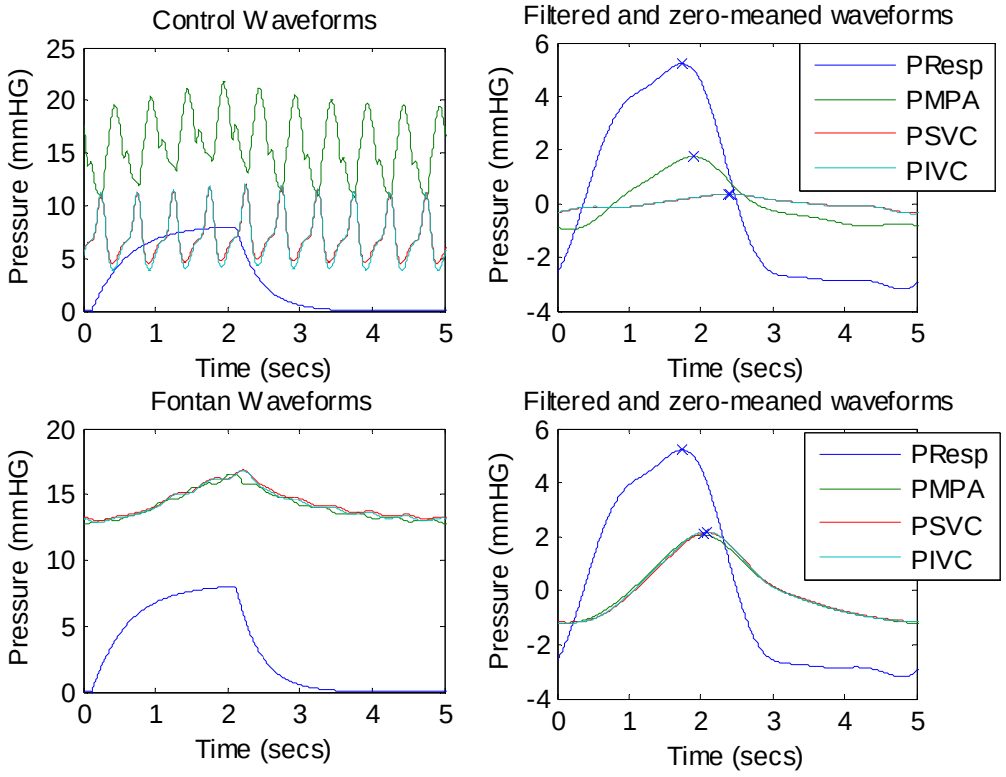

Figure 5.21 Model Pressures: inspiration (PResp), main pulmonary artery (PMPA), Superior Vena Cava (PSVC) and Inferior Vena Cava (PIVC). Top: Control

Situation, Bottom: Fontan Situation, Left: Original Waveforms. Right, Waveforms with means removed and lowpass filtered.

CHAPTER VI

DISCUSSION

The focus of this dissertation has been on providing overall statistics that give insights relative to four possible variations of the Fontan operation. Except for AP connection, the uniqueness of the study lies in the truly univentricular heart preparation in relatively small animals. Various labs have reported animal models of the Fontan circulation, but no other lab, to the best of our knowledge, has actually created the single ventricle physiology or used animals approximating the size of a child.

The preparation is challenging and getting the animals off bypass after the operation has been completed is difficult. In patients, the Fontan is normally implemented in stages, thus giving the circulation time to adapt to lesser modifications. Even so, many patients take considerable time to adapt to the completion stage, as indicated by the routine use of fenestrations that may or may not be closed and relatively long hospital stays. Recent studies in larger animals (50 kgs), in which the connection geometry is realistic even though the heart is not univentricular, suggest that one needs the use of ventricular assist devices (VADs) for animal survival. Though we would like to have access to this level of support, our surgeons do not view this as a viable alternative for patients given the size of the currently available devices.

Though the number of successful studies is small, certain trends have been observed, e.g.

1. Geometry wise, the TCPC and TCPX are similar and may be combined in later reports. The TCPC was implemented when the anatomy of the lamb was such that the IVC could be extended to reach the MPA without the use of a synthetic graft, which would not be possible in the human anatomy. In general, however, the TCPC (no synthetic material) performed better than the TCPX, thus indicating that the natural conduit would be preferable.
2 The TCPY, which differs primarily in the angles at which the SVC and IVC flows converge, in general, performed better than the TCPC and TCPX. Cardiac outputs were higher, which may be the most important factor to consider. Though this is not a common modification, our results suggest that the principle of this connection is worthy of consideration and may be more surgically practical than the "Optiflow" model that CFD and in vitro studies indicate would be most efficient.
3. Energy vs. energy loss? When examining CFD or *in vitro* models, the focus factor for efficiency is energy loss or percent energy loss. However, in *in vivo* studies, the most important factor is CO and/or the energy available to drive blood through the pulmonary circuit. Considering one without the other can give conflicting results. For example, as indicated above, CO was closest to normal in the TCPY and increased significantly when breathing rates and stroke volumes increased, as might be expected with exercise. However, if one looks at energy losses, the TCPY would not appear to be the most efficient. This conclusion is misleading for having more energy/flow is clearly the preferred situation, regardless of the energy lost in the conduit.

4. In general, varying the ventilation parameters has more impact on Fontan than normal circulations, displaying up to 40% shifts in energy losses between settings. A more thorough analysis of individual subjects is needed to understand these phenomena.
5. The results of the timing of respiratory influences are interesting in itself. Of particular interest is the finding that larger delays are observed at the caval levels for Fontan Circulations than for normal circulations, with delays at the pulmonary level being minimal. As the hemodynamic distance between the two sites is less for the Fontan circulation, a move in the opposite direction was expected. This finding will be pursued with lumped parameter modeling studies.

Data analysis is currently in progress of individual lamb hemodynamics that may help eliminate the interanimal variability observed. Impedances and overall resistances between inspiration and expiration are being examined. Future results will be submitted to their appropriate journals.

Future Studies.

As might be expected, given the complicated nature of the various operations, the interanimal variability and the small sample size, these studies in many ways provided more questions than answers. Some answers may be obtained by more thorough analysis of the data available. Others would benefit from larger numbers and different protocols.

1. As for the numerous *in vitro* studies that have been successfully published as part of this project, the most important information may come from careful study of individual subjects rather than from averaged data. For example, the averaged studies

do not really give justice to the influence of respiration in the Fontan Circulations, in which IVC flow is often totally occluded during inspiration.

2. Studies need to be designed to isolate and examine the various respiratory influences—at the pulmonary arteriole level, at the diaphragm level, at the individual chamber and vessel exteriors as the lungs expand and push vessels, etc. Even in our open chest preparation, which is theoretically simpler than a closed-chest situation, the timing effects are complicated. Suggestions in this area include: implementing a left sided bypass procedure to isolate the impact on the caval veins. The lungs could then be ventilated without influencing either the pulmonary vascular resistance (no flow) or arterial (fixed by pump) patterns. Short time/single beat interventions should be attempted in order to trace patterns through the various circuits. In stable preparations when time permits, attempts should be made to close the chest and repeat the ventilation protocol.
3. One of the major goals of this research has been to determine the importance of graft compliance. The limited comparison of the TCPX and TCPC connections suggests that a compliant graft is preferable. However, the gold standard, which we still hope to accomplish, is implanting a graft whose compliance can be changed in situ. Interanimal variability is too large to look at different materials in different animals without performing a very large number of operations. This is being investigated *in vitro* before being pursued *in vivo*.
4. As more patient respiration/hemodynamic data become available, efforts need to be made to compare the results. Our open chest studies have been criticized as only being relevant to the peri-operative period because flow rates decrease rather than

increase during inspiration, as is observed in normal closed chest subjects. Ironically, the first pattern observed in a Fontan patient using MRI techniques also showed decreased flow during inspiration. This may not be the norm, but understanding the factors that cause this scenario is important.

APPENDIX I:

COMPARISON OF HEMODYNAMICS IN LAMB MODELS OF THE FONTAN CIRCULATION

MANUSCRIPT DRAFT SUBMITTED TO CIRCULATION RESEARCH

M. E. Ketner[1], C. L. Lucas[1], M. R. Mill[2], B. Sheridan[2], W. Lucas[3], B. Steele[1], A. Yoganathan[4]
[1]Department of Biomedical Engineering, University of North Carolina-Chapel Hill and North Carolina State University, NC, USA
[2]Department of Cardiothoracic Surgery, University of North Carolina-Chapel Hill, NC, USA
[3]Department of Anesthesiology, University of North Carolina-Chapel Hill, NC, USA
[4]Wallace H. Coulter Department of Biomedical Engineering,
Georgia Institute of Technology & Emory University

Running Head: Hemodynamics in Lamb Models of the Fontan Circulation

Keywords: Animal models, Fontan, hemodynamics, Total Cavopulmonary

Word Count: 2864 words

Figure and Table Count: 7

ABSTRACT

Approximately two out of every one thousand live births have a complex congenital heart defect that effectively creates a univentricular physiology. As a result, the overloaded single ventricle pumps oxygenated and deoxygenated blood to parallel pulmonary and systemic circulations. Since 1971, when Fontan and Baudet were first successful in treating patients with tricuspid atresia, operations that place the pulmonary and systemic circulations

in series with the single pump have been termed “Fontan” Repairs. The original repair, termed atriopulmonary (AP), was implemented by implanting a shunt between the right atrium and main pulmonary artery. The current repair of choice bypasses the right side of the heart, connecting the dissected superior and inferior cava directly to the pulmonary arteries. Such repairs, termed total cavopulmonary connections (TCP), again have various modifications. This research investigated various Fontan modifications not available via computer simulation by implementing surgical designs in vivo in lambs and collecting pressure and flow data in various vessels and chambers. Data were obtained in 4 models: the AP connection and three models of the TCP connection: total cavopulmonary connection without a synthetic graft (TCPC), extracardiac total cavopulmonary connection with graft (TCPX), and the total cavopulmonary connection using a Y-shaped graft (TCPY). Though the number of successful implementations was small, results demonstrated that lambs can be used to model Fontan circulations and that small differences in connection geometries make a difference in the immediate post operation time frame.

INTRODUCTION

Approximately two out of every one thousand live births have a complex congenital heart defect that effectively creates a univentricular physiology.[1] Examples of such defects include multiple ventricular septal defects, tricuspid atresia, hypoplastic left heart syndrome, and double outlet ventricle. As a result of the altered physiology, the overloaded single ventricle pumps both oxygenated and deoxygenated blood to parallel pulmonary and systemic circulations, which leads to inadequate tissue oxygenation and cyanosis.

Prior to the development of surgical shunt procedures connecting systemic to pulmonary arteries (e.g., Blalock-Taussig [2] in 1945 and Potts [3] in 1946), survival of patients with blocked right heart pathways depended on the presence of coexisting defects, e.g., a patent ductus arteriosus and a septal defect, that enabled shunting of blood from the systemic to the pulmonary circulation. In 1948, the first right ventricular bypass was performed in dogs by Rodbard and Wagner, [4] which stimulated experimentation that led to Glenn's 1958 report of a clinical success with a cavopulmonary shunt as a palliative procedure for cyanotic congestive heart disease [5]. The shunt between the superior vena cava (SVC) and right pulmonary artery (RPA) is still widely used. For patients with pulmonary atresia, early repair procedures effecting a separation of pulmonary and systemic pathways included reconstruction of the pulmonary outflow tract with a synthetic extracardiac conduit (Rastelli. in 1965 [6]) or an aortic valved homograft (Ross and Somerville in 1966 [7]).

In 1971, Fontan and Baudet [8] successfully implemented in two patients with tricuspid atresia a palliative atriopulmonary (AP) connection consisting of a graft between the right atria (RA) and the main pulmonary artery (MPA). This resulted in separate pulmonary and systemic circulations with only one functional ventricle. The "Fontan" procedure, or one of its many modifications, has since become the repair option in anatomically and hemodynamically qualified patients [8].

During the 35 years since that first repair, surgical preferences have evolved from the AP connection to connections that remove the influence of the pumping right atrium, classified as total cavopulmonary (TCP) connections, which come in two varieties. In 1988, de Leval [9] introduced an intra-atrial or lateral tunnel TCP modification. This modification includes an end-to-side anastomosis of the SVC to the RPA, construction of an intra-atrial

tunnel using composite material, part of the RA wall, and use of a synthetic graft to channel the inferior vena cava (IVC) to the inferior side of the RPA. Marcelletti et al [10] introduced an extracardiac TCP modification in 1990. This implements a graft, usually of synthetic material, that connects the IVC to the inferior side of the RPA without disturbing the RA.

In spite of the general agreement that TCP repairs are superior to AP repairs, [11-13] practice still varies widely with surgeon relative to connection geometries (anastomosis sites, graft size, graft material, connection angles, etc.) In spite of the general agreement that connections should minimize energy losses and maintain normal distribution of total and IVC flow to both lungs, the need still exists for tools that will enable presurgical planning to achieve these goals.

The motivation for the studies undertaken for this report is the need for animal models that can be used to test hypotheses/planning tools not readily tested in patients or *in silico*. To date, the animals that have been used to develop ideas and practice techniques relative to Fontan operations have been predominantly adult dogs, sheep and pigs [14-26]. The focus of our laboratory has been the development of several Fontan modifications in lambs weighing between 10 and 25 kilograms, which are more comparable in size and age to the patient population of interest.

METHODS

Animals Studies

In-vivo experiments were performed in lambs one to three months in age, ranging from 10.0 to 25.0 kilograms. This weight range was chosen to closely approximate the anatomy and vessel geometries of children ranging from one month to three years old. All animals

were cared for in accordance with the "Guide for the Care and Use of Laboratory Animals" (NIH Publication No. 86-23, revised 1985) and were in accordance with the standards of the Institutional Animal Care and Use Committee of the University of North Carolina at Chapel Hill.

Surgical Procedure

The lamb was sedated using ketamine (30 mg/kg) intramuscularly and then administered isoflurane and oxygen throughout the procedure. Once sedated, the lamb was positioned on the table and its chest, right flank, thorax, and neck were shaved. Endotracheal intubation of the animal took place using an appropriately sized tube with a balloon and stilette. The tidal volume administered was 10 – 15 ml / kg without any positive end expiratory pressure or adjusted accordingly to maintain optimal arterial blood gas tensions. Measurements of respiration rate, carbon dioxide (CO_2) return, and pulse oximetry (placed on the tongue) were monitored. A Validyne pneumotachometer (Validyne Engineering, Northridge, CA) was introduced into the air circuit in order to monitor and record air flow. Also in the air circuit, a fluid filled polypropylene catheter was inserted and connected to a Statham P23Gb transducer (Statham Transducer P23Gb, Siemens) to measure airway pressure. Next, a cut down on the internal jugular was performed and a double lumen catheter was inserted. This allowed for intravenous fluid and pharmaceutical administration throughout the procedure. Once this was completed, the carotid artery was identified and a Millar Mikro-Tip Catheter (MPC-500, Millar Instruments, Houston, TX) pressure transducer was introduced and positioned as close to the aortic arch as possible in order to record and observe arterial pressure (AOP). Arterial blood gases were closely monitored throughout the

procedure and pharmaceutical adjustments were provided when needed. Blood gases were measured by an iSTAT analyzer (Abbott Laboratories, IL). Parameters monitored included hematocrit, hemoglobin, sodium, potassium, pH, PCO2, PO2, Calcium, O2 saturation, bicarbonate, and base excess.

A mid-sternotomy was performed that started at approximately the sixth interspace. Exposure was from the superior azygous vein to the diaphragm. The SVC was cleared and the azygous vein, if present, was tied off. The same was done for the IVC. The AO was then dissected and cleaned and the pulmonary arteries were exposed. The pericardium was opened and as much as possible was preserved in case a pericardial patch was needed during the operation.

Millar pressure transducers were placed in the MPA, SVC, IVC, RA, left atria (LA), and left ventricle (LV). To record blood flow, Transonic T206 Small Animal Blood Flow probes (Transonic Systems Inc., Ithaca, NY) were positioned around the LPA, MPA, SVC, IVC, and aorta. Conductive gel was placed between the vessel and transducer in order to improve the signal quality. Data were recorded at a rate of 200 Hertz for individual episodes of 5.12 seconds or 1024 data points/episode. Cardiopulmonary bypass was then performed using a bi-caval cannulation and arterial cannulation at the aortic arch. Once on bypass, one of the following Fontan connection geometries was constructed:

The AP connection (Figure 1A) consisted of a graft connected to the RA appendage. The graft was connected to the MPA by an end-to-side anastomosis. The tricuspid valve was closed using a pursestring suture. (Technique first reported by Haneda et al. [14])

The TCPC connection (Figure 1B): The IVC was transected and connected to the transected MPA via an end-to-end anastomosis. The SVC was subsequently attached to the

RPA via an end-to-side anastomosis. This connection used native vessels for the Fontan connection. No synthetic graft was used.

The TCPX connection (Figure 1C): The IVC was connected to the extracardiac graft using an end-to-end anastomosis. The RPA was then connected to the graft via an end-to-side anastomosis.

The TCPY connection (Figure 1D): The IVC was connected to the graft using an end-to-end anastomosis. The SVC was connected to the graft using an end-to-side anastomosis. The MPA was attached to the graft using an end-to-end anastomosis.

In all connections, an atrial septectomy was performed to allow perfusion and return of the right coronary blood flow.

Cardiopulmonary bypass times averaged approximately 90 minutes. Bypass pump rates were set at approximately one-third of normal cardiac output to maintain proper perfusion. Central venous pressure was monitored in order to assess and maintain blood volume while on bypass. Steroids were given prior to going on bypass. Blood gases were taken approximately every five minutes to control hemodynamic stability. Ventilation of the lungs was performed occasionally while on bypass in order to prevent fluid buildup in the lungs. Additional blood from a donor animal was heated to 37 degrees Celsius and then hemoconcentrated using an Minimax Plus (Medtronic Inc., Minneapolis MN) oxygenator system.

Upon procedure completion, pressure and flow transducers were reintroduced. The animal was then taken off bypass under Fontan conditions. Experimental protocol was performed and surviving lambs were euthanized using a lethal dose of concentrated potassium.

Data and Statistical Analysis

Data analysis was performed using MATLAB™ (The Mathworks Inc., Natick, MA). All values were expressed as mean ± SD. Statistical significance was determined using univariate and repeated measures analysis of variance. A p-value < 0.05 was regarded as significant. The post hoc Bonferroni test was used in order to compensate for type I error with multiple comparisons and the Tukey honestly significant difference test was used for multiple comparison tests across experimental groups.

Vascular Resistance Calculations

Systemic vascular resistance and pulumonary vascular resistance were calculated.

For normal and AP connections,

$$SVR\ (dyne \bullet \sec \bullet cm^{-5}) = 80 * \frac{(\overline{AOP} - \overline{RAP}) mmHg}{\overline{CO}\ (L \bullet \min^{-1})} \qquad (1)$$

where AOP is mean arterial pressure, RAP is mean right atrial pressure and CO is mean cardiac output.

For TCPC, TCPX, and TCPY connections, SVR was calculated by:

$$SVR\ (dyne \bullet \sec \bullet cm^{-5}) = 80 * \frac{(\overline{AOP} - \overline{PAP}) mmHg}{\overline{CO}\ (L \bullet \min^{-1})} \qquad (2)$$

where PAP is mean pulmonary artery pressure. Pulmonary artery pressure was used because the right atria was eliminated from the circulation. Pulmonary vascular resistance was calculated by:

$$PVR\ (dyne \bullet \sec \bullet cm^{-5}) = 80 * \frac{(\overline{PAP} - \overline{LAP}) mmHg}{\overline{CO}\ (L \bullet \min^{-1})} \qquad (3)$$

RESULTS

Representative results for one animal (TCPC model) are illustrated in Figure 2. Though differences in the TCP configurations were observed, the general pattern is consistent. Flow rates decrease, pulsatility is almost removed at the caval levels, caval pressures increase and respiration effects are magnified to the extent that flow may be occluded during inspiration. Specific results for each connection geometry are shown in Tables 1-4.

Bar charts illustrating before and after values across all connections are shown in Figure 3. To summarize, generalized findings for the variables considered are as follows: AOP decreased slightly (TCPC) or remained unchanged in all geometries. With the exception of AP, PAP increased slightly or remained unchanged. SVCP and IVCP rose significantly in all cases. LAP did not change significantly in any of the geometries. RAP increased significantly in AP connections but was not measured in the TCP geometries, in which the pressure in the RAP and LAP were assumed to be the same. All flow rates decreased; however, the TCPY flow was significantly higher than the flow for the other geometries. With the exception of the TCPC, flow percentages to pulmonary arteries remained relatively unchanged. In the AP and TCPC, percentages increased significantly to the SVC. With the exception of TCPY, PVR increased in all models. SVR only increased significantly in the AP model.

DISCUSSION

Though the number of successful studies is relatively small, these results demonstrate that lamb models of Fontan circulations can be accomplished. Except for AP connection,

the uniqueness of the study lies in the extracardiac connections and univentricular heart preparation in small lambs.

Various labs have reported animal models of the Fontan circulation, but no other lab, to the best of our knowledge, has actually created the single ventricle physiology or used animals approximating the size of a child. Hanada et al [14], creating AP shunts in dogs, had comparable findings relative to changes in hemodynamics. Gandhi, Bromberg, Rodefeld and colleagues [15-19] created AP and intra-atrial tunnel TCP connections in dogs to characterize the causes of atrial flutter and to suggest techniques for their reduction and reported that flutter could not be induced with proper placement of the suture line in relationship to the crista terminalis. Szabo and colleagues [20] established Fontan Circulations in dogs and examined cardiac contractility, determining that the increased ventricular/arterial coupling ratio and reduced mechanical efficiency would predict limited functional reserve after the Fontan operation. Mace and Colleagues [21] established Fontan circulations in pigs, determining that venous return parameters were changed. Though yielding valuable information about the effects of the Fontan circulation on venous and ventricular parameters, Fontan geometries created were not pertinent to surgical practice.

Lardo and colleagues used *in vitro* studies in explanted adult sheep hearts to better understand the energy losses associated with atriopulmonary (AP) and various TCP connections [22-24]. They compared energy losses in models of intra-atrial tunnels, extracardiac tunnels and extracardiac conduits with and without caval offsets and reported that extracardiac tunnels with offsets were most efficient. These studies are most analogous to our in vitro [27-29]and computational studies [30]in which boundary conditions are controlled.

The preparation is challenging and getting the animals off bypass after the operation has been completed is difficult. In patients, the Fontan is normally implemented in stages, thus giving the circulation time to adapt to lesser modifications. Even so, many patients take considerable time to adapt to the completion stage, as indicated by the routine use of fenestrations that may or may not be closed and relatively long hospital stays [31, 32]. A recent innovative modification of the Fontan circulation was created in 33-79 kg sheep by Rodefeld et al.[25] Axial flow pumps were placed percutaneously in the IVC and SVC percutaneously. Theoretically, the pumps would reverse the Fontan paradox of caval hypertension and pulmonary hypotension. Moreover, circulation hemodynamics resembling that of a two ventricle physiology was restored. Early results showed great promise. Hemodynamics remained stable for 1 hour and 6 hour durations postoperatively. Systemic venous pressure remained unchanged from normal control circulation conditions. Secondly, pulmonary arterial pressures were maintained in the vicinity of baseline measurements. With the exception of the more normalized blood flow as a result of the assist device, results were similar to our findings in the young lambs with respect to systemic and pulmonary pressures. In a similar study, Riemer et al [26]placed an axial flow pump into a TCPC circuit in large sheep, which resulted in an increase in cardiac output and IVC flow and a return to normal IVC, MPA, and LA pressures. Though we would like to have access to this level of support, this as not a viable alternative for most children given the size of the currently available devices.

Though patient prognosis after Fontan completion has improved considerably since 1971, patients still suffer from life long complications ranging from exercise intolerance to life threatening GI problems for which the genesis is not yet understood [33, 34]. Many designs

of TCP repairs are used in current practice, varying markedly from surgeon to surgeon and patient to patient. Rapid advances in MRI [33]and CFD technologies [35-37] are enabling investigators to study the hemodynamics on a patient-by-patient basis. While these studies provide valuable insights and are leading to exciting new tools for surgical planning, some studies can still only be done in animals. MRI studies are limited by the lack of blood pressure measurements and CFD studies, for the most part, are limited to open loop studies in rigid geometries. Only animal studies, with all of their inherent difficulties, can give a complete picture of how the closed loop body reacts to the altered circulation.

While the main goal of this paper is to describe methods for creating animal models of the Fontan Circulation over a range of patient possibilities, findings have suggested further investigations. For example, results suggested that the TCPY repair, which is unique to this study, is worthy of further investigation and the improved statistics for the TCPC relative to the TCPX configuration suggest that biological grafts, even when growth is not a factor, are better than synthetic grafts.

Acknowledgments

This work was supported by a BRP grant from the National Heart, Lung, and Blood Institute, HL67622.

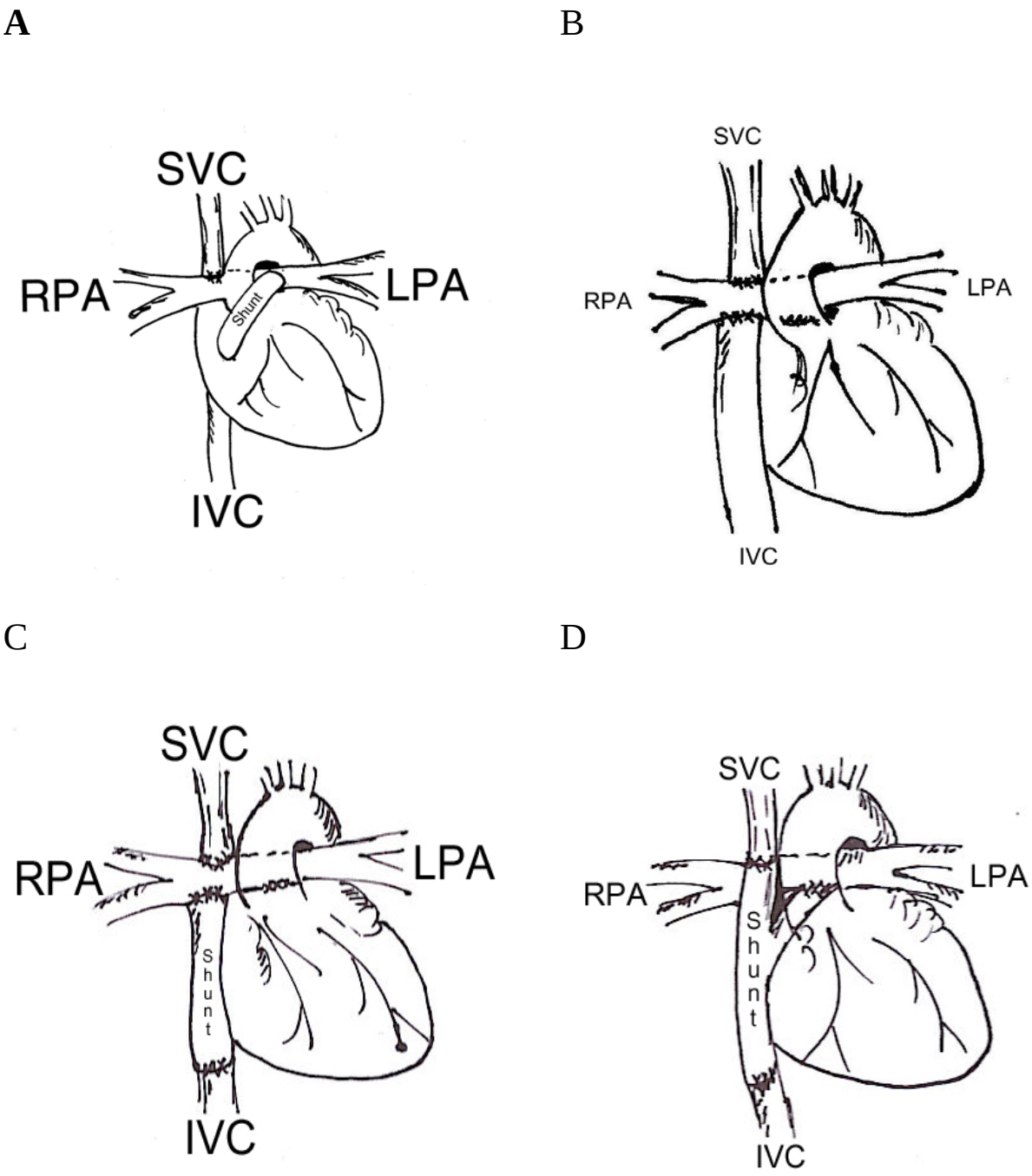

Figure 1. Schematic drawings of the A) AP, B) TCPC, C) TCPX, and D) TCPY Fontan modifications.

A

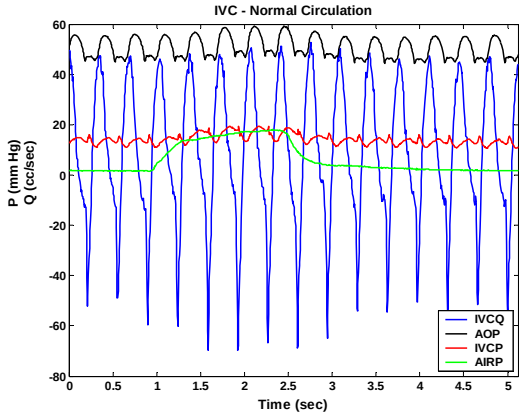

B

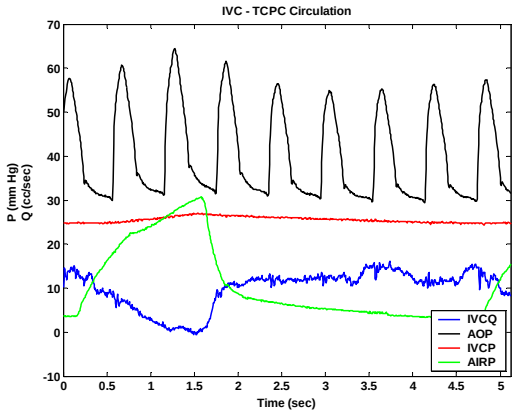

C

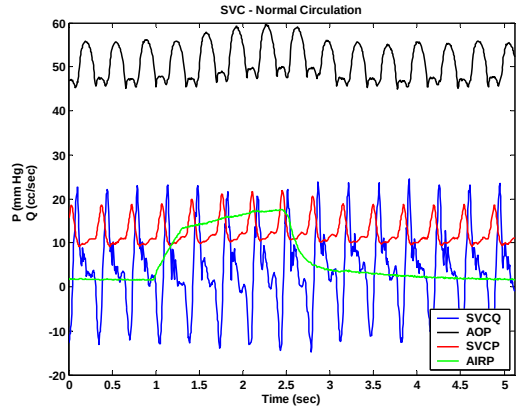

D

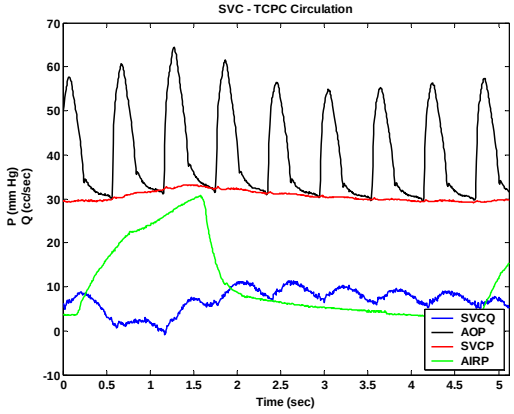

Figure 2. Representative waveforms depicting pressure (P) and flow (Q) of the inferior vena cava (IVC) under normal circulation (A and C) and TCPC circulations (B and D). Arterial pressure (AOP) and airway pressure (AIRP) are shown for reference.

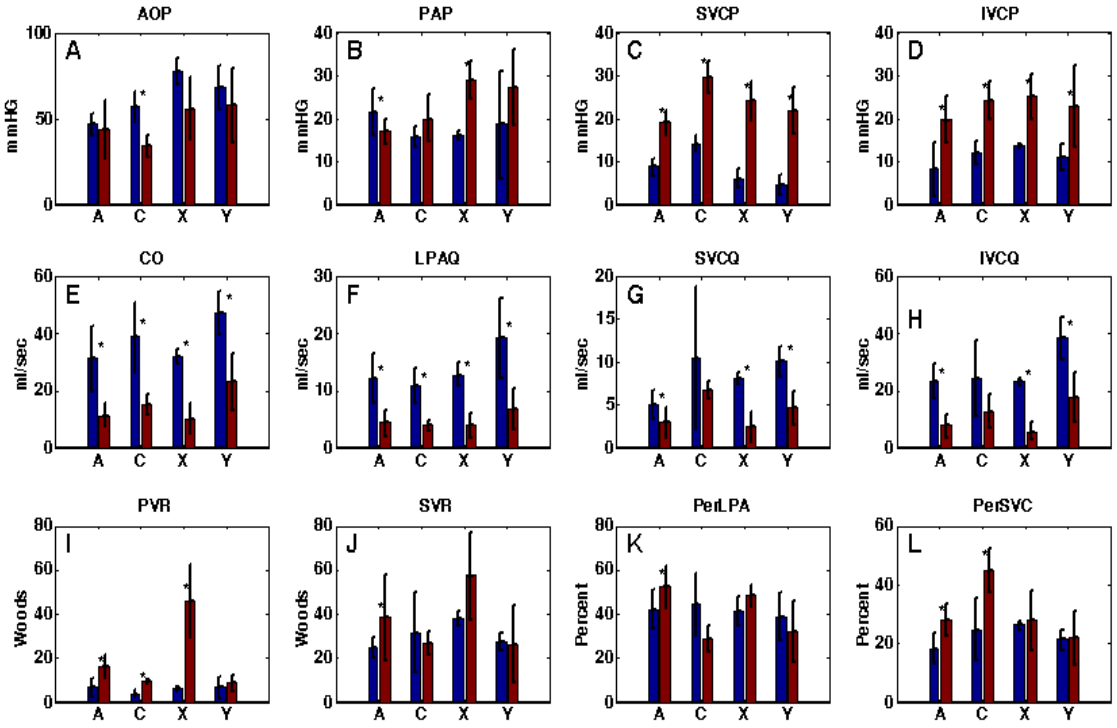

Figure 3. Comparison of before and after hemodynamics across connection geometries: A=AP, C=TCPC, X=TCPX and Y=TCPY.

A) Aortic Pressure (AOP), B) Pulmonary Artery Pressure (PAP), C) Systemic Venous Pressure (SVCP), D) Inferior Vena Cava Pressure (IVCP), E) Cardiac Output (C), F) Left Pulmonary Artery Flow (LPAQ), G) Superior Vena Cava Flow (SVCQ), H) Inferior Vena Cava Flow (IVCQ), I) Pulmonary Vascular Resistance (PVR), J) Systemic Vascular Resistance (SVR). K) % LPA Flow (PerLPA), L) % IVC Flow (PerIVC)

***Statistically significant differences with a $p<0.05$ as indicated**

Table 1:

	Normal **Mean ± SD** **(n=11)**	**AP Connection** **Mean ± SD** **(n=11)**
Pressures (mm Hg)		
Ao	46.7 ± 6.3	43.5 ± 17.0*
PA	21.5 ± 5.3	17.0 ± 2.9*
SVC	8.7 ± 2.0	19.0 ± 2.8*
IVC	8.1 ± 6.3	19.6 ± 5.4*
LA	8.1 ± 2.8	6.5 ± 2.6
RA	6.2 ± 3.2	15.7 ± 6.1*
Flows (cc/sec)		
PA	29.7 ± 10.9	9.3 ± 3.7*
SVC	5.1 ± 1.7	2.9 ± 1.7*
IVC	23.3 ± 6.3	7.7 ± 4.1*
LPA	12.1 ± 4.3	4.3 ± 2.3*
CO	31.3 ± 11.6	11.3 ± 4.1*
% LPA	42.2 ± 9.1	52.4 ± 9.7
% SVC	18.1 ± 5.2	27.9 ± 5.3
% IVC	81.9 ± 5.2	72.1 ± 5.3
Vascular Resistances		
PVR		
dyne·sec·cm^{-5}	536 ± 333.7	1270 ± 434.4*
Wood Units	6.7 ± 4.17	15.9 ± 5.4*
SVR		
dyne·sec·cm^{-5}	1987.1 ± 358.1	3065.6 ± 1550.3*
Wood Units	24.8 ± 4.5	38.4 ± 19.3*

Table 1. Overall hemodynamic values under normal and AP circulations in lambs.

***Statistically significant differences with a $p<0.05$ as indicated**

Table 2:

	Normal Mean ± SD (n=4)	TCPC Connection Mean ± SD (n=4)
Pressures (mm Hg)		
Ao	56.7 ± 8.9	33.9 ± 6.32*
PA	15.6 ± 2.4	20.0 ± 5.5
SVC	14.1 ± 1.8	29.5 ± 3.7*
IVC	12.1 ± 2.7	24.2 ± 4.2*
LA	13.0 ± 1.3	9.9 ± 4.6
Flows (cc/sec)		
SVC	10.5 ± 8.4	6.7 ± 1.0
IVC	24.3 ± 12.9	12.6 ± 6.0
LPA	10.9 ± 3.2	3.9 ± 0.8*
CO	38.8 ± 12.3	15.2 ± 3.3*
% LPA	44.2 ± 14.0	28.4 ± 5.8
% SVC	24.6 ± 10.7	44.7 ± 7.3*
% IVC	75.4 ± 10.7	55.3 ± 7.3*
Vascular Resistances		
PVR		
dyne·sec·cm^{-5}	314.4 ± 129.9	736.4 ± 54.1*
Wood Units	3.93 ± 1.6	9.2 ± 0.7*
SVR		
dyne·sec·cm^{-5}	2523.5 ± 1452.1	2137.5 ± 423.1
Wood Units	31.5 ± 18.2	26.7 ± 5.3

Table 2. Overall hemodynamic values under normal and TCPC circulations in lambs.

***Statistically significant differences with a $p<0.05$ as indicated**

Table 3:

	Normal Mean ± SD (n=4)	TCPX Connection Mean ± SD (n=4)
Pressures (mm Hg)		
Ao	77.4 ± 7.7	55.63 ± 18.2
PA	15.9 ± 1.0	28.9 ± 4.3*
SVC	5.9 ± 2.2	24.0 ± 4.6*
IVC	13.6 ± 0.3	25.2 ± 5.3*
LA	4.3 ± 0.5	6.5 ± 2.9
Flows (cc/sec)		
SVC	8.1 ± 0.8	2.4 ± 1.8*
IVC	23.0 ± 1.4	5.7 ± 3.1*
LPA	12.8 ± 2.1	3.9 ± 2.2*
CO	32.0 ± 2.5	10.2 ± 5.4*
% LPA	41.2 ± 6.7	48.4 ± 4.9
% SVC	26.0 ± 1.4	27.6 ± 10.1
% IVC	74.0 ± 1.4	72.4 ± 10.1
Vascular Resistances		
PVR		
dyne·sec·cm^{-5}	487.1 ± 72.8	3664.4 ± 1343.7*
Wood Units	6.1 ± 0.9	45.8 ± 16.8*
SVR		
dyne·sec·cm^{-5}	3021.4 ± 300.1	4579.8 ± 1603.5
Wood Units	37.8 ± 3.8	57.3 ± 20.0

Table 3. Overall hemodynamic values under normal and TCPX circulations in lambs.

***Statistically significant differences with a p<0.05 as indicated.**

Table 4:

	Normal Mean ± SD (n=5)	**TCPY Connection** Mean ± SD (n=5)
Pressures (mm Hg)		
Ao	68.4 ± 12.6	57.5 ± 21.7
PA	18.6 ± 12.6	27.2 ± 8.9
SVC	4.6 ± 2.2	21.8 ± 5.5*
IVC	10.9 ± 3.1	22.8 ± 9.6*
LA	9.3 ± 5.9	21.4 ± 13.9
Flows (cc/sec)		
PA	47.5 ± 10.3	19.7 ± 10.8*
SVC	10.1 ± 1.8	4.6 ± 2.0*
IVC	38.4 ± 7.3	17.9 ± 8.6*
LPA	19.1 ± 7.1	6.8 ± 3.6*
CO	47.2 ± 7.7	23.0 ± 9.9*
% LPA	38.9 ± 11.0	31.9 ± 14.0
% SVC	21.2 ± 3.4	21.8 ± 9.4
% IVC	78.9 ± 3.4	78.2 ± 9.4
Vascular Resistances		
PVR		
dyne·sec·cm^{-5}	543.8 ± 303.6	688.5 ± 267.8*
Wood Units	6.8 ± 4.8	8.6 ± 3.7*
SVR		
dyne·sec·cm^{-5}	2182.8 ± 299.1	2084.6 ± 1406.1
Wood Units	27.3 ± 3.7	26.1 ± 17.6

Table 4. Overall hemodynamic values under normal and TCPY circulations in lambs.

***Statistically significant differences with a $p<0.05$ as indicated.**

REFERENCES

1. Rowe RD, Freedom RM, Mehrizi A. *The Neonate with Congenital Heart Disease.* 2nd ed. Philadelphia, PA: W.B. Saunders Co.; 1981.

2. Blalock A, Taussig H.B. Surgical treatment of malformations of the heart in which there is pulmonary stenosis or pulmonary atresia. *JAMA*. 1945;128:128-189.

3. Potts WJ, Gibson S. Aorto-pulmonary anastomosis in congenital pulmonary steniosis. *JAMA*. 1948;137:343.

4. Rodbard S, Wagner D. Bypassing the right ventricle. *Proc Soc Exp Biol Med*. 1949;71:69–70.

5. Glenn WW. Circulatory bypass of the right side of the heart. IV. shunt between superior vena cava and distal right pulmonary artery; report of clinical application. *N Engl J Med*. 1958;259:117-120.

6. Rastelli GC, Ongley PA, Davis GD, Kirklin JW. Surgical Repair for Pulmonary valve atresia with coronary-pulmonary artery fistula: Report of Case. *Mayo Clin Proc*. 1965;40:521-527.

7. Ross DN, Somerville J. Correction of pulmonary atresia with a homograft aortic valve. *Lancet*. 1966;2:1446-1447.

8. Castaneda AR. From Glenn to Fontan. A continuing evolution. *Circulation*. 1992;86:II80-4.

9. de Leval MR, Kilner P, Gewillig M, Bull C. Total cavopulmonary connection: A logical alternative to atriopulmonary connection for complex Fontan operations. experimental studies and early clinical experience. *J Thorac Cardiovasc Surg*. 1988;96:682-695.

10. Marcelletti C, Corno A, Giannico S, Marino B. Inferior vena cava-pulmonary artery extracardiac conduit. A new form of right heart bypass. *J Thorac Cardiovasc Surg*. 1990;100:228-232.

11. Marcelletti CF, Hanley FL, Mavroudis C, et al. Revision of previous Fontan connections to total extracardiac cavopulmonary anastomosis: A multicenter experience. *J Thorac Cardiovasc Surg*. 2000;119:340-346.

12. Podzolkov VP, Zaets SB, Chiaureli MR, Alekyan BG, Zotova LM, Chernikh IG. Comparative assessment of Fontan operation in modifications of atriopulmonary and total cavopulmonary anastomoses. *Eur J Cardiothorac Surg*. 1997;11:458-465.

13. Laschinger JC, Redmond JM, Cameron DE, Kan JS, Ringel RE. Intermediate results of the extracardiac Fontan procedure. *Ann Thorac Surg*. 1996;62:1261-7; discussion 1266-7.

14. Haneda K, Konnai T, Sato N, Nicoloff NN, Mohri H. Acute hemodynamic changes after Fontan operation: An experimental study. *Tohoku J Exp Med*. 1993;169:113-119.

15. Rodefeld MD, Bromberg BI, Schuessler RB, Boineau JP, Cox JL, Huddleston CB. Atrial flutter after lateral tunnel construction in the modified Fontan operation: A canine model. *J Thorac Cardiovasc Surg*. 1996;111:514-526.

16. Bromberg BI, Schuessler RB, Gandhi SK, Rodefeld MD, Boineau JP, Huddleston CB. A canine model of atrial flutter following the intra-atrial lateral tunnel Fontan operation. *J Electrocardiol*. 1998;30 Suppl:85-93.

17. Gandhi SK, Bromberg BI, Schuessler RB, et al. Characterization and surgical ablation of atrial flutter after the classic Fontan repair. *Ann Thorac Surg*. 1996;61:1666-78; discussion 1678-9.

18. Gandhi SK, Bromberg BI, Rodefeld MD, et al. Lateral tunnel suture line variation reduces atrial flutter after the modified Fontan operation. *Ann Thorac Surg*. 1996;61:1299-1309.

19. Rodefeld MD, Gandhi SK, Huddleston CB, et al. Anatomically based ablation of atrial flutter in an acute canine model of the modified Fontan operation. *J Thorac Cardiovasc Surg*. 1996;112:898-907.

20. Szabo G, Buhmann V, Graf A, et al. Ventricular energetics after the Fontan operation: Contractility-afterload mismatch. *J Thorac Cardiovasc Surg*. 2003;125:1061-1069.

21. Mace L, Dervanian P, Bourriez A, et al. Changes in venous return parameters associated with univentricular Fontan circulations. *Am J Physiol Heart Circ Physiol*. 2000;279:H2335-43.

22. Lardo AC, Webber SA, Iyengar A, del Nido PJ, Friehs I, Cape EG. Bidirectional superior cavopulmonary anastomosis improves mechanical efficiency in dilated atriopulmonary connections. *J Thorac Cardiovasc Surg*. 1999;118:681-691.

23. Lardo AC, del Nido PJ, Webber SA, Friehs I, Cape EG. Hemodynamic effect of progressive right atrial dilatation in atriopulmonary connections. *J Thorac Cardiovasc Surg*. 1997;114:2-8.

24. Lardo AC, Webber SA, Friehs I, del Nido PJ, Cape EG. Fluid dynamic comparison of intra-atrial and extracardiac total cavopulmonary connections. *J Thorac Cardiovasc Surg*. 1999;117:697-704.

25. Rodefeld MD, Boyd JH, Myers CD, et al. Cavopulmonary assist: Circulatory support for the univentricular Fontan circulation. *Ann Thorac Surg*. 2003;76:1911-6; discussion 1916.

26. Riemer RK, Amir G, Reichenbach SH, Reinhartz O. Mechanical support of total cavopulmonary connection with an axial flow pump. *J Thorac Cardiovasc Surg*. 2005;130:351-354.

27. Ensley AE. *A Fluid Mechanic assessment of the Total Cavopulmonary Connection.* [MS Thesis]. Atlanta, GA: Georgia Institute of Technology; 2000.

28. Ensley AE, Lynch P, Chatzimavroudis GP, Lucas C, Sharma S, Yoganathan AP. Toward designing the optimal total cavopulmonary connection: An in vitro study. *Ann Thorac Surg*. 1999;68:1384-1390.

29. Ryu K, Healy TM, Ensley AE, Sharma S, Lucas C, Yoganathan AP. Importance of accurate geometry in the study of the total cavopulmonary connection: Computational simulations and in vitro experiments. *Ann Biomed Eng*. 2001;29:844-853.

30. Masters JC, Ketner M, Bleiweis MS, Mill M, Yoganathan A, Lucas CL. The effect of incorporating vessel compliance in a computational model of blood flow in a total cavopulmonary connection (TCPC) with caval centerline offset. *J Biomech Eng*. 2004;126:709-713.

31. Thompson LD, Petrossian E, McElhinney DB, et al. Is it necessary to routinely fenestrate an extracardiac Fontan? *J Am Coll Cardiol*. 1999;34:539-544.

32. Cetta F, Feldt RH, O'Leary PW, et al. Improved early morbidity and mortality after Fontan operation: The mayo clinic experience, 1987 to 1992. *J Am Coll Cardiol*. 1996;28:480-486.

33. Gersony DR, Gersony WM. Management of the postoperative Fontan patient. *Progress in Pediatric Cardiology*. 2003;17:73-79.

34. de Leval MR. The Fontan circulation: A challenge to william harvey? *Nat Clin Pract Cardiovasc Med*. 2005;2:202-208.

35. Pekkan K, Kitajima HD, de Zelicourt D, et al. Total cavopulmonary connection flow with functional left pulmonary artery stenosis: Angioplasty and fenestration in vitro. *Circulation*. 2005;112:3264-3271.

36. Pekkan K, de Zelicourt D, Ge L, et al. Physics-driven CFD modeling of complex anatomical cardiovascular flows-a TCPC case study. *Ann Biomed Eng*. 2005;33:284-300.

37. de Zelicourt DA, Pekkan K, Parks J, Kanter K, Fogel M, Yoganathan AP. Flow study of an extracardiac connection with persistent left superior vena cava. *J Thorac Cardiovasc Surg*. 2006;131:785-791.

APPENDIX II:

ENERGETICS OF POSITIVE PRESSURE VENTILATION IN LAMB FONTAN CIRCULATIONS

MANUSCRIPT DRAFT SUBMITTED TO ANNALS OF BIOMEDICAL ENGINEERING

M. E. Ketner[1], C. L. Lucas[1], M. R. Mill[2], B. Sheridan[2], W. Lucas[3], B. Steele[1], A. Yoganathan[4]
[1]Department of Biomedical Engineering, University of North Carolina-Chapel Hill and North Carolina State University, NC, USA
[2]Department of Cardiothoracic Surgery, University of North Carolina-Chapel Hill, NC, USA
[3]Department of Anesthesiology, University of North Carolina-Chapel Hill, NC, USA
[4]Wallace H. Coulter Department of Biomedical Engineering,
Georgia Institute of Technology & Emory University

Running Head: ENERGETICS OF VENTILATION IN LAMB FONTAN CIRCULATIONS

ABSTRACT

Current palliative solutions to repair congenital heart defects that effectively create a univentricular physiology, termed “Fontan” repairs, consist of bypassing the right side of the heart and connecting the systemic and pulmonary circulations in series with the univentricular pump. Positive pressure ventilation (PPV) has a particularly deleterious effect on children who have Fontan circulations. The aim of this study is to examine energy gains/losses under varying PPV parameters. The long term goal is to determine an optimal surgical management strategy and develop more accurate computer simulation models. In vivo studies were performed in lambs in which a Fontan circulation had been established.

Four modifications were examined: the atriopulmonary (AP) connection, total cavopulmonary connection without a synthetic graft (TCPC), extracardiac total cavopulmonary connection with graft (TCPX), and the total cavopulmonary connection using a Y-shaped graft (TCPY). Multiple pressure and flow transducers were introduced. Significant differences in power generation occurred across varying stroke volume and ventilation rates for all Fontan modifications examined. Power losses significantly differed across connection types. Results provide insight on PPV management and peri- and postoperative therapeutics.

Keywords: animal models, Fontan, hemodynamics

INTRODUCTION

A common congenital heart defect that occurs in children today impairs the atriopulmonary pathway and thus effectively creates a univentricular geometry [1]. Examples of such defects include multiple ventricular septal defects, tricuspid atresia, hypoplastic left heart syndrome, and double outlet ventricle. As a result of the altered physiology, the overloaded single ventricle pumps both oxygenated and deoxygenated blood to parallel pulmonary and systemic circulations, which leads to inadequate tissue oxygenation and cyanosis.

In 1971, Fontan and Baudet[2] successfully implemented an atriopulmonary (AP) connection (graft between the right atrium (RA) and main pulmonary artery (MPA)) in a patient with tricuspid atresia, effectively separating the parallel pulmonary and systemic circuits, placing them in series with the univentricular pump. The "Fontan" procedure or

one of its many modifications became the repair option of choice in patients who qualified, i.e., those who had reasonable anatomy and normal pulmonary vascular resistance [3].

During the 35 years since that first repair, surgical preferences have evolved from the AP connection to connections that remove the influence of the pumping right atrium, classified as total cavopulmonary (TCP) connections, which come in two varieties. The intra-atrial or lateral tunnel version, attributed to deLeval et al, [4] 1988, includes an end-to-side anastomosis of the superior vena cava (SVC) to the right pulmonary artery (RPA), construction of an intra-atrial tunnel using composite material, part of the RA wall, and use of a synthetic graft to channel the inferior vena cava (IVC) to the inferior side of the RPA. In the extracardiac version, attributed to Marcelleti et al, [5]1990, a graft, usually of synthetic material, connects the IVC to the inferior side of the RPA without disturbing the RA. Variations of TCP repairs are used almost exclusively in current practice [6-8], with each surgeon appearing to have her/his own preferences relative to features such as anastomosis sites, graft size, graft material, connection angles, etc.

Without the RV pump, one of the features of all TCP repairs is the increase in caval pressures to at least the level of the pulmonary artery pressure, i.e., from means in the 5-10 mmHg range to means in the 15 mmHg and above range. The resulting caval hypertension and possible pulmonary hypotension creates a situation, termed the "Fontan Paradox"[9] which is believed to be the underlying mechanisms for many complications following a Fontan procedure. Pulsatility is markedly reduced at caval and pulmonary levels, which may also have a negative impact on vessel function. Another feature of the post Fontan operation is a marked increase in the effects of respiration. Unlike many surgeries after which positive

pressure ventilation (PPV) has a positive effect relative to managing pulmonary edema, Fontan patients are weaned from PPV as soon as possible.

The motivation for the studies undertaken for this report is the need for a better understanding of this increased respiratory influence on the Fontan circulation. Improved understanding will enable more accurate computational models that should in turn lead to improved surgical management strategies and ventilation therapies. Though patient prognosis has improved considerably over the years, patients with Fontan circulations still suffer from complications, ranging from exercise intolerance to life threatening GI disorders [10, 11].

To this end, we have examined the effects of varying respiration rates and stroke volumes in lamb models of AP and TCP Fontan geometries. Results are presented in terms of power available at key junctions (SVC, IVC and LPA), and power conserved/lost across the connection geometry.

Power related variables are emphasized because fluid mechanical power loss is among the multiple variables being considered in optimizing Fontan connection geometries, hypothesizing that lowering the loss could reduce the workload on the single ventricle and increase exercise tolerance. This particular feature also has the advantage of being testable in vitro and in silico while controlling geometry features and boundary conditions. The effects of respiration, which include diaphragm movement, however, are multifaceted and difficult to model in vitro or in silico. Factors to be considered include internal influences on the pulmonary blood vessels and exterior influences on heart chambers and major vessels in the thoracic region.

METHODS

Animals Studies

In-vivo experiments were performed in lambs one to three months in age, ranging from 10.0 to 25.0 kilograms. This weight range was chosen to closely approximate the anatomy and vessel geometries of children ranging from one month to three years old. All animals were cared for in accordance with the "Guide for the Care and Use of Laboratory Animals" (NIH Publication No. 86-23, revised 1985) and were in accordance with the standards of the Institutional Animal Care and Use Committee of the University of North Carolina at Chapel Hill.

Surgical Procedure

The surgical procedure, which is described in more detail elsewhere[12], is summarized below: The lamb was sedated using ketamine intramuscularly and then administered isoflurane and oxygen throughout the procedure. A Validyne pneumotachometer was positioned in the air circuit to record air flow, a fluid filled polypropylene catheter was inserted and connected to a Statham P23Gb transducer to measure airway pressure and a Millar Mikro-Tip Catheter 500 was introduced into the aortic arch via the carotid artery to measure aortic pressure.

A mid-sternotomy was performed. Millar pressure transducers were placed in the MPA, SVC, IVC, RA, left atria (LA), and left ventricle (LV). Transonic T206 Small Animal Blood Flow Probes were positioned around the LPA, MPA, SVC, IVC, and aorta. Baseline data were recorded while the animal was ventilated at different rates and stroke volumes, as described below.

The animal was then placed on cardiopulmonary bypass and one of the following Fontan connection geometries was constructed:

The AP connection consisted of a graft connected to the RA appendage. The graft was connected to the MPA by an end-to-side anastomosis. The tricuspid valve was closed using a pursestring suture. (Technique first reported by Haneda et al.[13]).

The TCPC connection: The IVC was transected and connected to the transected MPA via an end-to-end anastomosis. The SVC was subsequently attached to the RPA via an end-to-side anastomosis. This connection used native vessels for the Fontan connection. No synthetic graft was used.

The TCPX connection: The IVC was connected to the extracardiac graft using an end-to-end anastomosis. The RPA was then connected to the graft via an end-to-side anastomosis.

The TCPY connection: The IVC was connected to the graft using an end-to-end anastomosis. The SVC was connected to the graft using an end-to-side anastomosis. The MPA was attached to the graft using an end-to-end anastomosis.

In all TCP connections, an atrial septectomy was performed to allow perfusion and return of the right coronary blood flow.

Upon procedure completion, the animal was taken off bypass and the Fontan circulation was imposed. Pressure and flow transducers that had been removed during the operation were reinserted and data were again collected at the different ventilation rates and stroke volumes. Surviving lambs were euthanized with a lethal dose of concentrated potassium.

Data Collection

The ventilation protocol was as follows: While maintaining a constant ventilation rate at 13 breaths/min, stroke volume was varied in 100 mL intervals from 300 to 700 mL/breath. Next, while maintaining a constant stroke volume at 400 mL, the ventilation rate was varied in 5 breaths/minute intervals from 8 to 23 breaths/minute. Furthermore, keeping air flow rate constant at 5200 mL/minute, all combinations of ventilatory rates and stroke volumes were performed. Multiple episodes of each parameter setting were recorded. Data were recorded at a rate of 200 Hertz for individual episodes of 5.12 seconds or 1024 data points/episode. Several episodes were recorded for each setting.

Power Calculations

Power gains/losses are calculated throughout multiple respiratory cycles and averaged. Kinetic energy was neglected and an average beat analysis of the mean and the first twenty harmonics was performed via:

$$P = P_o + \Sigma P_k \cos(k\Omega_o t + \theta_k) \qquad (1)$$

$$Q = Q_o + \Sigma Q_k \cos(k\Omega_o t + \phi_k). \qquad (2)$$

Where P and Q are pressure and flow respectively, P_o and Q_o are mean pressure and flow, P_k and Q_k are values at each harmonic, and θ_k and ϕ_k are the respective phase angles. Power is divided into its mean and pulsatile terms.

$$\dot{E}_{mean} = P_o * Q_o \qquad (3)$$

$$\dot{E}_{pulsatile} = \frac{1}{2}\sum_{k=1}^{20}(P_k * Q_k \cos(\theta_k - \phi_k)) \qquad (4)$$

For percent change calculations, minimum parameter settings were using as references: rate of 8 breaths/min, a stroke volume of 300mL, and a constant minute ventilation combination of 8 breaths/min and 650mL stroke volume.

To analyze the amount of power transferred through the Fontan connection across different geometries, a ratio of the amount of total power transferred to the left pulmonary artery was calculated.

$$\dot{E}_{LPA}\,(E\ Ratio) = \frac{\dot{E}_{LPA}}{\dot{E}_{SYS}} \qquad (5)$$

$$\dot{E}_{SYS} = \dot{E}_{SVC} + \dot{E}_{IVC} \qquad (6)$$

A comparable RPA ratio could not be calculated as placement of a flow probe around the right pulmonary artery was not possible after the Fontan circulation was implemented. The vessel is the main site of the cardiopulmonary anastomoses and the downstream length before the vessel branches into the upper and lower lobes is too short. Given the goals of the study, however, a rough estimation of total power conserved across the connection geometry was needed. Based on available data, equations 7 and 8 were used.

$$\frac{\dot{E}_{OUT}}{\dot{E}_{SYS}} \qquad (7)$$

$$\dot{E}_{OUT} = \overline{PAP} * \overline{CO} \qquad (8)$$

PAP and CO are expressed as means. These variables have been normalized such that a value of 1 implies complete conservation within the connection to a value of zero being complete loss across the Fontan connection site.

Data and Statistical Analysis

Data analysis was performed using MATLAB^{TM} (The Mathworks Inc., Natick, MA). All values were expressed as mean ± SD. Univariate and repeated measures analysis of variance were used to determine statistical significance. A p-value < 0.05 was regarded as significant. The post hoc Bonferroni test was used in order to compensate for type I error with multiple comparisons and the Tukey honestly significant difference test was used for multiple comparison tests across experimental groups.

RESULTS

Representative waveforms for one animal are illustrated in Figure 1. The general pattern is consistent for all the Fontan models. Flow rates decrease and pulsatility is almost removed at the caval levels. Systemic and pulmonary pressures increase that may lead to postoperative complications. Respiration effects produce marked changes in both pressures and flows. Flow may be occluded during inspiration. Average baseline hemodynamic values related to the above statement are shown in Table 1.

Percent power changes in the SVC, IVC and LPA under varying ventilation rates and stroke volumes are shown in Figure 2. Values were normalized to the 13 breathes/minute, 400 ml stroke volume situation as that was the usual configuration selected by the anesthesiologist while the chest was opened and baseline measurements were made. Power values corresponding to those ventilation settings can be found in Table 1.

Transfer ratios to the LPA are shown in figure 3. In general, ratios were little affected by ventilation parameters and mean levels were relatively consistent with the percentage of

flow going to the left lung, which were highest in AP and TCPX connections and significantly lower in TCPC connections.

Results are similar when efforts were made to measure total energy transfer as shown in the top row of Figure 4. Somewhat more variation was seen with ventilation parameters. The most notable change was the increase in ratios for the TCPY connection, which did have the best post operation baseline blood flow. Figure 4 (bottom row) includes comparable statistics for cardiac output at the different ventilation parameters. The most notable feature of this figure is the switch in the TCPX and TCPC positions. The comparison suggests, as would be expected, that efficiencies increase as CO decreases.

DISCUSSION

Though the number of studies is relatively small, these results demonstrate that our lamb models of Fontan circulations exhibit the expected increased sensitivity to respiration parameters (Figure 2). All models showed increased responsiveness relative to the normal circulation. Furthermore, though the mechanisms are not readily apparent, different connection geometries and materials, even in this simpler open-chest preparation appeared to react differently. The following are examples of generalizations relative group patterns observed. 1) With the exception of the TCPY connections, assuming that higher powers are preferable, results imply that all subjects might have fared better had stroke volumes increased to 500 ml and/or baseline ventilations rates were increased to 18 breathes/minutes. This should have been expected as anesthesiologists prefer to under ventilate and under perfuse during the operative period. 2) With the exception of TCPX, SVC and IVC power appears to go up and down in concert, contrary to the hypothesis that the SVC, which serves

the head, is more isolated from respiration influences than the IVC. 3) Likewise, the TCPX appeared to be the most compromised by unusually high or low rates and stroke volumes.

Findings support the concept that ventilation protocols could be designed to specifically improve the peri-operative care of Fontan patients. Rates and stroke volumes could be altered to maximize an appropriate power measurement, assuming such could be monitored. The resolution for this study was relatively large, with step sizes of 5 breaths/minute and 100 ml stroke volumes. Fifty percent power changes were often observed during one step in either direction, indicating that a finer resolution would be helpful. A logical next step in this direction would be to develop a technique for moving settings up or down based on real-time measurements of power levels. The technique would be evaluated against other protocols used by anesthesiologists and respiration therapists. Our Fontan animal models provide an ideal test bed for a new protocol.

Results presented in this report focus on group findings relative to the effects of ventilation parameters on different Fontan connection geometries. Of perhaps more interest, as has been true for patient studies, will be a more detailed analysis of individual animal data. Waveforms will be subjected to transfer function and correlation analyses to tease out the different influence pathways. Findings will be used to improve lumped parameter models of the entire circulation.

Various labs have reported animal models of the Fontan circulation [13-25], but no other lab, to the best of our knowledge, has actually created the single ventricle physiology in animals approximating the size of a child or used the models to investigate the effects of respiration. In vitro and CFD studies, however, have been used extensively to study power losses across different Fontan geometries, focusing particularly on the effects of offset

diameter, flaring, nonplanar geometry, compliance mismatch, etc. A unique in vitro study using explanted adult sheep hearts was designed by Lardo and colleagues to better understand the energy losses associated with atriopulmonary (AP) and various TCP connections [17-19]. They compared energy losses in models of intra-atrial tunnels, extracardiac tunnels and extracardiac conduits with and without caval offsets and reported that extracardiac tunnels with offsets were most efficient. These studies are most analogous to our in vitro [26-30]and computational studies[22, 23, 25] in which boundary conditions are controlled. In general, all studies confirm that caval offsets and flaring decrease energy losses. No attempt was made to control flaring in our animal models. Due to lamb anatomy, TCPC and TCPX configurations had little if any caval offset. The TCPY geometry, however, is somewhat more analogous to a recently described "optiflow" [30] model in which power losses are minimized by avoiding direct impact of SVC and IVC flows.

Using MRI obtained velocity measurements and a viscous dissipation function, power losses across geometries can be estimated in humans [31, 32]. The technology is being used to assess exercise tolerance in patients with Fontan circulations. Again, due to lack of pressure measurements, power available can not be measured using this technique.

The major advantage of the in vivo studies in lambs is the capability of measuring both pressure and flow waveforms needed for measuring power at input and output locations across the Fontan geometry, which is not yet possible via MRI studies in humans. The major disadvantage, particularly compared to in vitro and CFD studies, is the inability to control parameters. Our power loss percentages ranged from 10% to 70%. These values, however, appeared to be a function of cardiac output, which is perhaps the most important variable for optimization.

Acknowledgments

This work was supported by a BRP grant from the National Heart, Lung, and Blood Institute, HL67622.

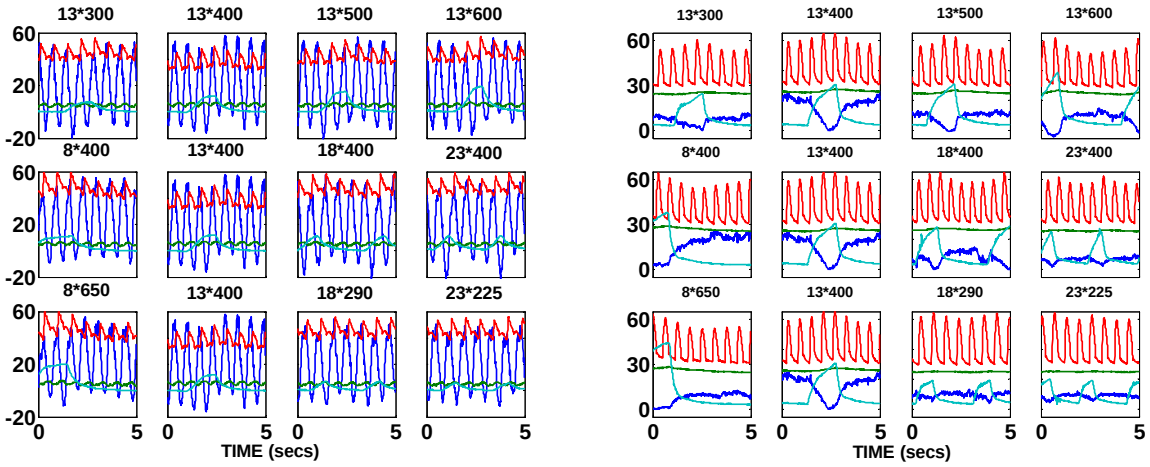

Figure 1. Left Panel: Normal Circulation: Top Row = 13 breathes/minute, various stroke volumes, Middle Row=400 cc stroke volume, various rates, Bottom Row=constant minute volume of 5200 cc/minute under varying stroke volumes and rates. Right Panel: Fontan Circulation: Same protocol.

A

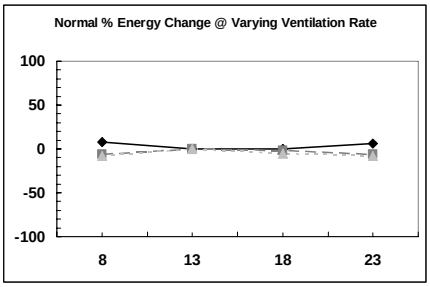
Normal % Energy Change @ Varying Ventilation Rate
100
50
0
-50
-100
8
13
18
23

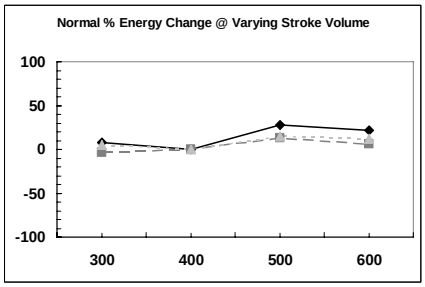
Normal % Energy Change @ Varying Stroke Volume
100
50
0
-50
-100
300
400
500
600

B

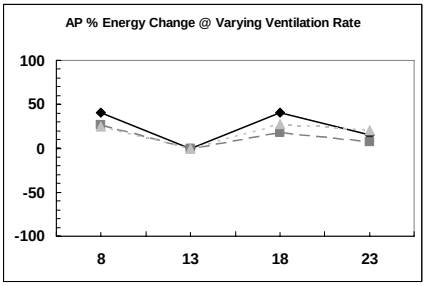
AP % Energy Change @ Varying Ventilation Rate
100
50
0
-50
-100
8
13
18
23

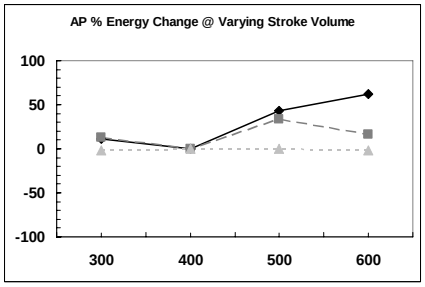
AP % Energy Change @ Varying Stroke Volume
100
50
0
-50
-100
300
400
500
600

C

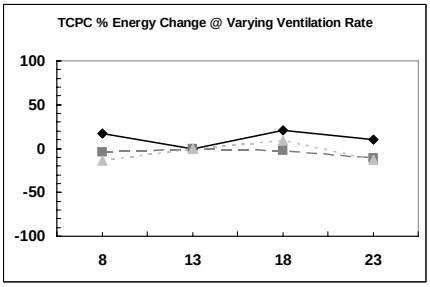
TCPC % Energy Change @ Varying Ventilation Rate
100
50
0
-50
-100
8
13
18
23

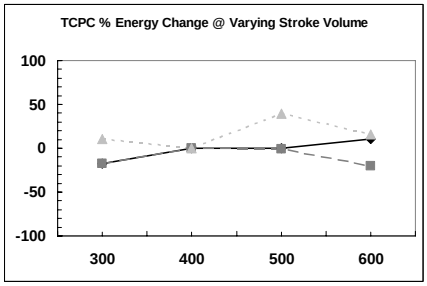
TCPC % Energy Change @ Varying Stroke Volume
100
50
0
-50
-100
300
400
500
600

D

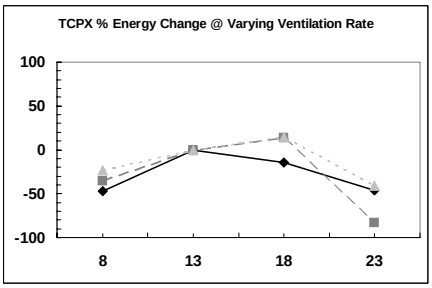
TCPX % Energy Change @ Varying Ventilation Rate
100
50
0
-50
-100
8
13
18
23

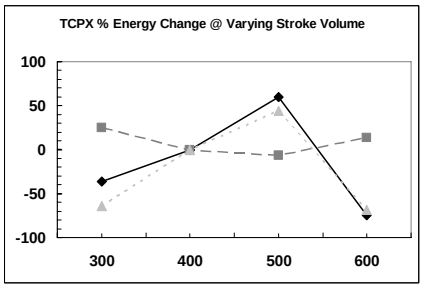
TCPX % Energy Change @ Varying Stroke Volume
100
50
0
-50
-100
300
400
500
600

E

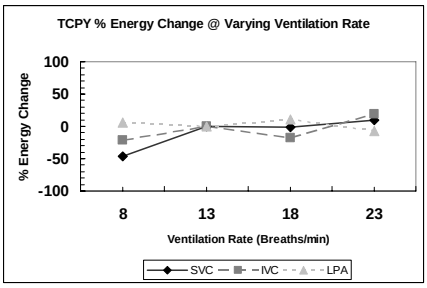
TCPY % Energy Change @ Varying Ventilation Rate
% Energy Change
100
50
0
-50
-100
8
13
18
23
Ventilation Rate (Breaths/min)
SVC
IVC
LPA

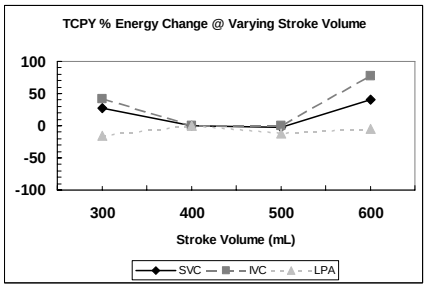
TCPY % Energy Change @ Varying Stroke Volume
100
50
0
-50
-100
300
400
500
600
Stroke Volume (mL)
SVC
IVC
LPA

Figure 2. Percent energy changes under varying ventilation rates (left column) and varying stroke volumes (right column). Each row represents a different model: A) Normal/Baseline, B) AP, C) TCPC, D) TCPX, E) TCPY. SVC = diamonds, IVC = Squares; LPA = triangles. References of a rate of 13 breaths/min and a stroke volume of 400 mL were used.

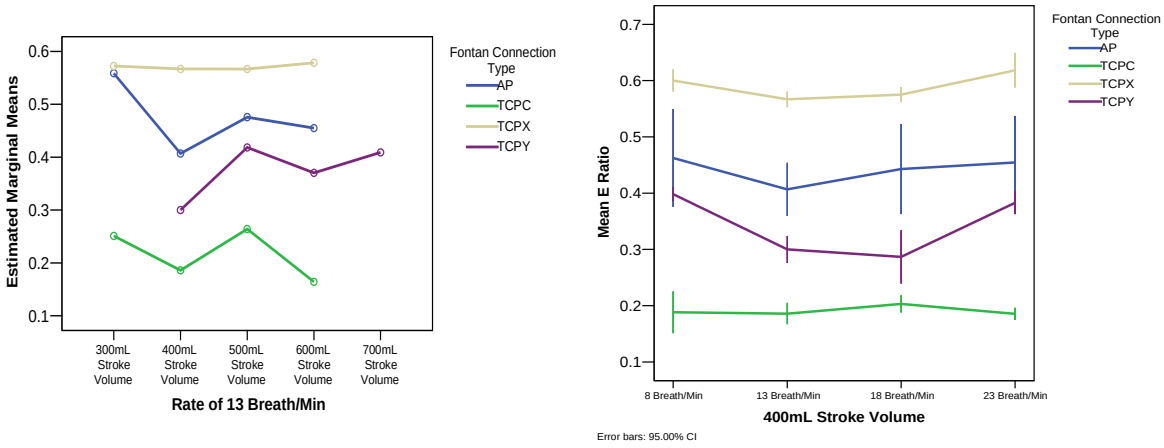

Figure 3. Left Panel: Ratio of left pulmonary artery energy to total systemic energy over varying stroke volumes with the rate fixed at 13 breaths/minute: Right Panel: Ratio over varying rates with the stroke volume fixed at 400 mL.

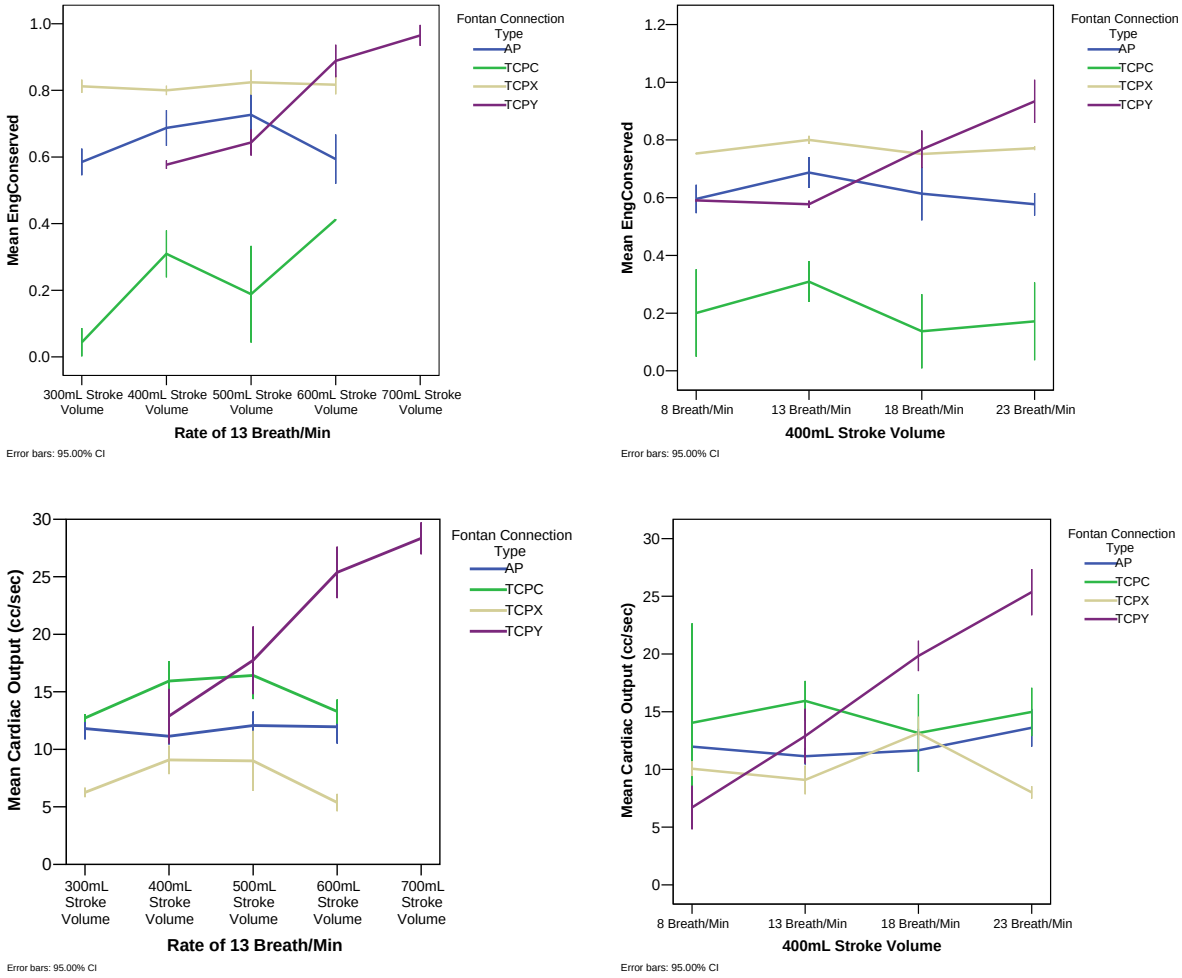

Figure 4. Upper Left: Ratio of pulmonary energy to total caval energy (percent energy conserved across the connection) over varying stroke volumes with the rate fixed at 13 breaths/minute: Upper Right: Ratio over varying rates with the stroke volume fixed at 400 mL. Lower Left: Cardiac output for the settings in the Upper Left Panel. Lower right: Cardiac output for the settings in the Upper Right Panel.

Table 1:

	Normal Mean ± SD (n=24)	AP Connection Mean ± SD (n=11)	TCPC Connection Mean ± SD (n=4)	TCPX Connection Mean ± SD (n=4)	TCPY Connection Mean ± SD (n=5)
Pressure (mm Hg)					
Ao	46.7 ± 6.3	43.5 ± 17.0	33.9 ± 6.32*	55.63 ± 18.2	57.5 ± 21.7
PA	21.5 ± 5.3	17.0 ± 2.9*	20.0 ± 5.5	28.9 ± 4.3*	27.2 ± 8.9
SVC	8.7 ± 2.0	19.0 ± 2.8*	29.5 ± 3.7*	24.0 ± 4.6*	21.8 ± 5.5*
IVC	8.1 ± 6.3	19.6 ± 5.4*	24.2 ± 4.2*	25.2 ± 5.3*	22.8 ± 9.6*
LA	8.1 ± 2.8	6.5 ± 2.6	9.9 ± 4.6	6.5 ± 2.9	21.4 ± 13.9
Flow ($cm^3 \cdot sec^{-1}$)					
SVC	5.1 ± 1.7	2.9 ± 1.7*	6.7 ± 1.0*	2.4 ± 1.8*	4.6 ± 2.0
IVC	23.3 ± 6.3	7.7 ± 4.1*	12.6 ± 6.0*	5.7 ± 3.1*	17.9 ± 8.6
LPA	12.1 ± 4.3	4.3 ± 2.3*	3.9 ± 0.8*	3.9 ± 2.2*	6.8 ± 3.6*
CO	31.3 ± 11.6	11.3 ± 4.1*	15.2 ± 3.3*	10.2 ± 5.4*	23.0 ± 9.9
Power (mWatt)					
SVC	5.30	4.69	17.00	10.35	13.87
IVC	26.54	14.88	41.34	20.34	60.32
LPA	37.68	17.16	13.44	17.78	37.87

Table 1. Overall average baseline hemodynamic values for open chest normal, atriopulmonary (AP), total cavopulmonary connection without a synthetic graft (TCPC), extracardiac total cavopulmonary with synthetic graft (TCPX), and total cavopulmonary connection with a Y-shaped anastomosis (TCPY) circulations. *Statistically significant differences with a $p<0.05$ as indicated.

REFERENCES

1. Rowe RD, Freedom RM, Mehrizi A. *The Neonate with Congenital Heart Disease.* 2nd ed. Philadelphia, PA: W.B. Saunders Co.; 1981.

2. Fontan F, Baudet E. Surgical repair of tricuspid atresia. *Surgical repair of tricuspid atresia*. 1971;26:240-248.

3. Castaneda AR. From glenn to fontan. A continuing evolution. *Circulation*. 1992;86:II80-4.

4. de Leval MR, Kilner P, Gewillig M, Bull C. Total cavopulmonary connection: A logical alternative to atriopulmonary connection for complex fontan operations. experimental studies and early clinical experience. *J Thorac Cardiovasc Surg*. 1988;96:682-695.

5. Marcelletti C, Corno A, Giannico S, Marino B. Inferior vena cava-pulmonary artery extracardiac conduit. A new form of right heart bypass. *J Thorac Cardiovasc Surg*. 1990;100:228-232.

6. Laschinger JC, Redmond JM, Cameron DE, Kan JS, Ringel RE. Intermediate results of the extracardiac fontan procedure. *Ann Thorac Surg*. 1996;62:1261-7; discussion 1266-7.

7. Marcelletti CF, Hanley FL, Mavroudis C, et al. Revision of previous fontan connections to total extracardiac cavopulmonary anastomosis: A multicenter experience. *J Thorac Cardiovasc Surg*. 2000;119:340-346.

8. Podzolkov VP, Zaets SB, Chiaureli MR, Alekyan BG, Zotova LM, Chernikh IG. Comparative assessment of fontan operation in modifications of atriopulmonary and total cavopulmonary anastomoses. *Eur J Cardiothorac Surg*. 1997;11:458-465.

9. Bull K. The fontan procedure: Lessons from the past. *Heart*. 1998;79:213-214.

10. de Leval MR. The fontan circulation: A challenge to william harvey? *Nat Clin Pract Cardiovasc Med*. 2005;2:202-208.

11. Gersony DR, Gersony WM. Management of the postoperative fontan patient. *Progress in Pediatric Cardiology*. 2003;17:73-79.

12. Ketner ME, Lucas CL, Mill MR, et al. Comparison of hemodynamics in lamb models of the fontan circulation. . 2006.

13. Haneda K, Konnai T, Sato N, Nicoloff NN, Mohri H. Acute hemodynamic changes after fontan operation: An experimental study. *Tohoku J Exp Med*. 1993;169:113-119.

14. Bromberg BI, Schuessler RB, Gandhi SK, Rodefeld MD, Boineau JP, Huddleston CB. A canine model of atrial flutter following the intra-atrial lateral tunnel fontan operation. *J Electrocardiol*. 1998;30 Suppl:85-93.

15. Gandhi SK, Bromberg BI, Rodefeld MD, et al. Lateral tunnel suture line variation reduces atrial flutter after the modified fontan operation. *Ann Thorac Surg*. 1996;61:1299-1309.

16. Gandhi SK, Bromberg BI, Schuessler RB, et al. Characterization and surgical ablation of atrial flutter after the classic fontan repair. *Ann Thorac Surg*. 1996;61:1666-78; discussion 1678-9.

17. Lardo AC, del Nido PJ, Webber SA, Friehs I, Cape EG. Hemodynamic effect of progressive right atrial dilatation in atriopulmonary connections. *J Thorac Cardiovasc Surg*. 1997;114:2-8.

18. Lardo AC, Webber SA, Friehs I, del Nido PJ, Cape EG. Fluid dynamic comparison of intra-atrial and extracardiac total cavopulmonary connections. *J Thorac Cardiovasc Surg*. 1999;117:697-704.

19. Lardo AC, Webber SA, Iyengar A, del Nido PJ, Friehs I, Cape EG. Bidirectional superior cavopulmonary anastomosis improves mechanical efficiency in dilated atriopulmonary connections. *J Thorac Cardiovasc Surg*. 1999;118:681-691.

20. Mace L, Dervanian P, Bourriez A, et al. Changes in venous return parameters associated with univentricular fontan circulations. *Am J Physiol Heart Circ Physiol*. 2000;279:H2335-43.

21. Riemer RK, Amir G, Reichenbach SH, Reinhartz O. Mechanical support of total cavopulmonary connection with an axial flow pump. *J Thorac Cardiovasc Surg*. 2005;130:351-354.

22. Rodefeld MD, Bromberg BI, Schuessler RB, Boineau JP, Cox JL, Huddleston CB. Atrial flutter after lateral tunnel construction in the modified fontan operation: A canine model. *J Thorac Cardiovasc Surg*. 1996;111:514-526.

23. Rodefeld MD, Gandhi SK, Huddleston CB, et al. Anatomically based ablation of atrial flutter in an acute canine model of the modified fontan operation. *J Thorac Cardiovasc Surg*. 1996;112:898-907.

24. Rodefeld MD, Boyd JH, Myers CD, et al. Cavopulmonary assist: Circulatory support for the univentricular fontan circulation. *Ann Thorac Surg*. 2003;76:1911-6; discussion 1916.

25. Szabo G, Buhmann V, Graf A, et al. Ventricular energetics after the fontan operation: Contractility-afterload mismatch. *J Thorac Cardiovasc Surg*. 2003;125:1061-1069.

26. de Zelicourt DA, Pekkan K, Parks J, Kanter K, Fogel M, Yoganathan AP. Flow study of an extracardiac connection with persistent left superior vena cava. *J Thorac Cardiovasc Surg*. 2006;131:785-791.

27. Ensley AE, Lynch P, Chatzimavroudis GP, Lucas C, Sharma S, Yoganathan AP. Toward designing the optimal total cavopulmonary connection: An in vitro study. *Ann Thorac Surg*. 1999;68:1384-1390.

28. Pekkan K, Kitajima HD, de Zelicourt D, et al. Total cavopulmonary connection flow with functional left pulmonary artery stenosis: Angioplasty and fenestration in vitro. *Circulation*. 2005;112:3264-3271.

29. Ryu K, Healy TM, Ensley AE, Sharma S, Lucas C, Yoganathan AP. Importance of accurate geometry in the study of the total cavopulmonary connection: Computational simulations and in vitro experiments. *Ann Biomed Eng*. 2001;29:844-853.

30. Soerensen DD, de Zelicourt D, Pekkan K, et al. Introduction of a new optimized total cavo-pulmonary connection. Submitted to *JTCVS*. 2006.

31. Healy TM, Lucas C, Yoganathan AP. Noninvasive fluid dynamic power loss assessments for total cavopulmonary connections using the viscous dissipation function: A feasibility study. *J Biomech Eng*. 2001;123:317-324.

32. Pekkan K, de Zelicourt D, Ge L, et al. Physics-driven CFD modeling of complex anatomical cardiovascular flows-a TCPC case study. *Ann Biomed Eng*. 2005;33:284-300.

APPENDIX III:

INTRODUCTION OF A NOVEL TOTAL CAVO-PULMONARY WITH Y-SHAPED GRAFT CONNECTION IMPLEMENTED IN LAMBS

MANUSCRIPT DRAFT SUBMITTED TO JOURNAL OF THORACIC AND CARDIOVASCULAR SURGERY

M. E. Ketner[1], C. L. Lucas[1], M. R. Mill[2], B. Sheridan[2], W. Lucas[3], B. Steele[1], A. Yoganathan[4]
[1]Department of Biomedical Engineering, University of North Carolina-Chapel Hill and North Carolina State University, NC, USA
[2]Department of Cardiothoracic Surgery, University of North Carolina-Chapel Hill, NC, USA
[3]Department of Anesthesiology, University of North Carolina-Chapel Hill, NC, USA
[4]Wallace H. Coulter Department of Biomedical Engineering,
Georgia Institute of Technology & Emory University

Running Head: Novel Y-Shaped TCPC

Keywords: CHD, Fontan, TCPC, Hemodynamics, Power loss

Word Count: *Abstract: 242 words *Text: 3796 words *References: 49 *Figures: 2 *Tables: 3

Abstract

BACKGROUND: Numerous congenital heart defects feature an essentially univentricular heart pumping to parallel pulmonary and systemic circuits. Since Fontan and Baudet first implemented an atriopulmonary (AP) connection in 1971, many surgical modifications, termed “Fontan” repairs, which place the pulmonary and systemic circuits in series with the univentricular heart, have been introduced to maximize hemodynamic energy and minimize postoperative complications. This report focuses on a novel total cavopulmonary connection

(TCP) that has been implemented in vivo in lamb models using a Y-shaped connection (TCPY).

METHODS: In vivo studies in lambs weighing 10 to 25 kilograms were performed implementing a TCPY Fontan modification. Multiple pressure and flow transducers were inserted and instantaneous data were recorded for both open chest normal and Fontan circulations. Hemodynamic parameters, systemic and pulmonary vascular resistances, and power losses were determined for normal and TCPY circulations.

RESULTS: The TCPY showed a 25±8.52 percent power loss across the connection region. No statistical differences were observed between normal and TCPY caval powers or systemic vascular resistance. Pulmonary vascular resistance increased in the TCPY model. Cardiac output decreased 49% between normal and TCPY conditions. Caval blood flow contributions and distribution to the lungs were consistent between normal and TCPY circulations. Respiration effects were magnified in the TCPY.

CONCLUSIONS: A new surgical technique for a TCP procedure using a Y-shaped connection has been successfully implemented in lambs. Results are promising and suggest that the TCPY procedure warrants further investigation as a clinical option.

Mini Abstract

A novel total cavopulmonary connection using a Y-shaped connection, which may have clinical feasibility, has been successfully implemented in lambs. Hemodynamic and power analyses are reported. Results show minimal power losses across the connection site and a maximization of cardiac output compared to similar Fontan modifications performed in lambs.

Introduction

Congenital heart disease that impairs the atriopulmonary pathway and creates a univentricular anatomy is prevalent in approximately two out of every one thousand live births [1]. Examples of such defects include multiple ventricular septal defects, tricuspid atresia, hypoplastic left heart syndrome, and double outlet ventricle. As a result of the altered physiology, the overloaded single ventricle pumps both oxygenated and deoxygenated blood to parallel pulmonary and systemic circulations, which leads to inadequate tissue oxygenation and cyanosis.

In 1971, Fontan and Baudet [2] successfully implemented an atriopulmonary (AP) connection (graft between the right atrium (RA) and main pulmonary artery (MPA)) in a patient with tricuspid atresia, effectively separating the parallel pulmonary and systemic circuits, placing them in series with the univentricular pump. The "Fontan" procedure or one of its many modifications became the repair option of choice in patients with reasonable anatomy [3].

Surgical modifications have evolved from the original AP connection to the total cavopulmonary connection (TCP) that removes right atrial influences. TCP procedures utilize either an intra-atrial or lateral tunnel baffle, attributed to deLeval [4], include an end-to-side anastomosis of the SVC to the RPA, construction of an intra-atrial tunnel using composite material, part of the RA wall, and use of a synthetic graft to channel the inferior vena cava (IVC) to the inferior side of the RPA. In the extracardiac version, attributed to Marcelletti in 1990 [5], a synthetic graft connects the IVC to the inferior side of the RPA without disturbing the RA.

In general, TCP repairs are considered superior to AP repairs [6-8]. However, connection geometries still vary according to surgeon preference. Current TCP geometries have improved hemodynamics but show an increase in poor clinical outcomes and numerous postoperative complications. Connection geometries create unequal hepatic blood flow distributions to the lungs resulting in pulmonary arteriovenous malformations and impaired lung development [9-11]. Reduced exercise tolerance, lower quality of life, and long term complications are common [12, 13].

Post Fontan elevated venous pressures and lymph production may compromise splanchnic bed functions. Protein-losing enteropathy (PLE), the severe loss of serum proteins into the intestine, is one of the most serious complications. Onset of PLE occurs approximately six months after the Fontan procedure [14]. At least 40% of Fontan patients have a raised level of one or more liver enzymes, 25% have a depletion of coagulation factors, and 7% have low serum albumin levels [15].

A recent innovative modification of the Fontan circulation, designed to reverse the Fontan paradox (venous hypertension and pulmonary hypotension), was performed in sheep by Rodefeld and colleagues [16]. To assist cavopulmonary blood flow, axial flow pumps were placed in the IVC and SVC percutaneously. Circulation hemodynamics resembling that of a two ventricle physiology were restored. Addition of an axial pump resulted in an increase in cardiac output and IVC flow. Furthermore, IVC, MPA, and LA pressures returned to normal values.

In spite of the general agreement that connections should minimize energy losses and maintain normal distribution of total and IVC flow to both lungs, the need still exists for new surgical techniques/tools that will enable presurgical planning to achieve these goals. The

motivation for this report is examination of a novel surgical technique (TCPY) successfully implemented in animal models without use of additional power supplies. Animal models allow for hemodynamic examination not available via in vitro and computer simulations. To date, the animals that have been used to develop ideas and practice techniques relative to Fontan operations have been predominantly adult dogs, pigs, or sheep [17-26].

Methods

Animal Studies

The focus of our laboratory has been the development of Fontan modifications in lambs weighing between 10 and 25 kilograms, which are comparable in size and age to the patient population of interest. All animals were cared for in accordance with the "Guide for the Care and Use of Laboratory Animals" (NIH Publication No. 86-23, revised 1985) and were in accordance with the standards of the Institutional Animal Care and Use Committee of the University of North Carolina at Chapel Hill.

TCPY Surgical Procedure

The lamb was sedated using ketamine (30 mg/kg) intramuscularly and then administered isoflurane and oxygen throughout the procedure. Once sedated, the lamb was positioned on the table and its chest, right flank, thorax, and neck were shaved. Endotracheal intubation of the animal took place using an appropriately sized tube with a balloon and stilette. The tidal volume administered was 10 – 15 ml / kg without any positive end expiratory pressure or adjusted accordingly to maintain optimal arterial blood gas tensions. Measurements of respiration rate, carbon dioxide (CO_2) return, and pulse oximetry (placed on the tongue) were monitored. A Validyne pneumotachometer (Validyne Engineering, Northridge, CA) was

introduced into the air circuit in order to monitor and record air flow. Also in the air circuit, a fluid filled polypropylene catheter was inserted and connected to a Statham P23Gb transducer (Statham Transducer P23Gb, Siemens) to measure airway pressure. Next, a double lumen catheter was inserted into the internal jugular vein. This allowed for intravenous fluid and pharmaceutical administration throughout the procedure. The carotid artery was then dissected and a Millar Mikro-Tip Catheter (MPC-500, Millar Instruments, Houston, TX) pressure transducer was introduced and positioned as close to the aortic arch as possible in order to record and observe arterial pressure (AOP). Arterial blood gases were closely monitored throughout the procedure and pharmaceutical adjustments were provided when needed. Blood gases were measured by an iSTAT analyzer (Abbott Laboratories, IL). Parameters monitored included hematocrit, hemoglobin, sodium, potassium, pH, PCO2, PO2, Calcium, O2 saturation, bicarbonate, and base excess.

A mid-sternotomy was performed that started at approximately the sixth interspace. Exposure was from the superior azygous vein to the diaphragm. The SVC was cleared and the azygous vein, if present, was tied off. The same was done for the IVC. The aorta (AO) and pulmonary arteries were then dissected. The pericardium was opened and as much as possible was preserved in case a pericardial patch was needed during the operation.

Millar pressure transducers were placed in the MPA, SVC, IVC, RA, left atria (LA), and left ventricle (LV). To record blood flow, Transonic T206 Small Animal Blood Flow probes (Transonic Systems Inc., Ithaca, NY) were positioned around the LPA, MPA, SVC, IVC, and AO. Data were recorded at a rate of 200 Hertz for individual episodes of 5.12 seconds or 1024 data points/episode. Cardiopulmonary bypass was then performed using a bi-caval

cannulation and arterial cannulation at the aortic arch. Once on bypass, the TCPY Fontan connection geometry was constructed.

The TCPY connection (Figure 1A and 1B) consists of the IVC connected to the synthetic graft via an end-to-end anastomosis (Figure 1C). The SVC was connected to the graft (Figure 1D) by one of two methods: 1) an end to side anastomosis or 2) an end to end anastomosis to one arm of a Y-shaped synthetic graft. The MPA was attached to the graft (Figure 1E) using an end-to-end anastomosis. An atrial septectomy was performed to allow perfusion and return of the right coronary blood flow.

Cardiopulmonary bypass times averaged 90 minutes. Bypass pump rates were set at approximately 33% of normal cardiac output to maintain proper perfusion. Central venous pressure was monitored in order to assess and maintain blood volume while on bypass. Steroids were given prior to going on bypass. Blood gases were taken approximately every five minutes to assess and control hemodynamic stability. Ventilation of the lungs was performed occasionally while on bypass in order to prevent fluid buildup in the lungs. Additional blood from a donor animal was heated to 37 degrees Celsius and then hemoconcentrated using an Minimax Plus (Medtronic Inc., Minneapolis MN) oxygenator system. Upon procedure completion, the animal was taken off bypass and the Fontan circulation was imposed. Surviving lambs were euthanized with a lethal dose of concentrated potassium.

Data and Statistical Analysis

Data analysis was performed using MATLAB™ (The Mathworks Inc., Natick, MA). All values were expressed as mean ± SD. Two-tailed unpaired variance t-tests were performed. Statistical significance was determined by a p-value < 0.05.

Vascular Resistance Calculations

Pulmonary vascular resistance (PVR) and systemic vascular resistance (SVR) were calculated. SVR was divided into the resistance of the head (Equation 1) and the resistance of the body (Equation 2) and overall SVR was calculated using equation 3.

$$(HRES) = R_{HEAD}\ (dyne \bullet \sec \bullet cm^{-5}) = 80 * \frac{(\overline{AOP} - \overline{SVCP})mmHg}{SVCQ\ (L * \min^{-1})} \quad (1)$$

$$(BRES) = R_{BODY}\ (dyne \bullet \sec \bullet cm^{-5}) = 80 * \frac{(\overline{AOP} - \overline{IVCP})mmHg}{\overline{IVCQ}\ (L * \min^{-1})} \quad (2)$$

$$SVR\ (dyne \bullet \sec \bullet cm^{-5}) = \frac{HRES * BRES}{HRES + BRES} = \frac{R_{HEAD} * R_{BODY}}{R_{HEAD} + R_{BODY}} \quad (3)$$

PVR was calculated via:

$$PVR\ (dyne \bullet \sec \bullet cm^{-5}) = 80 * \frac{(\overline{PAP} - \overline{LAP})mmHg}{\overline{PAQ}\ (L * \min^{-1})} \quad (4)$$

using average data measurements over multiple 5.12 second episodes each with multiple heartbeats.

Power Loss Calculations

Power gains/losses were calculated throughout. Data were acquired over multiple respiratory cycles and averaged. Kinetic energy was neglected and an average beat analysis of the mean and the first twenty harmonics was performed via:

$$P = P_o + \Sigma P_k \cos(k\Omega_o t + \theta_k) \quad (5)$$

$$Q = Q_o + \Sigma Q_k \cos(k\Omega_o t + \phi_k). \quad (6)$$

Where P and Q are vessel pressure and flow respectively, P_o and Q_o are mean pressure and flow, P_k and Q_k are values at each harmonic, and θ_k and ϕ_k are the respective phase angles. Power was divided into its mean and pulsatile terms.

$$\dot{E}_{mean} = P_o * Q_o \quad (7)$$

$$\dot{E}_{pulsatile} = \frac{1}{2}\sum_{k=1}^{20}(P_k * Q_k \cos(\theta_k - \phi_k)) \quad (8)$$

Power losses across the TCPY connection region were calculated using equation 9.

$$\dot{E}_{LOSS} = \dot{E}_{SYS} - \dot{E}_{PA} \quad (9)$$

$$\dot{E}_{SYS} = \dot{E}_{SVC} + \dot{E}_{IVC} \quad (10)$$

To illustrate power transferred to the left and right lungs, an LPA power was calculated and the ratio of LPA power to pulmonary power was calculated using equation 11.

$$\% \dot{E}_{LPA} = \frac{\dot{E}_{LPA}}{\dot{E}_{PA}} * 100 \quad (11)$$

A comparable RPA power measurement could not be acquired or calculated as placement of a flow probe around the right pulmonary artery was not possible after the Fontan circulation was implemented. The RPA is the main site of the cardiopulmonary

anastomoses and the downstream length before the vessel branches into the upper and lower lobes was insufficient for flow probe placement.

Results

Representative waveforms

Representative waveforms for one animal with a TCPY Fontan modification are illustrated in Figure 2. Hemodynamic comparison results between normal and TCPY animals are summarized in Table 1. An overall trend of caval flow decreases and pressure increases are observed in the Fontan circulations. SVC and IVC flows decreased by 36%, and 61% respectively. Pressures increased to values ranging in the 20-30 mmHg range, a significant increase from normal values. Essentially all pulsatility was removed from caval pressures and flows with the exception of the PA flow tracing. Small disturbances were observed that correlated to systole in the SVC pressure and flow waveforms. No systolic effect was seen in the IVC waveforms. Ventilation had a larger influence on both pressure and flow in the TCPY circulation compared to normal conditions. During inspiration, pressures increased and flows decreased (Figure 2).

Blood flow to the LPA decreased by 73% in the TCPY modification. However, no significant differences are observed in percentage of flow distributed to the left lung between normal and TCPY conditions. TCPY flow contribution from both the SVC and IVC were comparable to flow contributions within the normal circulation. Overall cardiac output decreased by 49% between circulations.

PVR increased significantly between normal and TCPY conditions. Body resistance (BRES) and head resistance (HRES) did not significantly change between circulations. Furthermore, normal and TCPY SVR measurements remained stable.

Power Analysis

Baseline measurements, a ventilation rate of 13 breaths/min at a stroke volume of 400 mL, were used in order to determine milliwatt power values for the systemic (SVC and IVC) and pulmonary (PA) circulations between normal and TCPY circulations. Results are illustrated in Table 2. No significant differences were observed for the systemic power values. With the inclusion of the right ventricle in the normal circulation, significant power differences occurred with a large decrease in power in the TCPY circulation that removed all right ventricle hemodynamic power contributions and pulsatility effects.

Table 3 summarizes the systemic and pulmonary power for the TCPY modification. LPA power is reported to illustrate power distribution to the left and right lungs. A 25% power loss was observed across the TCPY connection. Power transferred to the left lung was 44% of the total power leaving the connection. Power values expressed in milliwatts are also reported for reference.

Discussion

To date, our lab has successfully implemented this novel TCP procedure using a Y-shaped connection in six lambs. The number, though small, proves feasibility in-vivo. To our knowledge, no other lab has successfully created a true single ventricle physiology in animals that approximate the size of young patients. However, numerous investigators have reported animal model results of the Fontan circulation. Haneda [17] compared hemodynamics between normal and AP circulations in dogs. Dogs were used by Gandhi, Bromberg, and Rodefeld [18-22] to compare atrial flutter and suture line placements in AP and intra-atrial TCP connections. Ventricular function, cardiac contractility, and mechanical efficiency following the Fontan procedure were investigated by Szabo [27]. Adult pig models were used by Mace [23]

to determine venous return parameters and how they were affected by Fontan circulations. These findings were valuable, however, the geometries created were not possible for clinical use. This study examines a novel procedure that is clinically applicable. The TCPY is performed outside of the heart, which does not require intra-atrial suture lines, is a simpler surgical procedure than the intra-atrial tunnel, and may help reduce postoperative complications. Also, an extracardiac conduit will reduce cardiopulmonary bypass time.

A successful clinical modification of the classic extracardiac Fontan procedure was performed on a seventeen-year-old patient in Japan by Okano and colleagues using a Y-shaped bifurcated graft [28]. Although the anatomy and vessel geometry differ from our experimental setup, Okano illustrates the possibility of using Y-shaped grafts in a clinical setting. For Okano's patient, one arm of the graft connected the IVC to the LPA. The second arm connected the IVC to the RPA. This patient had bilateral SVCs and had undergone bilateral bidirectional Blalock-Taussig and Glenn procedures previously. This modification may be useful in patients with severe MPA defects or when geometries will not allow an unbifurcated graft.

Hemodynamic results comparing normal and TCPY conditions showed an increase in caval pressures, a decrease in CO, and a normal systemic arterial pressure (AOP). These findings are consistent with previous studies [27, 29-32]. An increase in PVR was observed that is consistent with other acute studies but has not been found in chronic Fontan patients [27, 33]. This may be due to the open chest preparation and lack of pulsatility in the system [34]. TCPY hemodynamics also illustrated little change in SVR, consistent with findings by Mace [23]. Pulsatility in the PA flow waveform may be due to physical heart motion acting on the synthetic graft due to the anterior graft placement with respect to the heart. The anterior

placement of the graft may also reduce lung and respiration effects on the caval flows and pressures that were observed in our previous studies.

A major reason for failing Fontan circulations is a large decrease in CO. The TCPY modification illustrated promising results conserving 51% of CO between normal and Fontan circulations. This may be the most important factor in optimization of surgical procedures and maximization of power across the connection region. Another advantage of the TCPY modification is its use of the native pulmonary artery branching. This allows for proper distribution of both SVC and IVC flows to the lungs, which may help reduce complications caused by lack of hepatic blood to one lung [9-11]. Our study produced a 35% flow contribution to the left lung under Fontan conditions compared to 26% under normal circulation. The TCPY modification does not instigate the head on collisions of caval flows (Figure 1) that are present in the TCP procedures currently used in practice. Head on collisions have been shown to have a harmful effect on power conservation. Thus, TCPY geometries may lead to a more beneficial streamlined flow profile and reduced recirculation regions. As a result, efficiencies will be increased and power conservation will be maximized across the connection.

This study investigated power losses in a closed loop in-vivo system in lambs that have not yet been reported from other labs. Therefore, comparison of power values to other investigator findings is not possible. Our lab has performed multiple TCP modifications and power comparisons will be reported in future manuscripts. This paper focuses on the uniqueness of the model geometry and feasibility in clinical practice and to report pre- and postoperative hemodynamic values for future comparison. The most comparable study was that performed by Lardo and colleagues who investigated power losses in explanted sheep

hearts in vitro between AP and various intra-atrial and extracardiac TCP connections [24-26]. A comparison to these findings can be seen by in vitro study results previously reported by our lab [35-39].

Computational fluid dynamics (CFD) results have also been reported by our lab [40, 41] as well as others [42-48]. In general, the CFD studies examined the effects of caval offsets, flaring, vessel diameters, and incidence angles for various TCP geometries. Results reported that caval offsets and flaring of anastomoses reduce power losses across the connection and that extracardiac tunnel procedures are more efficient. This study did not examine caval offsets nor control flaring in the animal models. As stated earlier, direct impact of SVC and IVC flows was avoided using the TCPY modification. In CFD models, boundary conditions are applied to open loop systems, which is quite different from examining a closed loop system with its many intrinsic feedback mechanisms—neuronal, mechanical, etc.

Recently, MRI methods have been utilized in humans to obtain three dimensional velocity measurements [12] enabling analysis on an individual patient basis. Using a viscous dissipation function, power losses are estimated [35, 41, 49]. Pressure measurements are not available and therefore power cannot be measured by this technique.

Certain limitations are inherent in these studies. Lambs having normal anatomy that had not been preconditioned with an overloaded ventricle were subjected to an operation that severely altered geometries and hemodynamics. Clinical practice divides the TCP procedure into multiple stages allowing for a more gradual hemodynamic adaptation. Normal pulmonary vasculature is also present and necessary for successful TCPY procedures. Although utmost attention is taken to control parameters, individual lamb variability and ability to adapt to modified hemodynamics cannot be controlled.

Disadvantages of the TCPY procedure are also present with current extracardiac TCP procedures. Implementation of a synthetic graft does not allow for patient growth. Also, introduction of synthetic material is more prone to thrombosis formation. In addition, fenestration may be necessary in order to help reduce the effects after cardiopulmonary bypass and to increase CO. Coming off cardiopulmonary bypass after the TCPY procedure was often difficult in our lamb models.

Future directions include increasing the total number of successful TCPY procedures. Respiration effects will be examined in more detail and power differences between inspiration and expiration will be investigated. Real time power calculations should be implemented into the data acquisition system and instantaneous manipulations and respiration therapies can be performed to optimize hemodynamics and minimize power losses.

Conclusion

A new surgical technique for a TCP procedure using a Y-shaped connection has been successfully implemented in lambs. This TCPY procedure warrants further investigation and may be a viable option for future clinical use. Currently, animal models allow for instantaneous pressure and flow measurements and hemodynamic and power analysis at input and output regions of the Fontan connection and at systemic vessel sites. This single ventricle closed loop analysis is not currently available by any other modality. This novel procedure preserved 51% of CO, a major component in success of TCP procedures. Blood flow contributions to each lung and hepatic distribution was similar to normal conditions. No change in SVR was observed and an expected increase in PVR. A 25±8.52 percent

power loss is lower than current results from CFD and in vitro studies. TCPY connection geometry does not implement direct impact of caval flows, therefore may minimize power losses through the connection.

Acknowledgments

This work was supported by a BRP grant from the National Heart, Lung, and Blood Institute, HL67622.

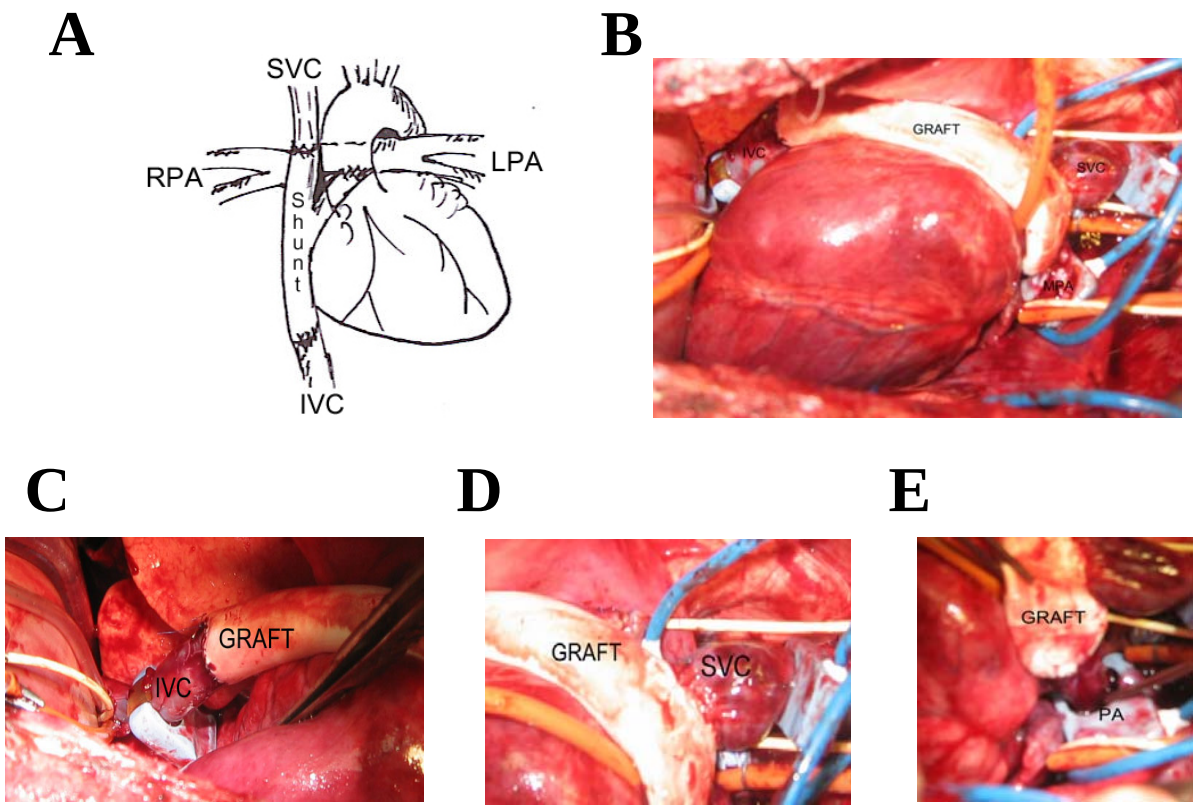

Figure 1. (A) Schematic of total cavopulmonary procedure with Y-shaped connection (TCPY). (B) TCPY connection implemented in lamb model illustrating graft position. Pictures of inferior vena cava, IVC, (C), superior vena cava, SVC, (D), and main pulmonary artery, PA (E) anastomoses. Flow (blue) and pressure (yellow) transducers are inserted at inlet (SVC and IVC) and outlet (MPA) vessels for instantaneous measurements.

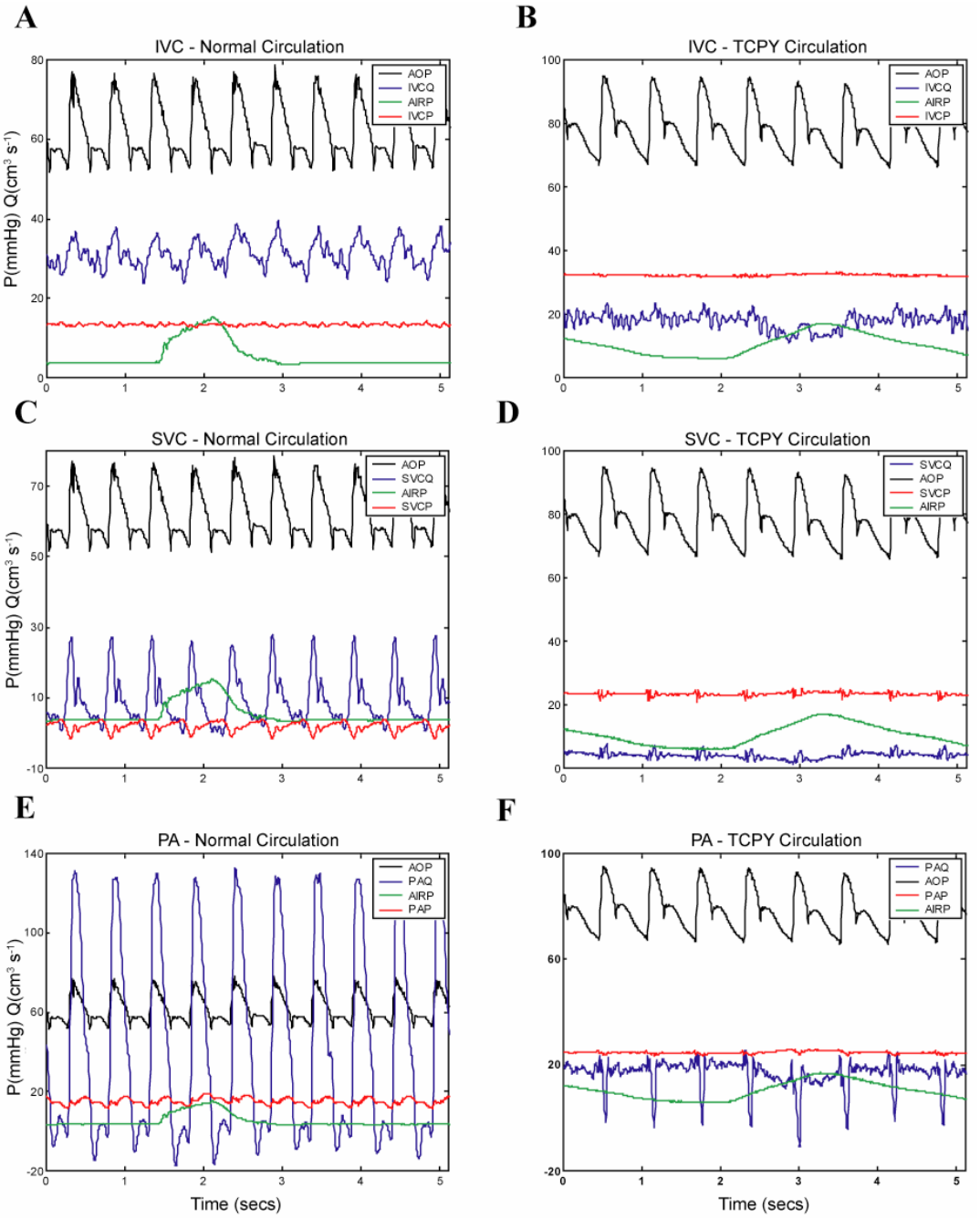

Figure 2. Lamb model example waveforms illustrating pressure (P) and flow (Q) of the inferior (IVC) vena cava, superior vena cava (SVC), and pulmonary artery (PA) under normal circulation (A, C, and E) and total cavopulmonary (TCPY) with a Y-shaped connection circulation (B, D, and F). For reference, arterial pressure (AOP) and airway pressure (AIRP) are shown.

Table 1:

	Normal Circulation Mean ± SD (n=6)	TCPY Circulation Mean ± SD (n=6)	p-value
Pressures (mm Hg)			
Ao	55.20 ± 19.65	58.50 ± 17.66	0.766
PA	16.98 ± 8.55	26.16 ± 8.63	0.094
SVC	5.35 ± 2.22	25.56 ± 9.32*	0.003
IVC	8.96 ± 2.35	28.59 ± 10.31*	0.005
LA	5.42 ± 3.13	10.32 ± 3.31*	0.025
Flows ($cm^3 \cdot sec^{-1}$)			
SVC	9.19 ± 2.02	5.86 ± 3.10	0.056
IVC	32.27 ± 15.06	12.45 ± 3.68*	0.022
LPA	21.04 ± 10.26	5.71 ± 3.72*	0.013
CO	38.77 ± 10.51	19.60 ± 5.37	0.005
% LPA	26.62 ± 21.99	34.12 ± 20.4	0.554
% SVC	25.36 ± 10.77	31.71 ± 10.12	0.317
% IVC	74.64 ± 10.77	68.29 ± 10.12	0.317
Vascular Resistances			
PVR			
$dyne \cdot sec \cdot cm^{-5}$	571.60 ± 531.12	1817.85 ± 827.24*	0.014
Wood Units	7.15 ± 6.64	22.72 ± 10.34*	
HRES			
$dyne \cdot sec \cdot cm^{-5}$	7300.97 ± 2291.98	8218.03 ± 3762.27	0.623
Wood Units	91.26 ± 28.65	102.73 ± 47.03	
BRES			
$dyne \cdot sec \cdot cm^{-5}$	2230.90 ± 1113.90	3156.97 ± 1147.52	0.187
Wood Units	27.89 ± 13.92	39.46 ± 14.34	
SVR			
$dyne \cdot sec \cdot cm^{-5}$	1636.57 ± 693.62	2185.70 ± 701.01	0.206
Wood Units	20.46 ± 8.67	27.32 ± 8.88	

Table 1. Comparison of overall hemodynamic values in lambs between normal and total cavopulmonary using a Y-shaped connection (TCPY) circulations. Systemic vascular resistance (SVR) was divided into the head resistance (HRES) and the body resistance (BRES). Two tailed unpaired variance T-test p-values are presented in the right column.

***Statistically significant differences reported with a p-value < 0.05.**

Table 2:

	Normal Circulation Mean ± SD (n=6)	TCPY Circulation Mean ± SD (n=6)	p-value
SVC Power (mW)	6.47 ± 2.67	18.53 ± 7.53	0.094
IVC Power (mW)	38.32 ± 19.15	45.91 ± 18.28	0.499
PA Power (mW)	84.91 ± 40.00	36.39 ± 20.21*	0.031

Table 2. Comparison of systemic (SVC and IVC) and pulmonary (PA) power in milliwatts (mW) between normal and TCPY circulations in lambs. Two tailed unpaired variance T-test p-values are presented in the right column.

***Statistically significant differences were reported with a p-value < 0.05 as indicated.**

Table 3:

Power	TCPY Connection Mean ± SD (n=6)
Systemic Power (mW)	64.44 ± 21.69
PA Power (mW)	36.39 ± 20.21
LPA Power (mW)	22.21 ± 11.75
% LPA Power	43.51 ± 19.60
Power Loss (mW)	28.05 ± 8.28
% Power Loss Across Connection	25.75 ± 8.52

Table 3. Systemic and pulmonary power values in milliwatts (mW) for lambs for the total cavopulmonary with Y-shaped connection (TCPY). Left pulmonary artery (LPA) percentage of total pulmonary power and total power loss across the connection region are shown.

REFERENCES

1. Rowe RD, Freedom RM, Mehrizi A. *The Neonate with Congenital Heart Disease.* 2nd ed. Philadelphia, PA: W.B. Saunders Co.; 1981.

2. Fontan F, Baudet E. Surgical repair of tricuspid atresia. *Surgical repair of tricuspid atresia*. 1971;26:240-248.

3. Castaneda AR. From Glenn to Fontan. A continuing evolution. *Circulation*. 1992;86:II80-4.

4. de Leval MR, Kilner P, Gewillig M, Bull C. Total cavopulmonary connection: A logical alternative to atriopulmonary connection for complex Fontan operations. experimental studies and early clinical experience. *J Thorac Cardiovasc Surg*. 1988;96:682-695.

5. Marcelletti C, Corno A, Giannico S, Marino B. Inferior vena cava-pulmonary artery extracardiac conduit. A new form of right heart bypass. *J Thorac Cardiovasc Surg*. 1990;100:228-232.

6. Marcelletti CF, Hanley FL, Mavroudis C, et al. Revision of previous Fontan connections to total extracardiac cavopulmonary anastomosis: A multicenter experience. *J Thorac Cardiovasc Surg*. 2000;119:340-346.

7. Podzolkov VP, Zaets SB, Chiaureli MR, Alekyan BG, Zotova LM, Chernikh IG. Comparative assessment of Fontan operation in modifications of atriopulmonary and total cavopulmonary anastomoses. *Eur J Cardiothorac Surg*. 1997;11:458-465.

8. Laschinger JC, Redmond JM, Cameron DE, Kan JS, Ringel RE. Intermediate results of the extracardiac Fontan procedure. *Ann Thorac Surg*. 1996;62:1261-7; discussion 1266-7.

9. Srivastava D, Preminger T, Lock JE, et al. Hepatic venous blood and the development of pulmonary arteriovenous malformations in congenital heart disease. *Circulation.* 1995;92:1217-1222.

10. Justino H, Benson LN, Freedom RM. Development of unilateral pulmonary arteriovenous malformations due to unequal distribution of hepatic venous flow. *Circulation*. 2001;103:E39-40.

11. Pike NA, Vricella LA, Feinstein JA, Black MD, Reitz BA. Regression of severe pulmonary arteriovenous malformations after Fontan revision and "hepatic factor" rerouting. *Ann Thorac Surg*. 2004;78:697-699.

12. Gersony DR, Gersony WM. Management of the postoperative Fontan patient. *Progress in Pediatric Cardiology*. 2003;17:73-79.

13. de Leval MR. The Fontan circulation: A challenge to william harvey? *Nat Clin Pract Cardiovasc Med*. 2005;2:202-208.

14. Lemes V, Murphy AM, Osterman FA, Laschinger JC, Kan JS. Fenestration of extracardiac Fontan and reversal of protein-losing enteropathy: Case report. *Pediatr Cardiol*. 1998;19:355-357.

15. Bull K. The Fontan procedure: Lessons from the past. *Heart*. 1998;79:213-214.

16. Rodefeld MD, Boyd JH, Myers CD, et al. Cavopulmonary assist: Circulatory support for the univentricular Fontan circulation. *Ann Thorac Surg*. 2003;76:1911-6; discussion 1916.

17. Haneda K, Konnai T, Sato N, Nicoloff NN, Mohri H. Acute hemodynamic changes after Fontan operation: An experimental study. *Tohoku J Exp Med*. 1993;169:113-119.

18. Rodefeld MD, Bromberg BI, Schuessler RB, Boineau JP, Cox JL, Huddleston CB. Atrial flutter after lateral tunnel construction in the modified Fontan operation: A canine model. *J Thorac Cardiovasc Surg*. 1996;111:514-526.

19. Rodefeld MD, Gandhi SK, Huddleston CB, et al. Anatomically based ablation of atrial flutter in an acute canine model of the modified Fontan operation. *J Thorac Cardiovasc Surg*. 1996;112:898-907.

20. Bromberg BI, Schuessler RB, Gandhi SK, Rodefeld MD, Boineau JP, Huddleston CB. A canine model of atrial flutter following the intra-atrial lateral tunnel Fontan operation. *J Electrocardiol*. 1998;30 Suppl:85-93.

21. Gandhi SK, Bromberg BI, Rodefeld MD, et al. Lateral tunnel suture line variation reduces atrial flutter after the modified Fontan operation. *Ann Thorac Surg*. 1996;61:1299-1309.

22. Gandhi SK, Bromberg BI, Schuessler RB, et al. Characterization and surgical ablation of atrial flutter after the classic Fontan repair. *Ann Thorac Surg*. 1996;61:1666-78; discussion 1678-9.

23. Mace L, Dervanian P, Bourriez A, et al. Changes in venous return parameters associated with univentricular Fontan circulations. *Am J Physiol Heart Circ Physiol*. 2000;279:H2335-43.

24. Lardo AC, Webber SA, Iyengar A, del Nido PJ, Friehs I, Cape EG. Bidirectional superior cavopulmonary anastomosis improves mechanical efficiency in dilated atriopulmonary connections. *J Thorac Cardiovasc Surg*. 1999;118:681-691.

25. Lardo AC, Webber SA, Friehs I, del Nido PJ, Cape EG. Fluid dynamic comparison of intra-atrial and extracardiac total cavopulmonary connections. *J Thorac Cardiovasc Surg*. 1999;117:697-704.

26. Lardo AC, del Nido PJ, Webber SA, Friehs I, Cape EG. Hemodynamic effect of progressive right atrial dilatation in atriopulmonary connections. *J Thorac Cardiovasc Surg*. 1997;114:2-8.

27. Szabo G, Buhmann V, Graf A, et al. Ventricular energetics after the Fontan operation: Contractility-afterload mismatch. *J Thorac Cardiovasc Surg*. 2003;125:1061-1069.

28. Okano T, Yamagishi M, Shuntoh K, et al. Extracardiac total cavopulmonary connection using a Y-shaped graft. *Ann Thorac Surg*. 2002;74:2195-2197.

29. Zellers TM, Driscoll DJ, Mottram CD, Puga FJ, Schaff HV, Danielson GK. Exercise tolerance and cardiorespiratory response to exercise before and after the Fontan operation. *Mayo Clin Proc*. 1989;64:1489-1497.

30. Shachar GB, Fuhrman BP, Wang Y, Lucas RV,Jr, Lock JE. Rest and exercise hemodynamics after the Fontan procedure. *Circulation*. 1982;65:1043-1048.

31. Kelley JR, Mack GW, Fahey JT. Diminished venous vascular capacitance in patients with univentricular hearts after the Fontan operation. *Am J Cardiol*. 1995;76:158-163.

32. Rosenthal M, Bush A, Deanfield J, Redington A. Comparison of cardiopulmonary adaptation during exercise in children after the atriopulmonary and total cavopulmonary connection Fontan procedures. *Circulation*. 1995;91:372-378.

33. Nawa S, Yamada M, Kino K, Teramoto S, Morita K. Post-Fontan care based on hemodynamic characteristics, with special reference to the central venous pressure. *Acta Med Okayama*. 1989;43:233-240.

34. Tamaki S, Kawazoe K, Yagihara T, Abe T. A model to simulate the haemodynamic effects of right heart pulsatile flow after modified Fontan procedure. *Br Heart J*. 1992;67:177-179.

35. de Zelicourt DA, Pekkan K, Parks J, Kanter K, Fogel M, Yoganathan AP. Flow study of an extracardiac connection with persistent left superior vena cava. *J Thorac Cardiovasc Surg*. 2006;131:785-791.

36. Ensley AE, Lynch P, Chatzimavroudis GP, Lucas C, Sharma S, Yoganathan AP. Toward designing the optimal total cavopulmonary connection: An in vitro study. *Ann Thorac Surg*. 1999;68:1384-1390.

37. Pekkan K, Kitajima HD, de Zelicourt D, et al. Total cavopulmonary connection flow with functional left pulmonary artery stenosis: Angioplasty and fenestration in vitro. *Circulation*. 2005;112:3264-3271.

38. Ryu K, Healy TM, Ensley AE, Sharma S, Lucas C, Yoganathan AP. Importance of accurate geometry in the study of the total cavopulmonary connection: Computational simulations and in vitro experiments. *Ann Biomed Eng*. 2001;29:844-853.

39. Sharma S, Goudy S, Walker P, et al. In vitro flow experiments for determination of optimal geometry of total cavopulmonary connection for surgical repair of children with functional single ventricle. *Journal of the American College of Cardiology*. 1996;27:1264-1269.

40. Masters JC, Ketner M, Bleiweis MS, Mill M, Yoganathan A, Lucas CL. The effect of incorporating vessel compliance in a computational model of blood flow in a total cavopulmonary connection (TCPC) with caval centerline offset. *J Biomech Eng*. 2004;126:709-713.

41. Healy TM, Lucas C, Yoganathan AP. Noninvasive fluid dynamic power loss assessments for total cavopulmonary connections using the viscous dissipation function: A feasibility study. *J Biomech Eng*. 2001;123:317-324.

42. Dubini G, de Leval MR, Pietrabissa R, Montevecchi FM, Fumero R. A numerical fluid mechanical study of repaired congenital heart defects. application to the total cavopulmonary connection. *J Biomech*. 1996;29:111-121.

43. Migliavacca F, Dubini G, Bove EL, de Leval MR. Computational fluid dynamics simulations in realistic 3-D geometries of the total cavopulmonary anastomosis: The influence of the inferior caval anastomosis. *J Biomech Eng*. 2003;125:805-813.

44. Hsia TY, Migliavacca F, Pittaccio S, et al. Computational fluid dynamic study of flow optimization in realistic models of the total cavopulmonary connections. *J Surg Res*. 2004;116:305-313.

45. Migliavacca F, Kilner PJ, Pennati G, et al. Computational fluid dynamic and magnetic resonance analyses of flow distribution between the lungs after total cavopulmonary connection. *IEEE Transactions on Biomedical Engineering*. 1999;46:393-399.

46. de Leval MR, Dubini G, Migliavacca F, et al. Use of computational fluid dynamics in the design of surgical procedures: Application to the study of competitive flows in cavo-pulmonary connections. *Journal of Thoracic and Cardiovascular Surgery*. 1996;111:502-513.

47. Migliavacca F, de Leval MR, Dubini G, Pietrabissa R. A computational pulsatile model of the bidirectional cavopulmonary anastomosis: The influence of pulmonary forward flow. *J Biomech Eng*. 1996;118:520-528.

48. Van Haesdonck JM, Mertens L, Sizaire R, et al. Comparison by computerized numeric modeling of energy losses in different Fontan connections. *Circulation*. 1995;92:II322-6.

49. Pekkan K, de Zelicourt D, Ge L, et al. Physics-driven CFD modeling of complex anatomical cardiovascular flows-a TCPC case study. *Ann Biomed Eng*. 2005;33:284-300.

APPENDIX IV:

MAGNETIC RESONANCE IMAGING OF FONTAN CIRCULATIONS

Background

Magnetic resonance imaging (MRI) is an evolving medium for studying the Fontan circulation and its many modifications. Early work by Julsrud et al consisted of vascular identification of the systemic veins, pulmonary arteries, and pulmonary veins. This information was used to determine vascular structure prior to surgery in patients being considered for a Fontan procedure (Julsrud, Ehman et al 1989). Advancements in MRI sequencing and design have broadened the spectrum for which MRI is now being utilized in Fontan patients.

MRI has also been utilized in determining anatomical geometries at various stages of Fontan surgical procedures. Left ventricular volume, mass, stroke volume, cardiac index, and ejection fraction were determined at all stages of Fontan construction. Results showed no significant differences between the surgical groups. However, statistical differences were present between MR datasets and angiography data. Angiography overestimated all parameters investigated (Fogel, Weinberg et al 1996).

Bolus blood tagging techniques were used to visualize blood flow patterns in the systemic pathway. Results showed laminar flow within the systemic vessels. Also, approximately 70% of the blood flow was found to be cardiac dependent, with the difference being respiratory dependent. Furthermore, blood flow during all phases of the cardiac cycle was determined. Results showed maximum flow occurring at end systole and during early diastole. Also, flow increased during inspiration (Fogel, Weinberg et al 1997).

As hemodynamic efficiency was proven to have a major effect on surgical outcome, MRI was also used to determine Fontan pathway phase velocity measurements. Three dimensional velocity vector maps were acquired throughout the cardiac cycle. Results demonstrated flow stagnation, regurgitation, and non-uniform flow patterns in the AP connection. Also, flow was greater in the TCPC geometries and more unidirectional. Vessel and shunt diameter was determined to affect hemodynamic efficiency with greater losses occurring as diameter increased. Laminar flow and decreased areas of disturbed flow were observed in TCPC geometries (Be'eri, Maier et al 1998).

Axial, circumferential, and radial shear stresses in the pulmonary arteries were also investigated using MRI three dimensional velocity phase contrast techniques (Morgan, Graham et al 1998). The TCPC connection had higher shear stresses than normal circulation. AP shear stresses were similar to normal circulations, but were less than TCPC stresses. Shear stresses are important for their contributions to cell function, vascular tone, vascular structure, endothelium release of vasodilators and constrictors, and thrombosis formation. Furthermore, pulmonary artery size is a dominant factor in flow determination and procedural outcome. This study used zero offset TCPC connections and stresses may be lower for offset modifications.

Cine MRI is a technique that was used in Fontan patients to determine blood flow distribution to the left and right lungs. Saturation pulses and gradient echo sequences enable blood flow distribution to be determined by decreases in signal intensity. Findings demonstrated SVC flow directed towards the RPA and IVC flow directed toward the LPA. However, equal amounts of IVC and SVC blood were present in the LPA because of the approximate 45% total systemic blood flow contribution from the IVC of a young child.

Therefore, the age of each Fontan state should be considered in determining the optimal flow pathway configuration (Fogel, Weinberg et al 1998).

Recent advances in MRI have broadened the scope of information now available to clinicians. Quantitative flow measurements can now be taken during exercise using a bicycle ergometer (Pedersen, Stenbog et al 2002). Results show a 100% increase in IVC flow and slight to minimal increase in SVC flow during exercise. The increase is due, primarily, to an increase in heart rate. Flow distribution to the lungs remained equally distributive indicating pulmonary resistance as the determinant of flow distribution of the TCPC connection. Also, MRI has been used to diagnose thrombosis in both the right atria and pulmonary arteries (Figure 1). The technique provides noninvasive diagnosis and enables monitoring of circulation evolvement after the Fontan procedure (Casolo, Rega et al 2006).

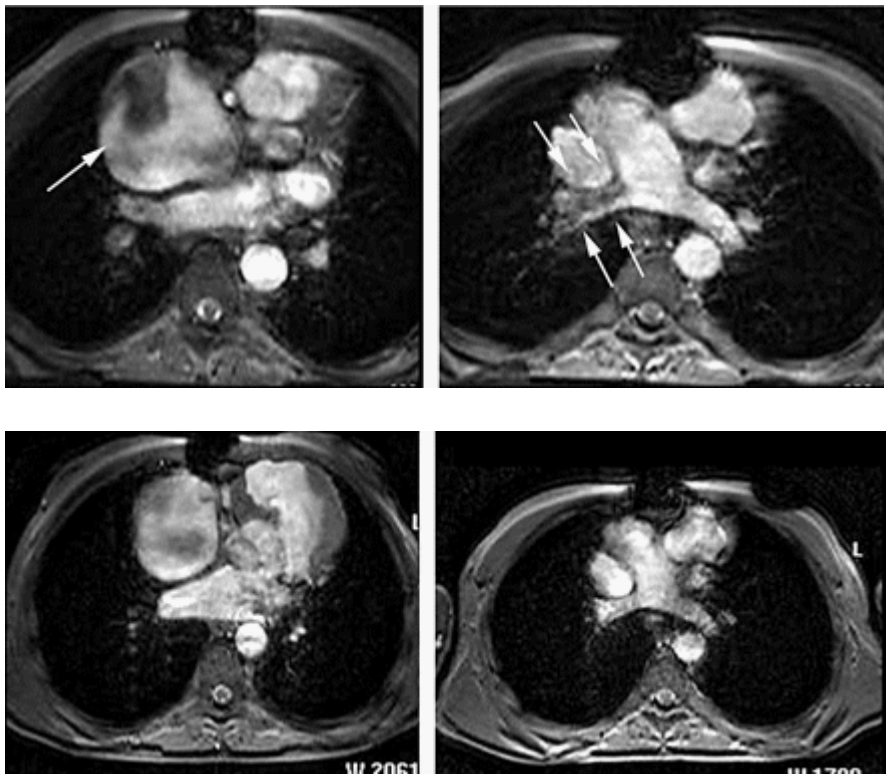

Figure 1. Cine magnetic resonance images of a right atrial mass with low signal

intensity (left) and right pulmonary artery thrombosis (right) shown with white arrows both a) before treatment and b) after oral anticoagulant treatment. (Casolo, Rega et al 2006).

MRI has progressed towards evaluation of single ventricle patients without the need for cardiac catheterization (Fogel 2005). Images provide 3D anatomy and structural information, evaluate systemic and pulmonary pathways, determine pulmonary artery size, determine degree of thrombosis, and provide velocity and flow distribution information. Blood flow turbulence, stagnation regions, regurgitation sites, and cardiac index are provided using various MR techniques. Furthermore, ventricular function and lung perfusion can also be assessed. These are just a few examples of the advancement of MR techniques for assessing single ventricle patients and demonstrates the need for further advancement and utilization of MR for evaluation and management in both pre and postoperative conditions.

Phase Contrast Concepts

Phase contrast MR measurements are possible because the transverse magnetization of spins that are in motion in the presence of a magnetic field gradient will have different spins from static spins. This phase shift is proportional to the velocity and the first moment of the gradient waveform. This can be expressed by:

$$\phi(T) = \gamma * v \int_0^T G(t) t dt$$

where $\Phi(T)$ is the phase shift at time T, γ is the gyromagnetic ratio, v is the velocity, and G is the gradient waveform (Pelc, Bernstein et al 1991). To eliminate errors such as magnetic field inhomogeneities, motion in other directions, and other small sources of error, multiple measurements are acquired. This allows for phase shifts to occur as the gradient waveform is

altered. To further eliminate error, a bipolar gradient pulse is used with changing magnitudes between images. Therefore, the phase change between images becomes:

$$\Delta\phi = 2\gamma G v \tau^2$$

where τ is the duration of the gradient, G is the gradient strength. The factor of two accounts for the bipolar gradient. This can be acquired in all three directions.

Two methods are commonly used to process the data. The first is the complex difference method that consists of two flow experiments followed by image reconstruction. The image signal therefore becomes

$$| \Delta S | = 2 | S_m \sin (\varphi_m/2)|$$

Where S_m is the moving spin contribution of the image and φ_m is the phase shift of the moving spins. This method has advantages of low storage required, the difference can be computed before reconstruction, the magnitude approaches zero if there is no motion (small φ_m), and output is independent of static signals. A disadvantage is that the directional information of the magnitude is disregarded.

To obtain directional flow by using the sign of the pixel values, a second approach of phase difference is utilized. Separate reconstructions of phase images must be performed that take processing time and computer storage. Once reconstructed, phase differences at each point are computed and the change in phase, $\Delta\Phi$, is computed by:

$$\Delta\Phi = \Phi_{S2} - \Phi_{S1} = \Phi_{S2}/\Phi_{S1}$$

where S1 and S2 are corresponding phase images. Velocity, *v*, can then be computed with direction via:

$$v = \Delta\Phi/ \gamma \Delta M$$

where M is the magnitude. This method has advantages of maintaining directional information allowing velocities and flow to be obtained in three dimensions. Also, magnitude images are easily obtained. A disadvantage is that stationary tissue degrades the images and underestimates velocity.

Specific Aim

Previously, Fontan patients had not been scanned using current phase velocity MRI techniques at the University of North Carolina at Chapel Hill (UNC). For this research, in order to help understand single ventricle anatomy and physiologies, the specific aims were to:

1) Explore feasibility and establish protocol at UNC for TCPC geometries and velocity mapping.
2) Recruit TCPC patient volunteers.
3) Obtain 3D velocity profiles of vessels of interest (left and right pulmonary arteries, inferior vena cava, and aortic arch).
4) Contribute to multi-institutional anatomic database in order to validate technique and aid in surgical planning.

Results

To date, fourteen patients have been successfully scanned at UNC. Patient details are shown in Table 1. For the first phase of this project, patients old enough to not require sedation were recruited. Recently, a sedation protocol has been approved allowing for recruitment of patients before the Glenn procedure, after the Glenn procedure, and after the

Fontan completion. UNC has successfully scanned three patients requiring sedation and two having the Glenn procedure prior to Fontan completion.

Patient	Age	Gender	CHD	Fontan Type
UNC 001	14	F	Double Outlet	Intra-atrial
UNC 002	9	M	Single Ventricle, Pulmonary Atresia	Intra-atrial
UNC 003	16	M	TGA, VSD, Pulmonary Atresia	Intra-atrial
UNC 004	7	M	Single Ventricle, Mitral Atresia	Intra-atrial
UNC 005	6	F	Tricuspid Atresia	Intra-atrial
UNC 006	11	M	VSD, DILV, TGA, HRH	Intra-atrial
UNC 007	16	F	DILV,Pulmonary Stenosis	Intra-atrial
UNC 008	5	M	TGA, Pulmonary Stenosis, HLV	Intra-atrial
UNC 009	2	M	HRV	Intra-atrial
UNC 010	8	M	HLV	Intra-atrial
UNC 011	14	M	Heterotaxy	Intra-atrial
UNC 012	10	F	Pulmonary Atresia	Intra-atrial
UNC 013	2	M	Pulmonary Atresia, HRV, ASD	Glenn
UNC 014	2	M	DILV, TGA, Pulmonary Atresia	Glenn

Table 1. Database of Fontan patients scanned at the University of North Carolina at Chapel Hill (UNC). M=Male, F=Female, CHD=Congenital Heart Defect, TGA=Transposition of the Great Arteries, VSD=Ventricular Septal Defect, DILV=Double Inlet Left Ventricle, HRH=Hypoplastic Right Heart, HLV=Hypoplastic Left Ventricle, HRV=Hypoplastic Right Ventricle, ASD=Atrial Septal Defect.

Overall MRI Protocol

MRI was performed at UNC using a 1.5 Tesla MRI system (Sonata; Siemens, Germany). Consent forms and protocol have been approved by the Institutional Review Board (IRB) and are in compliance with the Health Insurance Portability and Accountability Act (HIPAA). Morphological images were acquired in the transverse, coronal, and sagittal planes via rapid low resolution localizer or scout sequences. Two-dimensional Fast Imaging with Steady

Precession (FISP) and half-Fourier single shot turbo spin-echo (HASTE) sequences were used to acquire morphological information. Velocity maps using three-dimensional (3D) phase contrast (PC) imaging sequences were acquired both in-plane and through-plane of the systemic and pulmonary vessels. For this study, 3D PC images were acquired:

- In the SVC above the pulmonary anastomosis
- In the venous conduit below the pulmonary artery junction
- In the venous conduit above the IVC anastomosis
- In the RPA and LPA
- Azygous vein for patients with interrupted IVC
- In the Ao

For demonstrative purposes, patient UNC004 is illustrated in the following figures to display example protocol images. The bidirectional SVC to RPA anastomosis is identified for PC imaging. Figure 2 illustrates the image of the SVC, yellow arrow, and AO, red arrow a) prior to the SVC to RPA anastomosis and b) at the pulmonary artery anastomosis.

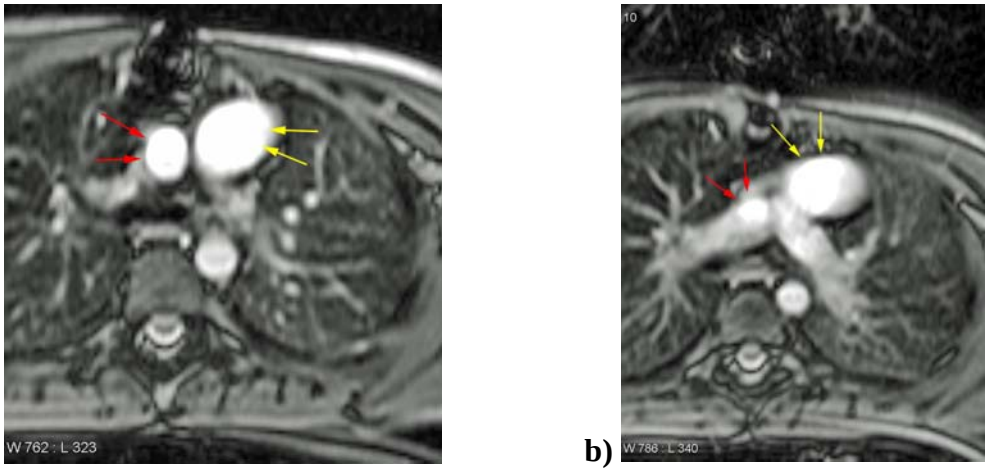

Figure 2. MRI images illustrating the SVC, yellow arrow, and AO, red arrow a)

prior to the SVC to RPA anastomosis and b) at the pulmonary artery anastomosis of a lateral tunnel Fontan modification. This is the bidirectional Glenn portion of the Fontan circulation.

The SVC is anastomosed to the right pulmonary artery. Branch pulmonary arteries are shown in Figure 3. The SVC anastomosis site (yellow arrow) and the beginning of the IVC baffle to the RPA anastomosis (red arrow) are shown. Caval offsets can be observed and measured for postprocessing information.

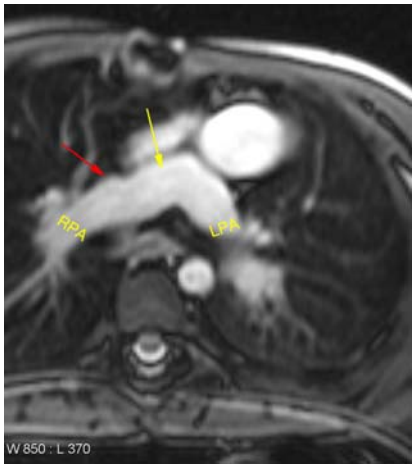

Figure 3. MRI of the left (LPA) and right pulmonary artery (LPA) at the superior vena cava (SVC) anastomosis site (yellow arrow). The flared initial baffle anastomosis region is shown with a red arrow.

The lateral tunnel anastomosis to the inferior side of the right pulmonary artery is shown in Figure 4. The aortic valve, pulmonary veins and atria are also shown.

a) 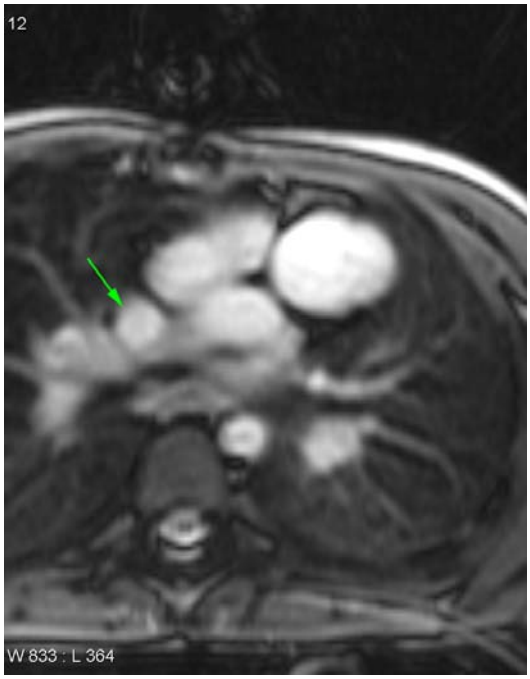

b) 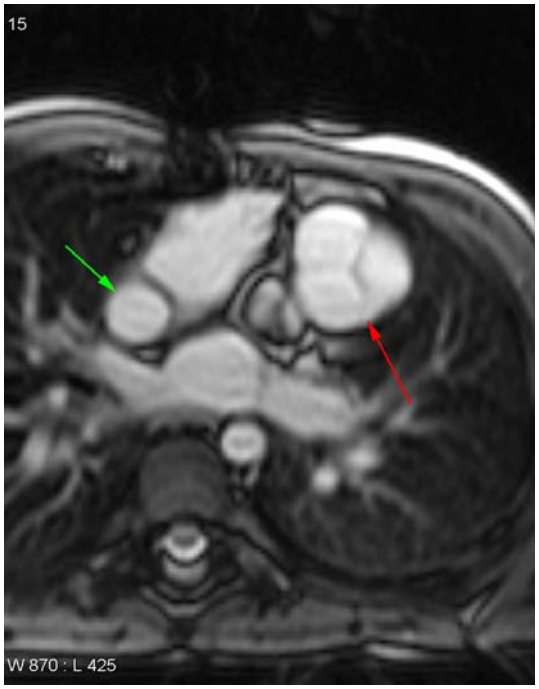

Figure 4. MRI of lateral tunnel baffle (green arrow) at the a) anastomosis site on the inferior side of the right pulmonary artery and location of the b) aortic valve (red).

An example of the single ventricle anatomy and the lateral tunnel baffle is shown in Figure 5. The ASD creating a single atria is also illustrated.

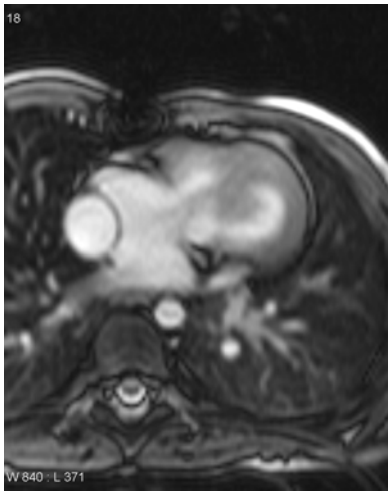

Figure 5. MRI of single ventricle anatomy with lateral tunnel Fontan modification. The ASD allowing communication of the atria is also shown.

Sagittal views allow for the entire conduit to be imaged. The IVC and lateral tunnel conduit are illustrated in Figure 6.

Figure 6. Sagittal view of inferior vena cava and lateral tunnel conduit in Fontan modification patient.

These morphological images allow vessel geometries to be determined for 3D reconstructions. Once reconstructed, CFD software packages are utilized to compare velocity map results with the MRI for accuracy to instill confidence that simulations can be used in future patient model predictors. Examples of PC magnitude and phase images of vessels are shown in Figure 7 and through the lateral tunnel conduit in Figure 8.

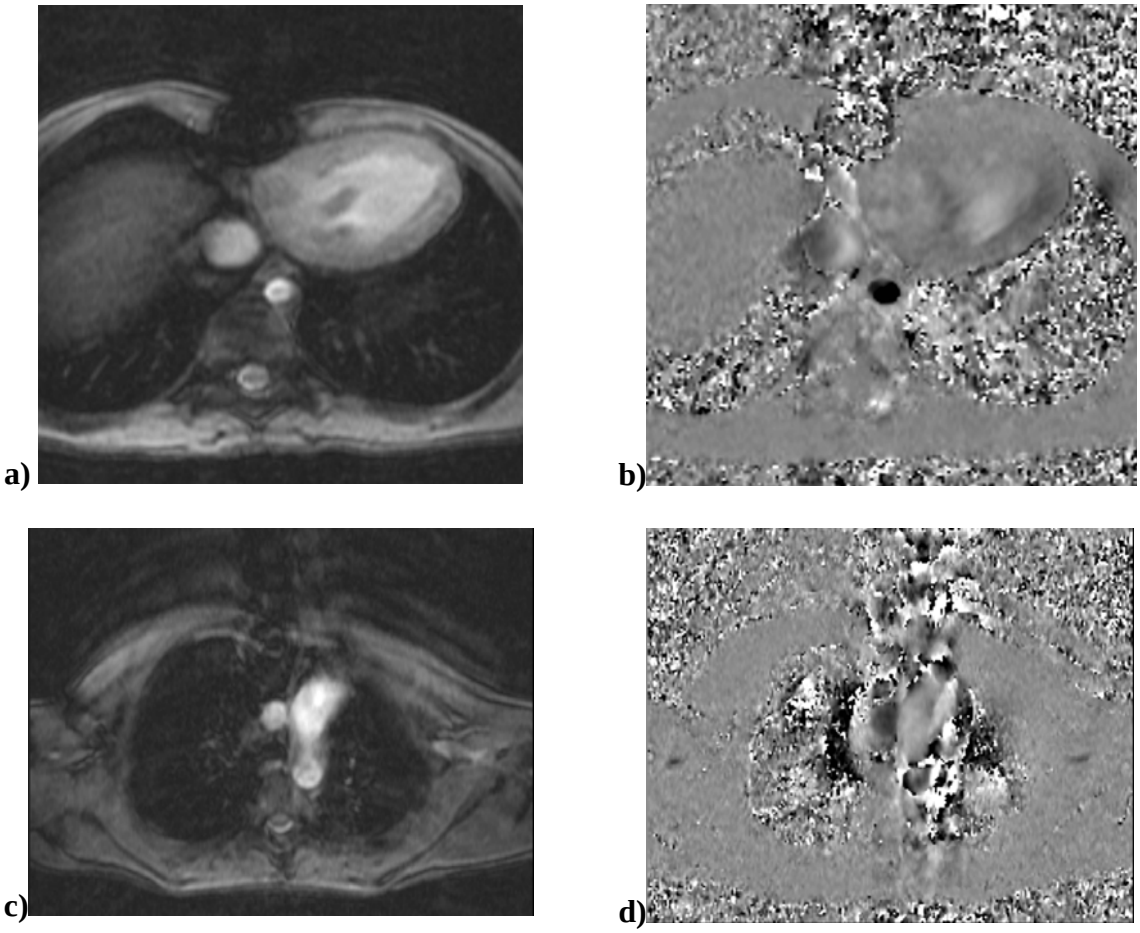

Figure 7. Example of phase contrast magnitude (a,c) and phase images (b,d) of the inferior vena cava through-plane (a and b) and aorta in-plane (c and d) used in determination of 3D velocity mapping.

a)  b) 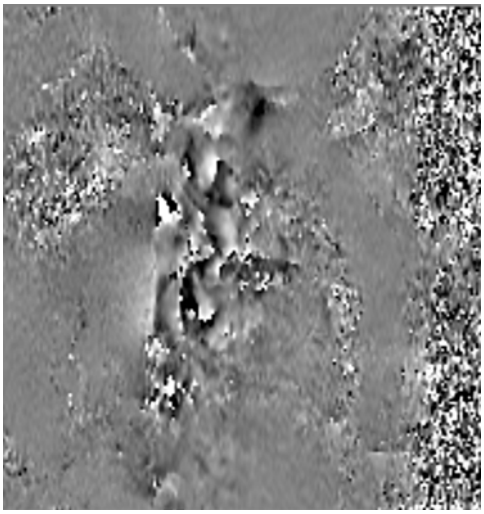

Figure 8. Example of phase contrast a) magnitude and b) phase images of lateral tunnel conduit.

Once MRI datasets are acquired, the information is sent the Georgia Institute of Technology, part of the Bioengineering Research Partnership. The data is imported, and software packages allow for determination of cross-sectional areas, flow rates, wall shear stresses, and average velocities. Flow ratios between the IVC:SVC and RPA:LPA are determined. Using this information along with data acquired via in-vivo, in-vitro, and CFD studies, flow patterns and surgical templates have been determined.

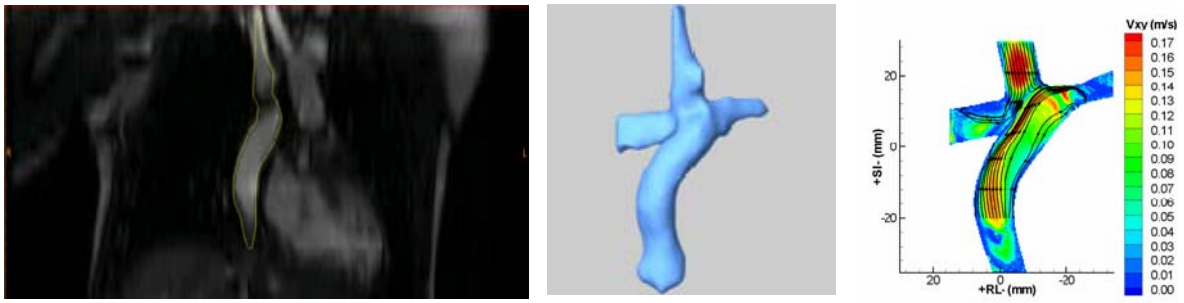

Figure 9. Segmented SVC and IVC on a) MRI and b) 3D anatomic reconstruction of Fontan patient from the coronal perspective. C) PIV TCPC flow field of at a cardiac output of 2 L/min and a 70/30 LPA/RPA flow rate ratio. (Yoganathan et al, 2006)

Conclusions

In the past two years, our lab has initiated and successfully scanned fourteen Fontan patients at UNC. Recent data sets have been used for 3D reconstruction and analysis (de Zelicourt et al, 2006). Patient recruitment is ongoing and patients are currently being scanned at different stages of the Fontan surgical procedure. Additional datasets are continuously being added to the multi-institutional database for further investigation and development of optimization techniques based on individual patient anatomy and vessel geometries.

The Imaging Protocol has recently been amended to incorporate the influences of inspiration and expiration on blood flow. Breath hold sequences at maximum inspiration and expiration of all four vessels of interest will be acquired in order to determine flow maps, ratios, and power losses.

Multiple scans of the same patient at all different stages of Fontan modifications are underway and necessary to examine blood flow changes between TCPC stages. Alterations in vessel size and shape will also be determined. In house sequencing techniques are also being developed to maximize signal to noise ratios. MRI will also be utilized in determining the effect of graft compliance on hemodynamics. Additionally, the effect of exercise on Fontan hemodynamics will be examined using a MRI stationary bike.

APPENDIX V:

INITIALIZE DATA FILE GUI

The following is the Matlab™ source code for the GUI process_data.m to universally initialize the data files for the lamb experiments. Following the GUI source code are essential callback subroutine codes.

process_data code

```
function fig = process_data()
% Copyright (C) 2006, Mark E. Ketner
% University of North Carolina at Chapel Hill, Department of Biomedical Engineering
% This software may be used, copied, or redistributed as long as it is not sold and this
% copyright notice is reproduced on each copy.  This program is provided as is without any
% implied warranties.
%
% If referenced, please send a copy to
% Mark Ketner
% Department of Biomedical Engineering
% University of North Carolina
% 152 MacNider Hall Campus Box 7575
% Chapel Hill, NC 27599
% E-mail:  mketner@bme.unc.edu
%%-------------------------------------------------------------------------------
% Usage:  process_data
%
% To be performed after .dat files are converted from voltages
% Main GUI window for which the following are created:
%
% 1.  lambXinfo.mat file
%     - inside file is variable of type structure with the following classes:
%       experiment: 'lambX'
%             date: '04/20/03'
%          connect: 'TCPC'
%              sex: 'M'
%           weight: 10
%            begin: 1
%              max: 16
%           fontan: 0
%         channels: 14
%        info_file: 42.0012
%        harm_file: 43.0012
%         ave_file: 44.0012
```

```
%    beatloc_file: 45.0012
%         chnumb: [16x18 double]
%
%    info.chnumb is an array giving column location for channels in the following order
%       - see newgetdata subroutine for structure
%
%   Creates new .mat files of size #episodes x FFT info x channel
%   stored in variable EpifftfX where X is A-Z corresponding A:1-50 B:51-100...
%
%   Creates average file that contains averages of each channel for each episode
%       - filename lambX.ave
%
%   Creates beat location file that stores starting point of each beat in episode
%       - filename lambXbt.dat

%   Creates new figure window for GUI
h0 = figure('Color',[0 0 0.25], ...
          'Name','INITIALIZE', ...
          'NumberTitle','off', ...
          'PaperPosition',[18 180 576 432], ...
          'PaperUnits','points', ...
          'Position',[23 87 325 625], ...
          'Tag','MainFig', ...
          'ToolBar','none');
%   Creates Workspace menu on toolbar
h1 = uimenu('Parent',h0, ...
          'Label','Workspace', ...
          'Tag','wkspace1');
%   Subcategories under Workspace Menu
h2 = uimenu('Parent',h1, ...
          'Label','Save Variables', ...
          'Tag','SaveVar1');
h2 = uimenu('Parent',h1, ...
          'Callback','clear', ...
          'Label','Clear Variables', ...
          'Tag','ClearVar1');
h2 = uimenu('Parent',h1, ...
          'Label','List Variables', ...
          'Tag','ListVar1');
h3 = uimenu('Parent',h2, ...
          'Callback','whos', ...
          'Label','Long List', ...
          'Tag','LongList1');
h3 = uimenu('Parent',h2, ...
          'Callback','who', ...
          'Label','Short List', ...
```

```
        'Tag','ShortList1');
%   Initialize Data file text
h1 = uicontrol('Parent',h0, ...
        'Units','points', ...
        'BackgroundColor',[0 0 0.25], ...
        'FontName','Avant Garde', ...
        'FontSize',14, ...
        'FontWeight','bold', ...
        'ForegroundColor',[1 1 1], ...
        'ListboxTop',0, ...
        'Position',[39 441 156.75 16.5], ...
        'String','INITIALIZE DATA FILES', ...
        'Style','text', ...
        'Tag','Title1');
%   Text "Connection"
h1 = uicontrol('Parent',h0, ...
        'Units','points', ...
        'BackgroundColor',[0 0 0.25], ...
        'FontName','Avant Garde', ...
        'ForegroundColor',[1 1 1], ...
        'ListboxTop',0, ...
        'Position',[52.5 350.25 59.25 9.75], ...
        'String','CONNECTION', ...
        'Style','text', ...
        'Tag','ConnTitle1');
%   Text "Experiment"
h1 = uicontrol('Parent',h0, ...
        'Units','points', ...
        'BackgroundColor',[0 0 0.25], ...
        'FontName','Avant Garde', ...
        'ForegroundColor',[1 1 1], ...
        'ListboxTop',0, ...
        'Position',[55.5 366.75 54 10.5], ...
        'String','EXPERIMENT', ...
        'Style','text', ...
        'Tag','ExperName2');
%   Edit text box for experiment name -- default: none
h1 = uicontrol('Parent',h0, ...
        'Units','points', ...
        'BackgroundColor',[1 1 1], ...
  'FontName','Arial', ...
  'FontWeight','bold',...
        'ForegroundColor',[0.7 0 0], ...
        'ListboxTop',0, ...
        'Position',[119.25 368.75 63.75 13.5], ...
        'String','none', ...
```

```
          'Style','edit', ...
          'Tag','experiment');
%   Text "Maximum Episode"
h1 = uicontrol('Parent',h0, ...
          'Units','points', ...
          'BackgroundColor',[0 0 0.250980392156863], ...
          'FontName','Avant Garde', ...
          'ForegroundColor',[1 1 1], ...
          'ListboxTop',0, ...
          'Position',[51.75 243.75 90.75 10.5], ...
          'String','MAXIMUM EPISODE', ...
          'Style','text', ...
          'Tag','maxeptitle');
%   Edit text box for maximum episode -- default: 500
h1 = uicontrol('Parent',h0, ...
          'Units','points', ...
          'BackgroundColor',[1 1 1], ...
  'ForegroundColor',[1 0 0], ...
  'FontName','Arial',...
  'FontSize',8,...
          'ListboxTop',0, ...
          'Position',[145.5 244.25 22.5 12.75], ...
          'String','500', ...
          'Style','edit', ...
          'Tag','max_episode');
%   Text "Beginning Episode"
h1 = uicontrol('Parent',h0, ...
          'Units','points', ...
          'BackgroundColor',[0 0 0.25], ...
          'FontName','Avant Garde', ...
          'ForegroundColor',[1 1 1], ...
          'ListboxTop',0, ...
          'Position',[43.5 260.25 102.75 12], ...
          'String','BEGINNING EPISODE', ...
          'Style','text', ...
          'Tag','epbegtitle');
%   Edit text box for beginning episode -- default: 1
h1 = uicontrol('Parent',h0, ...
          'Units','points', ...
          'BackgroundColor',[1 1 1], ...
          'ForegroundColor',[1 0 0], ...
          'ListboxTop',0, ...
          'Position',[145.5 261 23.25 12.75], ...
          'String','1', ...
          'Style','edit', ...
          'Tag','epbegin');
```

```
%   Text "Number Channels"
h1 = uicontrol('Parent',h0, ...
          'Units','points', ...
          'BackgroundColor',[0 0 0.25], ...
          'FontName','Avant Garde', ...
          'ForegroundColor',[1 1 1], ...
          'ListboxTop',0, ...
          'Position',[53.25 210.75 81.75 10.5], ...
          'String','NUMBER CHANNELS', ...
          'Style','text', ...
          'Tag','numchtitle');
%   Edit text box for number channels -- default: 12
h1 = uicontrol('Parent',h0, ...
          'Units','points', ...
          'BackgroundColor',[1 1 1], ...
          'ForegroundColor',[1 0 0], ...
          'ListboxTop',0, ...
          'Position',[145.5 210.75 22.5 12.75], ...
          'String','12', ...
          'Style','edit', ...
          'Tag','num_channels');
%   Popup menu for Connection -- options: AP,TCPC,TCPY,Controls,Other
h1 = uicontrol('Parent',h0, ...
          'Units','points', ...
          'BackgroundColor',[1 1 1], ...
          'FontName','Avant Garde', ...
    'FontSize',8, ...
    'FontWeight','bold',...
          'ForegroundColor',[1 0 0], ...
          'ListboxTop',0, ...
          'Position',[119.25 355.25 51.75 10.75], ...
          'String',{'AP','TCPC','TCPY','Controls','Other'}, ...
          'Style','popupmenu', ...
          'Tag','ConnectOpt', ...
          'Value',1);
%   Text "Event Date"
h1 = uicontrol('Parent',h0, ...
          'Units','points', ...
          'BackgroundColor',[0 0 0.25], ...
          'FontName','Avant Garde', ...
          'ForegroundColor',[1 1 1], ...
          'ListboxTop',0, ...
          'Position',[78 333 33 10.5], ...
          'String','EVENT DATE', ...
          'Style','text', ...
          'Tag','Event_date');
```

```
%   Edit text box for event date -- default: 04/20/06
h1 = uicontrol('Parent',h0, ...
          'Units','points', ...
          'BackgroundColor',[1 1 1], ...
    'ForegroundColor',[0.8 0 0], ...
    'FontWeight','bold',...
    'FontSize',8,...
          'ListboxTop',0, ...
          'Position',[119.25 333 55 13.5], ...
          'String','04/20/06', ...
          'Style','edit', ...
          'Tag','date');
%   Text "Sex"
h1 = uicontrol('Parent',h0, ...
          'Units','points', ...
          'BackgroundColor',[0 0 0.25], ...
          'FontName','Avant Garde', ...
    'ForegroundColor',[1 1 1], ...
          'ListboxTop',0, ...
          'Position',[87 315 19.5 10.5], ...
          'String','SEX', ...
          'Style','text', ...
          'Tag','Sex_title');
%   Popup menu for Sex -- options: M,F
h1 = uicontrol('Parent',h0, ...
          'Units','points', ...
          'BackgroundColor',[1 1 1], ...
          'FontName','Arial', ...
          'FontSize',8, ...
    'ForegroundColor',[1 0 0], ...
    'FontWeight','bold',...
          'ListboxTop',0, ...
          'Position',[119.25 317 27 13.5], ...
          'String',{'M','F'}, ...
          'Style','popupmenu', ...
          'Tag','sex', ...
          'Value',1);
%   Text "Weight (kgs)"
h1 = uicontrol('Parent',h0, ...
          'Units','points', ...
          'BackgroundColor',[0 0 0.25], ...
          'FontName','Avant Garde', ...
          'ForegroundColor',[1 1 1], ...
          'ListboxTop',0, ...
          'Position',[43.5 297.75 68.25 10.5], ...
          'String','WEIGHT (kgs)', ...
```

```
        'Style','text', ...
        'Tag','Weight_title');
%   Edit text box for weight -- default: 20
h1 = uicontrol('Parent',h0, ...
        'Units','points', ...
        'BackgroundColor',[1 1 1], ...
        'ForegroundColor',[1 0 0], ...
        'ListboxTop',0, ...
        'Position',[119.25 297.75 18 13.5], ...
        'String','20', ...
        'Style','edit', ...
        'Tag','weight');
%   Text "Fontan Episode"
h1 = uicontrol('Parent',h0, ...
        'Units','points', ...
        'BackgroundColor',[0 0 0.25], ...
        'FontName','Avant Garde', ...
        'ForegroundColor',[1 1 1], ...
        'ListboxTop',0, ...
        'Position',[60 227.25 79.5 10.5], ...
        'String','FONTAN EPISODE', ...
        'Style','text', ...
        'Tag','fontan_title');
%   Edit text box for fontan episode
h1 = uicontrol('Parent',h0, ...
        'Units','points', ...
        'BackgroundColor',[1 1 1], ...
        'ForegroundColor',[1 0 0], ...
        'ListboxTop',0, ...
        'Position',[145.5 227.5 22.5 12.75], ...
        'String','0', ...
        'Style','edit', ...
        'Tag','fontan_episode');
%   Comment box (dynamically changes) -- default: FILL OUT NECESSARY....
h1 = uicontrol('Parent',h0, ...
        'Units','points', ...
        'BackgroundColor',[0 0 0.25], ...
        'FontName','Avant Garde', ...
        'FontSize',10, ...
        'ForegroundColor',[0 1 1], ...
        'ListboxTop',0, ...
        'Position',[7.5 405 225 15], ...
        'String','FILL OUT NECESSARY FIELDS...HIT RUN', ...
        'Style','text', ...
        'Tag','comment');
%   Run Button -- callback initialize
```

```
h1 = uicontrol('Parent',h0, ...
        'Units','points', ...
        'BackgroundColor',[0.75 0.75 0.75], ...
        'Callback','initialize', ...
        'FontName','Avant Garde', ...
        'FontSize',16, ...
        'FontWeight','bold', ...
        'ForegroundColor',[0 0.50 0.25], ...
        'ListboxTop',0, ...
        'Position',[38.25 15 49.5 25.5], ...
        'String','RUN', ...
        'Tag','execute_button');
%   Stop Button -- callback close
h1 = uicontrol('Parent',h0, ...
        'Units','points', ...
        'BackgroundColor',[0.75 0.75 0.75], ...
        'Callback','status=findobj("Tag","status");set(status,"String","0");close(gcf);clear
status;return', ...
        'FontName','Avant Garde', ...
        'FontSize',16, ...
        'FontWeight','bold', ...
        'ForegroundColor',[0.5 0 0], ...
        'ListboxTop',0, ...
        'Position',[151.25 15 49.5 25.5], ...
        'String','STOP', ...
        'Tag','stop_button');
%   Text "Episode Information"
h1 = uicontrol('Parent',h0, ...
        'Units','points', ...
        'BackgroundColor',[0 0 0.25], ...
        'FontName','Avant Garde', ...
        'FontSize',10, ...
        'FontWeight','demi', ...
        'ForegroundColor',[1 1 0], ...
        'ListboxTop',0, ...
        'Position',[45.75 280.25 130.5 9.75], ...
        'String','EPISODE INFORMATION', ...
        'Style','text', ...
        'Tag','epis_title');
%   Text "General Information"
h1 = uicontrol('Parent',h0, ...
        'Units','points', ...
        'BackgroundColor',[0 0 0.25], ...
        'FontName','Avant Garde', ...
        'FontSize',10, ...
        'FontWeight','demi', ...
```

```
        'ForegroundColor',[1 1 0], ...
        'ListboxTop',0, ...
        'Position',[48 387 131.25 11.25], ...
        'String','GENERAL INFORMATION', ...
        'Style','text', ...
        'Tag','gen_title');
%   Text "Operations"
h1 = uicontrol('Parent',h0, ...
        'Units','points', ...
        'BackgroundColor',[0 0 0.25], ...
        'FontName','Avant Garde', ...
        'FontSize',10, ...
        'FontWeight','demi', ...
        'ForegroundColor',[1 1 0], ...
        'ListboxTop',0, ...
        'Position',[67.5 194.25 66.75 12], ...
        'String','OPERATIONS', ...
        'Style','text', ...
        'Tag','operation_title');
%   Text "File Information"
h1 = uicontrol('Parent',h0, ...
        'Units','points', ...
        'BackgroundColor',[0 0 0.25], ...
        'FontName','Avant Garde', ...
        'FontSize',10, ...
        'FontWeight','demi', ...
        'ForegroundColor',[1 1 0], ...
        'ListboxTop',0, ...
        'Position',[44.25 125 117 10.5], ...
        'String','FILE INFORMATION', ...
        'Style','text', ...
        'Tag','file_title');
%   Help Button -- callback process_data_help
h1 = uicontrol('Parent',h0, ...
        'Units','points', ...
        'BackgroundColor',[0.75 0.75 0.75], ...
        'Callback','inithelp', ...
        'FontName','Avant Garde', ...
        'FontSize',16, ...
        'FontWeight','bold', ...
        'ForegroundColor',[1 1 0], ...
        'ListboxTop',0, ...
        'Position',[94.75 15 49.5 25.5], ...
        'String','HELP', ...
        'Tag','help_button');
%   Checkbox for Saving General Information (lambXinfo.mat)
```

```
h1 = uicontrol('Parent',h0, ...
        'Units','points', ...
        'BackgroundColor',[0 0 0.25], ...
        'FontName','Avant Garde', ...
        'ForegroundColor',[1 1 1], ...
        'ListboxTop',0, ...
        'Position',[32.25 176.25 139.5 12], ...
        'String','SAVE GENERAL INFORMATION', ...
        'Style','checkbox', ...
        'Tag','info_save');
%   Checkbox for creating new harmonic files
h1 = uicontrol('Parent',h0, ...
        'Units','points', ...
        'BackgroundColor',[0 0 0.25], ...
        'FontName','Avant Garde', ...
        'ForegroundColor',[1 1 1], ...
        'ListboxTop',0, ...
        'Position',[32.25 159.75 158.25 10.5], ...
        'String','CREATE NEW HARMONIC .mat FILES', ...
        'Style','checkbox', ...
        'Tag','new_mat');
%   Checkbox for building/saving harmonic files
h1 = uicontrol('Parent',h0, ...
        'Units','points', ...
        'BackgroundColor',[0 0 0.25], ...
        'FontName','Avant Garde', ...
        'ForegroundColor',[1 1 1], ...
        'ListboxTop',0, ...
        'Position',[31.5 141.75 160.5 12], ...
        'String','BUILD/SAVE HARMONIC .mat FILES', ...
        'Style','checkbox', ...
        'Tag','build_mat');
%   Text "Information Stored in File"
h1 = uicontrol('Parent',h0, ...
        'Units','points', ...
        'BackgroundColor',[0 0 0.25], ...
        'FontName','Avant Garde', ...
        'ForegroundColor',[0.8 0.8 0.8], ...
        'ListboxTop',0, ...
        'Position',[28.5 108 132.75 9], ...
        'String','INFORMATION STORED IN FILE :', ...
        'Style','text', ...
        'Tag','StaticText1');
%   Text "Harmonics Stored in File"
h1 = uicontrol('Parent',h0, ...
        'Units','points', ...
```

```
        'BackgroundColor',[0 0 0.25], ...
        'FontName','Avant Garde', ...
        'ForegroundColor',[0.8 0.8 0.8], ...
        'ListboxTop',0, ...
        'Position',[34.5 91 127.5 9], ...
        'String','HARMONICS STORED IN FILE :', ...
        'Style','text', ...
        'Tag','StaticText2');
%   Text "Averages Stored in File"
h1 = uicontrol('Parent',h0, ...
        'Units','points', ...
        'BackgroundColor',[0 0 0.25], ...
        'FontName','Avant Garde', ...
        'ForegroundColor',[0.8 0.8 0.8], ...
        'ListboxTop',0, ...
        'Position',[43.5 72.5 113.25 10.5], ...
        'String','AVERAGES STORED IN FILE :', ...
        'Style','text', ...
        'Tag','StaticText3');
%   Text "Beat Locations Stored in File"
h1 = uicontrol('Parent',h0, ...
        'Units','points', ...
        'BackgroundColor',[0 0 0.25], ...
        'FontName','Avant Garde', ...
        'ForegroundColor',[0.8 0.8 0.8], ...
        'ListboxTop',0, ...
        'Position',[18 54 141 10.5], ...
        'String','BEAT LOCATIONS STORED IN FILE :', ...
        'Style','text', ...
        'Tag','StaticText4');
%   Text edit box for puting information filename
h1 = uicontrol('Parent',h0, ...
        'Units','points', ...
        'BackgroundColor',[1 1 1], ...
        'FontName','helvetica', ...
        'FontSize',7, ...
        'ForegroundColor',[1 0 0.50], ...
        'ListboxTop',0, ...
        'Position',[164.25 105.75 58.5 13.5], ...
        'Style','edit', ...
        'Tag','info_filename');
%   Text edit box for putting harmonic filename
h1 = uicontrol('Parent',h0, ...
        'Units','points', ...
        'BackgroundColor',[1 1 1], ...
        'FontName','helvetica', ...
```

```
        'FontSize',7, ...
        'ForegroundColor',[1 0 0.50], ...
        'ListboxTop',0, ...
        'Position',[164.25 88 58.5 12.75], ...
        'Style','edit', ...
        'Tag','harm_filename');
%   Text edit box for putting average filename
h1 = uicontrol('Parent',h0, ...
        'Units','points', ...
        'BackgroundColor',[1 1 1], ...
        'FontName','helvetica', ...
        'FontSize',7, ...
        'ForegroundColor',[1 0 0.50], ...
        'ListboxTop',0, ...
        'Position',[164.25 70.25 58.5 12.75], ...
        'Style','edit', ...
        'Tag','aver_filename');
%   Text edit box for putting beat location filename
h1 = uicontrol('Parent',h0, ...
        'Units','points', ...
        'BackgroundColor',[1 1 1], ...
        'FontName','helvetica', ...
        'FontSize',7, ...
        'ForegroundColor',[1 0 0.50], ...
        'ListboxTop',0, ...
        'Position',[164.25 51.75 58.5 13.5], ...
        'Style','edit', ...
        'Tag','beat_filename');
h1 = uicontrol('Parent',h0, ...
        'Units','points', ...
        'BackgroundColor',[1 1 1], ...
        'ListboxTop',0, ...
        'Position',[420 212.25 12 14.25], ...
        'String','0', ...
        'Style','edit', ...
        'Tag','status', ...
        'Visible','off');
if nargout > 0, fig = h0; end
```

Subroutine initialize.m code

```
%   usage: initalize
%
%   callback from process_data
% GET STATUS TAG
```

```
% status is zero initially
status=findobj('Tag','status');
comment=findobj('Tag','comment');
% DISABLE RUN PUSHBUTTON
h=findobj(gcbf,'Tag','execute_button');
set(h,'Visible','off')
% DISABLE HELP PUSHBUTTON
h=findobj(gcbf,'Tag','help_button');
set(h,'Visible','off')
% ********************************************************
%               GET DATA SUBROUTINE
% ********************************************************
% LOAD INFO DATA INTO WORKSPACE
% ALSO SAVES INFO DATA INTO FILE IF PROMPTED
% SEE help newgetdata FOR MORE DETAILS
[info]=getdata(status);
% CORRECT IF NO EXPERIMENT NAME IS GIVEN
H=findobj(gcbf,'Tag','status');
H=get(status,'String');
if H == '2'
  break
end
waitfor(status,'String','1');
status=findobj('Tag','status');
set(status,'String','0');
% ******************************************************
%           CREATE NEW .MAT FILES
% ******************************************************
% SEE IF OPERATION CREATE NEW MAT FILES BOX IS CHECKED
h=findobj(gcbf,'Tag','new_mat');
ex=get(h,'Value');
% IF CREATE NEW MAT FILES IS CHECKED
if ex == 1
  h=findobj(gcbf,'Tag','comment');
  set(h,'String','Creating New .mat Files....');
  % SEND WARNING ABOUT ERASING FILES
  % *******************************
  %               NEWMATGUI
  % *******************************
  % CHECKS TO MAKE SURE WANT TO ERASE FILES IF THEY EXIST
  % IF NOT, CONTINUES ON WITH PROGRAM
  % IF SO, CREATES EMPTY MAT FILES USING info
  makenewmatfiles
  % CALLS INITGUINEWMAT IF ANSWER YES
  % DOES NOTHING IF ANSWER NO
  h=findobj('Tag','indicator');
```

```
  waitfor(h,'String','1');
  close % CLOSES makenewmatfiles
end
% ************************************************
%          BUILD/SAVE HARMONIC FILES
% ************************************************
% SEE IF BUILD/SAVE HARMONIC .MAT FILES IS CHECKED
h=findobj(gcbf,'Tag','build_mat');
ch=get(h,'Value');
% IF BOX IS CHECKED, FIRST NEED TO RUN BAD FILES
% AND STORE IN FILE CALLED .....
if ch == 1
  set(comment,'String','Processing Bad Files....');
  [bad]=initbadfiles(info,status);
  waitfor(status,'String','1');
  set(status,'String','0');
  %  BUILD MAT FILES
  set(comment,'String','Building .mat files');
  newinitbuildmatfiles(info,bad,status,comment)
  waitfor(status,'String','1');
  set(status,'String','0');
  close(2)
end
comment=findobj(gcbf,'Tag','comment');
set(comment,'String','Back in main program');
% MAKE RUN PUSHBUTTON VISIBLE AGAIN
h=findobj(gcbf,'Tag','execute_button');
set(h,'Visible','on')
% MAKE HELP PUSHBUTTON VISIBLE AGAIN
h=findobj(gcbf,'Tag','help_button');
set(h,'Visible','on')
clear all
return
```

Subroutine getdata.m code

```
function [info]=getdata(status)
% SUBROUTINE GETDATA
% RETRIEVES DATA FROM INITIALIZE GUI
% INFORMATION STORED IN STRUCTURE info
%
% info USED FOR QUICK ACCESS OF DATA IN LATER PROGRAMS
% CHANGE COMMENT TO INFORM USER
comment=findobj(gcbf,'Tag','comment');
set(comment,'String','RECEIVING DATA.....');
pause(.1)
% GET NAME OF EXPERIMENT
```

```
% NAME
H=findobj(gcbf,'Tag','experiment');
experiment=get(H,'String');
info_filename=strcat(experiment,'info.mat');
% SAVE INFORMATION
H=findobj(gcbf,'Tag','info_save');
info_save=get(H,'Value');
% if name doesn't start with lamb, need to prompt user
% to change
no=strcmp(experiment,'none');
if no == 1
  set(comment,'String','Fill out Experiment Name');
  x={'No Experiment Name Entered !'
    'Please Enter Name and Try Again'
    'Thank You'};
  errordlg(x,'ERROR');
  % RESET INITIALIZE SUBROUTINE
  set(status,'String','2');
  % MAKE RUN PUSHBUTTON VISIBLE AGAIN
        h=findobj(gcbf,'Tag','execute_button');
  set(h,'Visible','on')
  h=findobj(gcbf,'Tag','help_button');
  set(h,'Visible','on')
  break
end
% SEE IF INFO FILE ALL READY EXISTS
% ex = 0 if doesn't exist
ex=exist(info_filename);
% IF FILE DOESN'T EXIST, GET DATA
if ex == 0 | info_save == 1
% ****************************************************************
%          GET INFORMATION FROM FIGURE
% ****************************************************************
% GENERAL INFORMATION
% NAME
H=findobj(gcbf,'Tag','experiment');
info.experiment=get(H,'String');
% DATE
H=findobj(gcbf,'Tag','date');
info.date=get(H,'String');
% CONNECTION TYPE
H=findobj(gcbf,'Tag','ConnectOpt');
connect_option=get(H,'Value');
connect=get(H,'String');
info.connect=connect{connect_option};
% SEX
```

```
H=findobj(gcbf,'Tag','sex');
sex_option=get(H,'Value');
sex=get(H,'String');
info.sex=sex{sex_option};
% WEIGHT
H=findobj(gcbf,'Tag','weight');
weight=get(H,'String');
info.weight=str2num(weight);
% EPISODE INFORMATION
% BEGINNING EPISODE
H=findobj(gcbf,'Tag','epbegin');
begin=get(H,'String');
info.begin=str2num(begin);
% MAXIMUM EPISODE
H=findobj(gcbf,'Tag','max_episode');
max=get(H,'String');
info.max=str2num(max);
% FONTAN EPISODE
H=findobj(gcbf,'Tag','fontan_episode');
fontan=get(H,'String');
info.fontan=str2num(fontan);
% CHANNEL INFORMATION
% NUMBER OF CHANNELS
H=findobj(gcbf,'Tag','num_channels');
channels=get(H,'String');
info.channels=str2num(channels);
% OPERATIONS
% SAVE INFORMATION
H=findobj(gcbf,'Tag','info_save');
info_save=get(H,'Value');
% CREATE NEW HARM FILES
H=findobj(gcbf,'Tag','new_mat');
newmat=get(H,'Value');
% BUILD/SAVE HARMONIC FILES
H=findobj(gcbf,'Tag','build_mat');
buildmat_save=get(H,'Value');
% SAVE AVERAGES
H=findobj(gcbf,'Tag','ave_save');
ave_save=get(H,'Value');
% SAVE HEART BEAT LOCATIONS
H=findobj(gcbf,'Tag','beatloc_save');
beatloc_save=get(H,'Value');
% GET FILENAME TAGS AND NAME FOR LATER
% INFO FILE
info_file=findobj(gcbf,'Tag','info_filename');
% HARMONIC FILE
```

```
harm_file=findobj(gcbf,'Tag','harm_filename');
% AVERAGE FILE
ave_file=findobj(gcbf,'Tag','aver_filename');
% BEAT LOCATION FILE
beatloc_file=findobj(gcbf,'Tag','beat_filename');
info.info_file=info_file;
info.harm_file=harm_file;
info.ave_file=ave_file;
info.beatloc_file=beatloc_file;
% CLEAR UNNECESSARY VARIABLES
clear info_file harm_file ave_file beatloc_file used val channels ...
  clear connect_option connect sex_option sex weight begin max fontan
% IF FILE ALL READY EXISTS
else
  % INFO FILE
        info_file=findobj(gcbf,'Tag','info_filename');
  set(comment,'String','Loading information file now')
  pause(.5)
  % LOAD lambXXinfo.mat
  info_f=strcat('load',info_filename,';');
  info_f=strrep(info_f,'l',' l');
  eval(info_f)
  % WRITE INFO FILENAME TO SCREEN
        set(info_file,'String',info_filename);
end
if ex == 0 | info_save == 1
  % GET CHANNEL INFORMATION
  multiple_channel
  h=findobj(gcf,'Tag','Pushbutton1');
  waitfor(h,'String','Wait');
  max=info.max;
  [channel_array]=makechannelarray(max);
  info.chnumb=channel_array;
end
% SAVE INFORMATION
H=findobj(gcbf,'Tag','info_save');
info_save=get(H,'Value');
% DOES USER WANT TO SAVE DATA
% info_save = 0 if no
% info_save = 1 if yes
if info_save == 1
  set(comment,'String','Saving information file')
  pause(1)
  % WRITE INFO FILENAME TO SCREEN
  set(info.info_file,'String',info_filename);
  info_f = strcat(info_filename,' info');
```

```
   info_f = strrep(info_f,'l',' l');
   info_f = strcat('save',info_f);
   eval(info_f)
end
set(status,'String','1')
set(comment,'String','End of Getdata Subroutine');
```

Subroutine makenewmatfiles.m code

```
function makenewmatfiles()
a = figure('Color',[0. 0. 0.25], ...
          'MenuBar','none', ...
          'Name','Are You Sure???', ...
          'NumberTitle','off', ...
          'Position',[360 350 278 140], ...
          'Tag','new_mat_warning');
b = uicontrol('Parent',a, ...
          'Units','points', ...
          'Callback','h=findobj(gcbf,"Tag","indicator");set(h,"String","1");newmat(info,status)',
...
          'FontSize',10, ...
          'FontWeight','bold', ...
          'Position',[40.5 5 50.25 30], ...
          'String','YES', ...
   'Tag','yes_b', ...
   'Visible','on');
b = uicontrol('Parent',a, ...
          'Units','points', ...
          'Callback','h=findobj(gcbf,"Tag","indicator");set(h,"String","1");', ...
          'FontSize',10, ...
          'FontWeight','bold', ...
          'Position',[123 5 49.5 30], ...
          'String','NO', ...
          'Tag','no_button');
b = uicontrol('Parent',a, ...
          'Units','points', ...
          'BackgroundColor',[0. 0. 0.25], ...
          'FontName','Arial', ...
          'FontSize',12, ...
          'FontWeight','normal', ...
          'ForegroundColor',[1 1 1], ...
          'Position',[1.5 36 206.25 38.25], ...
          'String','This will erase existing .mat files.  Are you sure you want to do this ?', ...
          'Style','text', ...
          'Tag','StaticText1');
b = uicontrol('Parent',a, ...
```

```
        'Units','points', ...
        'BackgroundColor',[0. 0. 0.25], ...
        'FontName','Arial', ...
        'FontSize',14, ...
        'FontWeight','normal', ...
        'ForegroundColor',[1 1 0], ...
        'Position',[59.25 75.5 90 21], ...
        'String','WARNING !!', ...
        'Style','text', ...
        'Tag','StaticText2');
b = uicontrol('Parent',a, ...
        'Units','points', ...
        'BackgroundColor',[1 1 1], ...
        'Position',[6.75 7.5 16.5 15], ...
        'String','0', ...
        'Style','edit', ...
        'Tag','indicator', ...
        'Visible','off');
```

Subroutine initbadfiles.m code

```
function [bad]=initbadfiles(info,status);
% USAGE : [BAD,NO_EXIST]=badfiles('EXPERIMENT')
% CYCLES THROUGH DATA FILES TO SEE WHICH ONES ARE BAD
% IF THEY ARE short, STORES EPISODE NUMBER IN ARRAY BAD
% IF EPISODES DO NOT EXIST, STORES IN NO_EXIST
NO_EXIST=[];
BAD=[];
% FIRST CHECK TO SEE IF BAD FILES HAVE ALLREADY
% BEEN STORED IN lambXbad.dat
nam=strcat(info.experiment,'bad.dat');
exis=exist(nam);
% IF FILE EXISTS, LOAD IT
if exis ~= 0
  %disp('loading file')
  nam = strrep(nam,'l',' l');
  nam = strcat('load',nam,';');
  eval(nam);
  X=strcat('bad=',info.experiment,'bad;');
  eval(X);
  set(status,'String','1');
  break
end
if exis == 0
        s=([1:1500]');
        i=1;
```

```
        m=1;
        % CYCLES THROUGH DATA FILES
        p=waitbar(0,'Processing Bad Files...Please Wait');
    set(p,'Position',[305 250 400 45]);
                for j=1:info.max
                g=s(j,1);
                E=g;
                g=int2str(g);
                V1=strcat(info.experiment,g,'.dat');
                V=strrep(V1,'l',' l');
                % CHECKS TO SEE IF DATA FILE EXISTS
                X=exist(V1,'file');
                U=strcat(info.experiment,g);
                % IF DATA FILE DOES NOT EXIST
                if X == 0
                % STORES EPISODE NUMBER IN NO_EXIST
                NO_EXIST(m)=E;
                m = m + 1;
                disp(strcat(V1,' does not exist'))
                end
        % IF DATA FILE EXISTS
                if X > 0
                W=strcat('load ',V);
                eval(W);
                s5=strcat('Epi=',U,';');
                eval(s5);
                % CHECK TO SEE IF DATA IS SHORT FILE
                if length(Epi) ~= 1024
                disp(strcat(U,' is a short file'))
                % IF SO, STORES EPISODE NUMBER IN BAD
                BAD(i)=E;
                i=i+1;
                end
                end
        waitbar(j/info.max,p);
        end
close(p)
end
bad=[0 BAD NO_EXIST];
sort(bad);
% SAVE BAD FILES TO FILE lambXbad.dat
sav_name=strcat('save ',info.experiment,'bad.dat bad -ascii -tabs');
sav_name=strrep(sav_name,'l',' l');
eval(sav_name)
set(status,'String','1');
return
```

Subroutine newinitbuildmatfiles.m code

```
% Usage: initbuildmatfiles(info,bad,status)
% Cyles through files building averaged curves (20 harmonics)
function initbuildmatfiles(info,bad,status,comment)
IRAY=[];
num=ceil(info.max/50);
tags='ABCDEFGHIJKLMNOPQRSTUVWXYZ';
tags=tags(1:num);
fepi='Epi';
% LOAD MAT FILES
pro=waitbar(0,'Loading .mat Files...');
for k=1:num
   mat_name = strcat(info.experiment,tags(k),'.mat');
   ex=exist(mat_name);
   % SEE IF mat FILES EXIST
   if ex == 0
      figure(1)
      h=findobj(gcbf,'Tag','execute_button');
      set(h,'Visible','on');
      h=findobj(gcbf,'Tag','help_button');
      set(h,'Visible','on');
      set(status,'String','1')
      x={'Need to run Create New .mat Files'
         'then run Build/Save .mat Files '};
      errordlg(x,'ERROR BUILDING .mat FILES');
      break
   end
   mat_name = strrep(mat_name,'l',' l');
   mat_load=strcat('load',mat_name);
   waitbar(k/num);
   eval(mat_load);
end
% pro is waitbar
close(pro)
% LOADS AVES FILE
aves_name = strcat(info.experiment,'.ave;');
aves_name = strrep(aves_name,'l',' l');
aves_load = strcat('load',aves_name);
eval(aves_load);
s6=strcat('aves=',info.experiment,';');
eval(s6);
% LOOP TO CALCULATE HARMONICS
plac=1;
proc=waitbar(0,'Processing .mat Files');
```

```
set(proc,'Position',[505 250 249 45]);
for i = info.begin:info.max
   badplus=0;
   no_data = 0;
   k=i;
   % CHECK TO SEE IF IT IS A BAD FILE
   for l = 1:length(bad)
      if bad(l) == i
         no_data = 1;
      end
   end
   % IF DATA FILE EXISTS ...
   if no_data == 0
      j=int2str(i);
      figure(1)
      x=strcat('Beginning of episode # ',j);
      set(comment,'String',x);
      f=strcat(info.experiment,int2str(i));
      s1='load';
      s3=strcat(f,'.dat');
      s3=strrep(s3,'l',' l');
      dat_name = strcat(s1,s3);
      eval(dat_name);
      s2='Epi=';
      s5=strcat(s2,f,';');
      eval(s5)
      C=Epi(:,info.chnumb(i,5)); %AOP COLUMN IN CHANNEL ARRAY
      % CALL TO initmatcalc
      % basically gives location of beats and if no difference in means
      % or low mean or high mean
      % Iray is array of beat locations
      % samp_beat is number of samples in a beat
      % code and defect are precautionary measures
      % badplus is if subroutine determines episode is bad, it adds it to
      % bad array a coulple of lines down from this
      [Iray,samp_beat,code,defect,badplus]=initmatcalc(C,i,plac);
      l=length(Iray);
      IRAY(i,1:l)=Iray;
      if defect == 1
         bad=[bad badplus];
      end
      if defect == 0
         if code==0
            % CALL TO BEATAVE
            [Epiave,Epifft]=initbeatave(Epi,Iray,samp_beat,info);
            %pause
```

```
            aves(k,:) = [Epifft(2,:)/samp_beat   60/(samp_beat*.005) Iray(1)];
            if (k>0 & k<=50) fp='EpifftfA';kk=k;
            elseif (k>50 & k<=100) fp='EpifftfB';kk=k-50;
            elseif (k>100 & k<=150) fp='EpifftfC';kk=k-100;
            elseif (k>150 & k<=200) fp='EpifftfD';kk=k-150;
            elseif (k>200 & k<=250) fp='EpifftfE';kk=k-200;
            elseif (k>250 & k<=300) fp='EpifftfF';kk=k-250;
            elseif (k>300 & k<=350) fp='EpifftfG';kk=k-300;
            elseif (k>350 & k<=400) fp='EpifftfH';kk=k-350;
            elseif (k>400 & k<=450) fp='EpifftfI';kk=k-400;
            elseif (k>450 & k<=500) fp='EpifftfJ';kk=k-450;
            elseif (k>500 & k<=550) fp='EpifftfK';kk=k-500;
            elseif (k>550 & k<=600) fp='EpifftfL';kk=k-550;
            elseif (k>600 & k<=650) fp='EpifftfM';kk=k-600;
            elseif (k>650) stop
            end
         else
            disp(strcat('problem  : ',f));
         end
         %       means of channels   time      1st beat location
         aves(k,:) =[Epifft(2,:)/samp_beat   60/(samp_beat*.005) Iray(1)];
         s10=strcat(fp,'(kk,:,:)=Epifft;');
         eval(s10);
      end
      % IF DATA FILE IS SHORT OR DOESN'T EXIST
      % need to update to include trouble files ??
      if no_data == 1 | code == 1 | defect == 1
         kk=k;
         aves(k,:)=0;
         Epifftf(kk,:,:)=0;
      end
      waitbar(i/info.max);
   end
end
close(proc)
% SAVE MAT FILES
for k=1:length(tags)
   f3=strcat(info.experiment,tags(k),'.mat');
   f3=strrep(f3,'l',' l');
   s8=strcat('save',f3,'  Epifftf',tags(k),';');
   eval(s8);
end
% SAVE AVE FILE
f4=strcat(info.experiment,'.ave');
f4 = strrep(f4,'l',' l');
s9=strcat('save',f4,' aves -ascii  -tabs;');
```

```
eval(s9);
% RESAVE BAD FILES INTO FILE
sav_name=strcat('save ',info.experiment,'bad.dat bad -ascii -tabs');
sav_name=strrep(sav_name,'l',' l');
eval(sav_name)
% SAVE HEART BEAT LOCATIONS OF EPISODES
sav_name=strcat('save',info.experiment,'bt.dat IRAY -ascii -tabs');
sav_name=strrep(sav_name,'l',' l');
eval(sav_name)
% DISPLAY FILENAMES IN GUI
figure(1)
harm_file=strcat(info.experiment,'X','.mat');
h=findobj(gcbf,'Tag','harm_filename');
set(h,'String',harm_file);
ave_file=strcat(info.experiment,'.ave');
h=findobj(gcbf,'Tag','aver_filename');
set(h,'String',ave_file);
beat_file=strcat(info.experiment,'bt.dat');
h=findobj(gcbf,'Tag','beat_filename');
set(h,'String',beat_file);
set(status,'String','1');
return
```

Subroutine initbeatave.m code

```
function [Epiave,Epifft]=initbeatave(Epi,I,N,info)
% function [Epiave,Epifft]=beatave(Epi,I,N)
% Epi = Record of channels of data being processed
% I = starting points of beats
% N = number of points in beat array
% Epiave = array of average beats
% Epifft = array of harmonics for average beat
N10=ceil(1.2*N);
nb=length(I);
Epifft=zeros(22,info.channels);
for ms=1:info.channels
        C=Epi(:,ms);
        FA=zeros(1,21)';
        hold off;
        repa=zeros(1,ceil(2*N));
        nrep=zeros(1,ceil(2*N));
        anbeat=0;
for k=2:nb
        ib=I(k-1);ie=I(k)-1;
        nbeat=(ie-ib+1);
        anbeat=anbeat+nbeat;
```

```
        FB=fft(C(ib:ie));
        FA=FA+FB(1:21);
        for m=1:ie-ib+1
        repa(m)=repa(m)+C(ib+m-1);
        nrep(m)=nrep(m)+1;
        end
        end
        m=1;
        clear rep
        while nrep(m)>0
                rep(m)=repa(m)/nrep(m);
                m=m+1;
        end
        anbeat=round(anbeat/(nb-1));
        FR=fft(rep,anbeat);
        FER=FR(1:21);
        FEE=[FER zeros(1,anbeat-41) conj(FER(21:-1:2))];
        repaf=real(ifft(FEE));
        FA=FA/(nb-1);
        FE=[FA.' zeros(1,anbeat-41) conj(FA(21:-1:2).')];
        repf=ifft(FE);
repf=(real(repf))';
temp(:,ms)=repaf';
Epifft(:,ms)=[N FER].';
end;
Epiave=zeros(anbeat,info.channels);
Epiave=temp;
```

Subroutine initmatcalc.m code

```
% SUBROUTINE TO BUILD .mat HARMONIC FILES
% CALLED FROM newinitbuildmatfiles
function [I,samp_beat,code,defect,badplus]=initmatcalc(C,episode,plac)
% PLACE FIGURE INFORMATION HERE
build=figure(2);
set(build,'Position',[50 165 620 400]);
%set(build,'MenuBar','none');
set(build,'Name','.mat File Information');
set(build,'NumberTitle','off');
clf
badplus=[0];
anbeat=0;
defect = 0;
code = 0;
FA=zeros(1,11)';
mean_ep=mean(C);
```

```
F=fft(C-mean(C),4096*4);
delf=60/(4096*4*.005); %resolution
% plot fft and data
figure(build);
subplot(2,2,1);plot(1:400,abs(F(1:400)),'r');hold on;title('FFT');
subplot(2,2,2);plot(1:1024,C);axis tight;hold on;title('AOP');
% CORRECTION IF DATA HAS NO PULSATILITY
if (max(C(1:400))-min(C(1:400))) < 2
  badplus(plac)=episode;
  plac=plac+1;
  defect = 1;code = 1;I=0;samp_beat=0;
  %disp('inside max/min if')
  break
end
% if mean is <= 15, bad episode
% store episode and break out of subroutine
if mean_ep <= 15 | mean_ep > 120
  badplus(plac)=episode;
  plac=plac+1;
  defect = 1;code = 1;I=0;samp_beat=0;
  break
end
[Y,Im]=max(abs(F(50:400)));
[X,In]=max(abs(F(50:50+floor((Im+50)/2))));
[zz,tes]=max(abs(F(50:Im-1)));
if zz>=.8*Y
   Im=tes
   Y=zz
   end
% NUMBER OF BEATS IN EPISODE
num_beat = floor(Im+49-1)/16;
% could put if statement if num_beats is less than a specified amount
if (num_beat <= 5)
  badplus(plac)=episode;
  plac=plac+1;
  defect = 1;code = 1;I=0;samp_beat=0;
  break
end
% HEART RATE
RATE = (Im+49-1)*delf;
% NUMBER OF SAMPLES PER BEAT
samp_beat = ceil(60/(RATE*.005));
% GIVE SOME LEEWAY FOR LONGER/SHORTER BEATS
beat_expand = ceil(1.5*samp_beat);%changed from 1.25
% FIND DERIVATIVE
[b]=initfirdif(5,40,.005);
```

```
ha = [0 hamming(9)' 0];
b=b.*ha;
n = [0:1023];
Xnew = C(1)+((C(2)-C(1))/1023)*n;
Xnew = C-Xnew';
dC=filter(b,[1],Xnew);
dC=dC(6:1024);
[Ytrig]=max(dC);
[YtrigC]=max(C);
subplot(2,2,3);plot(dC);hold on;title('Filter');plot(C,'r');axis tight
% FIND FIRST BEAT STARTING LOCATION
IS = 10;fcode = 0;Yd=0;R=1;YdC=0;
while (YdC<.3*YtrigC)*(fcode == 0)
  while YdC<.3*YtrigC
                [Yd Id]=max(dC(IS:R*samp_beat+IS));
                [YdC IdC]=max(C(IS:R*samp_beat+IS));
    R=1.1*R;
  end
       Id=Id+IS-1;
       IdC=IdC+IS-1;
  Bfact=floor(.25*samp_beat);
  if(IdC-Bfact)>0
    [Yd Id]=max(dC(IdC-Bfact:IdC));
    Id=Id+IdC-Bfact-1;
    fcode=1;
  else IS=ceil(IS+.75*samp_beat);
  end
end
fcode=0;
while fcode==0
  if Id==1
                IS=ceil(IS+.75*samp_beat);
                [Yd Id]=max(dC(IS:samp_beat+IS));
                [YdC IdC]=max(C(IS:samp_beat+IS));
    Id=Id+IS-1;
    subplot(2,2,2);plot([Id:1024],C(Id:1024),'g-.');
  end
  if (dC(Id-1)>=0)&((dC(Id)>=dC(Id-1))|((dC(Id)<dC(Id-1))&(dC(Id-1)>.25*Yd)))
    Id=Id-1;
   else fcode=1;
  end
end
% I(1) = BEGINNING BEAT LOCATION
I(1)=Id;
while (C(I(1)+3)-C(I(1)))<.3
  I(1)=I(1)+1;
```

```
end
subplot(2,2,2);plot([I(1):1024],C(I(1):1024),'k');pause(.2);
nb=floor((1024-5-I(1))/samp_beat);
[l,maxC(1)]=max(C(1:samp_beat));
% FIND MAX(C) FOR EACH BEAT
for k=2:nb-1
  [Y , maxC(k)] = max(C(maxC(k-1)+ceil(.75*samp_beat):maxC(k-1)+ceil(beat_expand)));
  maxC(k)=maxC(k-1)+ceil(.75*samp_beat) +maxC(k)-1;
end
% find max dC for each beat starting at second beat
for m = 2:length(maxC)
  [Y, maxdC(m-1)]=max(dC(maxC(m)-30:maxC(m)+10));
  maxdC(m-1)=maxC(m)-30+maxdC(m-1)-1;
end
% FIND BEGINNING OF BEATS
for k=2:nb-1
   ib=I(k-1);
   ie=maxdC(k-1);
   I(k)=ie;
   while(dC(ie-1)>=0)&((dC(ie)>=dC(ie-1))|((dC(ie)<dC(ie-1))&(dC(ie-1)>.25*Yd)))
     ie=ie-1;
     I(k)=I(k)-1;
   end
end
len=length(I);
if (I(2)-I(1))<.75*samp_beat
  I=I(2:len);
end
if I(2) == I(1)
  I=I(2:len);
end
repa=zeros(1,ceil(2*samp_beat));
nrep=zeros(1,ceil(2*samp_beat));
for k=2:nb-2
  ib=I(k-1);ie=I(k)-1;
  nbeat=(ie-ib+1);
  anbeat=anbeat+nbeat;
  FB=fft(C(ib:ie));
  FA=FA+FB(1:11);
  subplot(2,2,4);plot(C(ib:ie));hold on;
  for m=1:ie-ib+1
    if ((ib+m-1)>1024) | (m>size(repa))
      code=1;defect = 1;code = 1;I=0;samp_beat=0;
      return
    end
       repa(m)=repa(m)+C(ib+m-1);
```

```
        nrep(m)=nrep(m)+1;
end
end
m=1;
while nrep(m)>0
  rep(m)=repa(m)/nrep(m);
  m=m+1;
end
% PLOT OF AVERAGE BEAT AND INDIVIDUAL BEATS
subplot(2,2,4);title('Avg Beat');plot(rep,'r');axis tight;hold on;pause(.1);
anbeat=round(anbeat/(nb-2));
FR=fft(rep,anbeat);
FER=FR(1:21);
FEE=[FER zeros(1,anbeat-41) conj(FER(21:-1:2))];
repaf=ifft(FEE);
repaf=real(repaf);
FA=FA/(nb-2);
FE=[FA.' zeros(1,anbeat-21) conj(FA(11:-1:2).')];
repf=ifft(FE);
t=.005*(0:anbeat-1);
```

Subroutine makechannelarray.m code

```
function [channel_array]=makechannelarray(max)
% CALLED FROM GETDATA SUBROUTINE
% Returns channel_array(max episode,18)
% FOR FUTURE REFERENCE
% LPAQ IS COLUMN 1
% PAQ  IS COLUMN 2
% SVCQ IS COLUMN 3
% IVCQ IS COLUMN 4
% AOP  IS COLUMN 5
% SVCP IS COLUMN 6
% IVCP IS COLUMN 7
% PAP  IS COLUMN 8
% LAP  IS COLUMN 9
% RAP  IS COLUMN 10
% AIRP IS COLUMN 11
% AIRQ IS COLUMN 12
% AOQ  IS COLUMN 13
% LVP IS COLUMN  14
% NOTHING IN COLUMNS 15-18
% import maximum episode in order to zero initial array
channel_array=zeros(max,18);
% GET VALUES IF ALL BUTTON IS PRESSED
H=findobj(gcf,'Tag','all1');
```

```
val1=get(H,'Value');
H=findobj(gcf,'Tag','all2');
val2=get(H,'Value');
H=findobj(gcf,'Tag','all3');
val3=get(H,'Value');
H=findobj(gcf,'Tag','all4');
val4=get(H,'Value');
H=findobj(gcf,'Tag','all5');
val5=get(H,'Value');
H=findobj(gcf,'Tag','all6');
val6=get(H,'Value');
H=findobj(gcf,'Tag','all7');
val7=get(H,'Value');
H=findobj(gcf,'Tag','all8');
val8=get(H,'Value');
H=findobj(gcf,'Tag','all9');
val9=get(H,'Value');
H=findobj(gcf,'Tag','all10');
val10=get(H,'Value');
H=findobj(gcf,'Tag','all11');
val11=get(H,'Value');
H=findobj(gcf,'Tag','all12');
val12=get(H,'Value');
H=findobj(gcf,'Tag','all13');
val13=get(H,'Value');
H=findobj(gcf,'Tag','all14');
val14=get(H,'Value');
H=findobj(gcf,'Tag','all15');
val15=get(H,'Value');
% LOOP TO LOAD ARRAY IF ALL EPISODES IS CHECKED
for i=1:15
  code = 0;
  j = num2str(i);
  x=strcat('val',j);
  num=eval(x);
  p=strcat('ch',j);
  h=findobj(gcf,'Tag',p);
  name=popupstr(h);
  if strcmp(name,'LPAQ') == 1
    colum = 1;
  elseif strcmp(name,'PAQ') == 1
    colum = 2;
  elseif strcmp(name,'SVCQ') == 1
    colum = 3;
  elseif strcmp(name,'IVCQ') == 1
    colum =4;
```

```
  elseif strcmp(name,'AOP') == 1
    colum = 5;
  elseif strcmp(name,'SVCP') == 1
    colum = 6;
  elseif strcmp(name,'IVCP') == 1
    colum = 7;
  elseif strcmp(name,'PAP') == 1
    colum = 8;
  elseif strcmp(name,'LAP') == 1
    colum = 9;
  elseif strcmp(name,'RAP') == 1
    colum = 10;
  elseif strcmp(name,'AIRP') == 1
    colum = 11;
  elseif strcmp(name,'AIRQ') == 1
    colum = 12;
  elseif strcmp(name,'AOQ') == 1
    colum = 13;
  elseif strcmp(name,'LVP') == 1
    colum = 14;
  elseif strcmp(name,'none') == 1
    code = 1;
  end
if code == 0
  if num == 1
    x=strcat('num',j,'1');
    h=findobj(gcf,'Tag',x);
    number=popupstr(h);
    number=str2num(number);
    channel_array(1:max,colum)=number;
  end

  if num == 0
    % get first channel number
    x=strcat('num',j,'1');
    h=findobj(gcf,'Tag',x);
    first_ch=popupstr(h);
    first_ch=str2num(first_ch);
    % get second channel number
    x=strcat('num',j,'2');
    h=findobj(gcf,'Tag',x);
    second_ch=popupstr(h);
    second_ch=str2num(second_ch)
    %if second_ch ~= 'none'
    %   second_ch=str2num(second_ch)
    %end
```

```
    % get first array
    x=strcat('arr',j,'1');
    h=findobj(gcf,'Tag',x);
    one_array=get(h,'String');
    one_array=str2num(one_array);
    % get second array
    x=strcat('arr',j,'2');
    h=findobj(gcf,'Tag',x);
    two_array=get(h,'String');
    two_array=str2num(two_array);
    len1=length(one_array);
    len2=length(two_array);
    for i = 1:2:len1-1
      channel_array(one_array(i):one_array(i+1),colum) = first_ch;
    end
    if second_ch ~= 'none'
      for i = 1:2:len2-1
        channel_array(two_array(i):two_array(i+1),colum) = second_ch;
      end
    end
  end
end
end
close('CHANNEL SPECIFICATION')
return
```

Subroutine multiple_channel.m code

```
function fig = multiple_channel_information()
%   multiple_channel_information
%
%   CALLED FROM getdata
%
%   GUI FOR ENTERING IN CHANNEL INFORMATION
%   NAME OF CHANNEL AND WHICH EPISODES RECORDED
%   CAN CHANGE UP TO 2 CHANNELS PER PARAMETER
%   FIGURE FOR GUI
h0 = figure('Color',[0 0 0.25], ...
          'MenuBar','none', ...
          'Name','CHANNEL SPECIFICATION', ...
          'NumberTitle','off', ...
          'PaperPosition',[18 180 576 432], ...
          'PaperUnits','points', ...
          'Position',[18 87 675 645], ...
          'Tag','mult_ch_fig', ...
          'ToolBar','none');
```

```
%   POPUP MENU FOR CHANNEL 1
h1 = uicontrol('Parent',h0, ...
        'Units','points', ...
        'BackgroundColor',[1 1 1], ...
        'FontName','Arial', ...
        'FontWeight','bold', ...
        'ForegroundColor',[1 0 0], ...
        'ListboxTop',0, ...
        'Position',[21 434.25 46 14], ...
        'String',{'none','AIRQ','LPAQ','PAQ','SVCQ','IVCQ','AOQ','AOP','SVCP','IVCP','PA
P','LAP','RAP','LVP','AIRP'}, ...
        'Style','popupmenu', ...
        'Tag','ch1', ...
        'Value',1);
```

To eliminate repetitive entries, do same for popup menu for channels 2 through 15

```
% 1ST ARRAY FOR CHANNEL 1
h1 = uicontrol('Parent',h0, ...
        'Units','points', ...
        'BackgroundColor',[1 1 1], ...
        'FontName','Arial', ...
        'FontWeight','bold', ...
        'ListboxTop',0, ...
        'Position',[183 437.25 120 13.5], ...
        'String','[0 0]', ...
        'Style','edit', ...
        'Tag','arr11');
```

To eliminate repetitive entries, do same for array for channels 2 through 15

```
% POPUP MENU FOR CHANNEL NUMBER -- 15,1
h1 = uicontrol('Parent',h0, ...
        'Units','points', ...
        'BackgroundColor',[1 1 1], ...
        'FontName','Arial', ...
        'FontWeight','bold', ...
        'ForegroundColor',[0 0 1], ...
        'ListboxTop',0, ...
        'Position',[130.5 40.5 37.5 12.75], ...
        'String',{'none','1','2','3','4','5','6','7','8','9','10','11','12','13','14','15','16'}, ...
        'Style','popupmenu', ...
        'Tag','num151', ...
        'Value',1);
```

To eliminate repetitive entries, do same for array for channels 2.1 through 15.1

```
% POPUP MENU FOR CHANNEL NUMBER -- 1,2
h1 = uicontrol('Parent',h0, ...
        'Units','points', ...
        'BackgroundColor',[1 1 1], ...
        'FontName','Arial', ...
```

```
        'FontWeight','bold', ...
        'ForegroundColor',[0 0 1], ...
        'ListboxTop',0, ...
        'Position',[314.25 437.25 37.5 13.5], ...
        'String',{'none','1','2','3','4','5','6','7','8','9','10','11','12','13','14','15','16'}, ...
        'Style','popupmenu', ...
        'Tag','num12', ...
        'Value',1);
```

To eliminate repetitive entries, do same for array for channels 2.2 through 15.2

```
%  2ND ARRAY FOR CHANNEL 15
h1 = uicontrol('Parent',h0, ...
        'Units','points', ...
        'BackgroundColor',[1 1 1], ...
        'FontName','Arial', ...
        'FontWeight','bold', ...
        'ListboxTop',0, ...
        'Position',[365.25 40.5 120 12.75], ...
        'String','[0 0]', ...
        'Style','edit', ...
        'Tag','arr152');
```

To eliminate repetitive entries, do same for array for channels 2 through 15

```
% ALL BUTTONS FOR CHANNELS 1-15
h1 = uicontrol('Parent',h0, ...
        'Units','points', ...
        'BackgroundColor',[0 0 0.25098], ...
        'Callback','allaction', ...
        'FontName','Arial', ...
        'ForegroundColor',[1 1 0], ...
        'ListboxTop',0, ...
        'Position',[84.75 435 30 13.5], ...
        'String','ALL', ...
        'Style','radiobutton', ...
        'Tag','all1');
```

Repeat for all buttons 2 through 15

```
%  TEXT "CHANNEL"
h1 = uicontrol('Parent',h0, ...
        'Units','points', ...
        'BackgroundColor',[0 0 0.25098], ...
        'FontName','Arial', ...
        'FontSize',10, ...
        'FontWeight','bold', ...
        'ForegroundColor',[0.9 0.9 0.9], ...
        'ListboxTop',0, ...
        'Position',[121 460 60 10], ...
        'String','CHANNEL', ...
        'Style','text', ...
```

```
        'Tag','StaticText1');
h1 = uicontrol('Parent',h0, ...
        'Units','points', ...
        'BackgroundColor',[0 0 0.25098], ...
        'FontName','Arial', ...
        'FontSize',10, ...
        'FontWeight','bold', ...
        'ForegroundColor',[0.9 0.9 0.9], ...
        'ListboxTop',0, ...
        'Position',[305 460 60 10], ...
        'String','CHANNEL', ...
        'Style','text', ...
        'Tag','StaticText2');
% TEXT "[From To]
h1 = uicontrol('Parent',h0, ...
        'Units','points', ...
        'BackgroundColor',[0 0 0.25098], ...
        'FontName','Arial', ...
        'FontSize',10, ...
        'FontWeight','bold', ...
        'ForegroundColor',[0.9 0.9 0.9], ...
        'ListboxTop',0, ...
        'Position',[217 460 65 10], ...
        'String','[ From    To ]', ...
        'Style','text', ...
        'Tag','StaticText2');
h1 = uicontrol('Parent',h0, ...
        'Units','points', ...
        'BackgroundColor',[0 0 0.25098], ...
        'FontName','Arial', ...
        'FontSize',10, ...
        'FontWeight','bold', ...
        'ForegroundColor',[0.9 0.9 0.9], ...
        'ListboxTop',0, ...
        'Position',[395 460 65 10], ...
        'String','[ From    To ]', ...
        'Style','text', ...
        'Tag','StaticText2');
% TEXT "PARAMETER"
h1 = uicontrol('Parent',h0, ...
        'Units','points', ...
        'BackgroundColor',[0 0 0.25098], ...
        'FontName','Arial', ...
        'FontSize',10, ...
        'FontWeight','bold', ...
        'ForegroundColor',[0.9 0.9 0.9], ...
```

```
        'ListboxTop',0, ...
        'Position',[16 460 60 10], ...
        'String','PARAMETER', ...
        'Style','text', ...
        'Tag','StaticText1');
h1 = uicontrol('Parent',h0, ...
        'Units','points', ...
        'BackgroundColor',[0 0 0.25098], ...
        'Callback','allaction', ...
        'FontName','Arial', ...
        'ForegroundColor',[1 1 0], ...
        'ListboxTop',0, ...
        'Position',[84.75 36 30 13.5], ...
        'String','ALL', ...
        'Style','radiobutton', ...
        'Tag','all15');
h1 = uicontrol('Parent',h0, ...
        'Units','points', ...
        'BackgroundColor',[0 0 0.25098], ...
        'Callback','allaction', ...
        'FontName','Arial', ...
        'ForegroundColor',[1 1 0], ...
        'ListboxTop',0, ...
        'Position',[84.75 64.5 30 13.5], ...
        'String','ALL', ...
        'Style','radiobutton', ...
        'Tag','all14');
h1 = uicontrol('Parent',h0, ...
        'Units','points', ...
        'BackgroundColor',[0 0 0.25098], ...
        'Callback','allaction', ...
        'FontName','Arial', ...
        'ForegroundColor',[1 1 0], ...
        'ListboxTop',0, ...
        'Position',[84.75 93 30 13.5], ...
        'String','ALL', ...
        'Style','radiobutton', ...
        'Tag','all13');
% PUSHBUTTON -- FINISHED
h1 = uicontrol('Parent',h0, ...
        'Units','points', ...
        'BackgroundColor',[0.75 0.75 0.75], ...
        'Callback','h=findobj(gcf,"Tag", "Pushbutton1");set(h,"String","Wait");', ...
        'FontName','Arial', ...
        'ListboxTop',0, ...
        'Position',[152.25 10.5 69 13.5], ...
```

```
        'String','<< Finished >>', ...
        'Tag','Pushbutton1');
% HELP FOR GUI
h1 = uicontrol('Parent',h0, ...
        'Units','points', ...
        'Callback','chanhelp', ...
        'FontName','Arial', ...
        'ListboxTop',0, ...
        'Position',[285 10.5 69 13.5], ...
        'String','<< Help >>', ...
        'Tag','ch_help');
if nargout > 0, fig = h0; end
```

Subroutine initfirdif.m code

```
function [b]=initfirdif(N,f,T);
mid=N+1;
top=2*N+1;
wc=2*pi*f*T;
for i=1:N
        index=i-1;
   arg=wc*(index-mid);
        b(i)=(arg*cos(arg)-sin(arg))/(pi*(index-mid)^2*T);
        b(top+1-i)=-b(i);
end;
b(mid)=0.0;
return
```

APPENDIX VI:

DATA EXAMINATION GUI

The following is the Matlab™ source code for the GUI dataview.m to examine the hemodynamic variable data files for the lamb experiments. Following the GUI source code, necessary callback subroutine codes are included.

dataview code

```
function dataview()
% Copyright (C) 2006, Mark E. Ketner
% University of North Carolina at Chapel Hill, Department of Biomedical Engineering
% This software may be used, copied, or redistributed as long as it is not sold and this
% copyright notice is reproduced on each copy.  This program is provided as is without any
% implied warranties.
%
% If referenced, please send a copy to
% Mark Ketner
% Department of Biomedical Engineering
% University of North Carolina
% Campus Box 7575
% Chapel Hill, NC 27599
% E-mail:  mketner@bme.unc.edu
% Main GUI for Lamb Data Examination
% usage:  dataview
clc
close all
% Figure Window Information
a = figure('Color',[0 0 0], ...
        'MenuBar','none', ...
        'Name','PLOT MENU', ...
        'NumberTitle','off', ...
        'Position',[10 405 186 300], ...
        'Tag','plot_menu');
% One Channel Button
b = uicontrol('Parent',a, ...
        'Units','points', ...
        'Callback','OneChannel', ...
   'FontSize',10, ...
```

```
  'FontWeight','bold',...
          'Position',[9 157 125.25 25.5], ...
          'String','ONE CHANNEL', ...
          'Tag','Option1');
% Two Channel Button
b = uicontrol('Parent',a, ...
  'Units','points', ...
  'Callback','TwoChannels',...
  'FontSize',10, ...
  'FontWeight','bold',...
          'Position',[9 122.5 125.25 24.75], ...
          'String','TWO CHANNELS', ...
          'Tag','Option2');
% Multiple Channels Button
b = uicontrol('Parent',a, ...
  'Units','points', ...
  'Callback','MultChannels',...
  'FontSize',10, ...
  'FontWeight','bold',...
          'Position',[9 87.25 125.25 24.75], ...
          'String','MULTIPLE CHANNELS', ...
          'Tag','Option3');
% Make Movie Button
b = uicontrol('Parent',a, ...
          'Units','points', ...
  'FontSize',10, ...
  'FontWeight','bold',...
  'Callback','moviegui',...
          'Position',[7.5 51.5 125.25 24.75], ...
          'String','MAKE MOVIE', ...
          'Tag','Option6');
% Help Button
b = uicontrol('Parent',a, ...
          'Units','points', ...
          'Callback','dataviewhelp', ...
  'FontName','Helvetica', ...
  'ForegroundColor',[1 1 0],...
  'FontSize',10, ...
  'FontWeight','bold',...
          'Position',[9.75 10.5 49.5 25.5], ...
          'String','HELP', ...
          'Tag','help_button');
% Close Button
b = uicontrol('Parent',a, ...
          'Units','points', ...
          'Callback','close all,return', ...
  'FontName','Helvetica', ...
  'ForegroundColor',[1 0 0],...
  'FontSize',10, ...
  'FontWeight','bold',...
          'Position',[80.25 11.25 50.25 25.5], ...
```

```
        'String','CLOSE', ...
        'Tag','close_button');
% Text -- Plot Options
b = uicontrol('Parent',a, ...
        'Units','points', ...
        'BackgroundColor',[0 0 0], ...
        'FontName','Avant Garde', ...
        'FontSize',14, ...
        'FontWeight','bold', ...
        'ForegroundColor',[1 1 1], ...
        'Position',[18 193 103.5 19.5], ...
        'String','PLOT OPTIONS', ...
        'Style','text', ...
        'Tag','StaticText1');
```

Subroutine OneChannel.m code

```
function fig = OneChannel()
% GUI for Plot One Channel
% Callback from DataView
% FIGURE INFORMATION
h0 = figure('Color',[0 0 0], ...
        'MenuBar','none', ...
        'Name','PLOT ONE CHANNEL', ...
        'NumberTitle','off', ...
        'PaperPosition',[18 180 576 432], ...
        'PaperUnits','points', ...
        'Position',[10 210 272 515], ...
        'Tag','Opt1', ...
        'ToolBar','none');
% EXPERIMENT INFORMATION
h1 = uicontrol('Parent',h0, ...
        'Units','points', ...
        'BackgroundColor',[1 1 1], ...
        'FontWeight','bold', ...
        'ForegroundColor',[1 0 0], ...
        'ListboxTop',0, ...
        'Position',[125.25 351 51.75 15], ...
        'String',{'none'}, ...
        'Style','edit', ...
        'Tag','experiment', ...
        'Value',1);
% DISPLAY OPTION -- AVERAGE OR EPISODE
h1 = uicontrol('Parent',h0, ...
        'Units','points', ...
        'BackgroundColor',[1 1 1], ...
        'FontName','Avant Garde', ...
        'FontWeight','bold', ...
        'ForegroundColor',[1 0 0], ...
        'ListboxTop',0, ...
```

```
        'Position',[125.25 294.75 51.75 18], ...
        'String',{'Average','Episode'}, ...
        'Style','popupmenu', ...
        'Tag','matordat', ...
        'Value',1);
% CHANNEL OPTION POPUP MENU
h1 = uicontrol('Parent',h0, ...
        'Units','points', ...
        'BackgroundColor',[1 1 1], ...
        'FontName','Avant Garde', ...
        'FontWeight','bold', ...
        'ForegroundColor',[1 0 0], ...
        'ListboxTop',0, ...
        'Position',[125.25 323.25 51.75 18], ...
        'String',{'LPAQ','PAQ','SVCQ','IVCQ','AOP','SVCP','IVCP','PAP','LAP','RAP','AIRP','AIRQ'
,'AOQ','LVP','PVP','MISC'}, ...
        'Style','popupmenu', ...
        'Tag','channel', ...
        'Value',1);
% TEXT EDIT FOR GRAPH TITLE
h1 = uicontrol('Parent',h0, ...
        'Units','points', ...
        'BackgroundColor',[1 1 1], ...
        'ForegroundColor',[0 0 1], ...
        'ListboxTop',0, ...
        'Position',[21.75 179.25 150 15], ...
        'String','Place Graph Title Here', ...
        'Style','edit', ...
        'Tag','graphtitle');
% TEXT EDIT FOR BEGINNING EPISODE
h1 = uicontrol('Parent',h0, ...
        'Units','points', ...
        'BackgroundColor',[1 1 1], ...
        'ListboxTop',0, ...
        'Position',[135.75 258 30 15], ...
        'String','1', ...
        'Style','edit', ...
        'Tag','epbegin');
% TEXT EDIT FOR END EPISODE
h1 = uicontrol('Parent',h0, ...
        'Units','points', ...
        'BackgroundColor',[1 1 1], ...
        'ListboxTop',0, ...
        'Position',[135.75 228 30 15], ...
        'String','5', ...
        'Style','edit', ...
        'Tag','epend');
% CLOSE BUTTON
h1 = uicontrol('Parent',h0, ...
        'Units','points', ...
        'Callback','figure(3);close(3);close(gcbf);return', ...
```

```
        'FontWeight','bold', ...
        'ForegroundColor',[1 0 0], ...
        'ListboxTop',0, ...
        'Position',[53.25 21.75 84.75 25.5], ...
        'String','CLOSE', ...
        'Tag','close_button');
% CURRENT EPISODE
h1 = uicontrol('Parent',h0, ...
        'Units','points', ...
        'BackgroundColor',[1 1 1], ...
        'ListboxTop',0, ...
        'Position',[161.25 50.25 30 10.5], ...
        'String','0', ...
        'Style','text', ...
        'Tag','currentep', ...
        'Visible','off');
% TEXT 'EXPERIMENT'
h1 = uicontrol('Parent',h0, ...
        'Units','points', ...
        'BackgroundColor',[0 0 0], ...
        'FontSize',10, ...
        'FontWeight','bold', ...
        'ForegroundColor',[1 1 1], ...
        'ListboxTop',0, ...
        'Position',[28.5 352.5 66 13.5], ...
        'String','Experiment', ...
        'Style','text', ...
        'Tag','StaticText1');
% TEXT 'WAVEFORM TYPE'
h1 = uicontrol('Parent',h0, ...
        'Units','points', ...
        'BackgroundColor',[0 0 0], ...
        'FontSize',10, ...
        'FontWeight','bold', ...
        'ForegroundColor',[1 1 1], ...
        'ListboxTop',0, ...
        'Position',[15.75 298.5 92.25 11.25], ...
        'String','Waveform Type', ...
        'Style','text', ...
        'Tag','StaticText2');
% TEXT 'CHANNEL'
h1 = uicontrol('Parent',h0, ...
        'Units','points', ...
        'BackgroundColor',[0 0 0], ...
        'FontSize',10, ...
        'FontWeight','bold', ...
        'ForegroundColor',[1 1 1], ...
        'ListboxTop',0, ...
        'Position',[36 324.75 51.75 12.75], ...
        'String','Channel', ...
        'Style','text', ...
```

```
        'Tag','StaticText3');
% TEXT 'BEGINNING EPISODE'
h1 = uicontrol('Parent',h0, ...
        'Units','points', ...
        'BackgroundColor',[0 0 0], ...
        'FontSize',10, ...
        'FontWeight','bold', ...
        'ForegroundColor',[1 1 1], ...
        'ListboxTop',0, ...
        'Position',[13.5 257.25 102.75 12.75], ...
        'String','Beginning Episode', ...
        'Style','text', ...
        'Tag','StaticText4');
% TEXT 'ENDING EPISODE'
h1 = uicontrol('Parent',h0, ...
        'Units','points', ...
        'BackgroundColor',[0 0 0], ...
        'FontSize',10, ...
        'FontWeight','bold', ...
        'ForegroundColor',[1 1 1], ...
        'ListboxTop',0, ...
        'Position',[19.5 228.75 90 13.5], ...
        'String','Ending Episode', ...
        'Style','text', ...
        'Tag','StaticText5');
% TEXT 'CURRENT EPISODE'
h1 = uicontrol('Parent',h0, ...
        'Units','points', ...
        'BackgroundColor',[0.8 0.8 0.8], ...
        'ListboxTop',0, ...
        'Position',[156.75 62.25 37.5 22.5], ...
        'String','Current Episode', ...
        'Style','text', ...
        'Tag','currentep_text', ...
        'Visible','off');
% TEXT 'TITLE'
h1 = uicontrol('Parent',h0, ...
        'Units','points', ...
        'BackgroundColor',[0 0 0], ...
        'FontWeight','bold', ...
        'ForegroundColor',[1 1 1], ...
        'ListboxTop',0, ...
        'Position',[81.75 198 33 11.25], ...
        'String','Title', ...
        'Style','text', ...
        'Tag','StaticText7');
% PLOT BUTTON
h1 = uicontrol('Parent',h0, ...
        'Units','points', ...
        'Callback','plot1channel', ...
        'FontWeight','bold', ...
```

```
        'ForegroundColor',[0 0 1], ...
        'ListboxTop',0, ...
        'Position',[53.25 60 84.75 25.5], ...
        'String','PLOT', ...
        'Tag','plot_button');
% TEXT 'X AXIX LABEL'
h1 = uicontrol('Parent',h0, ...
        'Units','points', ...
        'BackgroundColor',[0 0 0], ...
        'FontWeight','bold', ...
        'ForegroundColor',[1 1 1], ...
        'ListboxTop',0, ...
        'Position',[66.75 162.75 63.75 11.25], ...
        'String','X Axis Label', ...
        'Style','text', ...
        'Tag','StaticText8');
% TEXT 'Y AXIS LABEL'
h1 = uicontrol('Parent',h0, ...
        'Units','points', ...
        'BackgroundColor',[0 0 0], ...
        'FontWeight','bold', ...
        'ForegroundColor',[1 1 1], ...
        'ListboxTop',0, ...
        'Position',[66 129.75 65.25 11.25], ...
        'String','Y Axis Label', ...
        'Style','text', ...
        'Tag','StaticText9');
% TEXT EDIT FOR X AXIS
h1 = uicontrol('Parent',h0, ...
        'Units','points', ...
        'BackgroundColor',[1 1 1], ...
        'ForegroundColor',[0 0 1], ...
        'ListboxTop',0, ...
        'Position',[58.5 147 75 14], ...
        'Style','edit', ...
        'Tag','xaxis_label');
% TEXT EDIT FOR Y AXIS
h1 = uicontrol('Parent',h0, ...
        'Units','points', ...
        'BackgroundColor',[1 1 1], ...
        'ForegroundColor',[0 0 1], ...
        'ListboxTop',0, ...
        'Position',[59.25 114.75 75 14], ...
        'Style','edit', ...
        'Tag','yaxis_label');
h1 = uicontrol('Parent',h0, ...
        'Units','points', ...
        'BackgroundColor',[0 0 0], ...
        'FontWeight','bold', ...
        'ForegroundColor',[1 1 0], ...
        'ListboxTop',0, ...
```

```
        'Position',[6 216.75 190.5 7.5], ...
        'String','-------------------------------------------------------------', ...
        'Style','text', ...
        'Tag','StaticText10');
h1 = uicontrol('Parent',h0, ...
        'Units','points', ...
        'BackgroundColor',[0 0 0], ...
        'FontWeight','bold', ...
        'ForegroundColor',[1 1 0], ...
        'ListboxTop',0, ...
        'Position',[4.5 104.25 190.5 7.5], ...
        'String','-------------------------------------------------------------', ...
        'Style','text', ...
        'Tag','StaticText10');
h1 = uicontrol('Parent',h0, ...
        'Units','points', ...
        'BackgroundColor',[0 0 0], ...
        'FontWeight','bold', ...
        'ForegroundColor',[1 1 0], ...
        'ListboxTop',0, ...
        'Position',[6 283.5 190.5 7.5], ...
        'String','-------------------------------------------------------------', ...
        'Style','text', ...
        'Tag','StaticText10');
% RADIO BUTTON FOR MULTIPLE PLOTS
h1 = uicontrol('Parent',h0, ...
        'Units','points', ...
        'BackgroundColor',[0 0 0], ...
        'FontName','Avant Garde', ...
        'FontSize',7, ...
        'ForegroundColor',[1 1 1], ...
        'ListboxTop',0, ...
        'Position',[45 4 120 15], ...
        'String','Multiple Plots For Averages', ...
        'Style','radiobutton', ...
        'Tag','multplot');
if nargout > 0, fig = h0; end
```

Subroutine plot1channel.m code

```
function plot1channel
% SUBROUTINE TO PLOT ONE CHANNEL OF LAMB DATA
% PLOTS EITHER AVERAGE OR EPISODE - WAVEFORM TYPE
% PLOTS ANY CHANNEL
% CALLBACK FROM OneChannel
% APRIL 10, 2006
% GET EXPERIMENT NAME
h=findobj(gcbf,'Tag','experiment');
experiment=popupstr(h);
% GET CHANNEL
h=findobj(gcbf,'Tag','channel');
```

```
channel=popupstr(h);
% GET WAVEFORM TYPE (Episode or Average)
h=findobj(gcbf,'Tag','matordat');
wave_type=popupstr(h);
% GET BEGINNING EPISODE
h=findobj(gcbf,'Tag','epbegin');
epbegin=get(h,'String');
epbegin=str2num(epbegin);
% GET ENDING EPISODE
h=findobj(gcbf,'Tag','epend');
epend=get(h,'String');
epend=str2num(epend);
% GET GRAPH TITLE
h=findobj(gcbf,'Tag','graphtitle');
graph_title=get(h,'String');
% GET GRAPH X AXIS LABEL
h=findobj(gcbf,'Tag','xaxis_label');
xaxis_label=get(h,'String');
% GET GRAPH Y AXIS LABEL
h=findobj(gcbf,'Tag','yaxis_label');
yaxis_label=get(h,'String');
% GET MULT PLOT FOR AVERAGES
mult=findobj(gcbf,'Tag','multplot');
mult_plot=get(h,'Value');
% LOAD INFO FILE HERE
temp=strcat(experiment,'info.mat');
temp=strrep(temp,'l',' l');
temp=strcat('load',temp);
eval(temp);
eval('charray=info.chnumb;')
% DETERMINE WHICH COLUMN OF CHARRAY TO USE
if strcmp(channel,'LPAQ') == 1
   channel = 1;
elseif strcmp(channel,'PAQ') == 1
   channel = 2;
elseif strcmp(channel,'SVCQ') == 1
   channel = 3;
elseif strcmp(channel,'IVCQ') == 1
   channel = 4;
elseif strcmp(channel,'AOP') == 1
   channel = 5;
elseif strcmp(channel,'SVCP') == 1
   channel = 6;
elseif strcmp(channel,'IVCP') == 1
   channel = 7;
elseif strcmp(channel,'PAP') == 1
   channel = 8;
elseif strcmp(channel,'LAP') == 1
   channel = 9;
elseif strcmp(channel,'RAP') == 1
   channel = 10;
```

```
elseif strcmp(channel,'AIRP') == 1
   channel = 11;
elseif strcmp(channel,'AIRQ') == 1
   channel = 12;
elseif strcmp(channel,'AOQ') == 1
   channel = 13;
elseif strcmp(channel,'LVP') == 1
   channel = 14;
elseif strcmp(channel,'PVP') == 1
   channel = 15;
elseif strcmp(channel,'MISC') == 1
   channel = 16;
end
s=([1:1800]');
% FOR EPISODE PLOT
if wave_type == 'Episode'
   set(mult,'Visible','off');
   curep=findobj(gcbf,'Tag','currentep');
   set(curep,'Visible','on');
   cureptext=findobj(gcbf,'Tag','currentep_text');
   set(cureptext,'Visible','on');
   if epend < epbegin
      x={'Ending Episode is Greater Than'
         'Beginning Episode'
         ' '
         'Please Try Again'};
      j=errordlg(x,'Episode Error');
      pause(3)
      close(j)
      return
   end
   for j=epbegin:epend
      %pause(.3)
      g=s(j,1);
      E=g;
      g=int2str(g);
      V=strcat(experiment,g,'.dat');
      X=exist(V,'file');
      U=strcat(experiment,g);
      set(curep,'String',g);
      if X > 0
         V=strrep(V,'l',' l');
         W=strcat('load',V);
         eval(W);
         s5=strcat('Epi=',U,';');
         eval(s5);
         ch1=charray(j,channel);
         if ch1 <= 0
            mesg={'Channel NOT meaured'
               'for this experiment. '
               ' '
```

```
            'Please try a different channel'};
          J=errordlg(mesg,'NO CHANNEL');
          pause(2)
          close(J)
          return
        end
        C1=Epi(:,ch1);
        t1=strcat(graph_title,' for Episode ',g);
        plo=figure(3);
        set(plo,'Position',[300 210 650 465]);
        set(plo,'Name','PLOT ONE CHANNEL');
        set(plo,'NumberTitle','off');
        clf
        axis tight
        plot(C1,'r');hold on;title(t1);xlabel(xaxis_label);ylabel(yaxis_label);
      end
      pause(.5)
    end
    set(curep,'Visible','off');
    set(cureptext,'Visible','off');
    set(mult,'Visible','on');
end
% FOR AVERAGE PLOT
if wave_type == 'Average'
    figure(2)
    multplot=findobj('Tag','multplot');
    mult_plot=get(multplot,'Value');
    if mult_plot ~=1
      plo=figure(3);
      set(plo,'Color',[1 1 1]);
      clf;
    end
    plo=figure(3);
    set(plo,'Color',[1 1 1]);
    % if want to plot multiple episodes on same plot
    % comment clf
    if mult_plot ~= 1
      clf
    end
    if epend < epbegin
      x={'Ending Episode is Greater Than'
        'Beginning Episode'
        ' '
        'Please Try Again'};
      j=errordlg(x,'Episode Error');
      pause(2)
      close(j)
      return
    end
    x=[];
    tags='ABCDEFGHIJKLMNOPQRSTUVWXY';
```

```
num=ceil(epend/50);
tags=tags(1:num);
for k=1:num
   f3=strcat(experiment,tags(k),'.mat;')
   f4=strrep(f3,'l',' l');
   f3;
   X=exist(strcat(experiment,tags(k),'.mat'),'file');
   if X > 0
      s8=strcat('load',f4);
      eval(s8);
   end
end
cray=['r- ';'r: ';'r-.';'r--';...
      'b- ';'b: ';'b-.';'b--';...
      'g- ';'g: ';'g-.';'g--';...
      'c- ';'c: ';'c-.';'c--';...
      'y- ';'y: ';'y-.';'y--';...
      'm- ';'m: ';'m-.';'m--';...
      'k- ';'k: ';'k-.';'k--'];
ck=0;
for k=epbegin:epend
   j=int2str(k);
   k=k;
   if (k>0 & k<=50) EpifftfA;kk=k;
   elseif (k>50 & k<=100) EpifftfB;kk=k-50;
   elseif (k>100 & k<=150) EpifftfC;kk=k-100;
   elseif (k>150 & k<=200) EpifftfD;kk=k-150;
   elseif (k>200 & k<=250) EpifftfE;kk=k-200;
   elseif (k>250 & k<=300) EpifftfF;kk=k-250;
   elseif (k>300 & k<=350) EpifftfG;kk=k-300;
   elseif (k>350 & k<=400) EpifftfH;kk=k-350;
   elseif (k>400 & k<=450) EpifftfI;kk=k-400;
   elseif (k>450 & k<=500) EpifftfJ;kk=k-450;
   elseif (k>500 & k<=550) EpifftfK;kk=k-500;
   elseif (k>550 & k<=600) EpifftfL;kk=k-550;
   elseif (k>600 & k<=650) EpifftfM;kk=k-600;
   elseif (k>650) stop
   end
   kk=kk;
   t=.005*[0:1000];
   ch1=charray(k,channel);
   if ch1 <= 0
      mesg={'Channel NOT meaured'
         'for this experiment. '
         ' '
         'Please try a different channel'};
      J=errordlg(mesg,'NO CHANNEL');
      pause(3)
      close(J)
      return
   end
```

```
      f=Epifftf(kk,:,ch1);
      fn=f(1);
      if f(1)>0
         C=freconstruct(f);
         C=[C];
         x(k)=mean(C);
         ckk=ck-28*floor(ck/28)+1;
         set(plo,'Position',[300 210 650 465]);
         set(plo,'Name','PLOT ONE CHANNEL AVERAGE');
         set(plo,'NumberTitle','off');
         hold on;plot(t(1:length(C)),C,cray(ckk,:));hold
on;title(graph_title);xlabel(xaxis_label);ylabel(yaxis_label);
         ck=ck+1;
         pause(.8)
      end
   end
end
```

Subroutine freconstruct.m code

```
function C=freconstruct(f)
% function C=freconstruct(f)
% C is reconstruction of single waveform based on N and 20 harmonics
N=f(1);
fe=[f(2:22) zeros(1,N-41) conj(f(22:-1:3))];
C=real(ifft(fe));
```

Subroutine TwoChannels.m code

This code is similar to OneChannel.m. Therefore, this code was omitted.

Subroutine MultChannels.m code

```
function fig = MultChannels()
% GUI for Plotting Multiple Channels
% Callback from DataView
%
% APRIL 10, 2004
% FIGURE INFORMATION
h0 = figure('Color',[0 0 0], ...
          'MenuBar','none', ...
          'Name','MULTIPLE CHANNELS', ...
          'NumberTitle','off', ...
          'PaperPosition',[18 180 576 432], ...
          'PaperUnits','points', ...
          'Position',[10 185 271 541], ...
          'Tag','Opt3', ...
          'ToolBar','none');
% TEXT EDIT FOR EXPERIMENT
h1 = uicontrol('Parent',h0, ...
```

```
        'Units','points', ...
        'BackgroundColor',[1 1 1], ...
        'FontWeight','bold', ...
        'ForegroundColor',[1 0 0], ...
        'ListboxTop',0, ...
        'Position',[120 370.5 51.75 15], ...
        'String','none', ...
        'Style','edit', ...
        'Tag','experiment', ...
        'Value',1);
% POPUP MENU FOR WAVEFORM TYPE -- AVERAGE OR EPISODE
h1 = uicontrol('Parent',h0, ...
        'Units','points', ...
        'BackgroundColor',[1 1 1], ...
        'FontName','Avant Garde', ...
        'ForegroundColor',[1 0 0], ...
        'ListboxTop',0, ...
        'Position',[120.75 363.75 51.75 18], ...
        'String',{'Average','Episode'}, ...
        'Style','popupmenu', ...
        'Tag','matordat', ...
        'Value',2, ...
        'Visible','off');
% TEXT EDIT FOR GRAPH TITLE
h1 = uicontrol('Parent',h0, ...
        'Units','points', ...
        'BackgroundColor',[1 1 1], ...
        'ForegroundColor',[0 0 1], ...
        'ListboxTop',0, ...
        'Position',[79.5 225 99.75 15], ...
        'String','Place Graph Title Here', ...
        'Style','edit', ...
        'Tag','graphtitle');
% TEXT EDIT FOR BEGINNING EPISODE
h1 = uicontrol('Parent',h0, ...
        'Units','points', ...
        'BackgroundColor',[1 1 1], ...
        'ListboxTop',0, ...
        'Position',[147 136.25 30 15], ...
        'String','1', ...
        'Style','edit', ...
        'Tag','epbegin');
% TEXT EDIT FOR ENDING EPISODE
h1 = uicontrol('Parent',h0, ...
        'Units','points', ...
        'BackgroundColor',[1 1 1], ...
        'ListboxTop',0, ...
        'Position',[147 105.5 30 15], ...
        'String','5', ...
        'Style','edit', ...
        'Tag','epend');
```

```
% CLOSE BUTTON
h1 = uicontrol('Parent',h0, ...
        'Units','points', ...
        'BackgroundColor',[0.75 0.75 0.75], ...
        'Callback','figure(3);close(3);close(gcbf);return', ...
        'FontWeight','bold', ...
        'ForegroundColor',[1 0 0], ...
        'ListboxTop',0, ...
        'Position',[54 21.75 84.75 25.5], ...
        'String','CLOSE', ...
        'Tag','close_button');
% TEXT 'CURRENT EPISODE'
h1 = uicontrol('Parent',h0, ...
        'Units','points', ...
        'BackgroundColor',[1 1 1], ...
        'ListboxTop',0, ...
        'Position',[163.5 36.75 30 10.5], ...
        'String','1', ...
        'Style','text', ...
        'Tag','currentep', ...
        'Visible','off');
% TEXT 'EXPERIMENT'
h1 = uicontrol('Parent',h0, ...
        'Units','points', ...
        'BackgroundColor',[0 0 0], ...
        'FontSize',10, ...
        'FontWeight','bold', ...
        'ForegroundColor',[1 1 1], ...
        'ListboxTop',0, ...
        'Position',[29.25 374.25 66 13.5], ...
        'String','Experiment', ...
        'Style','text', ...
        'Tag','StaticText1');
% TEXT 'BEGINNING EPISODE'
h1 = uicontrol('Parent',h0, ...
        'Units','points', ...
        'BackgroundColor',[0 0 0], ...
        'FontSize',10, ...
        'FontWeight','bold', ...
        'ForegroundColor',[1 1 1], ...
        'ListboxTop',0, ...
        'Position',[15.75 137.5 102.75 12.75], ...
        'String','Beginning Episode', ...
        'Style','text', ...
        'Tag','StaticText4');
% TEXT 'ENDING EPISODE'
h1 = uicontrol('Parent',h0, ...
        'Units','points', ...
        'BackgroundColor',[0 0 0], ...
        'FontSize',10, ...
        'FontWeight','bold', ...
```

```
            'ForegroundColor',[1 1 1], ...
            'ListboxTop',0, ...
            'Position',[22.125 107 90 13.5], ...
            'String','Ending Episode', ...
            'Style','text', ...
            'Tag','StaticText5');
h1 = uicontrol('Parent',h0, ...
            'Units','points', ...
            'BackgroundColor',[0 0 0], ...
            'ForegroundColor',[1 1 1], ...
            'ListboxTop',0, ...
            'Position',[159 48.75 37.5 22.5], ...
            'String','Current Episode', ...
            'Style','text', ...
            'Tag','currentep_text', ...
            'Visible','off');
% TEXT 'TITLE'
h1 = uicontrol('Parent',h0, ...
            'Units','points', ...
            'BackgroundColor',[0 0 0], ...
            'FontWeight','bold', ...
            'ForegroundColor',[1 1 1], ...
            'ListboxTop',0, ...
            'Position',[30 222.75 35.25 11.25], ...
            'String','Title', ...
            'Style','text', ...
            'Tag','StaticText7');
% PLOT BUTTON
h1 = uicontrol('Parent',h0, ...
            'Units','points', ...
            'BackgroundColor',[0.75 0.75 0.75], ...
            'Callback','plotmultchannels', ...
            'FontWeight','bold', ...
            'ForegroundColor',[0 0 1], ...
            'ListboxTop',0, ...
            'Position',[54 53.75 84.75 25.5], ...
            'String','PLOT', ...
            'Tag','plot_button');
% TEXT 'X AXIS LABEL'
h1 = uicontrol('Parent',h0, ...
            'Units','points', ...
            'BackgroundColor',[0 0 0], ...
            'FontWeight','bold', ...
            'ForegroundColor',[1 1 1], ...
            'ListboxTop',0, ...
            'Position',[15.75 203.25 63.75 11.25], ...
            'String','X Axis Label', ...
            'Style','text', ...
            'Tag','StaticText8');
% TEXT 'Y AXIS LABEL'
h1 = uicontrol('Parent',h0, ...
```

```
            'Units','points', ...
            'BackgroundColor',[0 0 0], ...
            'FontWeight','bold', ...
            'ForegroundColor',[1 1 1], ...
            'ListboxTop',0, ...
            'Position',[18 181.5 65.25 11.25], ...
            'String','Y Axis Label', ...
            'Style','text', ...
            'Tag','StaticText9');
% TEXT EDIT FOR X AXIS
h1 = uicontrol('Parent',h0, ...
            'Units','points', ...
            'BackgroundColor',[1 1 1], ...
            'ForegroundColor',[0 0 1], ...
            'ListboxTop',0, ...
            'Position',[91.875 204.75 75 14.25], ...
            'Style','edit', ...
            'Tag','xaxis_label');
% TEXT EDIT FOR Y AXIS
h1 = uicontrol('Parent',h0, ...
            'Units','points', ...
            'BackgroundColor',[1 1 1], ...
            'ForegroundColor',[0 0 1], ...
            'ListboxTop',0, ...
            'Position',[91.875 181.5 75 14.25], ...
            'Style','edit', ...
            'Tag','yaxis_label');
h1 = uicontrol('Parent',h0, ...
            'Units','points', ...
            'BackgroundColor',[0 0 0], ...
            'FontWeight','bold', ...
            'ForegroundColor',[1 1 0], ...
            'ListboxTop',0, ...
            'Position',[5.25 352.5 190.5 7.5], ...
            'String','------------------------------------------------------------', ...
            'Style','text', ...
            'Tag','StaticText10');
h1 = uicontrol('Parent',h0, ...
            'Units','points', ...
            'BackgroundColor',[0 0 0], ...
            'FontWeight','bold', ...
            'ForegroundColor',[1 1 0], ...
            'ListboxTop',0, ...
            'Position',[5.625 93.5 190.5 7.5], ...
            'String','------------------------------------------------------------', ...
            'Style','text', ...
            'Tag','StaticText10');
h1 = uicontrol('Parent',h0, ...
            'Units','points', ...
            'BackgroundColor',[0 0 0], ...
            'FontWeight','bold', ...
```

```
        'ForegroundColor',[1 1 0], ...
        'ListboxTop',0, ...
        'Position',[6.75 247.5 190.5 7.5], ...
        'String','-------------------------------------------------------------', ...
        'Style','text', ...
        'Tag','StaticText10');
h1 = uicontrol('Parent',h0, ...
        'Units','points', ...
        'BackgroundColor',[0 0 0], ...
        'FontWeight','bold', ...
        'ForegroundColor',[1 1 0], ...
        'ListboxTop',0, ...
        'Position',[5.625 158.75 190.5 7.5], ...
        'String','-------------------------------------------------------------', ...
        'Style','text', ...
        'Tag','StaticText10');
% TEXT 'GRAPH'
h1 = uicontrol('Parent',h0, ...
        'Units','points', ...
        'BackgroundColor',[0 0 0], ...
        'FontWeight','bold', ...
        'ForegroundColor',[1 1 1], ...
        'ListboxTop',0, ...
        'Position',[79.5 336.75 37.5 9.75], ...
        'String','GRAPH', ...
        'Style','text', ...
        'Tag','StaticText3');
% RADIO BUTTONS FOR INDIVIDUAL CHANNELS
h1 = uicontrol('Parent',h0, ...
        'Units','points', ...
        'BackgroundColor',[0 0 0], ...
        'FontName','Avant Garde', ...
        'ForegroundColor',[1 1 1], ...
        'ListboxTop',0, ...
        'Position',[35 314.625 38 13], ...
        'String','LPAQ', ...
        'Style','radiobutton', ...
        'Tag','RBLPAQ');
h1 = uicontrol('Parent',h0, ...
        'Units','points', ...
        'BackgroundColor',[0 0 0], ...
        'FontName','Avant Garde', ...
        'ForegroundColor',[1 1 1], ...
        'ListboxTop',0, ...
        'Position',[35 303 38 13], ...
        'String','PAQ', ...
        'Style','radiobutton', ...
        'Tag','RBPAQ');
h1 = uicontrol('Parent',h0, ...
        'Units','points', ...
        'BackgroundColor',[0 0 0], ...
```

```
        'FontName','Avant Garde', ...
        'ForegroundColor',[1 1 1], ...
        'ListboxTop',0, ...
        'Position',[35 291 38 13], ...
        'String','SVCQ', ...
        'Style','radiobutton', ...
        'Tag','RBSVCQ');
h1 = uicontrol('Parent',h0, ...
        'Units','points', ...
        'BackgroundColor',[0 0 0], ...
        'FontName','Avant Garde', ...
        'ForegroundColor',[1 1 1], ...
        'ListboxTop',0, ...
        'Position',[35 279 38 13], ...
        'String','IVCQ', ...
        'Style','radiobutton', ...
        'Tag','RBIVCQ');
h1 = uicontrol('Parent',h0, ...
        'Units','points', ...
        'BackgroundColor',[0 0 0], ...
        'FontName','Avant Garde', ...
        'ForegroundColor',[1 1 1], ...
        'ListboxTop',0, ...
        'Position',[35 267 38 13], ...
        'String','AOP', ...
        'Style','radiobutton', ...
        'Tag','RBAOP');
h1 = uicontrol('Parent',h0, ...
        'Units','points', ...
        'BackgroundColor',[0 0 0], ...
        'FontName','Avant Garde', ...
        'ForegroundColor',[1 1 1], ...
        'ListboxTop',0, ...
        'Position',[80 314.625 38 13], ...
        'String','SVCP', ...
        'Style','radiobutton', ...
        'Tag','RBSVCP');
h1 = uicontrol('Parent',h0, ...
        'Units','points', ...
        'BackgroundColor',[0 0 0], ...
        'FontName','Avant Garde', ...
        'ForegroundColor',[1 1 1], ...
        'ListboxTop',0, ...
        'Position',[80 302.25 38 13], ...
        'String','IVCP', ...
        'Style','radiobutton', ...
        'Tag','RBIVCP');
h1 = uicontrol('Parent',h0, ...
        'Units','points', ...
        'BackgroundColor',[0 0 0], ...
        'FontName','Avant Garde', ...
```

```
            'ForegroundColor',[1 1 1], ...
            'ListboxTop',0, ...
            'Position',[80 291 38 13], ...
            'String','PAP', ...
            'Style','radiobutton', ...
            'Tag','RBPAP');
    h1 = uicontrol('Parent',h0, ...
            'Units','points', ...
            'BackgroundColor',[0 0 0], ...
            'FontName','Avant Garde', ...
            'ForegroundColor',[1 1 1], ...
            'ListboxTop',0, ...
            'Position',[80 279 38 13], ...
            'String','LAP', ...
            'Style','radiobutton', ...
            'Tag','RBLAP');
    h1 = uicontrol('Parent',h0, ...
            'Units','points', ...
            'BackgroundColor',[0 0 0], ...
            'FontName','Avant Garde', ...
            'ForegroundColor',[1 1 1], ...
            'ListboxTop',0, ...
            'Position',[80 267 38 13], ...
            'String','RAP', ...
            'Style','radiobutton', ...
            'Tag','RBRAP');
    h1 = uicontrol('Parent',h0, ...
            'Units','points', ...
            'BackgroundColor',[0 0 0], ...
            'FontName','Avant Garde', ...
            'ForegroundColor',[1 1 1], ...
            'ListboxTop',0, ...
            'Position',[125 314.625 38 13], ...
            'String','AIRP', ...
            'Style','radiobutton', ...
            'Tag','RBAIRP');
    h1 = uicontrol('Parent',h0, ...
            'Units','points', ...
            'BackgroundColor',[0 0 0], ...
            'FontName','Avant Garde', ...
            'ForegroundColor',[1 1 1], ...
            'ListboxTop',0, ...
            'Position',[125 303 38 13], ...
            'String','AIRQ', ...
            'Style','radiobutton', ...
            'Tag','RBAIRQ');
    h1 = uicontrol('Parent',h0, ...
            'Units','points', ...
            'BackgroundColor',[0 0 0], ...
            'FontName','Avant Garde', ...
            'ForegroundColor',[1 1 1], ...
```

```
        'ListboxTop',0, ...
        'Position',[125 291 38 13], ...
        'String','AOQ', ...
        'Style','radiobutton', ...
        'Tag','RBAOQ');
h1 = uicontrol('Parent',h0, ...
        'Units','points', ...
        'BackgroundColor',[0 0 0], ...
        'FontName','Avant Garde', ...
        'ForegroundColor',[1 1 1], ...
        'ListboxTop',0, ...
        'Position',[125 279 38 13], ...
        'String','LVP', ...
        'Style','radiobutton', ...
        'Tag','RBLVP');
h1 = uicontrol('Parent',h0, ...
        'Units','points', ...
        'BackgroundColor',[0 0 0], ...
        'FontName','Avant Garde', ...
        'ForegroundColor',[1 1 1], ...
        'ListboxTop',0, ...
        'Position',[125 267 40 13], ...
        'String','PVP', ...
        'Style','radiobutton', ...
        'Tag','RBPVP');
% LEGEND BUTTON
h1 = uicontrol('Parent',h0, ...
        'Units','points', ...
        'BackgroundColor',[0.75 0.75 0.75], ...
        'Callback','multlegend', ...
        'FontSize',7, ...
        'ListboxTop',0, ...
        'Position',[9 165 40 12], ...
        'String','LEGEND', ...
        'Tag','mult_legend', ...
        'Visible','off');
if nargout > 0, fig = h0; end
```

Subroutine MultChannels.m code

```
function fig = MultChannels()
% GUI for Plotting Multiple Channels
% Callback from DataView
% APRIL 10, 2006
% FIGURE INFORMATION
h0 = figure('Color',[0 0 0], ...
        'MenuBar','none', ...
        'Name','MULTIPLE CHANNELS', ...
        'NumberTitle','off', ...
        'PaperPosition',[18 180 576 432], ...
```

```
        'PaperUnits','points', ...
        'Position',[10 185 271 541], ...
        'Tag','Opt3', ...
        'ToolBar','none');
% TEXT EDIT FOR EXPERIMENT
h1 = uicontrol('Parent',h0, ...
        'Units','points', ...
        'BackgroundColor',[1 1 1], ...
        'FontWeight','bold', ...
        'ForegroundColor',[1 0 0], ...
        'ListboxTop',0, ...
        'Position',[120 370.5 51.75 15], ...
        'String','none', ...
        'Style','edit', ...
        'Tag','experiment', ...
        'Value',1);
% POPUP MENU FOR WAVEFORM TYPE -- AVERAGE OR EPISODE
h1 = uicontrol('Parent',h0, ...
        'Units','points', ...
        'BackgroundColor',[1 1 1], ...
        'FontName','Avant Garde', ...
        'ForegroundColor',[1 0 0], ...
        'ListboxTop',0, ...
        'Position',[120.75 363.75 51.75 18], ...
        'String',{'Average','Episode'}, ...
        'Style','popupmenu', ...
        'Tag','matordat', ...
        'Value',2, ...
        'Visible','off');
% TEXT EDIT FOR GRAPH TITLE
h1 = uicontrol('Parent',h0, ...
        'Units','points', ...
        'BackgroundColor',[1 1 1], ...
        'ForegroundColor',[0 0 1], ...
        'ListboxTop',0, ...
        'Position',[79.5 225 99.75 15], ...
        'String','Place Graph Title Here', ...
        'Style','edit', ...
        'Tag','graphtitle');
% TEXT EDIT FOR BEGINNING EPISODE
h1 = uicontrol('Parent',h0, ...
        'Units','points', ...
        'BackgroundColor',[1 1 1], ...
        'ListboxTop',0, ...
        'Position',[147 136.25 30 15], ...
        'String','1', ...
        'Style','edit', ...
        'Tag','epbegin');
% TEXT EDIT FOR ENDING EPISODE
h1 = uicontrol('Parent',h0, ...
        'Units','points', ...
```

```
        'BackgroundColor',[1 1 1], ...
        'ListboxTop',0, ...
        'Position',[147 105.5 30 15], ...
        'String','5', ...
        'Style','edit', ...
        'Tag','epend');
% CLOSE BUTTON
h1 = uicontrol('Parent',h0, ...
        'Units','points', ...
        'BackgroundColor',[0.75 0.75 0.75], ...
        'Callback','figure(3);close(3);close(gcbf);return', ...
        'FontWeight','bold', ...
        'ForegroundColor',[1 0 0], ...
        'ListboxTop',0, ...
        'Position',[54 21.75 84.75 25.5], ...
        'String','CLOSE', ...
        'Tag','close_button');
% TEXT 'CURRENT EPISODE'
h1 = uicontrol('Parent',h0, ...
        'Units','points', ...
        'BackgroundColor',[1 1 1], ...
        'ListboxTop',0, ...
        'Position',[163.5 36.75 30 10.5], ...
        'String','1', ...
        'Style','text', ...
        'Tag','currentep', ...
        'Visible','off');
% TEXT 'EXPERIMENT'
h1 = uicontrol('Parent',h0, ...
        'Units','points', ...
        'BackgroundColor',[0 0 0], ...
        'FontSize',10, ...
        'FontWeight','bold', ...
        'ForegroundColor',[1 1 1], ...
        'ListboxTop',0, ...
        'Position',[29.25 374.25 66 13.5], ...
        'String','Experiment', ...
        'Style','text', ...
        'Tag','StaticText1');
% TEXT 'BEGINNING EPISODE'
h1 = uicontrol('Parent',h0, ...
        'Units','points', ...
        'BackgroundColor',[0 0 0], ...
        'FontSize',10, ...
        'FontWeight','bold', ...
        'ForegroundColor',[1 1 1], ...
        'ListboxTop',0, ...
        'Position',[15.75 137.5 102.75 12.75], ...
        'String','Beginning Episode', ...
        'Style','text', ...
        'Tag','StaticText4');
```

```
% TEXT 'ENDING EPISODE'
h1 = uicontrol('Parent',h0, ...
        'Units','points', ...
        'BackgroundColor',[0 0 0], ...
        'FontSize',10, ...
        'FontWeight','bold', ...
        'ForegroundColor',[1 1 1], ...
        'ListboxTop',0, ...
        'Position',[22.125 107 90 13.5], ...
        'String','Ending Episode', ...
        'Style','text', ...
        'Tag','StaticText5');
h1 = uicontrol('Parent',h0, ...
        'Units','points', ...
        'BackgroundColor',[0 0 0], ...
        'ForegroundColor',[1 1 1], ...
        'ListboxTop',0, ...
        'Position',[159 48.75 37.5 22.5], ...
        'String','Current Episode', ...
        'Style','text', ...
        'Tag','currentep_text', ...
        'Visible','off');
% TEXT 'TITLE'
h1 = uicontrol('Parent',h0, ...
        'Units','points', ...
        'BackgroundColor',[0 0 0], ...
        'FontWeight','bold', ...
        'ForegroundColor',[1 1 1], ...
        'ListboxTop',0, ...
        'Position',[30 222.75 35.25 11.25], ...
        'String','Title', ...
        'Style','text', ...
        'Tag','StaticText7');
% PLOT BUTTON
h1 = uicontrol('Parent',h0, ...
        'Units','points', ...
        'BackgroundColor',[0.75 0.75 0.75], ...
        'Callback','plotmultchannels', ...
        'FontWeight','bold', ...
        'ForegroundColor',[0 0 1], ...
        'ListboxTop',0, ...
        'Position',[54 53.75 84.75 25.5], ...
        'String','PLOT', ...
        'Tag','plot_button');
% TEXT 'X AXIS LABEL'
h1 = uicontrol('Parent',h0, ...
        'Units','points', ...
        'BackgroundColor',[0 0 0], ...
        'FontWeight','bold', ...
        'ForegroundColor',[1 1 1], ...
        'ListboxTop',0, ...
```

```
        'Position',[15.75 203.25 63.75 11.25], ...
        'String','X Axis Label', ...
        'Style','text', ...
        'Tag','StaticText8');
% TEXT 'Y AXIS LABEL'
h1 = uicontrol('Parent',h0, ...
        'Units','points', ...
        'BackgroundColor',[0 0 0], ...
        'FontWeight','bold', ...
        'ForegroundColor',[1 1 1], ...
        'ListboxTop',0, ...
        'Position',[18 181.5 65.25 11.25], ...
        'String','Y Axis Label', ...
        'Style','text', ...
        'Tag','StaticText9');
% TEXT EDIT FOR X AXIS
h1 = uicontrol('Parent',h0, ...
        'Units','points', ...
        'BackgroundColor',[1 1 1], ...
        'ForegroundColor',[0 0 1], ...
        'ListboxTop',0, ...
        'Position',[91.875 204.75 75 14.25], ...
        'Style','edit', ...
        'Tag','xaxis_label');
% TEXT EDIT FOR Y AXIS
h1 = uicontrol('Parent',h0, ...
        'Units','points', ...
        'BackgroundColor',[1 1 1], ...
        'ForegroundColor',[0 0 1], ...
        'ListboxTop',0, ...
        'Position',[91.875 181.5 75 14.25], ...
        'Style','edit', ...
        'Tag','yaxis_label');
h1 = uicontrol('Parent',h0, ...
        'Units','points', ...
        'BackgroundColor',[0 0 0], ...
        'FontWeight','bold', ...
        'ForegroundColor',[1 1 0], ...
        'ListboxTop',0, ...
        'Position',[5.25 352.5 190.5 7.5], ...
        'String','------------------------------------------------------------', ...
        'Style','text', ...
        'Tag','StaticText10');
h1 = uicontrol('Parent',h0, ...
        'Units','points', ...
        'BackgroundColor',[0 0 0], ...
        'FontWeight','bold', ...
        'ForegroundColor',[1 1 0], ...
        'ListboxTop',0, ...
        'Position',[5.625 93.5 190.5 7.5], ...
        'String','------------------------------------------------------------', ...
```

```
            'Style','text', ...
            'Tag','StaticText10');
h1 = uicontrol('Parent',h0, ...
            'Units','points', ...
            'BackgroundColor',[0 0 0], ...
            'FontWeight','bold', ...
            'ForegroundColor',[1 1 0], ...
            'ListboxTop',0, ...
            'Position',[6.75 247.5 190.5 7.5], ...
            'String','--------------------------------------------------------------', ...
            'Style','text', ...
            'Tag','StaticText10');
h1 = uicontrol('Parent',h0, ...
            'Units','points', ...
            'BackgroundColor',[0 0 0], ...
            'FontWeight','bold', ...
            'ForegroundColor',[1 1 0], ...
            'ListboxTop',0, ...
            'Position',[5.625 158.75 190.5 7.5], ...
            'String','--------------------------------------------------------------', ...
            'Style','text', ...
            'Tag','StaticText10');
% TEXT 'GRAPH'
h1 = uicontrol('Parent',h0, ...
            'Units','points', ...
            'BackgroundColor',[0 0 0], ...
            'FontWeight','bold', ...
            'ForegroundColor',[1 1 1], ...
            'ListboxTop',0, ...
            'Position',[79.5 336.75 37.5 9.75], ...
            'String','GRAPH', ...
            'Style','text', ...
            'Tag','StaticText3');
% RADIO BUTTONS FOR INDIVIDUAL CHANNELS
h1 = uicontrol('Parent',h0, ...
            'Units','points', ...
            'BackgroundColor',[0 0 0], ...
            'FontName','Avant Garde', ...
            'ForegroundColor',[1 1 1], ...
            'ListboxTop',0, ...
            'Position',[35 314.625 38 13], ...
            'String','LPAQ', ...
            'Style','radiobutton', ...
            'Tag','RBLPAQ');
h1 = uicontrol('Parent',h0, ...
            'Units','points', ...
            'BackgroundColor',[0 0 0], ...
            'FontName','Avant Garde', ...
            'ForegroundColor',[1 1 1], ...
            'ListboxTop',0, ...
            'Position',[35 303 38 13], ...
```

```
            'String','PAQ', ...
            'Style','radiobutton', ...
            'Tag','RBPAQ');
h1 = uicontrol('Parent',h0, ...
            'Units','points', ...
            'BackgroundColor',[0 0 0], ...
            'FontName','Avant Garde', ...
            'ForegroundColor',[1 1 1], ...
            'ListboxTop',0, ...
            'Position',[35 291 38 13], ...
            'String','SVCQ', ...
            'Style','radiobutton', ...
            'Tag','RBSVCQ');
h1 = uicontrol('Parent',h0, ...
            'Units','points', ...
            'BackgroundColor',[0 0 0], ...
            'FontName','Avant Garde', ...
            'ForegroundColor',[1 1 1], ...
            'ListboxTop',0, ...
            'Position',[35 279 38 13], ...
            'String','IVCQ', ...
            'Style','radiobutton', ...
            'Tag','RBIVCQ');
h1 = uicontrol('Parent',h0, ...
            'Units','points', ...
            'BackgroundColor',[0 0 0], ...
            'FontName','Avant Garde', ...
            'ForegroundColor',[1 1 1], ...
            'ListboxTop',0, ...
            'Position',[35 267 38 13], ...
            'String','AOP', ...
            'Style','radiobutton', ...
            'Tag','RBAOP');
h1 = uicontrol('Parent',h0, ...
            'Units','points', ...
            'BackgroundColor',[0 0 0], ...
            'FontName','Avant Garde', ...
            'ForegroundColor',[1 1 1], ...
            'ListboxTop',0, ...
            'Position',[80 314.625 38 13], ...
            'String','SVCP', ...
            'Style','radiobutton', ...
            'Tag','RBSVCP');
h1 = uicontrol('Parent',h0, ...
            'Units','points', ...
            'BackgroundColor',[0 0 0], ...
            'FontName','Avant Garde', ...
            'ForegroundColor',[1 1 1], ...
            'ListboxTop',0, ...
            'Position',[80 302.25 38 13], ...
            'String','IVCP', ...
```

```
            'Style','radiobutton', ...
            'Tag','RBIVCP');
    h1 = uicontrol('Parent',h0, ...
            'Units','points', ...
            'BackgroundColor',[0 0 0], ...
            'FontName','Avant Garde', ...
            'ForegroundColor',[1 1 1], ...
            'ListboxTop',0, ...
            'Position',[80 291 38 13], ...
            'String','PAP', ...
            'Style','radiobutton', ...
            'Tag','RBPAP');
    h1 = uicontrol('Parent',h0, ...
            'Units','points', ...
            'BackgroundColor',[0 0 0], ...
            'FontName','Avant Garde', ...
            'ForegroundColor',[1 1 1], ...
            'ListboxTop',0, ...
            'Position',[80 279 38 13], ...
            'String','LAP', ...
            'Style','radiobutton', ...
            'Tag','RBLAP');
    h1 = uicontrol('Parent',h0, ...
            'Units','points', ...
            'BackgroundColor',[0 0 0], ...
            'FontName','Avant Garde', ...
            'ForegroundColor',[1 1 1], ...
            'ListboxTop',0, ...
            'Position',[80 267 38 13], ...
            'String','RAP', ...
            'Style','radiobutton', ...
            'Tag','RBRAP');
    h1 = uicontrol('Parent',h0, ...
            'Units','points', ...
            'BackgroundColor',[0 0 0], ...
            'FontName','Avant Garde', ...
            'ForegroundColor',[1 1 1], ...
            'ListboxTop',0, ...
            'Position',[125 314.625 38 13], ...
            'String','AIRP', ...
            'Style','radiobutton', ...
            'Tag','RBAIRP');
    h1 = uicontrol('Parent',h0, ...
            'Units','points', ...
            'BackgroundColor',[0 0 0], ...
            'FontName','Avant Garde', ...
            'ForegroundColor',[1 1 1], ...
            'ListboxTop',0, ...
            'Position',[125 303 38 13], ...
            'String','AIRQ', ...
            'Style','radiobutton', ...
```

```
        'Tag','RBAIRQ');
h1 = uicontrol('Parent',h0, ...
        'Units','points', ...
        'BackgroundColor',[0 0 0], ...
        'FontName','Avant Garde', ...
        'ForegroundColor',[1 1 1], ...
        'ListboxTop',0, ...
        'Position',[125 291 38 13], ...
        'String','AOQ', ...
        'Style','radiobutton', ...
        'Tag','RBAOQ');
h1 = uicontrol('Parent',h0, ...
        'Units','points', ...
        'BackgroundColor',[0 0 0], ...
        'FontName','Avant Garde', ...
        'ForegroundColor',[1 1 1], ...
        'ListboxTop',0, ...
        'Position',[125 279 38 13], ...
        'String','LVP', ...
        'Style','radiobutton', ...
        'Tag','RBLVP');
h1 = uicontrol('Parent',h0, ...
        'Units','points', ...
        'BackgroundColor',[0 0 0], ...
        'FontName','Avant Garde', ...
        'ForegroundColor',[1 1 1], ...
        'ListboxTop',0, ...
        'Position',[125 267 40 13], ...
        'String','PVP', ...
        'Style','radiobutton', ...
        'Tag','RBPVP');
% LEGEND BUTTON
h1 = uicontrol('Parent',h0, ...
        'Units','points', ...
        'BackgroundColor',[0.75 0.75 0.75], ...
        'Callback','multlegend', ...
        'FontSize',7, ...
        'ListboxTop',0, ...
        'Position',[9 165 40 12], ...
        'String','LEGEND', ...
        'Tag','mult_legend', ...
        'Visible','off');
if nargout > 0, fig = h0; end
```

Subroutine plotmultchannels.m code

```
function plotmultchannels
% CALLED FROM DATAVIEW
% PLOTS MULTIPLE CHANNELS
% WAVEFORM TYPE EPISODE
% APRIL 10, 2006
```

```
% GETS VALUES FOR CHANNELS
h=findobj(gcf,'Tag','RBLPAQ');
rblpaq=get(h,'Value');
h=findobj(gcf,'Tag','RBPAQ');
rbpaq=get(h,'Value');
h=findobj(gcf,'Tag','RBSVCQ');
rbsvcq=get(h,'Value');
h=findobj(gcf,'Tag','RBIVCQ');
rbivcq=get(h,'Value');
h=findobj(gcf,'Tag','RBAOP');
rbaop=get(h,'Value');
h=findobj(gcf,'Tag','RBSVCP');
rbsvcp=get(h,'Value');
h=findobj(gcf,'Tag','RBIVCP');
rbivcp=get(h,'Value');
h=findobj(gcf,'Tag','RBPAP');
rbpap=get(h,'Value');
h=findobj(gcf,'Tag','RBLAP');
rblap=get(h,'Value');
h=findobj(gcf,'Tag','RBRAP');
rbrap=get(h,'Value');
h=findobj(gcf,'Tag','RBAIRP');
rbairp=get(h,'Value');
h=findobj(gcf,'Tag','RBAIRQ');
rbairq=get(h,'Value');
h=findobj(gcf,'Tag','RBAOQ');
rbaoq=get(h,'Value');
h=findobj(gcf,'Tag','RBLVP');
rblvp=get(h,'Value');
h=findobj(gcf,'Tag','RBPVP');
rbpvp=get(h,'Value');
% GET EXPERIMENT NAME
h=findobj(gcbf,'Tag','experiment');
experiment=popupstr(h);
% GET WAVEFORM TYPE (Episode or Average)
h=findobj(gcbf,'Tag','matordat');
wave_type=popupstr(h);
% GET BEGINNING EPISODE
h=findobj(gcbf,'Tag','epbegin');
epbegin=get(h,'String');
epbegin=str2num(epbegin);
% GET ENDING EPISODE
h=findobj(gcbf,'Tag','epend');
epend=get(h,'String');
epend=str2num(epend);
% GET GRAPH TITLE
h=findobj(gcbf,'Tag','graphtitle');
graph_title=get(h,'String');
% GET GRAPH X AXIS LABEL
h=findobj(gcbf,'Tag','xaxis_label');
xaxis_label=get(h,'String');
```

```
% GET GRAPH Y AXIS LABEL
h=findobj(gcbf,'Tag','yaxis_label');
yaxis_label=get(h,'String');
% load info file here
temp=strcat(experiment,'info.mat');
temp=strrep(temp,'l',' l');
temp=strcat('load',temp);
eval(temp);
eval('charray=info.chnumb;');
% figure information
mult=figure(3);
set(mult,'Position',[300 180 600 500]);
set(mult,'NumberTitle','off');
set(mult,'Name','MULTIPLE CHANNELS');
hold on;
s=([1:1800]');
% FOR EPISODE PLOT
if wave_type == 'Episode'
  clf;
  curep=findobj(gcbf,'Tag','currentep');
  set(curep,'Visible','on');
  cureptext=findobj(gcbf,'Tag','currentep_text');
  set(cureptext,'Visible','on');
  if epend < epbegin
    msg={'Ending Episode is Greater Than'
      'Beginning Episode'
      ' '
      'Please Try Again'};
    j=errordlg(msg,'Episode Error');
    pause(3)
    close(j)
    return
  end
  for j=epbegin:epend
    pause(.7)
    g=s(j,1);
    E=g;
    g=int2str(g);
    V=strcat(experiment,g,'.dat');
    X=exist(V,'file');
    U=strcat(experiment,g);
    set(curep,'String',g);
  if X > 0
    V=strrep(V,'l',' l');
    W=strcat('load',V);
    eval(W);
    s5=strcat('Epi=',U,';');
    eval(s5);
    if rblpaq == 1 & charray(j,1) > 0
      plot([.005:.005:1024*.005],Epi(:,charray(j,1)),'b--');hold on;
    end
```

```
        if rbpaq == 1 & charray(j,2) > 0
  plot([.005:.005:1024*.005],Epi(:,charray(j,2)),'m--');hold on;
end
if rbsvcq == 1 & charray(j,3) > 0
  plot([.005:.005:1024*.005],Epi(:,charray(j,3)),'c--');hold on;
end
if rbivcq == 1 & charray(j,4) > 0
  plot([.005:.005:1024*.005],Epi(:,charray(j,4)),'b');hold on;%g--
end
if rbaop == 1 & charray(j,5) > 0
  plot([.005:.005:1024*.005],Epi(:,charray(j,5)),'k');hold on;%r
end
if rbsvcp == 1 & charray(j,6) > 0
  plot([.005:.005:1024*.005],Epi(:,charray(j,6)),'g');hold on;
end
if rbivcp == 1 & charray(j,7) > 0
  plot([.005:.005:1024*.005],Epi(:,charray(j,7)),'r');hold on;%g
end
if rbpap == 1 & charray(j,8) > 0
  plot([.005:.005:1024*.005],Epi(:,charray(j,8)),'r');hold on;
end
if rblap == 1 & charray(j,9) > 0
  plot([.005:.005:1024*.005],Epi(:,charray(j,9)),'m');hold on;
end
if rbrap == 1 & charray(j,10) > 0
  plot([.005:.005:1024*.005],Epi(:,charray(j,10)),'c');hold on;
end
if rbairp == 1 & charray(j,11) > 0
  plot([.005:.005:1024*.005],Epi(:,charray(j,11)),'k');hold on;
end
if rbairq == 1 & charray(j,12) > 0
  plot([.005:.005:1024*.005],Epi(:,charray(j,12)),'r--');hold on;
end
if rbaoq == 1 & charray(j,13) > 0
  plot([.005:.005:1024*.005],Epi(:,charray(j,13)),'y');hold on;
end
if rblvp == 1 & charray(j,14) > 0
  plot([.005:.005:1024*.005],Epi(:,charray(j,14)),'b');hold on;
end
if rbpvp == 1 & charray(j,15) > 0
  plot([.005:.005:1024*.005],Epi(:,charray(j,15)),'g');hold on;
end
h=gca;
set(h,'FontName','Arial');
set(h,'FontSize',[12]);
set(h,'FontWeight','bold');
t1=strcat(graph_title,' -- Episode  #',g);
t1=graph_title;
title(t1);xlabel(xaxis_label);ylabel(yaxis_label);
pause
if E ~= epend
```

```
        clf;
      end

   end
end
end
curep=findobj(gcbf,'Tag','currentep');
set(curep,'Visible','off');
cureptext=findobj(gcbf,'Tag','currentep_text');
set(cureptext,'Visible','off');
jj=findobj(gcbf,'Tag','mult_legend');
set(jj,'Visible','on');
```

Subroutine moviegui.m code

```
function fig = moviegui()
% MOVIE GUI
% MAKES MOVIES AND AVI FROM DATA FILES
% LOADS AND PLAYS STORED MOVIES
% APRIL 10, 2006
% FIGURE INFORMATION
h0 = figure('Color',[0 0 0], ...
            'MenuBar','none', ...
            'Name','MOVIE EDITOR', ...
            'NumberTitle','off', ...
            'PaperPosition',[18 180 576 432], ...
            'PaperUnits','points', ...
            'Position',[24 169 229 546], ...
            'Tag','mainmovie', ...
            'ToolBar','none');
% TEXT 'MOVIE EDITOR'
h1 = uicontrol('Parent',h0, ...
            'Units','points', ...
            'BackgroundColor',[0 0 0], ...
            'FontSize',12, ...
            'FontWeight','demi', ...
            'ForegroundColor',[1 1 1], ...
            'ListboxTop',0, ...
            'Position',[35.25 381 107.25 16.5], ...
            'String','MOVIE EDITOR', ...
            'Style','text', ...
            'Tag','StaticText1');
% Frame
h1 = uicontrol('Parent',h0, ...
            'Units','points', ...
            'BackgroundColor',[0 0 0], ...
            'ForegroundColor',[0.5 0.5 0.5], ...
            'ListboxTop',0, ...
```

```
        'Position',[13.5 207.75 141.75 153.75], ...
        'Style','frame', ...
        'Tag','Frame1');
% TEXT 'LAMB INFORMATION'
h1 = uicontrol('Parent',h0, ...
        'Units','points', ...
        'BackgroundColor',[0 0 0], ...
        'ForegroundColor',[1 1 0], ...
        'ListboxTop',0, ...
        'Position',[47.25 346.5 89.25 9.75], ...
        'String','LAMB INFORMATION', ...
        'Style','text', ...
        'Tag','StaticText4');
% TEXT 'EXPERIMENT'
h1 = uicontrol('Parent',h0, ...
        'Units','points', ...
        'BackgroundColor',[0 0 0], ...
        'ForegroundColor',[1 1 1], ...
        'ListboxTop',0, ...
        'Position',[21.75 321 45 12], ...
        'String','Experiment', ...
        'Style','text', ...
        'Tag','StaticText2');
% ONE CHANNEL RADIOBUTTON
h1 = uicontrol('Parent',h0, ...
        'Units','points', ...
        'BackgroundColor',[0 0 0], ...
        'Callback','chanselect', ...
        'ForegroundColor',[1 1 1], ...
        'ListboxTop',0, ...
        'Position',[21.75 297 63 15], ...
        'String','One Channel', ...
        'Style','radiobutton', ...
        'Tag','onechanbutt');
% POPUP MENU CHANNEL ONE
h1 = uicontrol('Parent',h0, ...
        'Units','points', ...
        'BackgroundColor',[1 1 1], ...
        'FontName','arial', ...
        'ListboxTop',0, ...
        'Position',[93.75 297.75 45 15], ...
        'String',{'LPAQ','PAQ','SVCQ','IVCQ','AOP','SVCP','IVCP','PAP','LAP','RAP','AIRP','AIRQ'
,'AOQ','LVP','PVP','MISC'}, ...
        'Style','popupmenu', ...
        'Tag','onechanselect', ...
        'Value',1, ...
        'Visible','off');
% TWO CHANNEL RADIOBUTTON
h1 = uicontrol('Parent',h0, ...
        'Units','points', ...
        'BackgroundColor',[0 0 0], ...
```

```
        'Callback','chanselect', ...
        'ForegroundColor',[1 1 1], ...
        'ListboxTop',0, ...
        'Position',[21.75 272.25 66.75 15.75], ...
        'String','Two Channels', ...
        'Style','radiobutton', ...
        'Tag','twochanbutt');
% POPUP MENU CHANNEL TWO
h1 = uicontrol('Parent',h0, ...
        'Units','points', ...
        'BackgroundColor',[1 1 1], ...
        'FontName','arial', ...
        'ListboxTop',0, ...
        'Position',[93.75 274.5 45 15], ...
        'String',{'LPAQ','PAQ','SVCQ','IVCQ','AOP','SVCP','IVCP','PAP','LAP','RAP','AIRP','AIRQ'
,'AOQ','LVP','PVP','MISC'}, ...
        'Style','popupmenu', ...
        'Tag','twoselone', ...
        'Value',1, ...
        'Visible','off');
% POPUP MENU CHANNEL TWO
h1 = uicontrol('Parent',h0, ...
        'Units','points', ...
        'BackgroundColor',[1 1 1], ...
        'FontName','arial', ...
        'ListboxTop',0, ...
        'Position',[93.75 252 45 15], ...
        'String',{'LPAQ','PAQ','SVCQ','IVCQ','AOP','SVCP','IVCP','PAP','LAP','RAP','AIRP','AIRQ'
,'AOQ','LVP','PVP','MISC'}, ...
        'Style','popupmenu', ...
        'Tag','twoseltwo', ...
        'Value',1, ...
        'Visible','off');
% TEXT 'EPISODES [START:END]
h1 = uicontrol('Parent',h0, ...
        'Units','points', ...
        'BackgroundColor',[0 0 0], ...
        'ForegroundColor',[1 1 1], ...
        'ListboxTop',0, ...
        'Position',[15.75 231.75 75 10.5], ...
        'String','Episodes [start:end]', ...
        'Style','text', ...
        'Tag','StaticText6');
% TEXT EDIT BOX FOR EPISODES
h1 = uicontrol('Parent',h0, ...
        'Units','points', ...
        'BackgroundColor',[1 1 1], ...
        'ListboxTop',0, ...
        'Position',[93.75 228.75 45 15], ...
        'Style','edit', ...
        'Tag','episnums');
```

```
% TEXT EDIT FOR EXPERIMENT
h1 = uicontrol('Parent',h0, ...
        'Units','points', ...
        'BackgroundColor',[1 1 1], ...
        'ListboxTop',0, ...
        'Position',[93.75 321 45 15], ...
        'String','none', ...
        'Style','edit', ...
        'Tag','experiment', ...
        'Value',1);
% FRAME
h1 = uicontrol('Parent',h0, ...
        'Units','points', ...
        'BackgroundColor',[0 0 0], ...
        'ForegroundColor',[0.5 0.5 0.5], ...
        'ListboxTop',0, ...
        'Position',[12.75 127.5 143.25 72.75], ...
        'Style','frame', ...
        'Tag','Frame2');
% SAVE MULTIPLE EPISODES RADIOBUTTON
h1 = uicontrol('Parent',h0, ...
        'Units','points', ...
        'BackgroundColor',[0 0 0], ...
        'ForegroundColor',[1 1 1], ...
        'ListboxTop',0, ...
        'Position',[34.5 164.25 99.75 14.25], ...
        'String','Save Multiple Episodes', ...
        'Style','radiobutton', ...
        'Tag','multepis');
% SAVE RADIOBUTTON
h1 = uicontrol('Parent',h0, ...
        'Units','points', ...
        'BackgroundColor',[0 0 0], ...
        'Callback','saveselect', ...
        'ForegroundColor',[1 1 1], ...
        'ListboxTop',0, ...
        'Position',[34.5 148.5 45 15], ...
        'String','Save', ...
        'Style','radiobutton', ...
        'Tag','savebutt');
% TEXT EDIT FILENAME
h1 = uicontrol('Parent',h0, ...
        'Units','points', ...
        'BackgroundColor',[1 1 1], ...
        'ListboxTop',0, ...
        'Position',[85.5 135 45 15], ...
        'Style','edit', ...
        'Tag','filename', ...
        'Visible','off');
% TEXT EDIT FILENAME
h1 = uicontrol('Parent',h0, ...
```

```
        'Units','points', ...
        'BackgroundColor',[0 0 0], ...
        'ForegroundColor',[1 1 1], ...
        'ListboxTop',0, ...
        'Position',[42 138 45 11.25], ...
        'String','Filename', ...
        'Style','text', ...
        'Tag','filetext', ...
        'Visible','off');
% TEXT 'FILE INFORMATION'
h1 = uicontrol('Parent',h0, ...
        'Units','points', ...
        'BackgroundColor',[0 0 0], ...
        'ForegroundColor',[1 1 0], ...
        'ListboxTop',0, ...
        'Position',[45 179.25 84 14.25], ...
        'String','FILE INFORMATION', ...
        'Style','text', ...
        'Tag','StaticText7');
% FRAME
h1 = uicontrol('Parent',h0, ...
        'Units','points', ...
        'BackgroundColor',[0 0 0], ...
        'ForegroundColor',[0.5 0.5 0.5], ...
        'ListboxTop',0, ...
        'Position',[12.75 10.5 143.25 109.5], ...
        'Style','frame', ...
        'Tag','Frame1');
% MESSAGE BOARD
h1 = uicontrol('Parent',h0, ...
        'Units','points', ...
        'BackgroundColor',[0.75 0.75 0.75], ...
        'ForegroundColor',[0 0 1], ...
        'ListboxTop',0, ...
        'Position',[13.5 367.5 144 10.5], ...
        'String','Message Board', ...
        'Style','text', ...
        'Tag','messboard');
% MAKE MOVIE BUTTON
h1 = uicontrol('Parent',h0, ...
        'Units','points', ...
        'BackgroundColor',[0.75 0.75 0.75], ...
        'Callback','makemovie', ...
        'ListboxTop',0, ...
        'Position',[35.25 45 99.75 25.5], ...
        'String','Make Movie', ...
        'Tag','makemovbutt');
% LOAD SAVED MOVIE
h1 = uicontrol('Parent',h0, ...
        'Units','points', ...
        'BackgroundColor',[0.75 0.75 0.75], ...
```

```
        'Callback','loadmovie', ...
        'ListboxTop',0, ...
        'Position',[35.25 75 99.75 24.75], ...
        'String','Load/Play Saved Movie', ...
        'Tag','loadmovbutt');
% TEXT 'OPERATIONS'
h1 = uicontrol('Parent',h0, ...
        'Units','points', ...
        'BackgroundColor',[0 0 0], ...
        'ForegroundColor',[1 1 0], ...
        'ListboxTop',0, ...
        'Position',[47.25 102 79.5 12], ...
        'String','OPERATIONS', ...
        'Style','text', ...
        'Tag','StaticText8');
% INFO BUTTON
h1 = uicontrol('Parent',h0, ...
        'Units','points', ...
        'BackgroundColor',[0.75 0.75 0.75], ...
        'Callback','movieinfo', ...
        'ListboxTop',0, ...
        'Position',[24 20.25 45 15], ...
        'String','INFO', ...
        'Tag','infobutt');
% CLOSE BUTTON
h1 = uicontrol('Parent',h0, ...
        'Units','points', ...
        'BackgroundColor',[0.75 0.75 0.75], ...
        'Callback','close all;return', ...
        'ListboxTop',0, ...
        'Position',[99.75 18.75 45 15], ...
        'String','CLOSE', ...
        'Tag','closebutt');
if nargout > 0, fig = h0; end
```

Subroutine chanselect.m code

```
function chanselect
H=findobj(gcf,'Tag','onechanbutt');
onechanbutt=get(H,'Value');
H=findobj(gcf,'Tag','twochanbutt');
twochanbutt=get(H,'Value');
if onechanbutt == 1
  h=findobj(gcf,'Tag','twochanbutt');
  set(h,'Visible','off');
  h=findobj(gcf,'Tag','onechanselect');
  set(h,'Visible','on');
end
if onechanbutt == 0
  h=findobj(gcf,'Tag','twochanbutt');
```

```
  set(h,'Visible','on');
  h=findobj(gcf,'Tag','onechanselect');
  set(h,'Visible','off');
end
if twochanbutt == 1
  h=findobj(gcf,'Tag','onechanbutt');
  set(h,'Visible','off');
  h=findobj(gcf,'Tag','twoselone');
  set(h,'Visible','on');
  h=findobj(gcf,'Tag','twoseltwo');
  set(h,'Visible','on');
end
if twochanbutt == 0
  h=findobj(gcf,'Tag','onechanbutt');
  set(h,'Visible','on');
  h=findobj(gcf,'Tag','twoselone');
  set(h,'Visible','off');
  h=findobj(gcf,'Tag','twoseltwo');
  set(h,'Visible','off');
end
```

Subroutine saveselect.m code

```
function saveselect
H=findobj(gcf,'Tag','savebutt');
savebutt=get(H,'Value');
if savebutt == 1
  h=findobj(gcf,'Tag','filename');
  set(h,'Visible','on');
  h=findobj(gcf,'Tag','filetext');
  set(h,'Visible','on');
end
if savebutt == 0
  h=findobj(gcf,'Tag','filename');
  set(h,'Visible','off');
  h=findobj(gcf,'Tag','filetext');
  set(h,'Visible','off');
end
```

Subroutine movieinfo.m code

```
function movieinfo
help ={' '
  ' '
  'IF LOADING/PLAYING A MOVIE'
  ' '
  '1.  Press Load/Play Saved Movie button'
  '2.  When prompted as to which file..'
  '       Select avi movie'
  '       you wish to view'
  '3.  Close movie window when finished'
```

```
  ' '
  'IF MAKING A MOVIE'
  ' '
  '1.  Select which lamb experiment'
  '2.  Select One Channel or Two Channels'
  '3.  Choose which channel(s) to view'
  '4.  Type episodes to view'
  '       Ex. 1:4'
  '5.  If want to save file:'
  '    Click Save button and enter filename'
  '6.  Press Make Movie button'
  '7.  Resize movie window to preferred size'
  '8.  Fill out Graph Information'
  '9.  Check Done box'
  ' '
  'Mark E. Ketner'
  'March 21, 2006'
  'Version 3.0'};
x=msgbox(help,'MOVIE HELP','help');
set(x,'Position',[15 100 200 310]);
```

Subroutine makemovie.m code

```
function makemovie
% MAKE OTHER OPERATION INVISIBLE
h=findobj(gcbf,'Tag','loadmovbutt');
set(h,'Visible','off');
h=findobj(gcbf,'Tag','playmovbutt');
set(h,'Visible','off');
% MESSAGE BOARD
messboard=findobj(gcbf,'Tag','messboard');
set(messboard,'String','In Make Movie Subroutine');
% ***************************
% GET INFORMATION FROM WINDOW
% ***************************
% GET EXPERIMENT
h=findobj(gcbf,'Tag','experiment');
experiment=popupstr(h);
% GET ONE CHANNEL RADIOBUTTON VALUE
h=findobj(gcbf,'Tag','onechanbutt');
onechanbutt=get(h,'Value');
% GET TWO CHANNEL RADIOBUTTON VALUE
h=findobj(gcbf,'Tag','twochanbutt');
twochanbutt=get(h,'Value');
% IF ONE BUTTON IS CHECKED, GET CHANNEL
if onechanbutt == 1
  h=findobj(gcbf,'Tag','onechanselect');
  onechanselect=popupstr(h);
end
% IF TWO BUTTON IS CHECKED, GET BOTH CHANNELS
if twochanbutt == 1
```

```
  h=findobj(gcbf,'Tag','twoselone');
  twoselone=popupstr(h);
  h=findobj(gcbf,'Tag','twoseltwo');
  twoseltwo=popupstr(h);
end
% GET EPISODES
h=findobj(gcbf,'Tag','episnums');
episnums=get(h,'String');
episnums=str2num(episnums);
% GET BITMAP DUPLICATE BUTTON VALUE
h=findobj(gcbf,'Tag','bitmapbutt');
bitmapbutt=get(h,'Value');
% GET MULTIPLE EPISODE VALUE
h=findobj(gcbf,'Tag','multepis');
multepis=get(h,'Value');
% GET SAVE FILE VALUE
h=findobj(gcbf,'Tag','savebutt');
savebutt=get(h,'Value');
% IF SAVE VALUE IS CHECKED, GET FILENAME
if savebutt == 1
  h=findobj(gcbf,'Tag','filename');
  filename=get(h,'String');
  % ERROR MESSAGE IF NO FILENAME ENTERED
  if isempty(filename)
    x={'ERROR.....'
      ' '
      'MUST ENTER A FILENAME'
      ' '};
    errordlg(x,'PLEASE ENTER FILENAME');
    set(messboard,'String','See Error Message');
    return
  end
end
% IF NEITHER ONE NOR TWO CHANNEL IS SELECTED
if onechanbutt == 0 & twochanbutt == 0
  x={'ERROR.....'
    ' '
    'YOU MUST SELECT EITHER'
    'ONE OR TWO CHANNELS   '
    ' '};
  errordlg(x,'PLEASE SELECT CHANNEL');
  set(messboard,'String','See Error Message');
  return
end
% ERROR MESSAGE IF NO EPISODES ENTERED
if isempty(episnums)
  x={'ERROR.....'
    ' '
    'PLEASE ENTER EPISODE NUMBERS'
    'EXAMPLE [1:4]              '
    ' '};
```

```
  errordlg(x,'ENTER EPISODES');
  set(messboard,'String','SEE ERROR MESSAGE!!!!');
  return
end
% LOAD EXPERIMENT INFO FILE
set(messboard,'String','LOADING INFO FILE');
temp=strcat(experiment,'info.mat');
temp=strrep(temp,'l',' l');
temp=strcat('load',temp);
eval(temp);
eval('charray=info.chnumb;')
% FIND MINIMUM # IN EPISODES
minepis=min(episnums);
% FIND MAXIMUM # IN EPISODES
maxepis=max(episnums);
% if file already exists ask if they want to overwrite it
%minepistr=num2str(minepis);
if savebutt == 1
x=strcat(filename,'.avi');
y = exist(x);
if y == 2
  set(messboard,'String','SEE QUESTION BOX');
  button = questdlg('OVERWRITE EXISTING FILE?','OVERWRITE','Yes','No','No');
  switch button
  case 'Yes',
    %disp('answered yes')
  case 'No',
    %disp('answered no')
    return
  end
end
end
% DETERMINE WHICH COLUMN OF CHARRAY TO USE
% one channel
if onechanbutt == 1
  if strcmp(onechanselect,'LPAQ') == 1
    channel1 = 1;
  elseif strcmp(onechanselect,'PAQ') == 1
    channel1 = 2;
  elseif strcmp(onechanselect,'SVCQ') == 1
    channel1 = 3;
  elseif strcmp(onechanselect,'IVCQ') == 1
    channel1 = 4;
  elseif strcmp(onechanselect,'AOP') == 1
    channel1 = 5;
  elseif strcmp(onechanselect,'SVCP') == 1
    channel1 = 6;
  elseif strcmp(onechanselect,'IVCP') == 1
    channel1 = 7;
  elseif strcmp(onechanselect,'PAP') == 1
    channel1 = 8;
```

```
  elseif strcmp(onechanselect,'LAP') == 1
    channel1 = 9;
  elseif strcmp(onechanselect,'RAP') == 1
    channel1 = 10;
  elseif strcmp(onechanselect,'AIRP') == 1
    channel1 = 11;
  elseif strcmp(onechanselect,'AIRQ') == 1
     channel1 = 12;
  elseif strcmp(onechanselect,'AOQ') == 1
     channel1 = 13;
  elseif strcmp(onechanselect,'LVP') == 1
     channel1 = 14;

  end
end
% two channels
if twochanbutt == 1
  if strcmp(twoselone,'LPAQ') == 1
    channel1 = 1;
  elseif strcmp(twoselone,'PAQ') == 1
    channel1 = 2;
  elseif strcmp(twoselone,'SVCQ') == 1
    channel1 = 3;
  elseif strcmp(twoselone,'IVCQ') == 1
    channel1 = 4;
  elseif strcmp(twoselone,'AOP') == 1
    channel1 = 5;
  elseif strcmp(twoselone,'SVCP') == 1
    channel1 = 6;
  elseif strcmp(twoselone,'IVCP') == 1
    channel1 = 7;
  elseif strcmp(twoselone,'PAP') == 1
    channel1 = 8;
  elseif strcmp(twoselone,'LAP') == 1
    channel1 = 9;
  elseif strcmp(twoselone,'RAP') == 1
    channel1 = 10;
  elseif strcmp(twoselone,'AIRP') == 1
    channel1 = 11;
  elseif strcmp(twoselone,'AIRQ') == 1
     channel1 = 12;
  elseif strcmp(twoselone,'AOQ') == 1
     channel1 = 13;
  elseif strcmp(twoselone,'LVP') == 1
     channel1 = 14;
  end
  if strcmp(twoseltwo,'LPAQ') == 1
    channel2 = 1;
  elseif strcmp(twoseltwo,'PAQ') == 1
    channel2 = 2;
  elseif strcmp(twoseltwo,'SVCQ') == 1
```

```
    channel2 = 3;
  elseif strcmp(twoseltwo,'IVCQ') == 1
    channel2 = 4;
  elseif strcmp(twoseltwo,'AOP') == 1
    channel2 = 5;
  elseif strcmp(twoseltwo,'SVCP') == 1
    channel2 = 6;
  elseif strcmp(twoseltwo,'IVCP') == 1
    channel2 = 7;
  elseif strcmp(twoseltwo,'PAP') == 1
    channel2 = 8;
  elseif strcmp(twoseltwo,'LAP') == 1
    channel2 = 9;
  elseif strcmp(twoseltwo,'RAP') == 1
    channel2 = 10;
  elseif strcmp(twoseltwo,'AIRP') == 1
    channel2 = 11;
  elseif strcmp(twoseltwo,'AIRQ') == 1
     channel2 = 12;
  elseif strcmp(twoseltwo,'AOQ') == 1
     channel2 = 13;
  elseif strcmp(twoseltwo,'LVP') == 1
     channel2 = 14;
  end
end
% CREATE NEW FIGURE WINDOW
fig3=figure(3);
set(fig3,'Color',[1 1 1]);
set(fig3,'MenuBar','none');
set(fig3,'Name','MOVIE WINDOW');
set(fig3,'NumberTitle','off');
set(fig3,'Position',[265 170 626 530]);
set(messboard,'String','Resize Window Now - Press Return');
pause;
% **********************
% FOR ONE CHANNEL MOVIE
% **********************
if onechanbutt == 1
  % IF MULTIPLE EPISODES IS CHECKED - DON'T CLEAR GRAPH
  if multepis ~= 1
    clf;
  end
  % GET GRAPH INFORMATION
  set(messboard,'String','Fill Out Graph Information');
  graphinfo1
  H=findobj(gcf,'Tag','donecheck');
  get(H,'Value');
  waitfor(H,'Value',1);
  h=findobj(gcf,'Tag','graph_title');
  graph_title=get(h,'String');
  h=findobj(gcf,'Tag','xaxis_label');
```

```
  xaxis_label=get(h,'String');
  h=findobj(gcf,'Tag','yaxis_label');
  yaxis_label=get(h,'String');
  close
  x=[];
  tags='ABCDEFGHIJKLMNOPQRSTUVWXYZ';
  num=ceil(maxepis/50);
  tags=tags(1:num);
  for k=1:num
    f3=strcat(experiment,tags(k),'.mat;');
    f4=strrep(f3,'l',' l');
    X=exist(strcat(experiment,tags(k),'.mat'),'file');
%     X=exist(f3,'file');
    if X > 0
      s8=strcat('load',f4);
      eval(s8);
    end
  end
cray=['r- ';'r: ';'r-.';'r--';...
    'b- ';'b: ';'b-.';'b--';...
    'g- ';'g: ';'g-.';'g--';...
    'c- ';'c: ';'c-.';'c--';...
    'y- ';'y: ';'y-.';'y--';...
    'm- ';'m: ';'m-.';'m--';...
    'k- ';'k: ';'k-.';'k--'];
ck=0;
numepis=length(episnums);
fr=1;
   title(graph_title);xlabel(xaxis_label);ylabel(yaxis_label);
if savebutt==1
   u=strcat('aviobj=avifile('',filename,'.avi',"compression","indeo5","fps",3,"quality",100)');
   eval(u)
end
for k=1:numepis
    num=k;
    k=episnums(k);
    j=int2str(k);
    if (k>0 & k<=50) Epifftf=EpifftfA;kk=k;
    elseif (k>50 & k<=100) Epifftf=EpifftfB;kk=k-50;
    elseif (k>100 & k<=150) Epifftf=EpifftfC;kk=k-100;
    elseif (k>150 & k<=200) Epifftf=EpifftfD;kk=k-150;
    elseif (k>200 & k<=250) Epifftf=EpifftfE;kk=k-200;
    elseif (k>250 & k<=300) Epifftf=EpifftfF;kk=k-250;
    elseif (k>300 & k<=350) Epifftf=EpifftfG;kk=k-300;
    elseif (k>350 & k<=400) Epifftf=EpifftfH;kk=k-350;
    elseif (k>400 & k<=450) Epifftf=EpifftfI;kk=k-400;
    elseif (k>450 & k<=500) Epifftf=EpifftfJ;kk=k-450;
    elseif (k>500 & k<=550) Epifftf=EpifftfK;kk=k-500;
    elseif (k>550 & k<=600) Epifftf=EpifftfL;kk=k-550;
    elseif (k>600) stop
    end
```

```
      kk=kk;
      t=.005*[0:1000];
      ch1=charray(k,channel1);
      if ch1 <= 0
        mesg={'Channel NOT meaured'
          'for this experiment. '
          ' '
          'Please try a different channel'};
        J=errordlg(mesg,'NO CHANNEL');
        pause(3)
        close(J)
        return
      end
      f=Epifftf(kk,:,ch1);
      fn=f(1);
      if f(1)>0
        C=freconstruct(f);
        C=[C];
        x(k)=mean(C);
        ckk=ck-28*floor(ck/28)+1;hold on;
        h=plot(t(1:length(C)),C,cray(ckk,:));
        set(h,'EraseMode', 'xor');
        ck=ck+1;
        if ck == 1
          V=axis;
          axis([V(1) V(2)+.15 V(3)-10 V(4)+10])
        end
        F(:,fr)=getframe(gcf);
        fr=fr+1;
          if savebutt==1
            frame=getframe(gcf);
            aviobj=addframe(aviobj,frame);
          end
     end
    set(messboard,'String','Finished');
end
clf;axes('Position',[0 0 1 1]);
movie(F,1,2)
    if savebutt==1
     aviobj=close(aviobj)
   end
end
% **********************
% FOR TWO CHANNEL MOVIE
% **********************
if twochanbutt == 1
  % IF MULTIPLE EPISODES IS CHECKED - DON'T CLEAR GRAPH
  if multepis ~= 1
    clf;
  end
  % GET GRAPH INFORMATION
```

```
  set(messboard,'String','Fill Out Graph Information');
  graphinfo2
  H=findobj(gcf,'Tag','donecheck');
  get(H,'Value');
  waitfor(H,'Value',1);
  h=findobj(gcf,'Tag','graph_title');
  graph_title=get(h,'String');
  h=findobj(gcf,'Tag','xaxis_label');
  xaxis_label=get(h,'String');
  h=findobj(gcf,'Tag','yaxis_label');
  yaxis_label=get(h,'String');
  h=findobj(gcf,'Tag','graph_title2');
  graph_title2=get(h,'String');
  h=findobj(gcf,'Tag','xaxis_label2');
  xaxis_label2=get(h,'String');
  h=findobj(gcf,'Tag','yaxis_label2');
  yaxis_label2=get(h,'String');
  close
  x=[];
  tags='ABCDEFGHIJKLMNOPQRSTUVWXYZ';
  num=ceil(maxepis/50);
  tags=tags(1:num);
  for k=1:num
    f3=strcat(experiment,tags(k),'.mat;');
    f4=strrep(f3,'l',' l');
    X=exist(strcat(experiment,tags(k),'.mat'),'file');
    if X > 0
      s8=strcat('load',f4);
      eval(s8);
    end
  end
cray=['r- ';'r: ';'r-.';'r--';...
    'b- ';'b: ';'b-.';'b--';...
    'g- ';'g: ';'g-.';'g--';...
    'c- ';'c: ';'c-.';'c--';...
    'y- ';'y: ';'y-.';'y--';...
    'm- ';'m: ';'m-.';'m--';...
    'k- ';'k: ';'k-.';'k--'];
ck=0;
numepis=length(episnums);
fr=1;
   title(graph_title);xlabel(xaxis_label);ylabel(yaxis_label);
if savebutt==1
   u=strcat('aviobj=avifile('',filename,'.avi'',''compression'',''indeo5'',''fps'',3,''quality'',100)');
   eval(u)
end
for k=1:numepis
    k=episnums(k);
    j=int2str(k);
    if (k>0 & k<=50) Epifftf=EpifftfA;kk=k;
    elseif (k>50 & k<=100) Epifftf=EpifftfB;kk=k-50;
```

```
    elseif (k>100 & k<=150) Epifftf=EpifftfC;kk=k-100;
    elseif (k>150 & k<=200) Epifftf=EpifftfD;kk=k-150;
    elseif (k>200 & k<=250) Epifftf=EpifftfE;kk=k-200;
    elseif (k>250 & k<=300) Epifftf=EpifftfF;kk=k-250;
    elseif (k>300 & k<=350) Epifftf=EpifftfG;kk=k-300;
    elseif (k>350 & k<=400) Epifftf=EpifftfH;kk=k-350;
    elseif (k>400 & k<=450) Epifftf=EpifftfI;kk=k-400;
    elseif (k>450 & k<=500) Epifftf=EpifftfJ;kk=k-450;
    elseif (k>500 & k<=550) Epifftf=EpifftfK;kk=k-500;
    elseif (k>550 & k<=600) Epifftf=EpifftfL;kk=k-550;
    elseif (k>600) stop
    end
    kk=kk;
    t=.005*[0:1024];
    ch1=charray(k,channel1);
    ch2=charray(k,channel2);
    if ch1 <= 0 | ch2 <= 0
      mesg={'Channel NOT meaured'
        'for this experiment. '
        ' '
        'Please try a different channel'};
      J=errordlg(mesg,'NO CHANNEL');
      pause(3)
      close(J)
      return
    end
    f=Epifftf(kk,:,ch1);
    fn=f(1);
    f2=Epifftf(kk,:,ch2);
    fn2=f(1);
    if f(1)>0
      C=freconstruct(f);
      C=[C];
      x(k)=mean(C);
      C2=freconstruct(f2);
      C2=[C2];
      ckk=ck-28*floor(ck/28)+1;
      subplot(2,1,1)
      hold on;plot(t(1:length(C)),C,cray(ckk,:));hold
on;title(graph_title);xlabel(xaxis_label);ylabel(yaxis_label);
      subplot(2,1,2)
      hold on;plot(t(1:length(C2)),C2,cray(ckk,:));hold
on;title(graph_title2);xlabel(xaxis_label2);ylabel(yaxis_label2);
      ck=ck+1;
      F(:,fr)=getframe(gcf);
      fr=fr+1;
        if savebutt==1
          frame=getframe(gcf);
          aviobj=addframe(aviobj,frame);
        end
      end
```

```
    end
  set(messboard,'String','Finished');
  clf;axes('Position',[0 0 1 1]);
  movie(F,1,2)
   if savebutt==1
    aviobj=close(aviobj);
  end
end
% MAKE OTHER OPERATIONS VISIBLE
h=findobj(gcbf,'Tag','loadmovbutt');
set(h,'Visible','on');
h=findobj(gcbf,'Tag','playmovbutt');
set(h,'Visible','on');
```

Subroutine loadmovie.m code

```
function loadmovie
% called from moviegui
% loads movies previously saved and plays
% MAKE OTHER OPERATION INVISIBLE
h=findobj(gcbf,'Tag','makemovbutt');
set(h,'Visible','off');
h=findobj(gcbf,'Tag','playmovbutt');
set(h,'Visible','off');
% CHANGE MESSAGE BOARD
messboard=findobj(gcbf,'Tag','messboard');
set(messboard,'String','Load Movie Subroutine');
% PUT IN DIALOG BOX TO TELL HOW TO LOAD MOVIES
presdir=pwd;
% GET FIRST MOVIE FILE OF SERIES
[fname,pname]=uigetfile('*.avi','MATLAB MOVIE FILES','Location',[400 400]);
if fname == 0
  set(messboard,'String','Must Select Movie to Load')
  h=findobj(gcbf,'Tag','makemovbutt');
  set(h,'Visible','on');
  h=findobj(gcbf,'Tag','playmovbutt');
  set(h,'Visible','on');
  return
end
cd(pname);
mov=aviread(fname);
% AVI FIGURE WINDOW PROPERTIES
h=figure;
set(h,'Name','MOVIE PLAYER');
set(h,'NumberTitle','off');
set(h,'Position',[275 40 650 650]);
set(h,'Color',[1 1 1]);
axes('Position',[0 0 1 1]);
set(messboard,'String','Resize Window Now - Press Return');
pause;
set(messboard,'String','Plotting movie');
```

```
% PLAY MOVIE ONCE AT 2 FRAMES PER SECOND
movie(mov,1,2)
cd(presdir)
% MAKE OTHER OPERATION VISIBLE
h=findobj(gcbf,'Tag','makemovbutt');
set(h,'Visible','on');
h=findobj(gcbf,'Tag','playmovbutt');
set(h,'Visible','on');
% END OF SUBROUTINE
set(messboard,'String','Finished')
```

REFERENCES

Alexi-Meskishvili, V., S. Ovroutski, et al. (2000). "Optimal conduit size for extracardiac Fontan operation." Eur J Cardiothorac Surg **18**(6): 690-5.

Be'eri, E, S. E. Maier, et al (1998). "In vivo evaluation of Fontan pathway flow dynamics by multidimensional phase-velocity magnetic resonance imaging" Circulation. **98**(25): 2873-82.

Bridges, N. D., J. E. Lock, et al. (1990). "Baffle Fenestration With Subsequent Transcatheter Closure: Modification of the Fontan Operation for Patients at Increased Risk." Circulation **82**(5): 1681-1689.

Bull, K. (1998). "The Fontan procedure: lessons from the past (editorial)." Heart **79**(3): 213-4.

Cetta, F., R. H. Feldt, et al. (1996). "Improved Early Morbidity and Mortality After Fontan Operation: The Mayo Clinic Experience, 1987 to 1992." Journal of the American College of Cardiology **28**(2): 480-6.

Coon, P. D., J. Rychik, et al. (2001). "Thrombus formation after the Fontan operation." Ann Thorac Surg **71**(6): 1990-4.

Cosolo, G., L. Rega, et al (2004). "Detection of right atrial and pulmonary artery thrombosis after the Fontan procedure by magnetic resonance imaging" Heart **90**: 825.

de Leval, M., P. Kilner, et al. (1988). "Total cavopulmonary connection: a logical alternative to atriopulmonary connection for complex Fontan operations. Experimental studies and early clinical experience." Journal of Thoracic & Cardiovascular Surgery **96**(5): 682-95.

de Leval, M. R., G. Dubini, et al. (1996). "Use of computational fluid dynamics in the design of surgical procedures: application to the study of competitive flows in cavopulmonary connections." Journal of Thoracic and Cardiovascular Surgery **111**(3): 502-513.

de Zelicourt DA, Pekkan K, Parks J, Kanter K, Fogel M, Yoganathan AP. Flow study of an extracardiac connection with persistent left superior vena cava. *J Thorac Cardiovasc Surg*. 2006;131:785-791.

Eicken, A., S. Fratz, et al. (2003). "Hearts late after fontan operation have normal mass, normal volume, and reduced systolic function: a magnetic resonance imaging study." J Am Coll Cardiol **42**(6): 1061-5.

Fogel, M. A., P. M. Weinberg, et al (1996). "Late Ventricular Geometry and Performance Changes of Functional Single Ventricle Throughout Staged Fontan Reconstruction Assessed by Magnetic Resonance Imaging" Journal of American College of Cardiology **28**: 212-21.

Fogel, M. A., P. M. Weinberg, et al (1997). "The Nature of flow in the systemic venous pathway measured by magnetic resonance blood tagging in patients having the Fontan operation" Journal of Thoracic and Cardiovascular Surgery **114**(6): 1032-41.

Fogel, M. A., P. M. Weinberg, et al (1999). "Caval Contribution to Flow in the Branch Pulmonary Arteries of Fontan Patients With a Novel Application of Magnetic Resonance Presaturation Pulse" Circulation **99**(9): 1215-21.

Fogel, M. A. (2005). "Is Routine Catheterization Necessary in the Management of Patients with Single Venticles Across Staged Fontan Reconstruction? No!" Pediatric Cardiology **26**: 154-8.

Fontan, F. and E. Baudet (1971). "Surgical repair of tricuspid atresia." Thorax **26**: 240-248.

Freedom, R. M. (1998). "Subaortic Obstruction and the Fontan Operation." Annals of Thoracic Surgery **66**(2): 649-52.

Freedom, R. M., D. Nykanen, et al. (1998). "The physiology of the bidirectional cavopulmonary connection." Annals of Thoracic Surgery **66**: 664-7.

Gandhi, S. K., B. I. Bromberg, et al. (1997). "Spontaneous Atrial Flutter in a Chronic Canine Model of the Modified Fontan Operation." Journal of the American College of Cardiology **30**(4): 1095-103.

Gardiner, H. M., R. Dhillon, et al. (1996). "Prospective Study of the Incidence and Determinants of Arrhythmia After Total Cavopulmonary Connection." Circulation **94**(9): II17-II21.

Gates, R. N., H. Laks, et al. (1997). "The Fontan Procedure in Adults." Annals of Thoracic Surgery **63**(4): 1276-82.

Geggel, R. L. (1997). "Update on the modified Fontan procedure." Current Opinion in Cardiology **12**(1): 51-62.

Gentles, T. L., K. Gauvreau, et al. (1997). "Functional Outcome After the Fontan Operation: Factors Influencing Late Morbidity." Journal of Thoracic & Cardiovascular Surgery **114**(3): 392-403;discussion 404-5.

Gentles, T. L., J. E. Mayer, et al. (1997). "Fontan Operation in Five Hundred Consecutive Patients: Factors Influencing Early and Late Outcome." Journal of Thoracic & Cardiovascular Surgery **114**(3): 376-91.

Goldman, A. P., R. E. Delius, et al. (1996). "Pharmacological Control of Pulmonary Blood Flow With Inhaled Nitric Oxide After the Fenestrated Fontan Operation." Circulation **94**(9 Suppl II): 44-48.

Gundry, S. R., A. J. Razzouk, et al. (1997). "The Optimal Fontan Connection: A Growing Extracardiac Lateral Tunnel with Pedicled Percardium." Journal of Thoracic & Cardiovascular Surgery **114**(4): 552-8.

Julsrud, PR, R. L. Ehman, et al (1989). "Extracardiac vasculature in candidates for Fontan Surgery: MR imaging." Radiology **173(2)**: 503-6.

Kim, Y. H., P. G. Walker, et al. (1995). "Hemodynamics of the Fontan Connection: An In-Vitro Study." Journal of Biomechanical Engineering **117**: 423-428.

Laks, H., J. M. Pearl, et al. (1991). "Partial Fontan: Advantages of an Adjustable Interatrial Communication." Annals of Thoracic Surgery **52**: 1084-95.

Lardo, A. C., S. A. Webber, et al. (1999). "Fluid dynamic comparison of intra-atrial and extracardiac total cavopulmonary connections." Journal of Thoracic and Cardiovascular Surgery **117**(4): 697-704.

Lemes, V., A. M. Murphy, et al. (1998). "Fenestration of Extracardiac Fontan and Reversal of Protein-Losing Enteropathy: Case Report." Pediatric Cardiology **19**(4): 355-7.

Lofland, G. K., (2001). "The enhancement of hemodynamic performance in Fontan circulation using pain free spontaneous ventilation." European Journal of Cardio-thoracic Surgery **20**: 114-9.

Marcelletti, C., A. Corno, et al. (1990). "Inferior vena-cava-pulmonary artery extracardiac conduit." Journal of Thoracic & Cardiovascular Surgery **100**: 228-232.

Masuda, M., H. Kado, et al. (1998). "Clinical Results of the Staged Fontan Procedure in High-Risk Patients." Annals of Thoracic Surgery **65**(6): 1721-5.

McElhinney, D. B., S. M. Marianeschi, et al. (1998). "Additional Pulmonary Blood Flow With the Bidirectional Glenn Anastomosis: Does It Make a Difference?" Annals of Thoracic Surgery **66**: 668-672.

McElhinney, D. B., V. M. Reddy, et al. (1996). "Revision of Previous Fontan Connections to Extracardiac or Intraatrial Conduit Cavopulmonary Anastomosis." Annals of Thoracic Surgery **62**(5): 1276-82.

Mendelsohn, A., E. Bove, et al. (1994). "Central pulmonary artery growth patterns after the bidirectional Glenn procedure." Journal of Thoracic & Cardiovascular Surgery **107**: 1284-90.

Morgan, V. L., T. P. Graham, et al (1998). "Alterations in pulmonary artery flow patterns and shear stress determined with three-dimensional phase-contrast magnetic resonance imaging in Fontan patients" Journal of Thoracic & Cardiovascular Surgery **116**(2): 294-304.

Norwood, W. I. and M. L. Jacobs (1993). "Fontan's Procedure in Two Stages." The American Journal of Surgery **166**: 548-551.

Okano, T., M. Yamagishi, et al. (2002). "Extracardiac total cavopulmonary connection using a Y-shaped graft." Ann Thorac Surg **74**(6): 2195-7.

Pedersen, E. M., E. V. Stenbog, et al (2002). "Flow during exercise in the total cavopulmonary connection measured by magnetic resonance velocity mapping" Heart **87**(6): 554-8.

Petrossian, E., V. M. Reddy, et al. (1999). "Early Results Of The Extracardiac Conduit Fontan Operation." Journal of Thoracic & Cardiovascular Surgery **117**(4): 688-96.

Riemer, R. G. Amir, S. Reichenbach, O. Reinhartz (2005). "Mechanical support of total cavopulmonary connection with an axial flow pump. " Journal of Thoracic and Cardiovascular Surgery, Volume **130**(2): 351-354.

Rodefeld, M. D., J. H. Boyd, et al. (2003). "Cavopulmonary assist: circulatory support for the univentricular Fontan circulation." Ann Thorac Surg **76**(6): 1911-6; discussion 1916.

Sano, S., K. Ishino, et al. (2003). "Right ventricle-pulmonary artery shunt in first-stage palliation of hypoplastic left heart syndrome." The Journal of Thoracic and Cardiovascular Surgery **126**(2): 504-510.

Sharma, S., A. E. Ensley, et al. (2001). "In Vivo Flow Dynamics of the Total Cavopulmonary Connection From Three-Dimensional Multislice Magnetic Resonance Imaging." Annals of Thoracic Surgery **71**: 889-98.

Shemin, R., W. Merrill, et al. (1979). "Evaluation of right atrial-pulmonary artery conduits for tricuspid atresia." Journal of Thoracic and Cardiovascular Surgery **77**: 685-690.

Tam, V. K. H., B. E. Miller, et al. (1999). "Modified Fontan Without Use of Cardiopulmonary Bypass." Annals of Thoracic Surgery **68**: 1698-704.

Thompson, L. D., E. Petrossian, et al. (1999). "Is It Necessary to Routinely Fenestrate an Extracardiac Fontan?" Journal of the American College of Cardiology **34**(2): 539-44.

van Son, J. A., M. V. Reddy, et al. (1995). "Extracardiac Modification of the Fontan Operation without use of Prosthetic Material." Journal of Thoracic & Cardiovascular Surgery **110**(6): 1766-1768.

Veldtman, G. R., A. Nishimoto, et al. (2001). "The Fontan procedure in adults." Heart **86**(3): 330-5.